NASA

National
Aeronautics and
Space
Administration

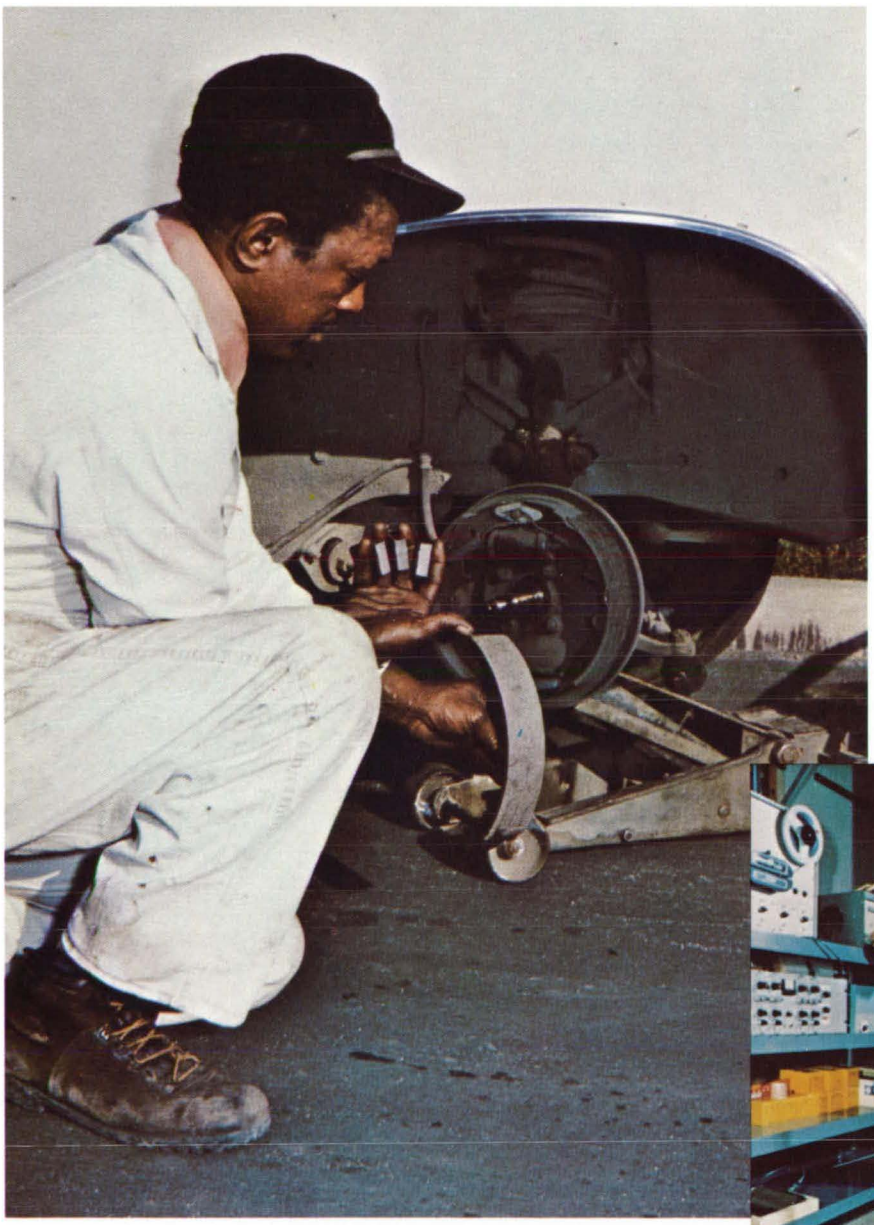

Materials developed at the Ames Research Center for high-temperature environments are being evaluated for applications as improved brake-lining materials.

To aid in physical therapy, walking patterns are analyzed by RF transmission of neuromotor sensor data, using sensors and electronics developed at NASA's Ames Research Center.

Vol. 1, No. 3

FALL 1976

About the NASA Technology Utilization Program

The National Aeronautics and Space Act of 1958, which established NASA and the United States civilian space program, requires that "The Administration shall provide for the widest practicable and appropriate dissemination of information concerning its activities and the results thereof."

To help carry out this objective the NASA Technology Utilization (TU) Program was established in 1962. It offers a variety of valuable services to facilitate the transfer of aerospace technology to nonaerospace applications, thus assuring American taxpayers maximum return on their investment in space research; thousands of spinoffs of NASA research have already occurred in virtually every area of our economy.

The TU Program has worked for engineers, scientists, technicians, and businessmen. And it can work for you.

NASA Tech Briefs

Tech Briefs is published quarterly and is free to any U.S. citizen or organization. It is both a current-awareness medium and a problem-solving tool. Potential products ... industrial processes ... basic and applied research ... shop and lab techniques ... computer software ... new sources of technical data ... concepts ... you will find them all in NASA Tech Briefs. The first section highlights a few of the potential new products contained in Tech Briefs. The remainder of the volume is organized by technical category to help you quickly review new developments in your areas of interest. Finally, a subject index makes each issue a convenient permanent reference file.

Further Information on Innovations

Although many articles are complete in themselves, others are backed up by Technical Support Packages (TSP's). TSP's are available without charge and may be ordered by simply completing the enclosed TSP Request Card. Further information on some innovations is available for a nominal fee from other sources, as indicated at the ends of the articles. In addition, Technology Utilization Officers at NASA Field Centers will assist you directly when necessary. (See page A4.)

Patent Licenses

Many of the inventions described are under consideration for patents or have been patented by NASA. Unless NASA has decided not to apply for a patent, the patent status is described at the end of each article. For further information about the Patent Program see page A8.

Other Technology Utilization Services

To assist engineers, industrial researchers, business executives, city officials, and other potential users in applying space technology to their problems, NASA sponsors six Industrial Applications Centers. Their services are described on page A6. In addition, an extensive library of computer programs is available through COSMIC, the Technology Utilization Program's outlet for NASA-developed software. (See page A5.)

Applications Program

To help solve public-sector problems in such areas as safety, health, transportation, and environmental protection, NASA TU Applications Teams, staffed by professionals from a variety of disciplines, work with Federal agencies, local governments, and health organizations to identify critical problems amenable to technical solutions. Among their many significant contributions are a rechargeable heart pacemaker, a lightweight fireman's breathing apparatus, aids for the handicapped, and safer highways.

Reader Feedback

We hope you find the information in NASA Tech Briefs useful. A reader feedback card has been included because we want your comments and suggestions on how we can further help you apply NASA innovations and technology to your needs. Please use it, or if you need more space, write us a letter.

NASA Tech Briefs

National Aeronautics and Space Administration

FALL 1976
Volume 1, Number 3

COVERS: The photographs on the front and back covers illustrate recent developments by NASA and its contractors that have resulted in commercial and nonaerospace spinoffs.

About This NASA Publication

NASA Tech Briefs, a quarterly publication, is distributed free to U.S. citizens to encourage commercial application of U.S. space technology. For information on publications and services available through the NASA Technology Utilization Program, write to the Director, Technology Utilization Office, P. O. Box 8756, Baltimore/Washington International Airport, Maryland 21240.

"The Administrator of National Aeronautics and Space Administration has determined that the publication of this periodical is necessary in the transaction of the public business required by law of this Agency. Use of funds for printing this periodical has been approved by the Director of the Office of Management and Budget through August 31, 1977."

Change of Address

Change of Address: If you wish to have NASA Tech Briefs forwarded to your new address, use one of the Subscriptions cards enclosed in the back of this volume of NASA Tech Briefs. Be sure to check the appropriate box indicating change of address.

Communication Concerning Editorial Matter

For editorial comments or general communications about NASA Tech Briefs, you may use the self-addressed Feedback card in the back of NASA Tech Briefs, or write to: The Publications Manager, Technology Utilization Office (Code KT), NASA Headquarters, Washington, DC 20546. Technical questions concening specific articles should be directed to the Technology Utilization Officer of the sponsoring NASA Center (addresses listed on page A4.)

NASA TU SERVICES

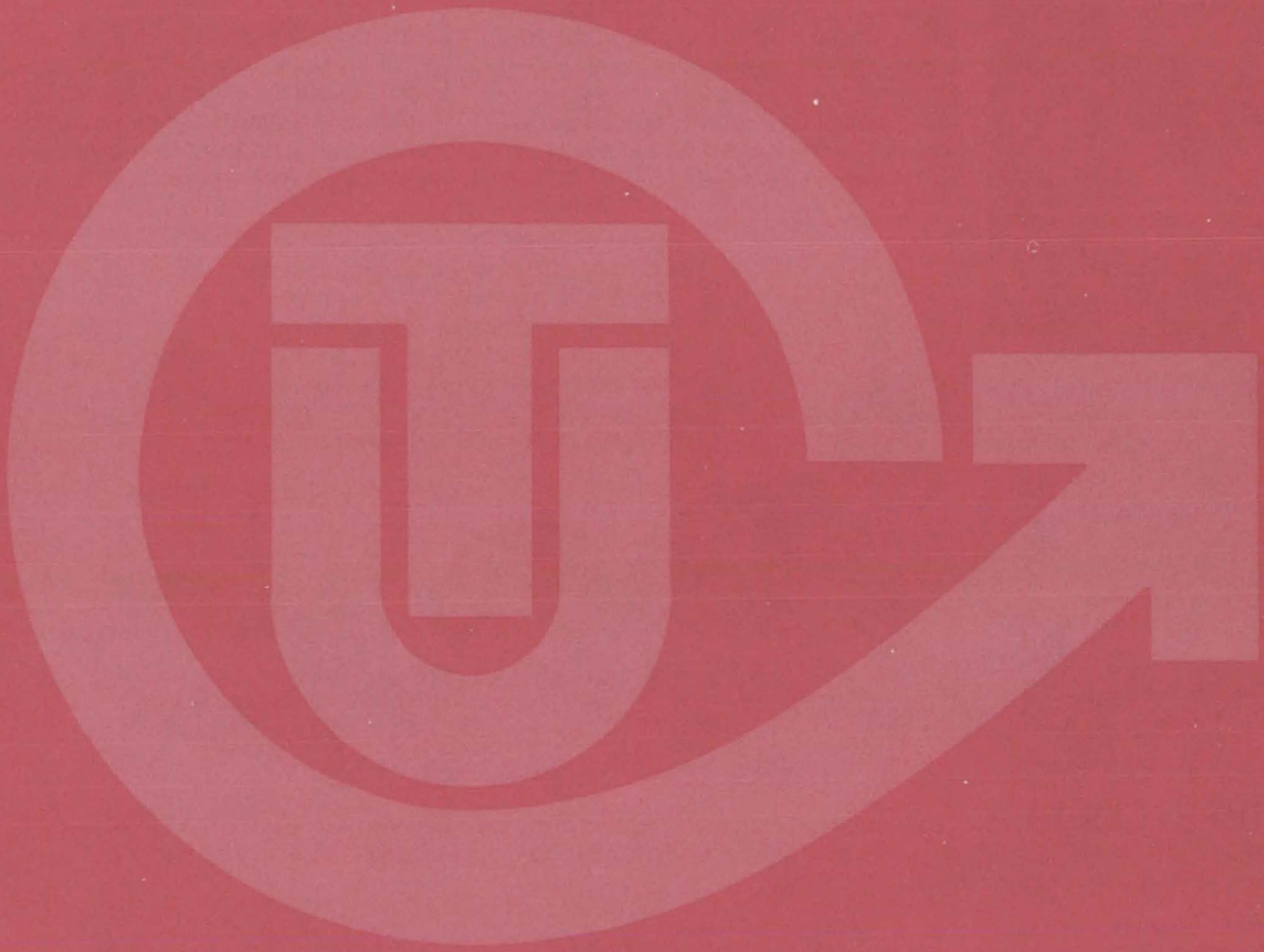

THE NASA TECHNOLOGY UTILIZATION OFFICERS

They will help you apply the innovations described in Tech Briefs.

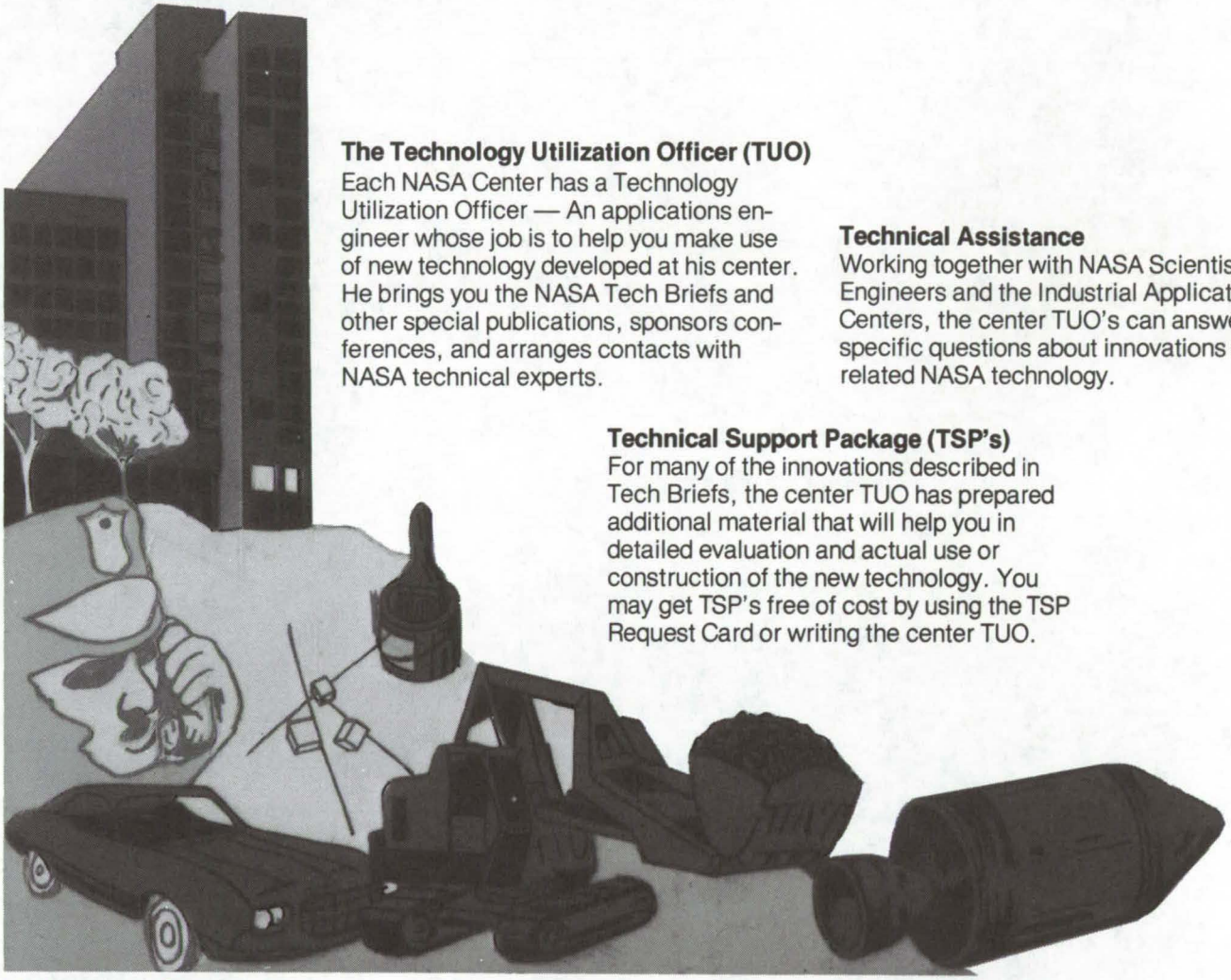

The Technology Utilization Officer (TUO)
Each NASA Center has a Technology Utilization Officer — An applications engineer whose job is to help you make use of new technology developed at his center. He brings you the NASA Tech Briefs and other special publications, sponsors conferences, and arranges contacts with NASA technical experts.

Technical Assistance
Working together with NASA Scientists and Engineers and the Industrial Applications Centers, the center TUO's can answer specific questions about innovations and related NASA technology.

Technical Support Package (TSP's)
For many of the innovations described in Tech Briefs, the center TUO has prepared additional material that will help you in detailed evaluation and actual use or construction of the new technology. You may get TSP's free of cost by using the TSP Request Card or writing the center TUO.

Who to Contact. Of course, many technical questions about Tech Briefs are answered in the TSP's, but when no TSP is available, or you have further questions, write the Technology Utilization Officer at the center that sponsored the research at the address listed below.

Charles K. Kubokawa
Ames Research Center
Code AU: 230-2
Moffett Field, CA 94035
(415) 965-5554

Clinton T. Johnson
Hugh L. Dryden Flight Research Center
P. O. Box 273
Edwards, CA 93523
(805) 258-3311, Ext. 568

Donald S. Friedman
Goddard Space Flight Center
Code 704.1
Greenbelt, MD 20771
(301) 982-6242

John T. Wheeler
Johnson Space Center
Code AT3
Houston, TX 77058
(713) 483-3809

Raymond J. Cerrato
John F. Kennedy Space Center
Code SA-RTP
Kennedy Space Center, FL 32899
(305) 867-2780

John Samos
Langley Research Center
Mail Stop 139A
Hampton, VA 23665
(804) 827-3281

Paul Foster
Lewis Research Center
21000 Brookpark Rd.
Cleveland, OH 44135
(216) 433-4000, Ext. 6832

Aubrey D. Smith
Marshall Space Flight Center
Code AT01
Marshall Space Flight Center, AL 35812
(205) 453-2224

John C. Drane
NASA Resident Legal Office-JPL
4800 Oak Grove Drive
Pasadena, CA 91103
(213) 354-6420

Gilmore H. Trafford
Wallops Flight Center
Wallops Island, VA 23337
(804) 824-3411, Ext 201

Louis Mogavero, Director
Technology Utilization Office
Code KT
NASA Headquarters
Washington, DC 20546
(202) 755-3103

COSMIC

(Computer Software Management & Information Center)

AN ECONOMICAL SOURCE OF COMPUTER PROGRAMS DEVELOPED BY THE GOVERNMENT.

COSMIC is sponsored by NASA to give you access to over 1400 computer programs developed by NASA and the Department of Defense, and selected programs from other government agencies. It is one of the Nation's largest software libraries.

COSMIC charges very reasonable fees for programs to help cover part of their expenses—and NASA pays for the remainder. Programs generally cost from $500 to $1000, but a few are more expensive and many are less. Documentation is available separately and very inexpensively.

COSMIC collects and stores software packages, insures that they are complete, prepares special announcements (such as Tech Briefs), publishes an indexed software catalog, and reproduces programs for distribution. COSMIC helps customers to identify their software needs, follows up to determine the successes and problems, and provides updates and error corrections. In some cases, NASA engineers can offer guidance to users in installing or running a program.

COSMIC programs range from management (pert scheduling) to information science (retrieval systems) and computer operations (hardware and software). Hundreds of engineering programs perform such tasks as structural analysis, electronic circuit design, chemical analysis, and design of fluid systems. Others determine building energy requirements, optimize mineral exploration, and draw maps of water-covered areas using NASA satellite data. In fact, the chances are, if you use a computer, you can use COSMIC.

COSMIC is eager to help you get the programs you need. For more information about services or software available from COSMIC, fill out and mail the COSMIC Request Card in this issue.

COSMIC: Computer Software and Management Information Center

Suite 112, Barrow Hall, Athens, Georgia 30602 Phone: (404) 542-3265

WHERE IS THE WORLD'S LARGEST BANK OF TECHNICAL DATA

?

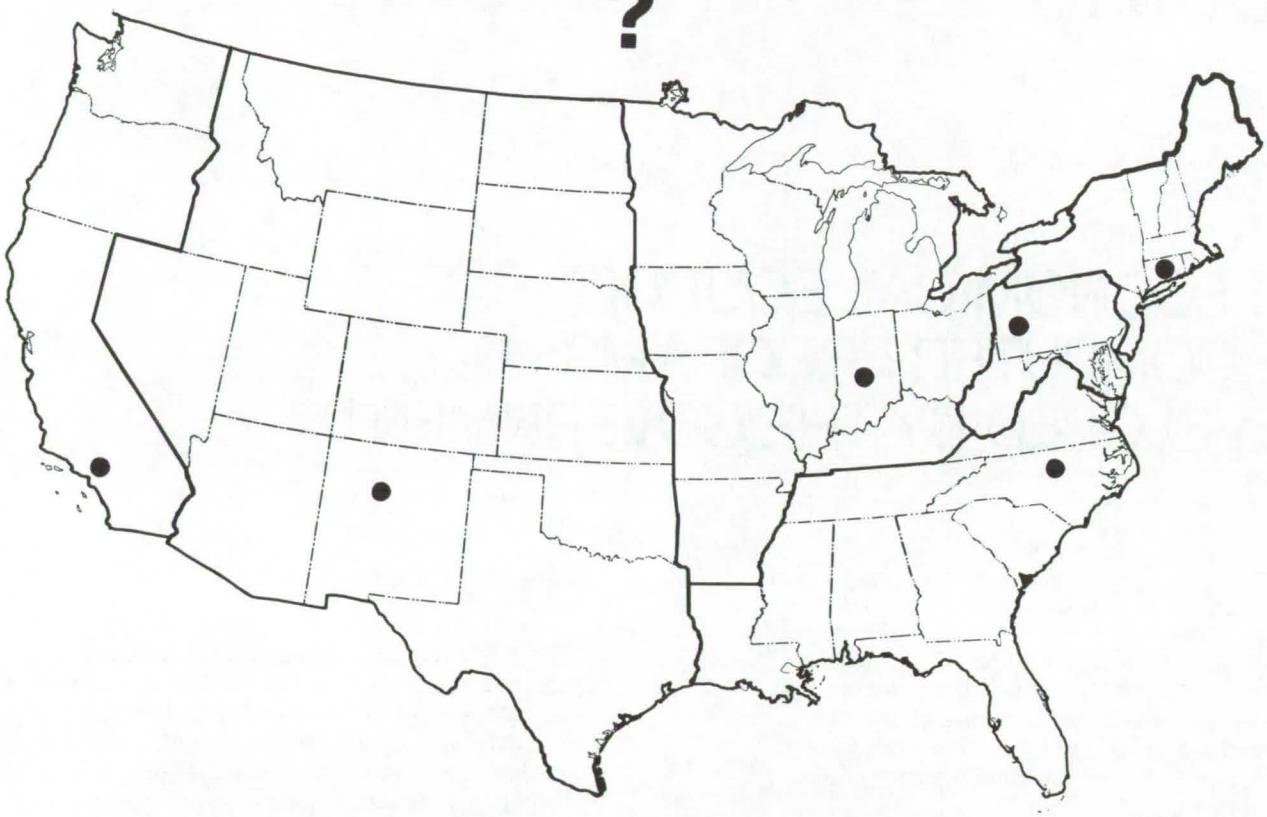

It's in Bloomington and Pittsburgh, it's in Storrs, Connecticut and Research Triangle Park, North Carolina; and it's in Albuquerque and Los Angeles.

NASA IAC's — INDUSTRIAL

You can get more information and more data on more technical subjects through NASA's network of IAC's than anywhere else in the world. About 8,000,000 documents and growing at the rate of 50,000 more each month!

Major sources include:

- 750,000 NASA Technical Reports
- Selected Water Resources Abstracts
- NASA Scientific and Technical Aerospace Reports
- Air Pollution Technical Information Center
- NASA International Aerospace Abstracts
- Chem Abstracts Condensates
- Engineering Index
- Nuclear Science Abstracts
- NASA Tech Briefs
- Government Reports Announcements

and many other specialized files on food technology, textile technology, metallurgy, medicine, business, economics, social sciences, and physical science.

The IAC's are one of the most economical ways of staying competitive in today's world of exploding technology. The help available from the network ranges from literature searches through expert technical assistance.

Literature Searches

Help in designing your search, typically from 30 to 300 abstracts in as narrow or broad an area as you need, and complete reports when you need them. The most complete "search before research" available!

Current Awareness

Consult with our applications engineers to design your personal program — selected monthly or quarterly abstracts on new developments in your speciality. It's like having your own journal!

Technical Assistance

Our applications engineers will help you evaluate and apply your literature-search results. They can help find answers to your technical problems and put you in touch with scientists and engineers at NASA Field Centers.

To obtain more information about how NASA's IAC's can help you —
Check the IAC box on the TSP Request Card in this issue,
Or write or call the IAC nearest you.

APPLICATIONS CENTERS

How to get reports and other documents discussed in this issue of Tech Briefs

Many of the innovations in Tech Briefs are described in detail in reports available at a reasonable cost through one or more of the IAC's. To order a report, call or write the IAC referenced at the end of the Tech Brief article at the address below. Be sure to list the titles and accession numbers (N76-..., N75-..., etc.) of those you wish to purchase.

Aerospace Research Application Center (ARAC)
Indiana University-Purdue University at Indianapolis
1201 E. 38th St.
Indianapolis, IN 46205
E. Guy Buck, Director
(317) 264-4644

Knowledge Availability Systems Center (KASC)
University of Pittsburgh
Pittsburgh, PA 15260
Edmond Howle, Director
(412) 624-5211

New England Research Application Center (NERAC)
Mansfield Professional Park
Storrs, CT 06268
Dr. Daniel U. Wilde, Director
(203) 486-4533

North Carolina Science & Technology
Research Center (NC/STRC)
P. O. Box 12235
Research Triangle Park, NC 27709
Peter J. Chenery, Director
(919) 549-0671

Technology Application Center (TAC)
University of New Mexico
Albuquerque, NM 87131
Dr. Carey O'Bryan, Director
(505) 277-4000

Western Research Application Center (WESRAC)
University of Southern California
University Park
Los Angeles, CA 90007
Radford King, Director
(213) 746-6132

NASA INVENTIONS AVAILABLE FOR LICENSING

Over 3,500 NASA inventions are available for licensing in the United States - both exclusive and nonexclusive.

Nonexclusive Licenses

Nonexclusive licenses for commercial use are encouraged to promote competition and to achieve the widest use of inventions. They must be used by a negotiated target date but are usually royalty free.

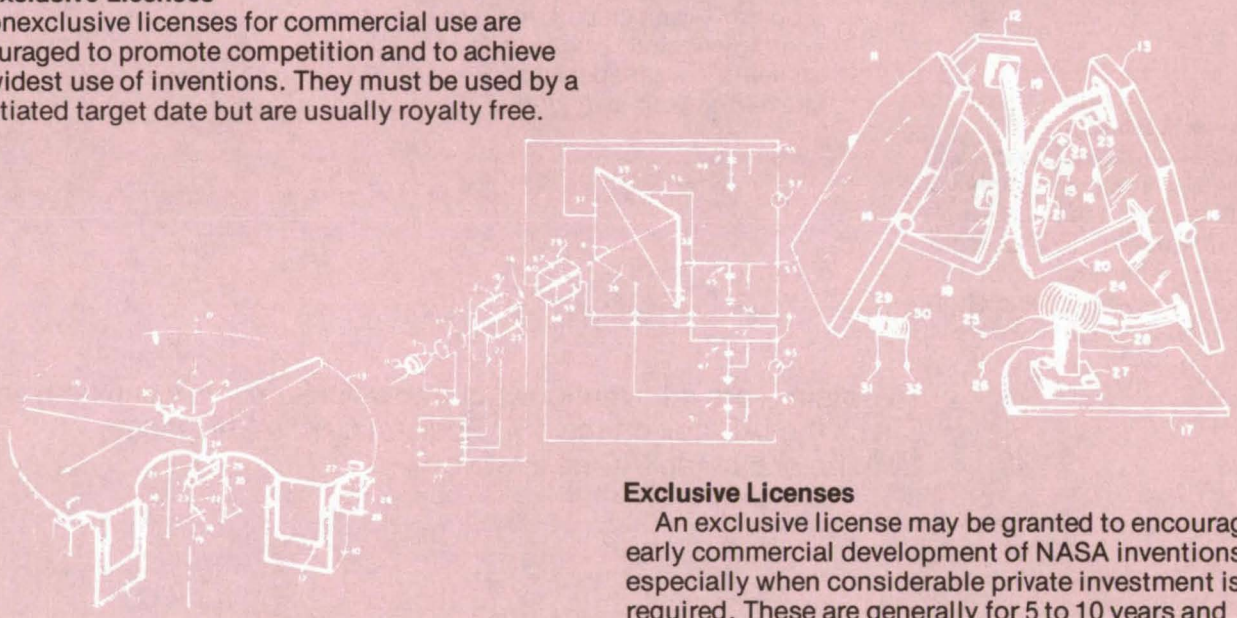

Exclusive Licenses

An exclusive license may be granted to encourage early commercial development of NASA inventions, especially when considerable private investment is required. These are generally for 5 to 10 years and usually require royalties based on sales or use.

The NASA patent licensing program also provides for licensing of NASA-owned foreign patents. In addition to inventions described in Tech Briefs, "NASA Patent Abstract Bibliography," containing abstracts of all NASA inventions, can be purchased from: National Technical Information Service, Springfield, Va., 22151. This document is updated semi-annually.

Patent Licenses and the NASA Tech Brief

Many of the inventions reported in Tech Briefs are patented or are under consideration for a patent at the time they are published. When this is the case, the current patent status is described at the end of the article; otherwise, there is no statement about patents. **If you want to know more about the patent program or are interested in license for a particular invention, write the Patent Counsel at the NASA Field Center** that sponsored the research. Be sure to refer to the NASA reference number at the end of the Tech Brief.

Robert F. Kempf
NASA Headquarters, Code GP
400 Maryland Ave., S.W.
Washington, DC 20546
(202) 755-3932

Darrell G. Brekke
Ames Research Center
Mail Code: 200-11A
Moffett Field, CA 94035
(415) 965-5104

John O. Tresansky
Goddard Space Flight Center
Mail Code: 204
Greenbelt, MD 20771
(301) 982-2351

Marvin F. Matthews
Lyndon B. Johnson Space Center
Mail Code: AM
Houston, TX 77058
(713) 483-4871

James O. Harrell
John F. Kennedy Space Center
Mail Code: SA-PAT
Kennedy Space Center, FL 32899
(305) 867-2544

Howard J. Osborn
Langley Research Center
Mail Code: 313
Hampton, VA 23665
(804) 827-3725

Norman T. Musial
Lewis Research Center
Mail Code: 500-113
21000 Brookpark Road
Cleveland, OH 44135
(216) 433-4000 Ext. 346

Leon D. Wofford, Jr.
Marshall Space Flight Center
Mail Code: CC01
Marshall Space Flight Center, AL 35812
(205) 453-0020

Monte F. Mott
NASA Resident Legal Office-JPL
4800 Oak Grove Drive
Pasadena, CA 91103
(213) 354-2700

NEW PRODUCT IDEAS

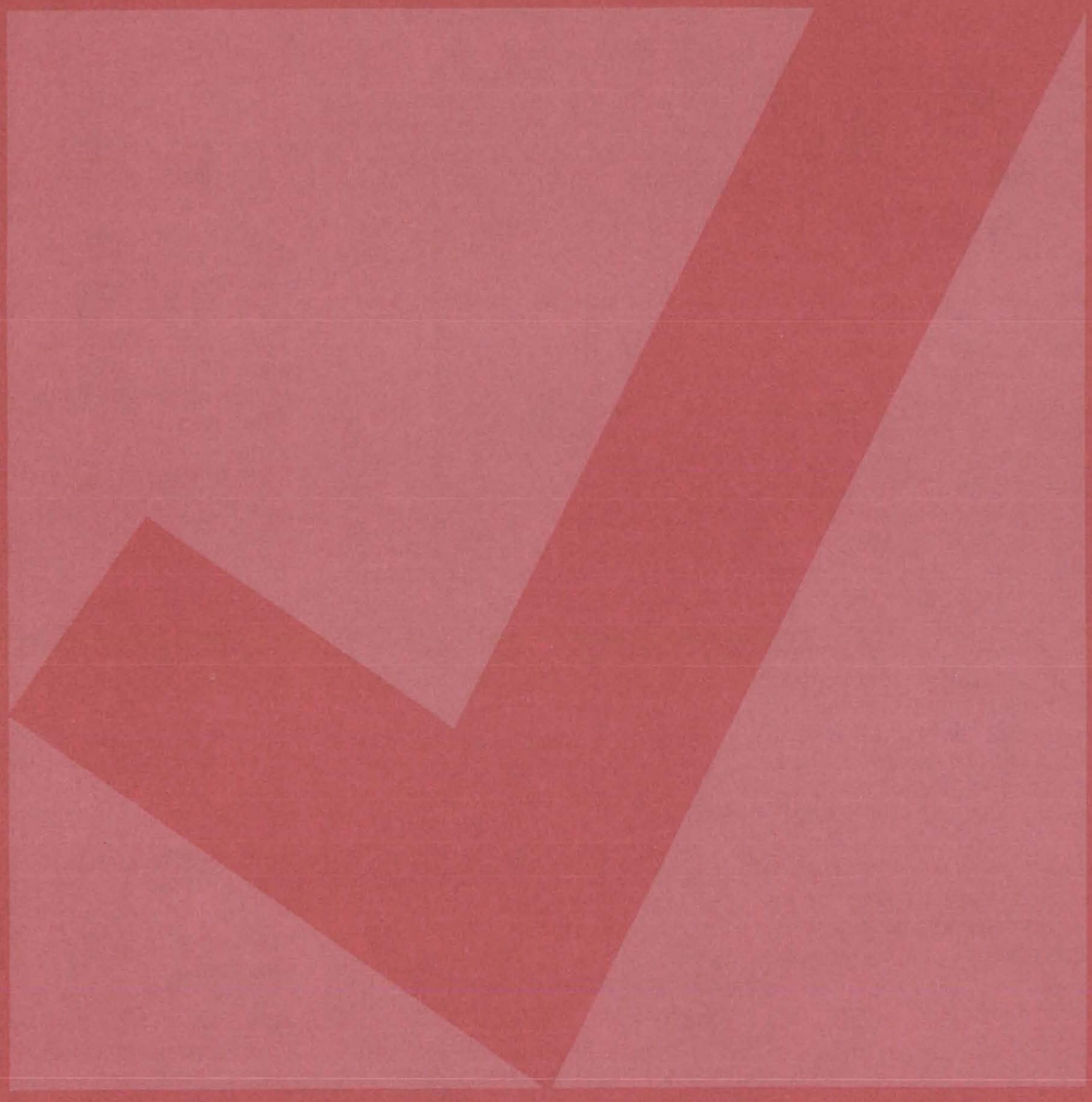

NEW PRODUCT IDEAS are just a few of the many innovations described in this issue of NASA Tech Briefs and having promising commercial applications. Each is discussed further on the referenced page in the appropriate section in this issue. If you are interested in developing a product from these or other NASA innovations, you can receive further technical information by requesting the TSP referenced at the end of the full-length article or by writing the Technology Utilization Office of the sponsoring NASA center (see page A4). NASA's patent-licensing program to encourage commercial development is described on page A8.

Automated EEG Acquisition

A new, recording and telemetry system could allow electroencephalographic analysis of patients — a valuable diagnostic technique currently limited to large specialized facilities — to become nearly a routine procedure. New recording equipment can be used by relatively untrained operators. New electronics process the waveforms and transmit them by telephone. Equipment for centralized analysis allows a large specialized hospital or other facility to receive transmitted waveforms, analyze them, and send the results back to the remote site. Computer-assisted analysis expands the capability of the central facility and allows numerous remote sites to be served. The system includes a special recording cap with replaceable electrodes, a telemetry (telephone line) system with a printer and voice communication, centralized data analysis circuits, and supporting software.
(See page 393.)

Pinhole Diffraction Filter

A new type of optical filter could serve as a simple way of reducing radiation flux levels for UV photon counters, as a calibration filter for photon-counting systems, as an optical low-pass filter, or as a color-balancing filter. The device is the optical analog of an electronic attenuating filter; it consists of a series of alined pinholes or slit arrays through which light passes. The light is attenuated as it passes through each pinhole in the series. The particular application (e.g., low-pass filtering and spectral filtering) determines the pinhole dimensions.
(See page 359.)

Precision Centering Vise

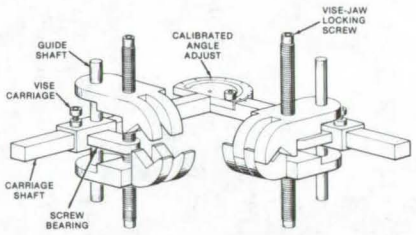

A new vise will hold stainless-steel tubing and fittings in the precise alinement required for induction brazing. Tube ends are automatically alined, regardless of differences in diameters. Tubing is not crushed or deformed. The vise is particularly useful where existing supports or walls cannot be used to anchor tubes. The vise consists of two clamping assemblies with dual lockable jaws and two carriages. The carriages ride on a support that can be adjusted for the particular fitting to be brazed.
(See page 440.)

Disposable Biomedical Electrode

New snap-on biomedical electrodes save costs by allowing the reuse of a special electrode-positioning cap used for EEG's. The electrodes could provide similar savings in the many other instances where biomedical electrodes are used with or as a part of other apparatus. The electrodes are molded units that are snapped into place like clothing fasteners. Simple to make,

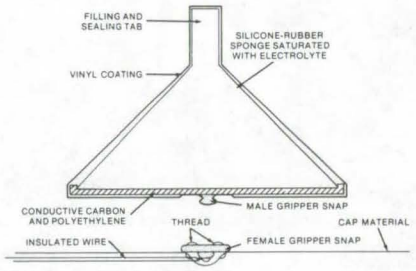

they consist of an electrolyte-saturated sponge coated with vinyl and supported on a conductive carbon/polyethylene base, on which the metal snap is also mounted.
(See page 392.)

Inexpensive Low-Voltage Solid-State Alarm

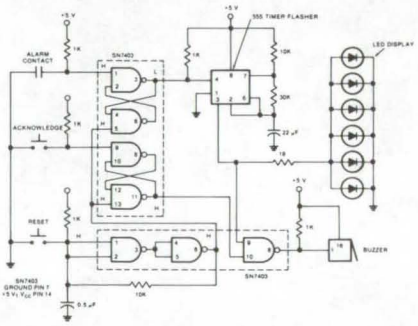

A versatile monitor/alarm circuit can be used to warn when prescribed limits of temperature, liquid level, pressure, or similar properties are exceeded. Although accurate and reliable, the device is more compact, lighter, and less expensive to manufacture than typical alarm circuits. It has both an audio and a visual warning output. Inputs can be, for example, from thermostats, pressure switches, or floating switches. When the input sensor is in a normal state, the alarm circuit is quiescent; when the system exceeds the preset limits and the sensor is activated, a buzzer sounds and LED's begin flashing.
(See page 344.)

Improved Load Handler

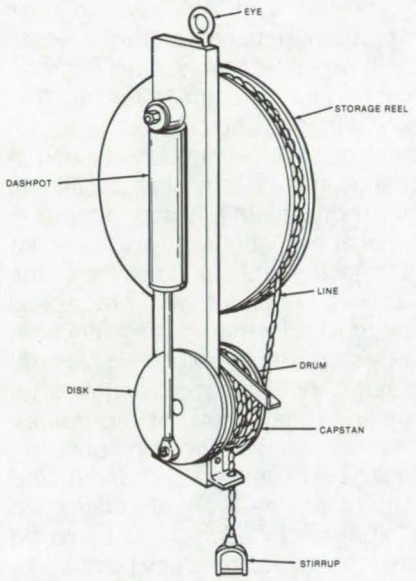

A simply-made rope-and-pulley arrangement lowers objects at a constant speed, relatively independent of the object weight. It could be used as an emergency escape device, for materials handling, or as part of a large system.
(See page 443.)

High-Torque Open-End Wrench

A new wrench combines the flexibility of an open-end wrench with the high-torque close-clearance capability of box and socket wrenches. It is an easy-to-use, inexpensive, simple tool that can be used in hard-to-get-at spots and has a wide

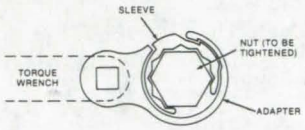

range of applications. In one trial use, it transmitted over 750 inch-pounds to a steel gland nut on a 3/4-inch tube. It can be used (as an adapter) with available ratchet and torque wrench handles.
(See page 437.)

Flame-Resistant Elastomeric Polymers

A new family of flame-resistant elastomeric polymers could be used in products for the automobile, textile, upholstery, and paint industries. The compounds are fluorinated urethanes and neoprenes. They were originally produced as materials for scaling and vibration dampening, but could be used in other applications requiring the high elongation and recovery properties of rubbers. Other possible applications include lens caps, helmet linings, coated fabrics, and packaging foams. The formulations have limiting oxygen indices (LOI's) from 50 to 100. They can be extruded through dies to produce elastic fibers, compression molded, dissolved in solvents as required for coatings, and calendered to produce film and embossed sheeting.
(See page 384.)

Fabrication and Applications of Electrets

Electrets are permanently charged dielectrics: electrical analogs of magnets. Recent research has significantly lowered their production costs, allowed new materials to be used, and suggested new applications. Using high-voltage corona discharge, electrets can generally be made in minutes at room temperature, compared to hours at elevated temperatures required previously. For the first time, electrets have been made from single crystals (gadolinium molybdate) and quartz. New applications include quartz electrets for quartz-crystal microbalances and filters or particle collectors for pollution studies.
(See page 460.)

Miniature Carbon Dioxide Sensor

Precision optical elements are used in a dual-wavelength IR spectrometer that measures CO_2 concentration in air. Accuracy is ± 5 percent, response time is instantaneous, and interference from oxygen, nitrogen, or water vapor is less than 0.5 percent. Power consumption is low, and the device has no moving parts. The instrument uses two wavelengths: one absorbed by CO_2 and the other not. Differences in optical absorbance by the sample are detected and processed electronically to generate a display of CO_2 concentration.
(See page 370.)

Frame for Daylight Photocopying

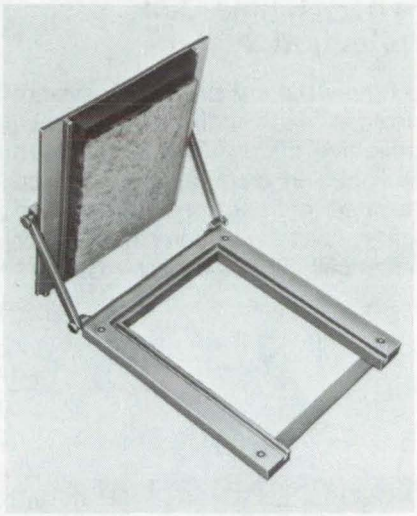

An inexpensive frame can be used with Polaroid (or equivalent) film to copy film negatives or positives without a darkroom. The photo to be copied is placed over a light source, the frame is loaded, and the tab is removed from the film. After exposure, the tab is reinserted for development.
(See page 438.)

Molecular Beam Generator

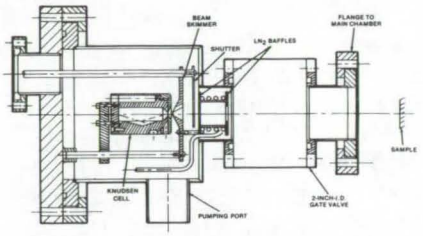

Vacuum deposition techniques formerly limited to metals, oxides, and certain dielectrics can be carried out with heavy organic molecules. A molecular beam generator, developed originally for laboratory use, can deposit films at rates from 6 to 15 angstroms per minute. The apparatus includes a nozzle and aperture especially designed for large organic molecules.
(See page 380.)

Battery Single-Cell Protection System

A new battery protection system provides each cell with its own protective circuit. The circuits are packaged in modules that can be mounted on each cell or on the battery case. A comparator, for each cell, continuously monitors voltage; when prescribed high or low limits are exceeded, a bypass removes the cell from the circuit. When the cell voltage returns to normal, the bypass is removed, during either the charge or discharge mode. Since no cell can be driven beyond the set voltage limits,

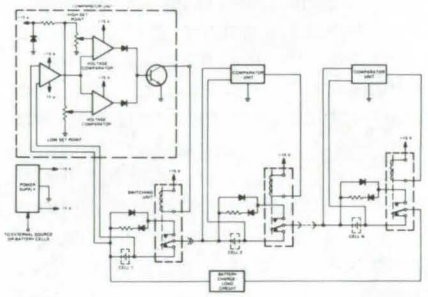

this system will extend the life of the battery. It also allows deeper discharge of the battery without cell reversal, allowing a smaller and lighter battery, equipped with the protection circuit, to be used in place of a larger battery.
(See page 328.)

Quartz-Crystal-Oscillator Hygrometer

A new dewpoint hygrometer uses a quartz-crystal oscillator to measure the dewpoint and thus the humidity of a gas. It is more accurate than psychrometers and hair hygrometers, and it could be less expensive to manufacture than optical dewpoint-condensation hygrometers. The new hygrometer requires no calibration, and its output is an electronic signal produced upon a change in frequency of an oscillating quartz crystal. In addition to meteorological and laboratory applications, this instrument is ideal for the hundreds of automatic processing and environmental-control applications requiring knowledge or control of humidity. It is small, requires no human observation or operation, and has an electrical output that could be digitized and integrated with most any type of processing equipment. In addition, it could be used to measure "dewpoints" of vapors other than water, as required in many chemical processes. The principle of operation is simple. An oscillating quartz crystal is heated or cooled until moisture begins to condense on its surface. This occurs at the dewpoint, and the condensation causes a shift in the crystal oscillating frequency that can be detected by relatively simple circuitry.
(See page 375.)

PATENT LICENSES RECENTLY GRANTED BY NASA FOR COMMERCIAL USE OF NASA-OWNED INVENTIONS

The patent licenses listed below have been recently awarded by NASA as part of its program to encourage the commercial application of its new technology. For information on how you may obtain nonexclusive or exclusive license for the commercial use of NASA inventions, see page A8 of this issue.

A nonexclusive license to Varian Associates, Palo Alto, California, for U.S. Patent No. 3,869,624, covering an invention entitled "Peak-Holding Circuit for Extremely Narrow Pulses."

A nonexclusive license to Lumidor Products Corporation, Miami, Florida, for U.S. Patent No. 3,895,912, covering an invention entitled "Carbon Monoxide Monitor."

An exclusive license to Owens Enterprises, Incorporated, Wilmington, California, for U.S. Patent No. 3,915,148, covering an invention entitled "Thermostatically Controlled Non-Tracking Type Solar Energy Concentrator."

Electronic Components and Circuits

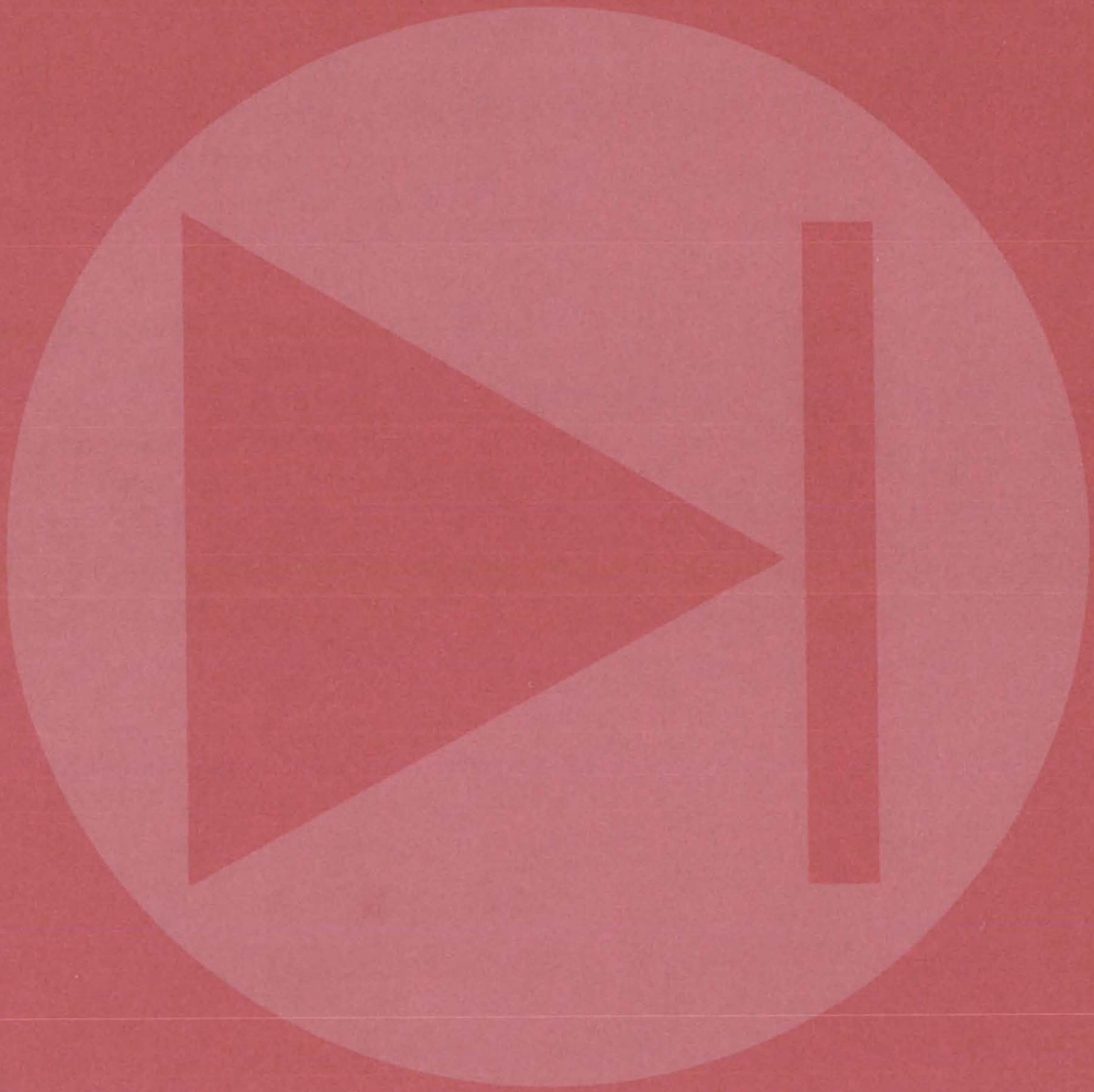

A Nonsaturating DC-to-DC Parallel Power Converter

The elimination of collector-current overlap avoids component damage from transients.

Goddard Space Flight Center, Greenbelt, Maryland

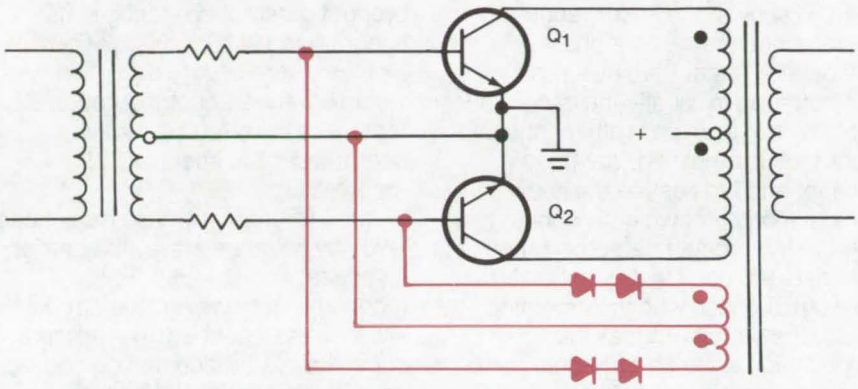

CONVERTER WITH FEEDBACK COMPENSATION

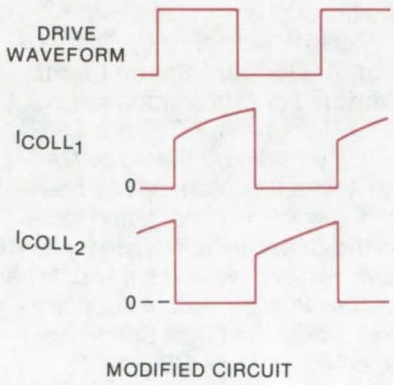

MODIFIED CIRCUIT

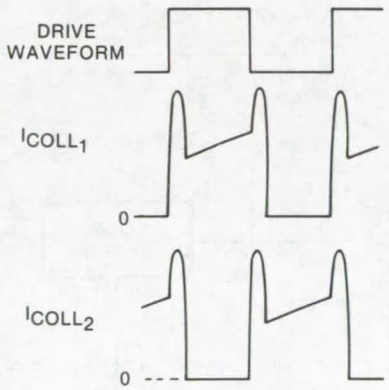

CONVENTIONAL CIRCUIT

The Improved DC-to-DC Converter is essentially a conventional circuit modified with a pair of diode rectifiers coupled to the switching transistors via a feedback winding. As can be seen in the waveforms above, the collector-current overlap between transistors is eliminated in the new circuit. This technique may be used with nonsaturating parallel-transistor converters operating from a voltage source which remains fixed or varies over a small range.

A modified dc-to-dc power converter eliminates collector-current overlap that causes transients due to the stored charge in the base-emitter junction of the 50-percent duty-cycle switching transistors. This improvement is especially useful at high-switching frequencies, where such transients are a common cause of component damage and excessive electromagnetic interference. In addition, this circuit is efficient, reliable, and self-adjusting under varying loads.

The circuit (see figure) has a center-tapped low-voltage feedback winding on the converter transformer primary. The ends of this winding are connected, through two series-connected fast-recovery rectifiers, to the bases of the converter transistors. The center tap of the feedback winding is common with the center tap of the base drive winding.

The feedback winding prevents the application of base drive from the drive transformer to turn on the off transistor until the conducting transistor turns fully off. This is accomplished by shunting the base drive through the feedback winding, thus preventing drive from being applied to the off transistor. The diodes allow only turnoff currents to flow from the bases. The feedback-winding voltage reverses polarity when either transistor collector comes out of saturation (which indicates charge depletion in the base-emitter junction). This reversal of polarity allows the off transistor to receive base drive from the drive winding.

Other advantages of this circuit are as follows:

a. The exact amount of stored charge is accounted for instead of a certain maximum amount which could result in current transients at lighter loads and reduced efficiency at full design load.
b. There are no critical resistor values, there is no interdependence of design parameters, and there are no excessive peak currents or excessive base-emitter reverse voltages.
c. Circuit complexity is minimized with good efficiency, reliability, and low EMI (electromagnetic interference).

This work was done by Thomas LaVigna of **Goddard Space Flight Center** *and Gale Gant and Lawrence Jan of Xerox Corp. No further documentation is available.*
GSC-12047

A Linear Phase Demodulator

A phase demodulator with a linear operating region of ± 150° and the ability to demodulate suppressed carrier signals

Goddard Space Flight Center, Greenbelt, Maryland

Phase demodulators generally have had at least one of two disadvantages: Either their linear operating region is limited to about ±50° or they will not lock to the input signal spectrum if it does not contain a carrier component.

A proposed linear phase demodulator circuit operates on a feedback principle to reduce the modulation index of the received signal, and thus reinserts a carrier component in the suppressed carrier signal. It can demodulate phase-shift-keyed (PSK) signals which do not have a carrier component, and it has a linear region of ±150°.

A block diagram of the demodulator is shown; the linear range is determined mainly by a phase modulator rather than by a product detector, as is usually the case. The data output from an ordinary phase-lock loop is amplified, reversed in phase, and fed back to the linear phase modulator which is connected before the product detector. Since the data fed back to the modulator are out of phase with the incoming data, the circuit reduces the modulation index and restores some of the sideband power to the carrier. Therefore the loop can lock to signals which have no carrier power prior to the phase modulator.

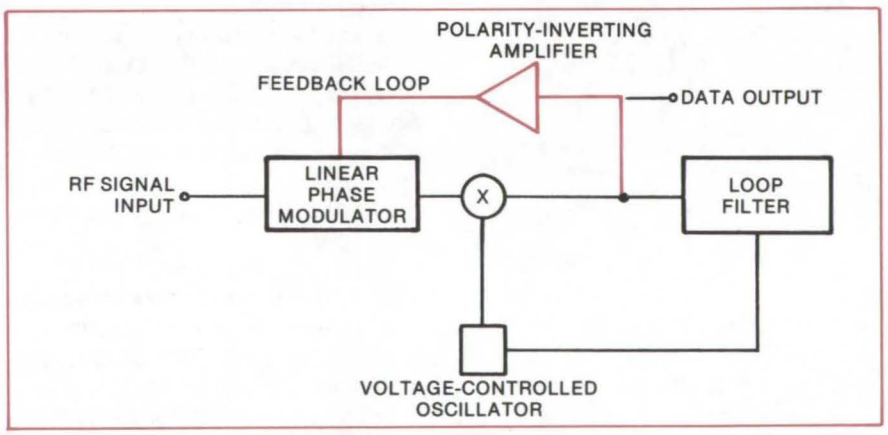

The **Linear Phase Demodulator** is shown with the components that must be added to a conventional phase-lock loop to obtain linear performance in color.

The loop tends to keep the product detector operating in its linear region at high modulation indices where severe distortion would otherwise occur. Another feature of the circuit is that it compresses the spectrum of the received signal.

If the RF input is phase modulated ±90° by a square wave, the carrier disappears completely (PSK modulation); however, the circuit will lock as described. The amount of carrier restoration can be controlled by adjusting the gain of the feedback amplifier. The circuit can also be used to detect biphase and quadriphase modulation.

This work was done by Ronnie R. Rippy of **Goddard Space Flight Center.** *For further information, Circle 1 on the TSP Request Card.*

This invention is owned by NASA, and a patent application has been filed. Inquiries concerning nonexclusive or exclusive license for its commercial development should be addressed to the Patent Counsel, Goddard Space Flight Center [see page A8]. Refer to GSC-12018.

Fluorescent Dimming Ballast

A high-frequency inverter and a saturable inductor control a fluorescent lighting system.

Lyndon B. Johnson Space Center, Houston, Texas

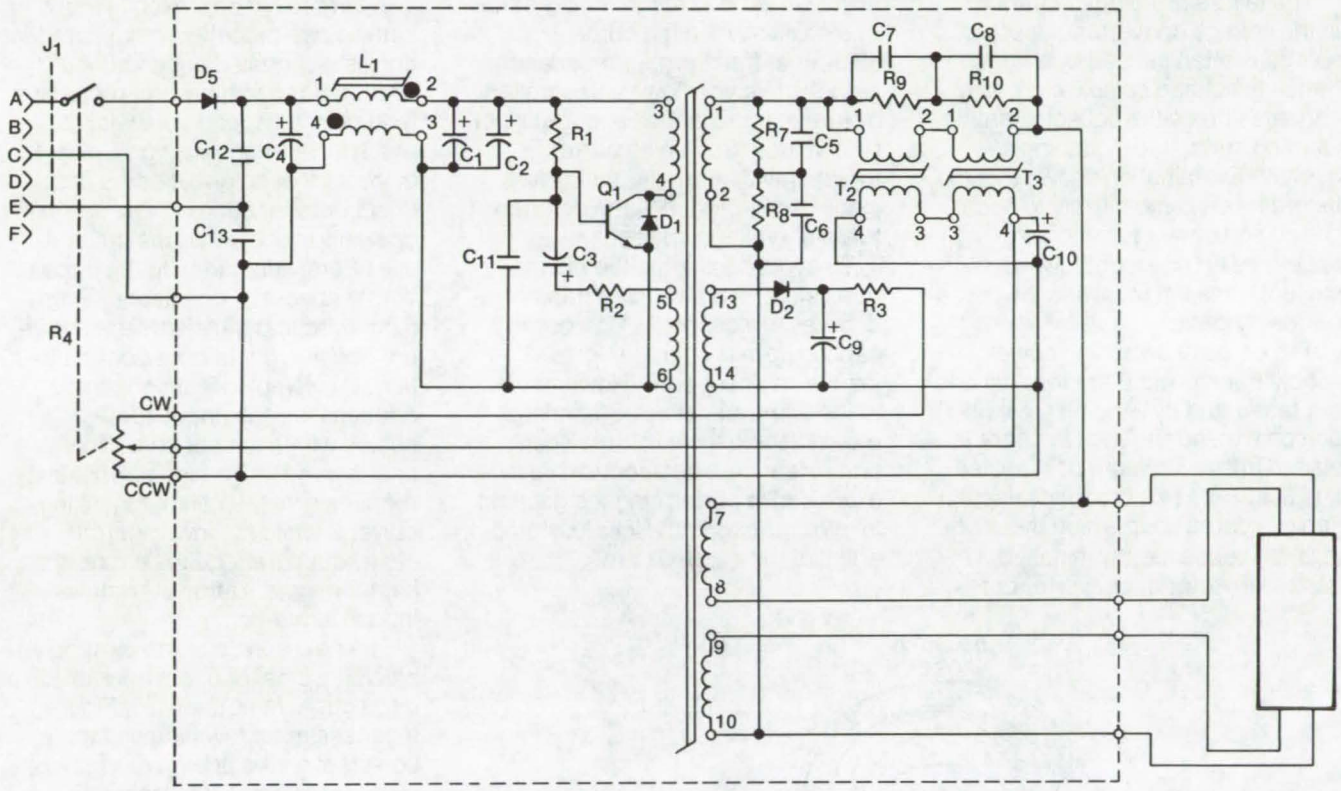

The **Control Circuit** for fluorescent lights has two inductors. By reversing one of the four windings, the energy present in one set of windings does not appear across the other; and a very small dc control current passing through one set of windings can saturate the magnetic material in both cores and change the impedance of the controlled path. Lamps can operate from about 2 percent full brightness up to 100 percent.

A magnetic amplifier approach has been adapted for dimming fluorescent lights operating from a 20-kHz power supply. Filament power is unaffected, and only the ballast is controlled.

Other advantages of this circuit approach are:

- No significant circuit changes are required, as the magnetic amplifier appears simply as a variable inductance.
- Few circuit elements are needed, efficiency is high, temperature stability is good, and the circuit can withstand large overloads and transients without failure.
- At the 20-kHz operating frequency small magnetic cores can achieve the desired impedance.
- There is no electromagnetic interference because the switching of the magnetic material is slow.

A small dc bias (see figure) is applied to the saturable inductors that control the ac signal, changing the effective inductance. Two magnetic elements are employed (T_2 and T_3) to act on both ac polarities, and one set of windings is connected in opposition to isolate the power and control paths. None of the ac lamp power appears in the control circuit, resulting in high efficiency. A high-current transistor is used for fast switching, and a small value of inductance is used to get the required minimum brightness.

The brightness control is operated at a low power level and is isolated from the primary lighting circuit. It governs the dc control current to the magnetic amplifier, which is obtained from a small impedance-matched supply (D_2 and C_9). R_4 has a logarithmic dimming-to-rotation correlation with a linear potentiometer. This is desirable as human visual response is approximately logarithmic. The dimming performance is excellent, and brightness control is stable and repeatable.

This work was done by Paul Lutus of ILC Technology for **Johnson Space Center.** *For further information, Circle 2 on the TSP Request Card.*
MSC-14937

Toroidal Converter Core

The protection of a gap core is combined with the low-current requirement of a cut core.

Caltech/JPL, Pasadena, California

The failure of switching transistors in the voltage converter of a power source is often caused by a large transient voltage spike which appears across the collector-emitter junction during the switching sequence. Examination shows that the failure mode is most likely to occur during equipment turn-on and appear as an unexpectedly-large current transient following the first switching cycle.

The cores of switching power supply transformers are toroidal and are fabricated by winding steel ribbon on a mandrel. Then the core is placed in an aluminum box, sealed, and fluidized. This produces uncut gapless cores upon which the windings are subsequently installed. Ungapped inverter or converter cores, however, tend to magnetically saturate easily. When the core saturates, transformer impedance reduces to a very low value, limited by circuit impedances and transistor beta values. Such high current, together with normal transformer inductance, produces the destructive high-voltage spikes.

To avoid destroying the driving transistors, the switching transformer cores are gapped. Core loss in a gapped core is not much greater than in an uncut core. However, due to the characteristics of magnetic materials and the very small gap size, great care and control must be exercised in performing the gapping to avoid affecting the low-loss properties of the gapped core.

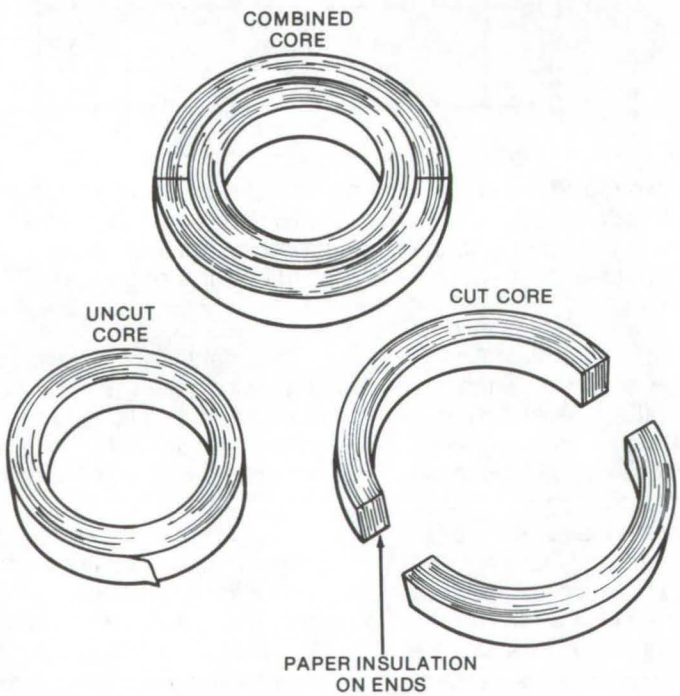

Figure 1. The **Cut/Uncut Toroidal Core** is made by combining two cores. The cores are made by winding steel ribbon on a mandrel and impregnating with epoxy to bond the layers together. The gap is made by cutting across a wound and bonded core. The rough ends are ground or lapped.

An improved approach is found in a new "two-piece" toroidal core that consists of nested cut and uncut sections. It combines the protective feature of a gapped core with the much lower magnetizing-current requirement of an uncut core. The uncut core functions under normal operating conditions; the cut core still offers inductance to the circuit during abnormal conditions. Thus, high switching transients are avoided. The cut/uncut core configuration is assembled in a concentric relationship: the uncut core is nested within the cut core. The uncut core, with a high permeability, requires a very small magnetizing current, while the lower-permeability cut core requires a much higher magnetization current to induce saturation.

The new core is made by simply placing a smaller uncut core inside a large cut core as shown in Figure 1. If necessary, a few wraps of the ribbon steel on the uncut core may be removed to make it fit inside the larger cut core. Both cores are coated with a thin layer of epoxy to round off the sharp corners and protect the insulation on the wire wrap. To provide uniform characteristics for the gapped core, a gap dimension of 1 mil (0.0025 cm) has been selected, since any variations produced by thermal cycling during manufacture will not affect this gap length greatly. The gap is obtained by inserting a sheet of paper or film material between the core ends during bonding.

The cores are normally made of nickel steel, a relatively expensive material. However, the desired features of the composite core can be obtained more economically by using different materials, such as silicon steel, for the cut and uncut portions of the core. A comparison

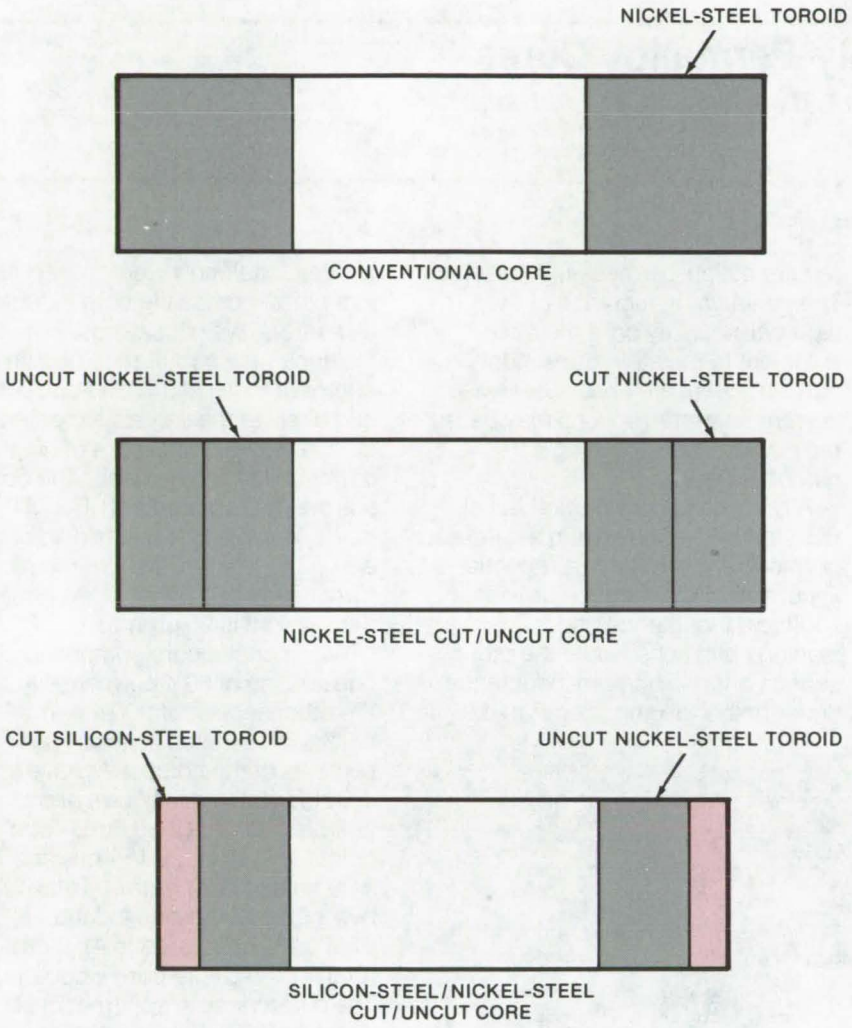

Figure 2. A **Comparison of Core Configurations** shows the relative amounts of material required for cores of substantially the same properties.

Fabrication and Applications of Electrets

Electrets, permanently charged dielectrics, can be made less expensively, faster, and more effectively with several new techniques. The electrets can be made in a much shorter period of time by using a high-voltage corona spray to charge the dielectric. New methods include charge injection, Tesla-coil charging, and molten spray. Electrets of increased strength can be made from Teflon, polyethylene, Mylar, and polycarbonates. Other, new, electret materials include quartz and single crystals. New applications include filters and particle collectors.
(See page 460.)

Reduced Costs for Solar-Cell Modules

Solar-cell production costs are reduced by embossing the encapsulating plastic film to position and secure the cells. The electrical circuit is printed on the plastic film at the time the cells are encapsulated. The process can be used with standard-contact and wraparound-contact cells.
(See page 458.)

Time-Domain Reflectometry for Cable Fault Isolation

Time-domain reflectometry (TDR) has been adapted to the detection of multiple-cable faults. Faults can be isolated at specific splices in multiple cables. If the multiple cable displays classical lumped circuit characteristics, inductance and resistance parameters will remain relatively constant over the cable length; capacitance and conductance will change at each splice. Knowing the approximate distance to splices, a functional wire in the bundle can be used to find the TDR length. The actual distance may be determined when a faulty splice is displayed on the TDR cathode-ray screen.
(See page 411.)

of various cores are shown in Figure 2. Silicon steel has a higher flux density than the nickel steel, and it can be seen that less silicon steel is required for a composite core in which the silicon-steel portion is the gapped section.

This work was done by Colonel W. T. McLyman of **Caltech/JPL.** *For further information, Circle 3 on the TSP Request Card.*

This invention is owned by NASA, and a patent application has been filed. Inquiries concerning nonexclusive or exclusive license for its commercial development should be addressed to the Patent Counsel, NASA Resident Legal Office-JPL *[see page A8].* *Refer to NPO-13413.*

Composite Stacked Moly-Permalloy Cores

Core size can be reduced using a composite core.

Caltech/JPL, Pasadena, California

The inductive value and resultant physical size of moly-Permalloy powder cores (used in inductive energy-storage power conversion circuits) are presently based on the tradeoff between minimum load conditions placed on the supply and the periods of heavy current demand. The minimum value of inductance is chosen to limit the peak collector current of the switching transistors. Supplies subjected to heavy dc loading require low-permeability cores which require higher currents to saturate, but supplies subjected to light loading require a high-permeability core. The minimum inductance of the high-permeability core must be sufficient to maintain transistor current flow at all times. Otherwise current flow interruptions may cause the power supply to deregulate output voltage.

A composite core comprised of two sections, each having a different permeability, results in a reduction in core size. One section provides sufficient inductance under light loading conditions, while the other section offers minimum inductance under heavy loading. Compared to conventional moly-Permalloy core inductors, composite core inductors also offer a weight savings. For instance, in a circuit requiring an inductor of 1 mH at full load current and 6 mH at the lightest expected load, a conventional core of 60 μ permeability can be used. The core has an inside diameter (I.D.) of 0.95 in. (2.41 cm) and an outside diameter (O.D.) of 1.57 in. (3.98 cm). Core height is 0.57 in. (1.44 cm); bare weight is 90 grams.

A composite core comprised of one section of 60 μ permeability and the other section of 300 μ permeability can be used instead. Both sections of the composite have an I.D. of 0.58 in. (1.47 cm) and an O.D. of 1.06 in. (2.69 cm). Total height is 0.44 in. (1.11 cm), and bare weight is 72 grams. Total cubic bulk of the composite inductor is 27.4 cm^3, compared to 41.6 cm^3 total for the single-core inductors. The differences in apparent bulk between the two core types are illustrated.

This work was done by Colonel W. T. McLyman of **Caltech/JPL.** *For further information, Circle 4 on the TSP Request Card.*
NPO-13578

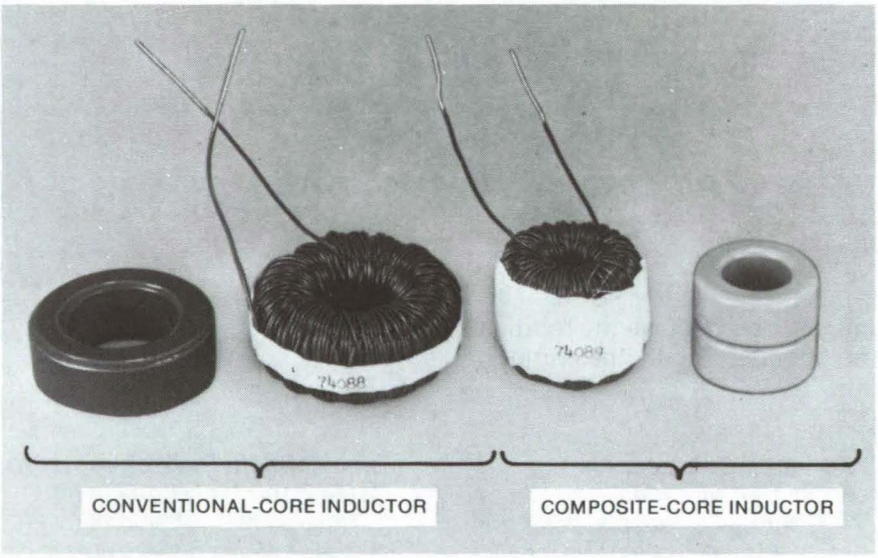

A **Comparison of Cores** shows the reduction in size possible with the composite core. The core (shown with and without windings) on the left is a conventional one. On the right is a composite core.

Band-Elimination Filter

A helical resonator is employed to produce a stable highly-selective band-elimination filter.

Marshall Space Flight Center, Alabama

In receiving systems, it is often a requirement to receive frequencies above and below a strong undesired center component. Therefore it is important to be able to attenuate undesired frequency components at the receiver end of a system. A technique for attenuating a 24-MHz signal component (in an optical radar system), while distorting other desired components as little as possible, uses a multistage stagger-tuned notch filter with a helical resonator as the frequency-controlling element.

Some features of the filter are the following:

- High selectivity
- Controlled bandwidth by cascading identical stages and stagger tuning
- Adjustable notch depth
- Good isolation between stages
- Gain set by proper choice of resistors
- Spurious responses eliminated
- Practical component values

The entire band-elimination filter consists of seven single-stage notch filters (one filter is shown in the illustration). The 60-dB (relative) bandwidth is 100 kHz, and the 3-dB (relative) bandwidth is 300 kHz. For greater bandwidth, several stages are cascaded and stagger tuned. Overall gain except for the filter "notch" was measured at 40 dB with a low-frequency cutoff at 2,500 Hz and a high-frequency cutoff beyond 50 MHz.

The helical resonators are the components critical to the performance of the band-elimination filter, and high-frequency assembly techniques must be followed in the fabrication. Coil L_1 is wound on a paper form 1 inch in diameter and 1.75 inches long. A spiral groove with 18 turns per inch is cut in the form to receive AWG 22-gage magnet wire. The winding is started 0.5 inch from the bottom and is continued for 27 turns. The tap is brought out 4 turns from the bottom.

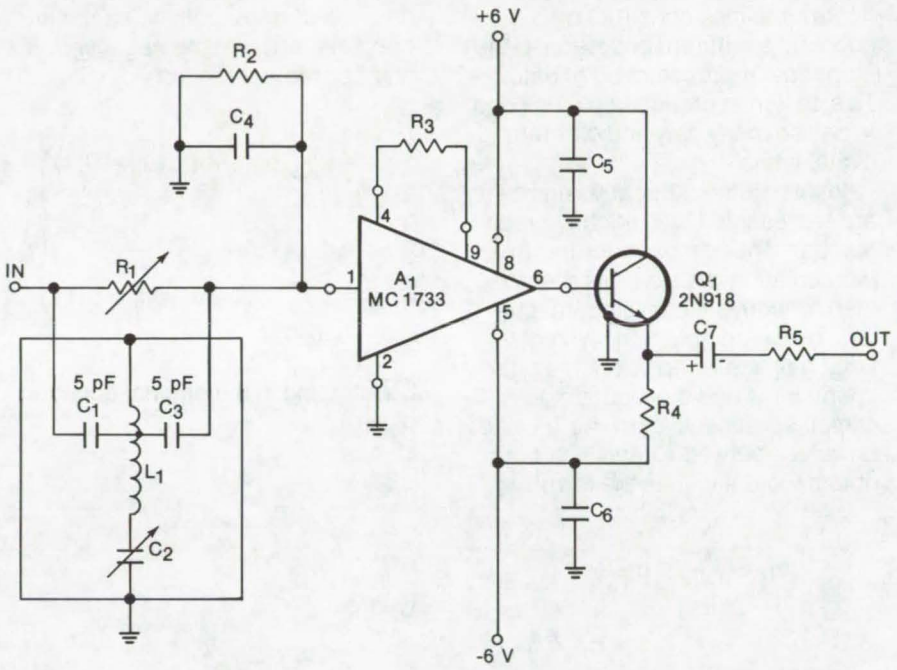

A **Single-Stage Notch Filter** is composed of components R_1, L_1, C_1, C_2, and C_3. Amplifier A_1 and Q_1 serve as wideband gain elements. Resistor R_3 is used to set the overall stage gain. Capacitor C_4 and resistor R_2 establish the high-frequency cutoff. Resistor R_2 provides a dc return for A_1 and an impedance match for the filter at the notch frequency. Q_1 is required if the stage is required to drive a cable or if a voltage output greater than about 250 mV is desired.

The outer shell is made from 2-inch-diameter copper tubing 2.5 inches long. A feedthrough solder terminal is soldered to the shell to receive the bottom end of L_1. Two press-in Teflon feedthrough terminals are mounted in the shell. Capacitors C_1 and C_3 are mounted from these terminals to the tap of the coil on the inside of the shell. Resistor R_1 is mounted to these terminals on the outside of the shell. Capacitor C_2 is mounted through the shell, and the ungrounded end is connected to the top of L_1.

The paper form and shell are fixed to the PC board. The shell bottom is grounded to and shielded by the ground plane of the PC board. The top of the shell is shielded so that the interaction between resonators is minimized.

This work was done by Glenn B. Shelton of Sperry Support Services for **Marshall Space Flight Center.** *For further information, Circle 5 on the TSP Request Card.*

Inquiries concerning rights for the commercial use of this invention should be addressed to the Patent Counsel, Marshall Space Flight Center [see page A8]. Refer to MFS-23303.

Counting Digital Filter

Radix (-2) is utilized for more efficient manipulation of data.

Caltech/JPL, Pasadena, California

A new basic concept for digital filters simplifies construction by adopting a different approach to the numerical representation of data. This design approach could be used to devise many new and different digital filters.

In this method, negative numbers are represented by a negative radix number. The hardware for this implementation is much less complex than for conventional sign/magnitude or 2's-complement systems. Letting a_i and x_i represent the filter coefficients and the input data samples, respectively, where i takes on values between 1 and K, an output word then has the form

$$y_m = \sum_{i=0}^{K-1} x_{m-i}a_i \qquad (1)$$

J_X bits are assigned to each input data word, and J_a bits to each filter coefficient. Using the negative radix number representation

$$\left.\begin{aligned} a_i &= \sum_{j=0}^{J_a-1} u_{ij}(-2)^j \quad (u_{ij}=0,1) \\ x_i &= \sum_{j=0}^{J_X-1} v_{ij}(-2)^j \quad (v_{ij}=0,1) \end{aligned}\right\} \qquad (2)$$

Substituting in the original equation gives

$$y_m = \sum_{r=0}^{J-1} h_r(-2)^r \qquad (3)$$

where

$$J = J_a + J_X - 1$$

$$h_r = \sum_{j=0}^{K-1} \sum_{i=0}^{J_a-1} u_{ji}v_{m-j,r-1} \qquad (4)$$

or, rearranging via the polynomial algorithm

$$y_m = (\ldots(h_{J-1}(-2)+h_{J-2})(-2)+\ldots+h_1)(-2)+h_0 \qquad (5)$$

Equations (4) and (5) embody the basic strategy of the proposed machine. Each element of the double sum in (4) is a product of two 1-bit entities. Such a product is either 0 or 1, and practically speaking, no multiplication is involved in its evaluation. A dual input AND gate is all that is needed. Equation (4) is a summation of KJ_a such terms. Thus, if we design a system in which KJ_a dual input gates are fed by the pairs

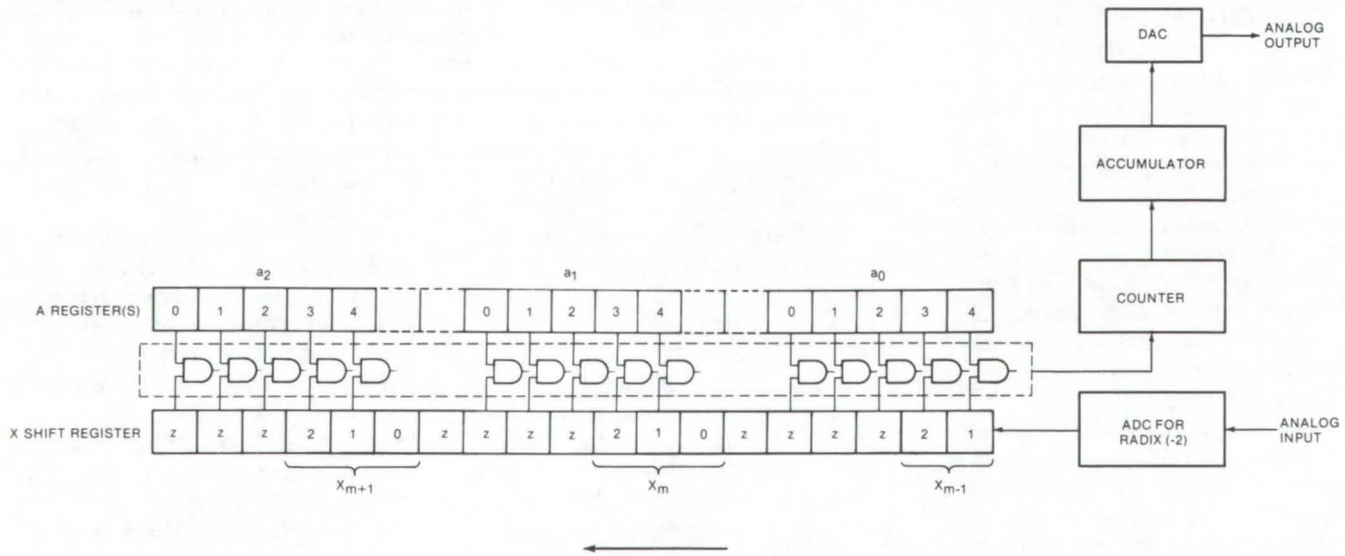

The **Counting Digital Filter** has four basic elements: (1) A fixed register (A) holds the coefficients a_i prescribing the filter transfer function. Its contents normally stay fixed throughout a specific filter simulation. They may, however, be varied in the course of the filtering to realize an adaptive filter. (2) A shift register (X) holds the input words x_i. These are fed in on the right, one bit at a time. The A and X registers are cross-linked by AND gates. (3) A counter computes the number of TRUE gates after every shift of register X. Each such count equals a specific h_r. (4) An accumulator combined J counter outputs through a shift-and-add sequence to generate the output word y_m.

of bits specified in (4), a count of the number of TRUE gates will equal h_r.

The realization of (5) can now be carried out in the following sequence of operations in an accumulator: shift, change sign, add, shift, etc. Both the counter and the accumulator are standard positive radix devices, and the output y_m is obtained in positive binary representation.

The a_j's are usually computed on a general-purpose binary computer. Their negative binary representation can be obtained by incorporating in the coefficient program a subroutine converting from positive binary to negative binary representation.

The overall design of the filter is shown in the figure. The negative radix converter is combined with the ADC in a single functional unit that directly converts the analog input to its negative binary representation.

Implementations of this design approach are described in further articles in this issue: "Circulating-Lines Digital Filter" (NPO-11831), "Partitioned Counting Digital Filter" (NPO-11832), and "Hybrid Digital-Analog Implementation of Digital Filters" (NPO-11833).

This work was done by Shalhav Zohar of **Caltech/JPL.** *For further information, Circle 6 on the TSP Request Card.*

This invention has been patented by NASA [U.S. Patent No. 3,732,409]. Inquiries concerning nonexclusive or exclusive license for its commercial development should be addressed to the Patent Counsel, NASA Resident Legal Office-JPL *[see page A8].* *Refer to NPO-11821.*

Circulating-Lines Digital Filter

Costs are lowered by allowing speed reduction.

Caltech/JPL, Pasadena, California

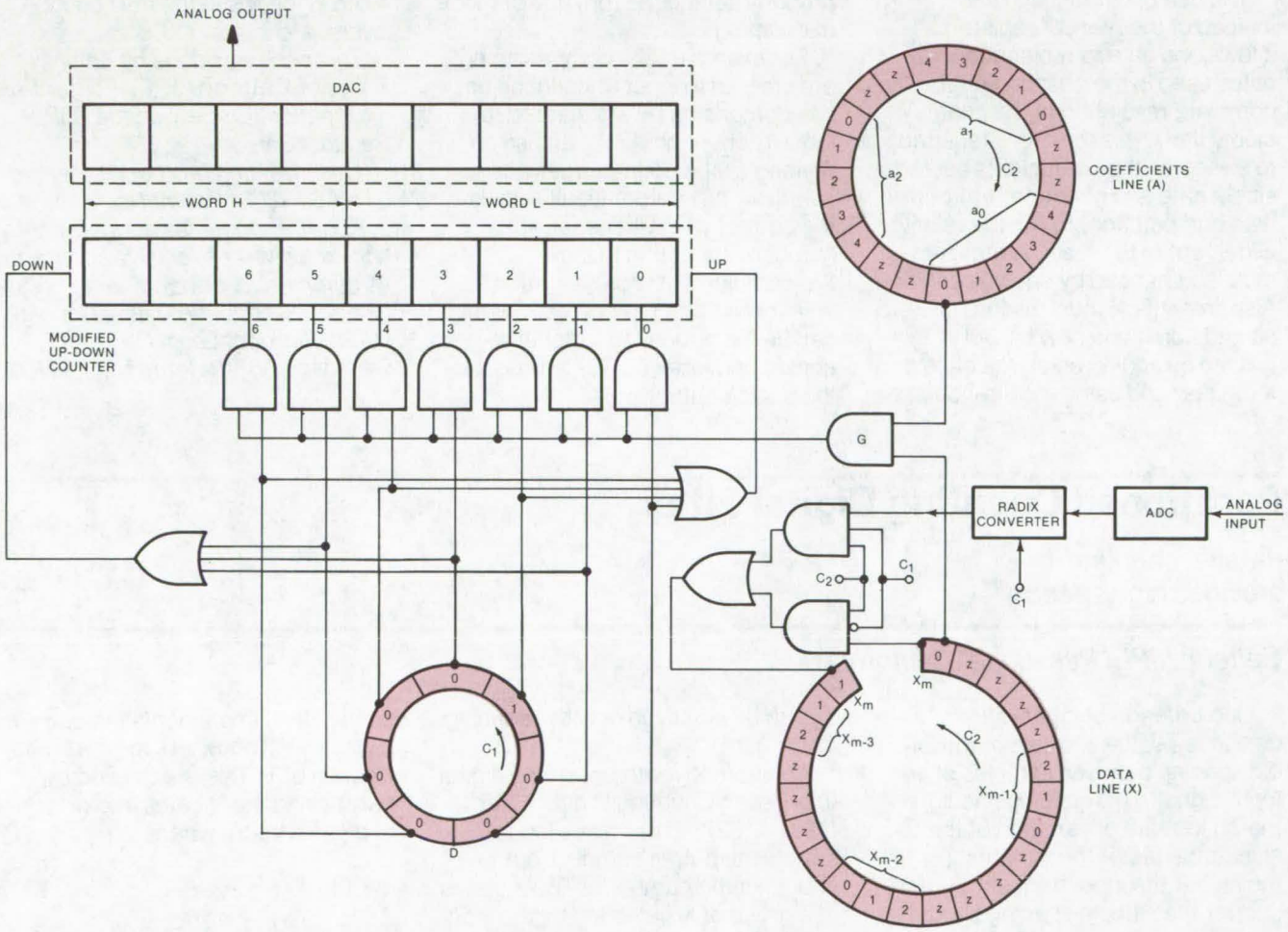

The **Circulating-Lines Digital Filter** has an array of line segments of various lengths which may be switched into the circulating lines by the machine operator. The flexibility and possibilities of such an arrangement are quite attractive yet may be obtained with a relatively modest investment in hardware.

The circulating-lines digital filter was designed for cases where filter speed is not critical; by sacrificing speed, the filter can be made at a much lower cost. It is a version of the counting digital filter described in the previous article: "Counting Digital Filter" (NPO-11821). Thus, terms and symbols which are not explained here are defined there.

In the counting digital filter, data words are fed into the X register with the most significant bits first. This means that the h_r's are computed in the time sequence h_{J-1}, h_{J-2}, ..., h_0. In the present case, it is more convenient to feed the least significant bits first, generating the h_r's in the time sequence h_0, h_1, ... h_{J-1}. Since serial analog-to-digital converters (ADC's) produce the most significant bit first, this sequencing means that it is necessary to wait for the complete conversion of a word prior to using any of its bits.

The use of circulating lines instead of the A and X registers allows one gate to replace the KJ_a gates used in the counting filter. One complete revolution of the coefficients line, A, is therefore required to sweep all the coefficients past the single gate and generate h_r. For the next computation, h_{r+1}, the relative alinement of the X and A registers must be changed by one bit position. Also, register X must discard one old bit and admit one new bit. All of this is done by adding an extra cell to the X register and using the flip-flop implementing it to inject new data bits.

The filter is shown in the figure. The input to the extra cell of the X register is routed, by using three gates controlled by clock sequences C_1 and C_2. Clock C_2 steps the circulating lines, while clock C_1 controls the serial radix converter and hence the rate of feeding new bits.

A modified up/down counter counts the "true" outputs of gate G to obtain h_r and the output word y_m. Unlike the standard up/down counter, there are inputs to all bit positions. This is permissible because the bit rate is low and only one input is activated at a time. Thus, rather than counting (up or down) by ones only, this counter can count by any power of 2. The output word y_m is constructed by steering the sequence of bits from gate G to the proper input terminal and by properly setting the (up/down) mode of counting.

For example, bits comprising h_0 are steered to input 0, counting up; bits comprising h_1 are steered to input 1, counting down; and so on. As long as the counter does not overflow, this automatically yields the correct y_m, with negative numbers appearing in their 2's-complement representation. This means that the counter output can be fed directly to a digital-to-analog converter (DAC) to produce the analog output.

The output of gate G is directed to the proper counter input by circulating-line D, which has J cells. One cell is set to 1, and the rest are set to 0. Being controlled by clock C_1, line D automatically enables bit r input when the bits comprising h_r are coming out of gate G. Circulating-line D also controls the up/down mode by the use of two OR gates.

Final output is transferred to the DAC, without interrupting the input data flow, by segregating the counter flip-flops into words L and H as shown in the figure. Data from these two words are transferred at different times. Word L is copied out when the gate connected to the lowest bit of word H is activated. Zeroing of word L follows in the next count cycle. Word H is copied out immediately after its assembly is complete, that is, at the same time the first bit of the next filter-output word enters the counter. Zeroing of word H follows in the next count cycle.

This work was done by Shalhav Zohar of **Caltech/JPL.** *For further information, Circle 7 on the TSP Request Card.*

This invention has been patented by NASA [U.S. Patent No. 3,732,409]. Inquiries concerning nonexclusive or exclusive license for its commercial development should be addressed to the Patent Counsel, NASA Resident Legal Office-JPL *[see page A8].* *Refer to NPO-11831.*

Partitioned Counting Digital Filter

Parallel counting provides high speed.

Caltech/JPL, Pasadena, California

One criterion of digital filter design is T_S, the shortest permissible spacing between samples of an input signal. This spacing should match the rate of variation of the signal; the faster the variation (or the higher the input frequency), the shorter the sample spacing should be. In present designs, T_S almost equals T, the time it takes to compute an output sample. Hence, a low T_S can be achieved only by reducing T.

An alternative, the counting digital filter [see "Counting Digital Filter" (NPO-11821) in this issue], constructs the output sample from counts of the number of TRUE states of a group of N gates fed by the input and coefficients bits. The partitioned counting digital filter, which is a high-speed variation of the counting digital filter, implements the count in a way which allows T_S to be a small fraction of T. This is achieved by partitioning the N gates into groups of q gates each, where

$$q = 2^r - 1 \quad (r = 2, 3, \ldots)$$

and counting all of these groups in parallel (simultaneously). The elementary q-bit counters can be very

fast. This is particularly so when q = 3, in which case the elementary counter is essentially the well-known full adder.

While the result of such an operation is not the final count and has to be processed further by repeated implementation of partitioned counting, the initial set of q-bit counters is ready to process the next bit as soon as its outputs have been transferred for further processing.

The large number of elementary counters required means that the investment in hardware is quite high. However, the resulting speed increase is significant. Thus, the speed increase over the single-counter method is given by the factor $(N+1)/2q$. For large N and small q ($q_{min} = 3$), this factor may be quite large.

This work was done by Shalhav Zohar of **Caltech/JPL.** *For further information, Circle 8 on the TSP Request Card.*

This invention has been patented by NASA [U.S. Patent No. 3,732,409]. Inquiries concerning nonexclusive or exclusive license for its commercial development should be addressed to the Patent Counsel, NASA Resident Legal Office-JPL [see page A8]. Refer to NPO-11832.

Hybrid Digital-Analog Implementation of Digital Filters

Lower precision
allows higher speed.

Caltech/JPL, Pasadena, California

The hybrid device described here is a modification of the counting digital filter [described earlier in this issue in the article "Counting Digital Filter" (NPO-11821)] permitting a new set of tradeoffs. The speed of the counter in the counting digital filter is a major design parameter. Fine control of the usual cost/speed tradeoff is exercised through this parameter. In the hybrid device, high speed is obtained not through higher cost but rather through lower precision. This is mainly effected by substituting an analog device for the digital counter.

The device is shown in the figure, in which the A register holds the filter coefficients a_i. It can be shown that the filtered output sample y_m is given by

$$y_m = \sum_{r=0}^{J-1} h_{mr}(-2)^r$$

in which h_{mr} is simply a count of the TRUE gates in the figure and J is about double the number of bits per word. Each gate controls the analog switch shown below it (closed when TRUE). Switch S_0 feeds the resistor network with a voltage proportional to $(-2)^r$. With h_{mr} of the switches closed, the current through point Q is proportional to $h_{mr}(-2)^r$.

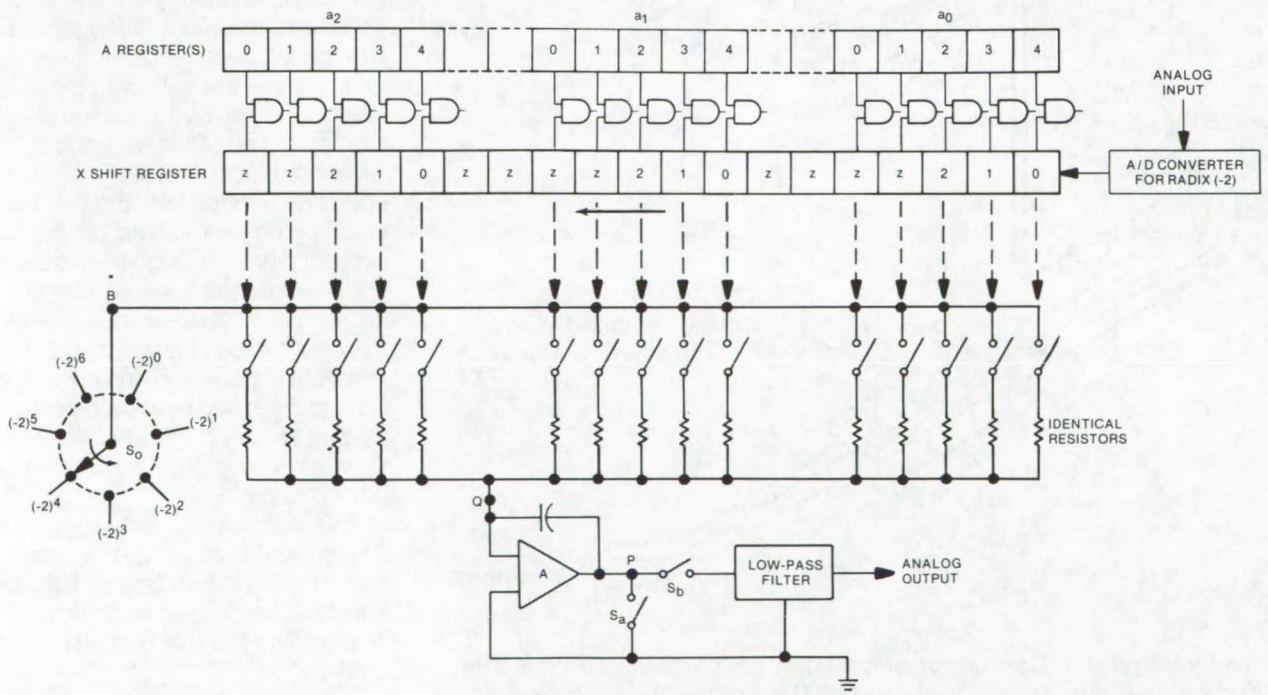

The **Hybrid Digital-to-Analog Filter** as shown above illustrates the general principles of operation. The switches shown, for instance, refer to logic-controlled semiconductor devices.

Switch S_0 is synchronized with the shifting of the X shift register, so that all J terms comprising y_m are generated sequentially as currents through Q. The integrator fed by these currents then performs the mathematical operation of summing (accumulating), so that when all J currents have been generated, the voltage at the integrator output point P is proportional to y_m. Switch S_b should then close momentarily, feeding the output low-pass filter with a pulse proportional to y_m.

The new cycle for the generation of y_{m+1} starts with the opening of S_b, momentary closing of S_a to discharge the integrator capacitor, and the feeding of the new sequence of J currents comprising y_{m+1}. While this design has a potential for very high speed, it should be realized that it suffers from the inherent lower precision of analog devices.

This work was done by Shalhav Zohar of **Caltech/JPL.** *For further information, Circle 9 on the TSP Request Card.*

This invention has been patented by NASA [U.S. Patent No. 3,732,409]. Inquiries concerning nonexclusive or exclusive license for its commercial development should be addressed to the Patent Counsel, NASA Resident Legal Office-JPL [see page A8]. Refer to NPO-11833.

Electrical-Splicing Connector

An inexpensive quick-connect splicer does not require removal of insulation.

Marshall Space Flight Center, Alabama

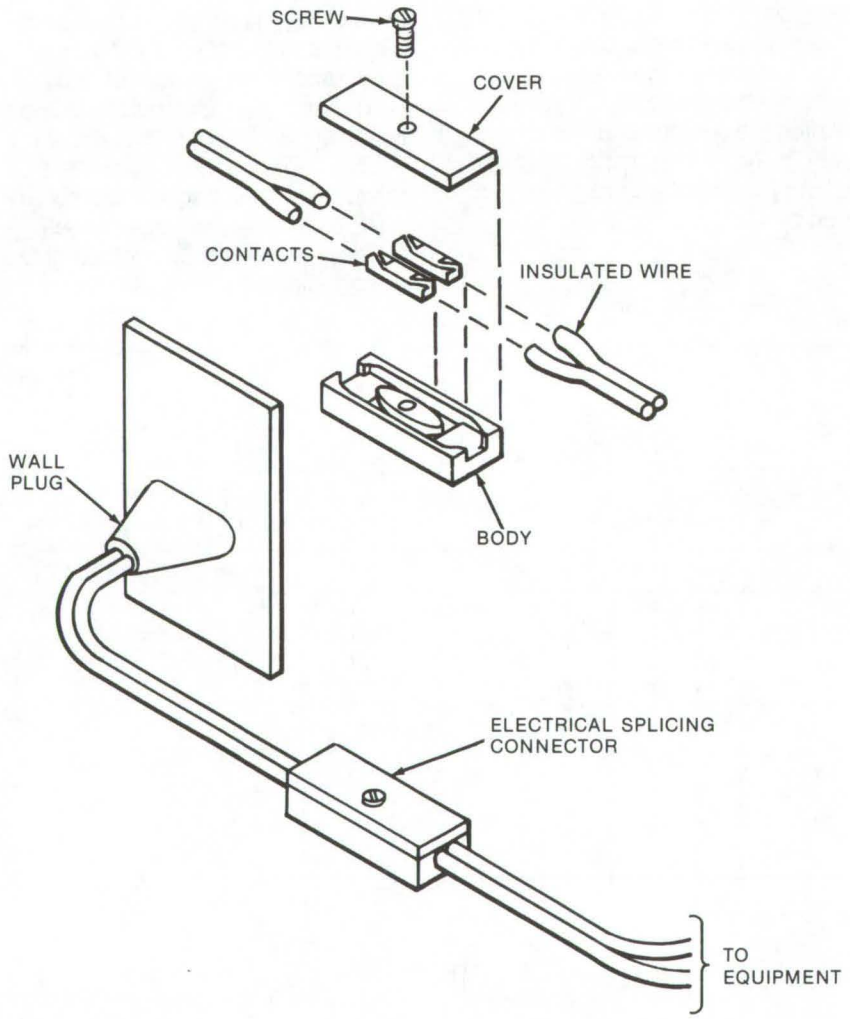

The **In-Line Splicing Connector** shown can be made in various sizes, depending on the intended application. The connection can be made without removing insulation, and the case insulates the splice.

When breadboarding a circuit, the technician can easily spend a disproportionate amount of time soldering and unsoldering leads and preparing splices as the design evolves. A quick-connect splicing connector can save him time, especially when he is working on prototype boards with several interconnecting test leads.

A quick-connect splicing connector offers a very simple method of splicing two wires together without having to remove the insulation and reinsulate with friction tape. To use the tool, both ends of the wires to be spliced are cut flush; the insulation is not removed. Both ends of the contact are opened, and the wires are placed inside. Then both ends are crimped until the double sharp prongs at each end of the contact pierce through the insulation and make contact with the conductor. At this stage the contacts and the wire can be placed into their respective grooves of the connector body and pushed down. Complete by placing the cover on top and threading the screw into the cover hole and down into the body.

This work was done by Eugene J. Stringer of Rockwell International Corp. for **Marshall Space Flight Center.** *For further information, Circle 10 on the TSP Request Card.*
MFS-24254

Foldback Current-Limiting for Hybrid Regulator

Power loss and temperature sensitivity are reduced.

Marshall Space Flight Center, Alabama

In high-current regulators it is usually very costly and inefficient to design the output transistor to handle rated current under short-circuit conditions. This problem is normally overcome by using a foldback current-limiting technique in which the load current is proportionally reduced as the regulator output voltage is pulled down by an overload condition.

Foldback current-limiting techniques in which readily-available integrated circuit (IC) regulators are used are well known, but they are not without disadvantages especially in high-current configurations. The magnitude of the short-circuit current is highly temperature sensitive since the foldback limiting point is controlled by the base-emitter voltage of the foldback-controlled current-pass transistor. Another disadvantage is the need for a high-wattage current-sensing resistor; short-circuit current flowing through the resistor forces the regulator to shut down, but it also produces a significant power loss at the rated load.

An improved foldback current limiting technique utilizes an operational amplifier to amplify and subtract the voltage across the current sensing resistor from the regulated output voltage as shown in the figure. The difference signal drives transistor Q1, which is connected to the compensation/shut-down terminal of the LM105 regulator. This terminal is internally connected to the base of the driver transistor in the LM105; hence, the regulator will shut down as base current is shunted away from the transistor and out through Q1. During normal operating conditions, the output of the amplifier is negative, and Q1 is turned off. As the load current is increased, the voltage across the current sensing resistor will increase, and the output of the amplifier will become positive, turning Q1 on and drawing drive current away from the LM105. This action reduces the current output of the regulator; consequently, the output voltage drops. The reduction in output voltages increases the amplifier output which further limits the output current. Hence, as the regulated output voltage drops due to an overload, the value of the output current is also proportionally reduced.

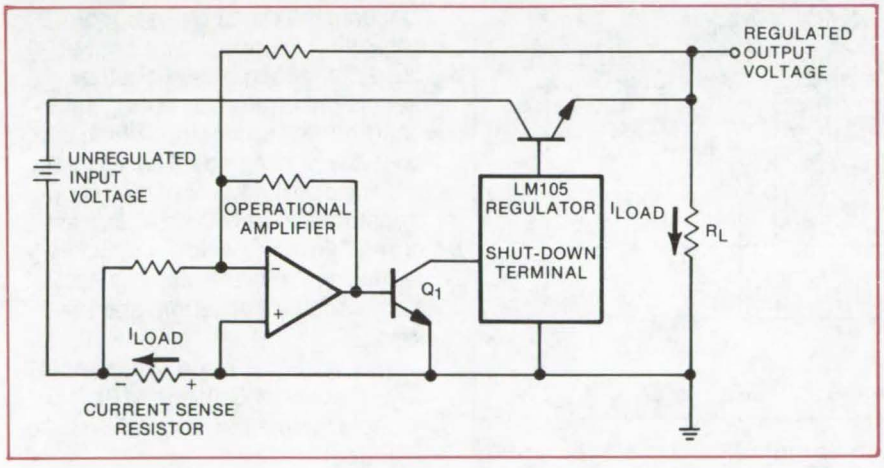

The **Foldback Current Technique** shown above was developed for a 6-ampere regulator utilizing an LM105.

Since a high gain amplifier is used in the current sensing feedback circuit, the temperature sensitivity of the short circuit current is greatly reduced. In addition, a relatively small current-sensing resistor may be used, eliminating the power loss problem found in conventional circuits.

This work was done by Chester H. Crider of IBM Corp. for **Marshall Space Flight Center.** *For further information, Circle 11 on the TSP Request Card.*

Inquiries concerning rights for the commercial use of this invention should be addressed to the Patent Counsel, Marshall Space Flight Center [see page A8]. *Refer to MFS-22995.*

Feedback Arrangement for Regenerative Switches

New arrangement for regenerative switches results in more reliable operation.

Caltech/JPL, Pasadena, California

Conventional regulators and dc converters used in regenerative switches are similar to those shown in the schematic, with the exception that feedback windings L_4 and L_5 are connected in series with the collectors of transistors Q_1 and Q_2 and primary L_1 of switching transformer T_2. In such arrangements the transistors associated with the primary of drive transformer T_1 control switching timing primarily, and the amount of base drive provided for transistors Q_1 and Q_2 is insufficient to pass on each switching action the amount of current required for typical loadings of the device. Additional base drive is provided by adding windings L_4 and L_5 to transformer T_1 and by connecting them to provide positive feedback or regenerative action.

This circuit has a disadvantage in that when first turned on, on initial transistor turnoff, the level of residual flux left in the transformer core varies randomly, so that on some occasions the core of transformer T_2 becomes saturated on the next transistor turn-on. Core saturation results in very low transformer impedance, and the current that can flow in the collector circuit is then limited only by other circuit impedances and transistor beta. Since this high collector current flow also passes through either winding L_4 or L_5 to provide regeneration, this high current flow, in conjunction with leakage inductance, results in the production of high-voltage spikes which could destroy the transistors.

Such occurrences can be prevented if the feedback arrangement is changed as shown in the schematic, in which windings L_4 and L_5 are in series with secondaries L_2 and L_3 of transformer T_2. When the core of transformer T_2 saturates, there can be no flux change; and hence no current flows in windings L_4 and L_5. The regenerative effect is lost until the core comes out of saturation. Hence the amount of current that can be switched by transistors Q_1 and Q_2 during such occurrences is only that which is possible with the small base drive provided by the primary circuit of transformer T_1. This provides fast current limiting, which is usually effective on the first switching cycle, to protect the transistors and the load.

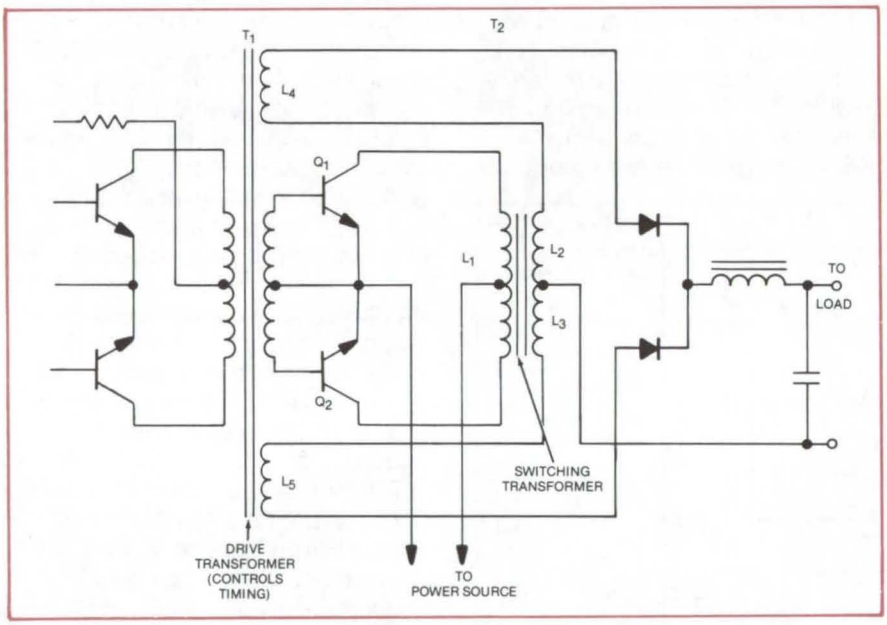

The **Load-Current Feedback Technique** samples load current instead of collector current. This makes it possible to operate the switching transistors at their maximum capacities for pulse loads.

This work was done by Colonel W. T. McLyman of **Caltech/JPL.** *For further information, Circle 12 on the TSP Request Card.*
NPO-13060

Low-Cost Pressure-Data Encoder

A simple method of linearly translating pressure variations to pulse-width changes

Caltech/JPL, Pasadena, California

Regenerative switches, used in conventional regulators and dc converters are similar to those shown in the schematic, with the exception new encoder, simpler and less expensive than its electromechanical counterpart, directs a digitally encoded signal to the radar transponder which, when queried, transmits the ship's altitude automatically.

The encoder output is linearly proportional to altitude. It compares a pressure-proportional voltage to an exponentially decaying voltage generated by a simple RC timing circuit. A pulse is thereby generated; pulse width is proportional to altitude. This pulse gates a counter which outputs a digital word in a specified altitude code to the transponder.

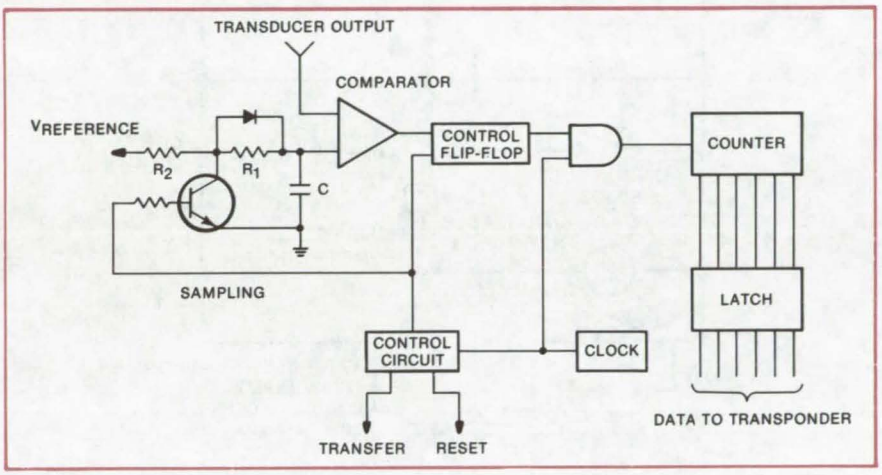

Comparator of **Altitude Encoder** is fed a fixed exponentially decaying pulse and a transducer output which is proportional to pressure. As altitude varies, comparator output pulse width changes similarly. The counter encodes the variable-width pulse in modified gray code for the radar transponder and in binary-coded decimal for the readout circuit.

A simplified schematic of the encoder is shown. The time constant generated by R_2 and C is less than one-tenth that of the sample time, to assure accuracy. The control circuit clocks the transistor which determines the charging rate of the capacitor. Comparator output is a pulse having a width determined by the transducer. The control circuit, besides sourcing a clock pulse to the sampling transistor, also controls the start of the counter. Total count is determined by pulse width.

This work was done by Richard B. Kolbly and Solomon R. Hedges of **Caltech/JPL.** *For further information, Circle 13 on the TSP Request Card.*
NPO-13692

Low-Voltage Motor Heater

A portable, automatic, and easy to use device for rapidly drying electric motors of varying sizes and voltages

John F. Kennedy Space Center, Florida

Because dampness can lead to premature motor failure, several methods are used for drying motors. These include heat lamps, fans, nitrogen drying, silica gel, and baking in an oven. These methods are time consuming, and none of them is completely successful. Another method that dries motors more completely is the application of a current at low-voltage to the motor windings. However, this method is also time consuming and costly when apparatus is put together specifically for only a few motors.

A new low-voltage motor heater has been designed. It can be used with motors of many sizes and voltages and will dry them within a few hours. The system is portable, can be operated by a single person, and can be used in difficult-to-reach locations.

The heater is shown in Figure 1. A controlled voltage source is applied to the windings of a motor to produce heat and dry it. To keep motor-shaft rotation to a minimum the voltage is kept low: from 0 to 28 V. The current required depends upon the size of the motor being heated. For example, a 20 hp, 440 V motor with a Locked Rotor Amperage (LRA) of 156 A draws approximately 8.5 A at 24 V. The heater, with a capacity of 125 A, is designed to dry a number of motors at the same time.

The unit operates from a 115-V, 60-Hz power source with a current requirement of about 30 A. A stepdown transformer is used to obtain the low-voltage range. A variable transformer is used to regulate the voltage within the 0-to-28-V range, and two voltmeters and two ammeters are used to monitor and calculate the load and wattage. To prevent overheating of the motor a regulated thermostat, with thermoprobe and readout, is included. The

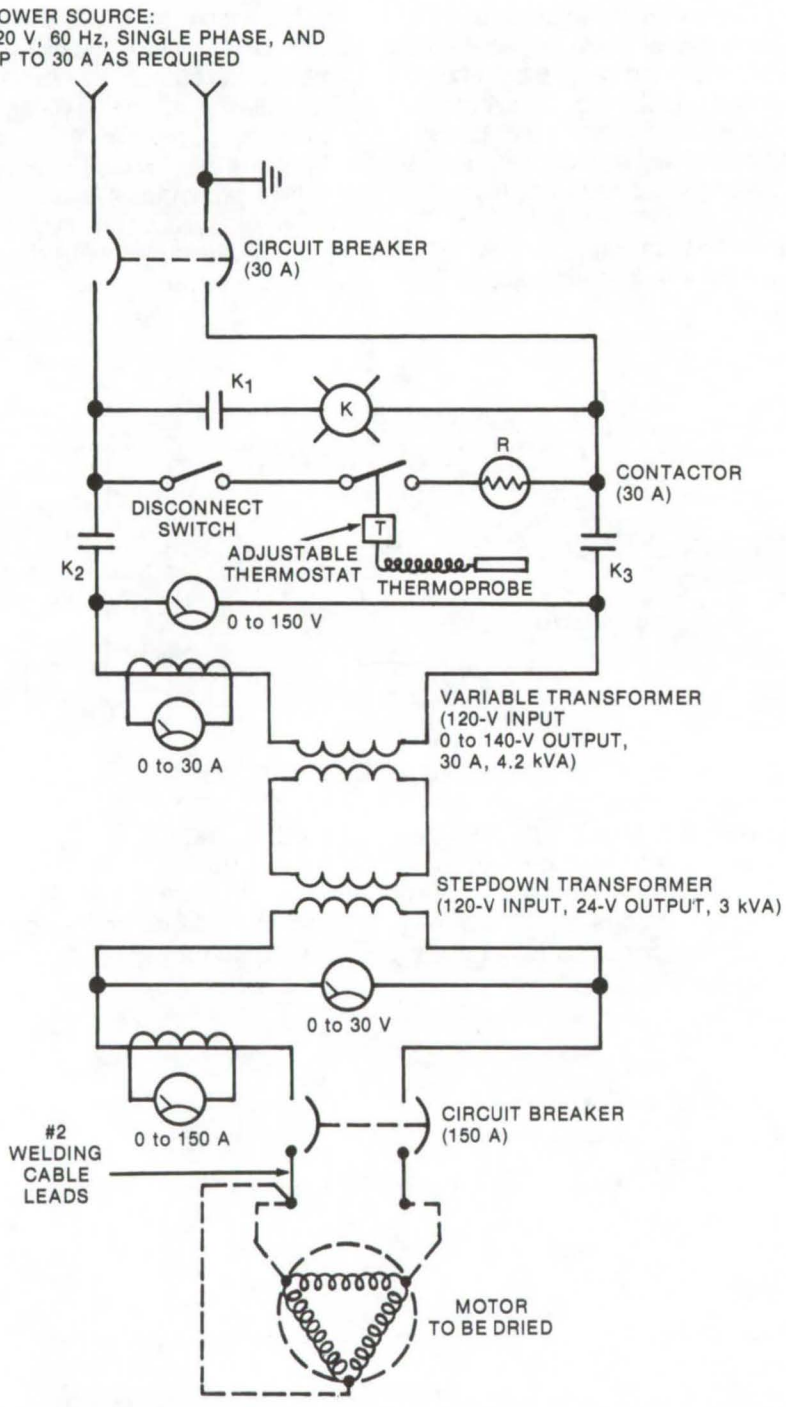

Figure 1. The **Low-Voltage Motor Heater** has a stepdown transformer for low-voltage range, a variable transformer for holding within the 0-to-28-volt range, and voltmeters and ammeters to monitor load and wattage. The regulated thermostat controls a contactor, permitting the heater to cycle.

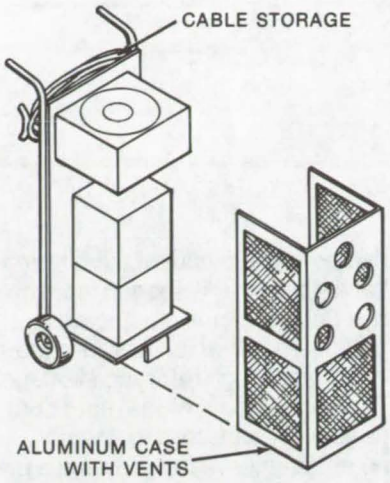

Figure 2. The **Low-Voltage Motor Heater Unit** is mounted on a two-wheel handcart, weighs about 45.4 kg, and takes up about 0.3 m^2. The power supply required is up to 30 A, 115 Vac, single phase.

thermoprobe is placed at the motor hot spot (not at the bearings), and controls a contactor which permits the heater to cycle. Manufacturer's allowable heat ranges, including information on the normal running temperature at the hot spot, must be available for reference, to allow the controller to be set. The unit incorporates circuit breaker protection. The entire unit is mounted on a two-wheel handcart (Figure 2) weighing about 45 kg (100 lb) and taking up about 0.3 m^2 (3 ft^2) of floor space.

The unique feature of the heater is its adaptability to a wide range of motor sizes. Only common handtools are required to use the heater, and it can be used to service two or more motors simultaneously. Once set up and stabilized, the low-voltage motor heater can be left unattended.

This work was done by Kenneth R. Bezant of Trans World Airlines Inc. for **Kennedy Space Center.** *For further information, Circle 14 on the TSP Request Card.*
KSC-10651

Multiple-Layer Printed-Wiring Trace Connector

A new connector repairs improperly plated-through holes.

Langley Research Center, Hampton, Virginia

A major reason for discarding a multilayer printed-wire board is plated-through-hole barrel failure. Fabricators of multilayer boards presently use copper plating to join the conductor paths of the layers. Due to a mismatch of thermal expansion characteristics of the materials used, plated-through-hole barrels fail. Now a new method, a nickel-plated spring-steel printed-wiring foil connector, is used to reduce the reject rate of printed-wiring boards by offering a means of repairing these holes.

The connector consists of a hollow pin slit along its length. Its outer surface has sharp inverted-V edges which run its entire length (see the figure). As the connector mates with the copper pads within the hole, the connector edges slightly indent the pads of the foil to assure a positive contact and thereby to maintain contact with the pads during thermal movement of the board in all planes.

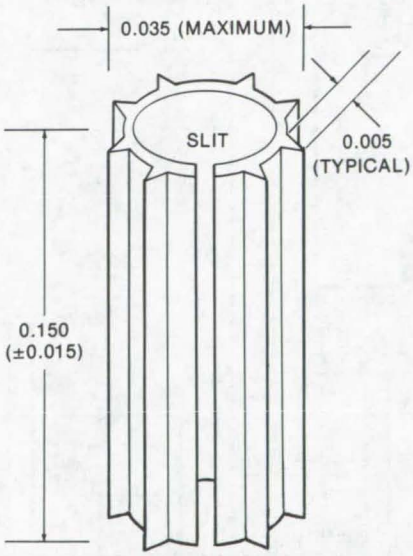

The **Printed-Wiring Connector** is a hollow pin, with a lengthwise slit, that is inserted into improperly plated-through holes. The edges of the connector make positive contact with the copper pads within the hole.

This work was done by Donald E. Pizzeck of **Langley Research Center.** *For further information, Circle 15 on the TSP Request Card.*

This invention has been patented by NASA [U.S. Patent No. 3,964,813]. Inquiries concerning nonexclusive or exclusive license for its commercial development should be addressed to the Patent Counsel, Langley Research Center [see page A8]. Refer to LAR-11709.

Battery Single-Cell Protection System

Individual modules protect each cell of a battery from undervoltage and overvoltage.

Lewis Research Center, Cleveland, Ohio

A battery protection system has been developed in which each cell of a multicell battery has its own protective circuit. The protective circuit (Figure 1) consists of a solid-state comparator unit and a high-current switching device combined into a single module, which can be mounted directly on each cell of the battery as part of the cell or battery case construction (Figure 2).

Batteries, particularly sealed batteries, require close voltage monitoring to make certain they are in good working condition. The comparator unit continuously monitors each cell. When the cell voltage either exceeds a predetermined high level or falls below a predetermined low level, the relay activates a bypass circuit across the cell which removes the cell from the circuit. The bypass circuit may include a cell-voltage simulation network (Figure 1) or, for some applications, can be reduced to a shorting bar. As soon as the cell returns to normal voltage, the bypass is removed, and the cell is returned to service in the battery regardless of whether the battery is in a charging or discharging mode of operation.

The comparator circuit comprises a differential amplifier connected across a cell with one input of each of the two voltage comparators connected to the output of the differential amplifier. The second input of one comparator is connected to a potentiometer which provides a predetermined high reference voltage. The second input of the other comparator is connected to another potentiometer which provides a predetermined low reference voltage. A driver transistor connected to the comparator output is activated when an out-of-limit voltage is sensed by either comparator.

Since no cell in the battery is allowed to be driven beyond the predetermined voltage limits, the life of the battery can be increased. Also the battery can be discharged much

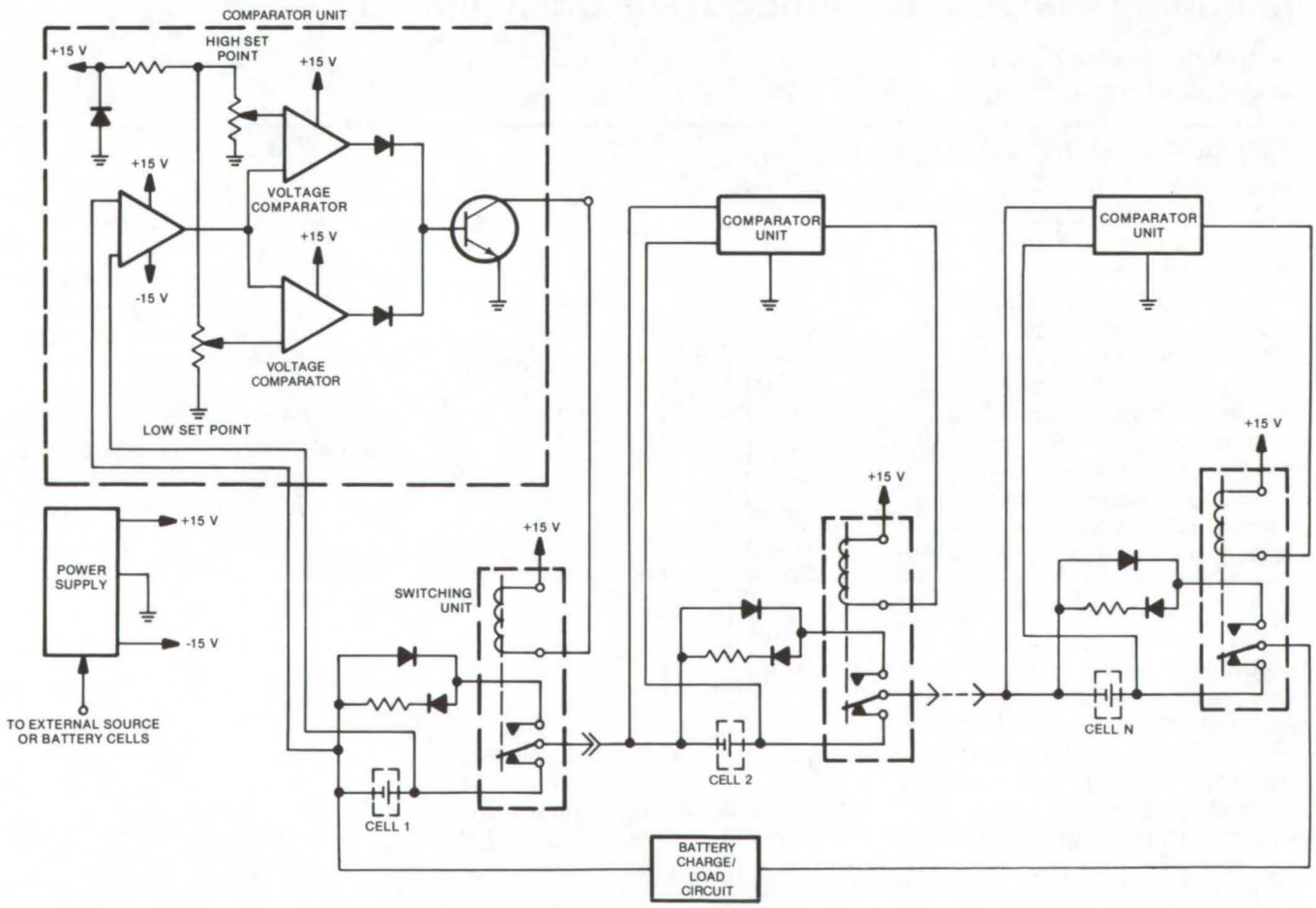

Figure 1. The **Single-Cell Protection Circuit,** for which the fundamental circuit is shown above, protects individual cells in a multicell battery.

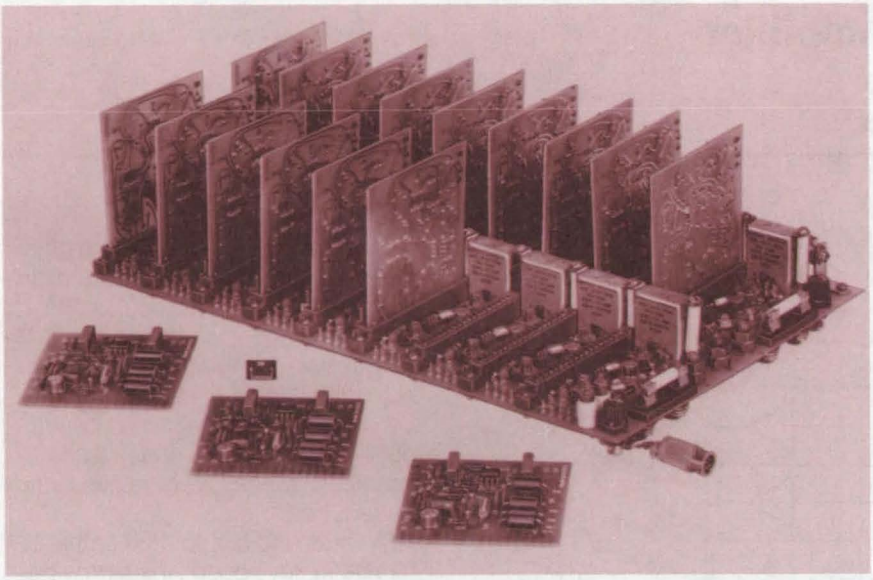

Figure 2. The **Experimental Protection Package** shown was designed for a 28-volt, 18-cell AgZn battery.

deeper without danger of cell reversal and consequent explosion. Deeper discharge increases the available useful energy from a battery; therefore, a smaller, lighter battery with the protection circuit could be used in place of a larger, heavier battery without the protection circuit. Development is continuing; a recent module is shown in Figure 3.

This work was done by Ralph D. Thomas and William J. Nagle of **Lewis Research Center.** *For further information, Circle 16 on the TSP Request Card.*

Inquiries concerning rights for the commercial use of this invention should be addressed to the Patent Counsel, Lewis Research Center *[see page A8]*. *Refer to LEW-12039.*

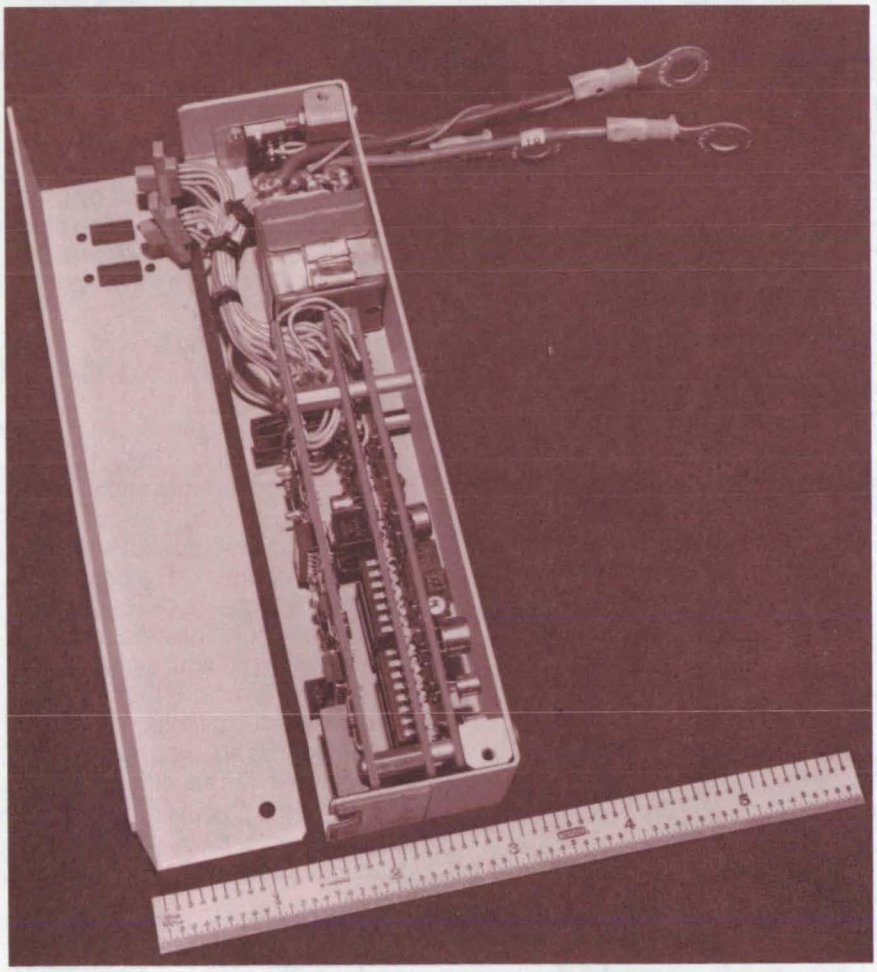

Figure 3. An **Improved Single-Cell Protection Module**

Wideband Distribution Amplifier

Temperature-stable amplifier
has 0.1 to 100 MHz frequency range.

Caltech/JPL, Pasadena, California

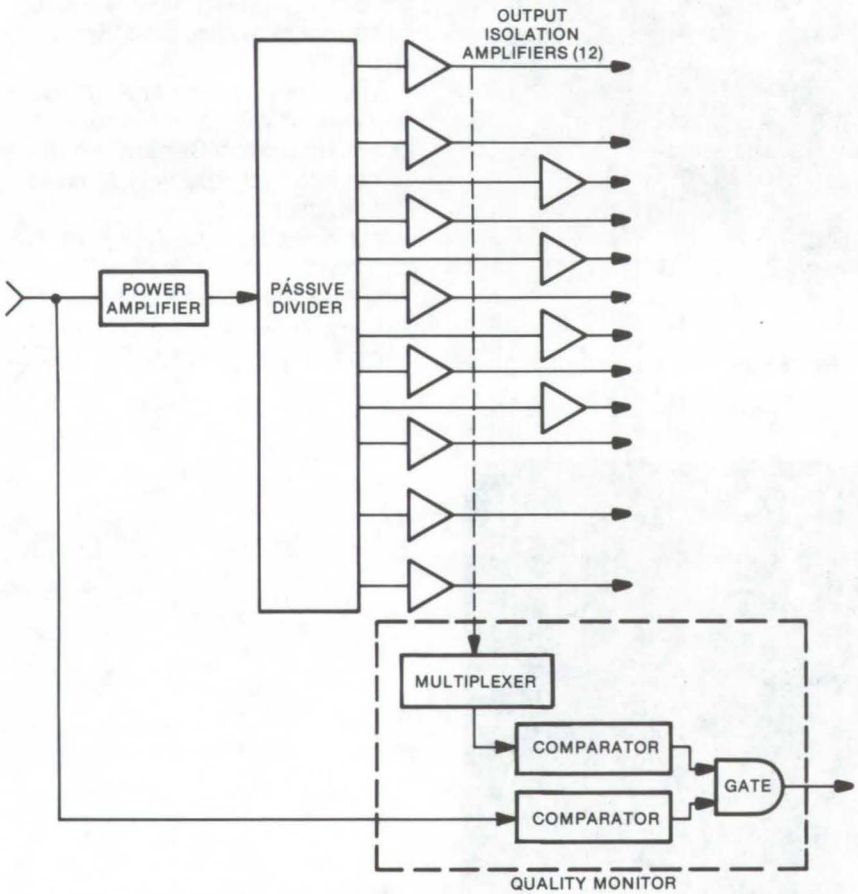

The **Wideband Amplifier** has been implemented with machined compartment techniques and semirigid coax and with stripline transmission and flexible coax. Phase stability is less than 1.5° from 0° to 50° C, and output-to-output isolation is better than 80 dB at 10 MHz and 70 dB at 100 MHz.

Stringent specifications are often placed on frequency-standard distribution systems. In particular, the criteria for phase shift and output-to-output isolation are primary design objectives. In addition, the distribution amplifiers in the chain should not be temperature sensitive nor should RF tuning over the passband be required.

A wideband distribution amplifier has been developed which provides 12 outputs isolated from each other by 70 dB at 100 MHz, a frequency range of 0.1 to 100 MHz, less than 2° phase shift over a temperature change of from 0° to 50° C, and a computer-level output to monitor module signal quality. As illustrated, the power amplifier drives a passive power divider and the 12 output isolation amplifiers. The high output-to-output isolation is achieved by using the 30-dB (minimum) isolation of the power divider and the reverse isolation of the output isolation amplifiers. In the mechanical design, stripline transmission and flexible coaxial-cable techniques further maintain isolation.

In the module signal-quality monitor, hot-carrier diodes detect the power level at the input and at the 12 outputs. The outputs are sampled by a multiplexer the output of which is fed to a comparator. The detected input power signal goes to a separate comparator. The detected input and multiplexer output signals are compared in a gate. If the input is out of its specified limits, the gate shuts off and is so indicated. If the input is within the specified limits and one of the outputs drops out of its preset limits, an external system detector latches until the problem is solved.

This work was done by Conrad F. Foster of **Caltech/JPL.** *For further information, Circle 17 on the TSP Request Card.*
NPO-13256

Overload-Protector/Fault-Indicator Circuit

Power driver circuits are protected by a current limiter with status lights.

Caltech/JPL, Pasadena, California

In large installations, status indication circuits may be located far from the equipment being monitored. The power source energizing the status circuits, which are often comprised of power-transistor-driven incandescent indicators, is adversely affected by initially-high surge currents when the lamps are first triggered on. The interconnecting cables and their associated connectors also impose large momentary fault current conditions on the power supply if the cables, upon removal from the connector, are accidentally short circuited while troubleshooting.

To overcome the effects of the current surges a three-terminal current limiter is incorporated in the power supply to increase its overload current protection. The integrated-circuit limiter (component 78M24 in the schematic) has a maximum peak current passthrough of approximately 2 A; the limiter provides about 500 mA under steady-state conditions. Since the limiter is internally protected by built-in thermal shutdown, it is not mounted with a heat sink and is therefore self-protecting. The status indicators are sourced from a 28.0-volt supply, but the limiter maximum voltage output is 24 volts. The reference terminal is biased slightly above ground to permit the limiter to operate at the output voltage requirement.

When the regulator is overloaded, it reduces the output voltage to a safe value via internal current limiting. The output voltage reduction increases the voltage differential across the limiter source/output terminals. The light-emitting diodes (LED's) connected across the terminals turn on, thus indicating a fault in the circuit being powered.

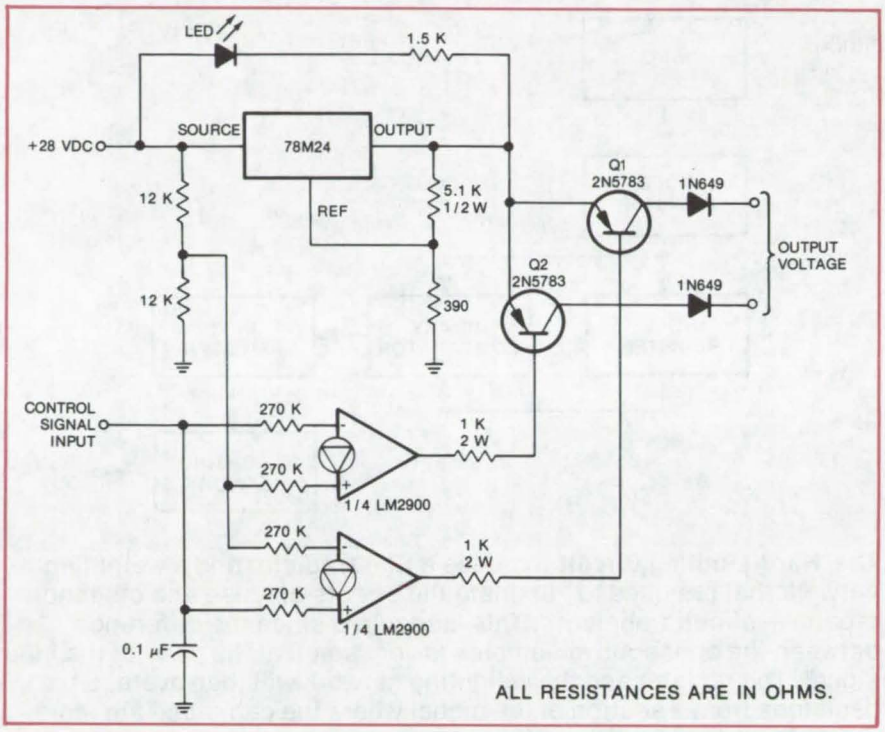

The Overload-Protector/Fault-Indicator Circuit incorporates a three-terminal current limiter (78M24) to increase the overall reliability and by eliminating transistor burnouts resulting from shorted interconnection lines and other overloads. Fast-acting LED's across the limiters show the status of the transistor output circuits.

After the fault is corrected the circuit returns to normal operation, and the LED is extinguished.

A separate current-control signal from the monitored circuit also can be used to turn off the power supply. The signal is fed to a pair of operational amplifiers. The amplifiers are connected for complementary output current required by the circuits being powered. The amplifiers, type LM2900 or equivalent, do not have closed-loop feedback to control gain. This provides full open-loop gain to drive the output transistors Q_1 and Q_2. The 1N649 diodes, in series with each of the transistor collector terminals, are used to prevent high transient currents (resulting from driving inductive loads) from destroying the output transistors. The diodes also protect the circuit if it is connected to a source higher than 28 volts.

This work was done by John R. Paluka of **Caltech/JPL** *and Stephen F. Moore of Resdel Engineering Corp. For further information, Circle 18 on the TSP Request Card.*
NPO-13592

Low-Frequency Sine Wave Hard-Limiting Technique

An effective technique separates the desired sine wave voltage from a bias voltage.

Caltech/JPL, Pasadena, California

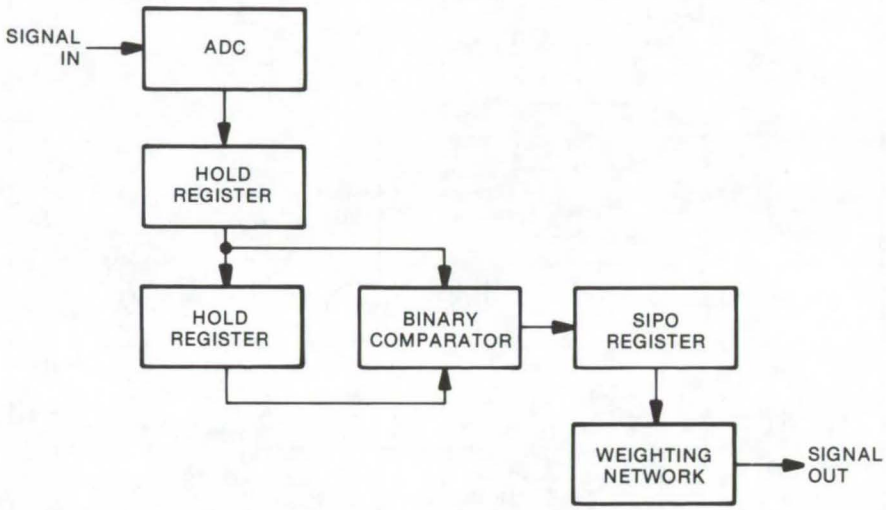

The **Hard-Limiting Circuit** includes a SIPO register and a weighting network that are used to eliminate the effects of noise and other non-repetitive circuit transients. This is required since the difference between the consecutive samples is very small at the peak of the input signal. The register and the weighting network will then average the decisions from a section of the signal where the decisions are more dependable (or where the differences between the two consecutive samples are larger).

Hard limiting a sine wave with a fixed value of superimposed dc bias is easily accomplished by using an analog flip-flop circuit such as a Schmitt trigger. If the bias varies slowly and if the frequency is sufficiently high, the signal can be capacitively coupled to the Schmitt trigger. In some applications, however, the frequency is too low for capacitive coupling to be practical.

A hard limiter for a low-frequency sine wave (of varying frequency, amplitude, and bias) is implemented by using digital-processing techniques. The sign of the signal slope changes at the signal peaks. This sign change, which is independent of amplitude, frequency, and bias, is used to detect the peaks and to implement a square wave of equivalent frequency. The detected signal is hard limited and is a square-wave replica of the original signal.

In the system, shown in the block diagram, the signal is sampled at a high rate by using an 8- to 10-bit-resolution analog-to-digital converter. The output of the ADC is held in a register for a full word time. A second hold register is added so that two consecutive data words are available simultaneously. These two data words are compared for relative size by using a simple binary comparator.

The output from this comparator is a single-term binary output indicating which word is greater. These consecutive "zero"/"one" decisions are stored in a serial-in/parallel-out (SIPO) shift register. Connected to the parallel outputs of the SIPO register is a static weighting network which indicates that at least half of the variables in the register are "ones" regardless of position in the register.

This work was done by Tage O. Anderson of **Caltech/JPL.** *For further information, Circle 19 on the TSP Request Card.*
NPO-13230

Signal Level Detector

A digital, frequency-independent circuit monitors sine waves of variable frequency.

Caltech/JPL, Pasadena, California

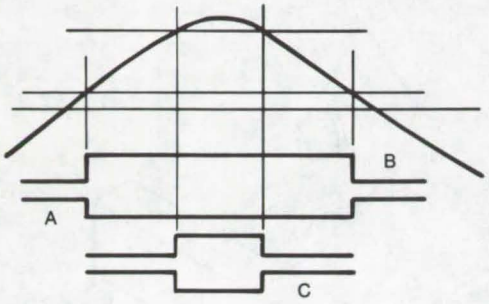

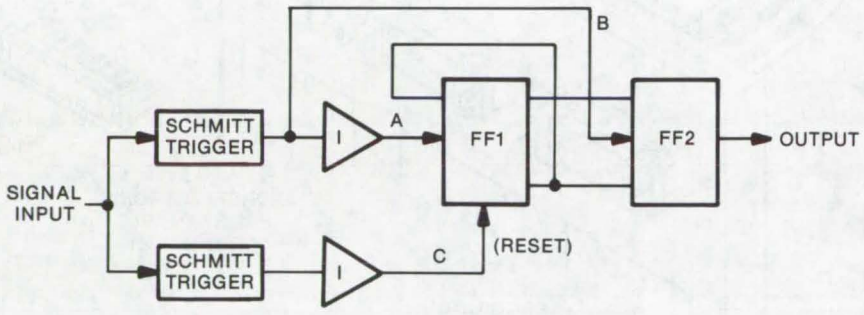

The **Signal Level Detector** frequency range depends on the limits of the logic family used. The operational performance of the unit is limited to the accuracy imposed by the Schmitt trigger threshold levels, which depend somewhat on temperature and on component variations from unit to unit.

It is difficult to detect reliably the level of a variable-frequency sine-wave signal. Since the signal varies in time and amplitude, analog filters and measuring devices are not accurate or economical. Previous digital and hybrid-circuit measurement schemes referenced the incoming sine-wave signal to a fixed signal crossover point or to an arbitrary level lower than the one detected. The circuits, all frequency-dependent, measure the amplitude of the sine wave after a fixed period of time has elapsed. Other circuits recognize that at a lower fixed level the duration of the signal above reference is longer or shorter than the reference duration.

A level detector which is frequency-independent is shown. It is implemented via two Schmitt-trigger circuits, a pair of inverters (I), and two flip-flop stages. One trigger is set to an arbitrary low level and could be considered to operate as a crossover detector. The other Schmitt trigger is adjusted to output a pulse at the dropout threshold of the sine-wave input.

The leading edge of the output of the lowest set trigger sets flip-flop 1 (F/F 1). The trailing edge transfers the content of F/F 1 to flip-flop 2 (F/F 2). The output from the dropout threshold resets F/F 1. The content of F/F 1 at the time of transfer is then high or low, depending on whether the signal peak amplitude is above or below the dropout threshold. The output from F/F 2 is the steady-state, indicating dropout.

This work was done by Tage O. Anderson of **Caltech/JPL.** *For further information, Circle 20 on the TSP Request Card.*
NPO-13272

Plug-In Circuit Monitor

A programable microelectronic module is used as a circuit monitor.

Lyndon B. Johnson Space Center, Houston, Texas

Normally, electronic-circuit functions are monitored during routine maintenance by probing each circuit element with an analytical tool. Guides published by the circuit manufacturer describe the anticipated results of the analysis and enable the technician to judge the circuit operation in terms of this standard. This procedure although qualitatively thorough is outmoded when applied to many present electronic systems, since it is only economical when checking a few discrete components, but not when checking complex modules (such as those with integrated circuits or large-scale integrated assemblies).

In a proposed monitoring scheme an intelligent electronic circuit is used to monitor other circuits within a module and to warn of imminent failure of the module under surveillance. The circuit monitor is housed in a rectangular connector and plugs into a mating jack, which was originaly designed to terminate multiple-wire flat-conductor cable (FCC).

The FCC premolded rectangular connector is lightweight, easy to replace, and highly reliable. Changing a monitor circuit merely requires the removal of one connector-encased circuit and the slipping in of another connector (programed with another circuit-surveillance function) in its place. After the required components are bonded to the back part of the connector, electrical interconnection is made between these components and the contacts of the connector. It is then encapsulated with epoxy-resin compound. An elastomeric material applied to the flat packs within the connector provides a cushioning effect and helps to secure the electronics. A seal and a polymeric cover are then installed on the back of the connector to moisture-proof the monitor.

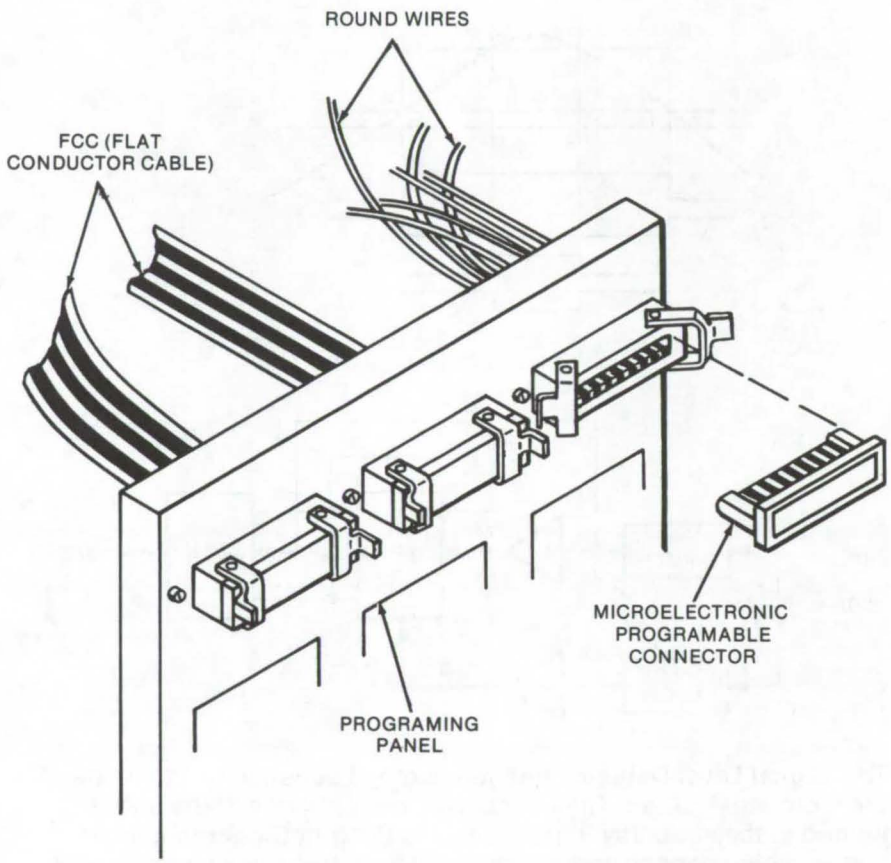

The **Plug-In Circuit Monitor** can be made from existing premolded rectangular connectors, slightly modified into programable microelectronic units.

This work was done by Eugene J. Stringer of Rockwell International Corp. for **Johnson Space Center.** *For further information, Circle 21 on the TSP Request Card.*
MSC-19455

Microprogramable Module

A new concept eliminates the need for patch panels.

Lyndon B. Johnson Space Center, Houston, Texas

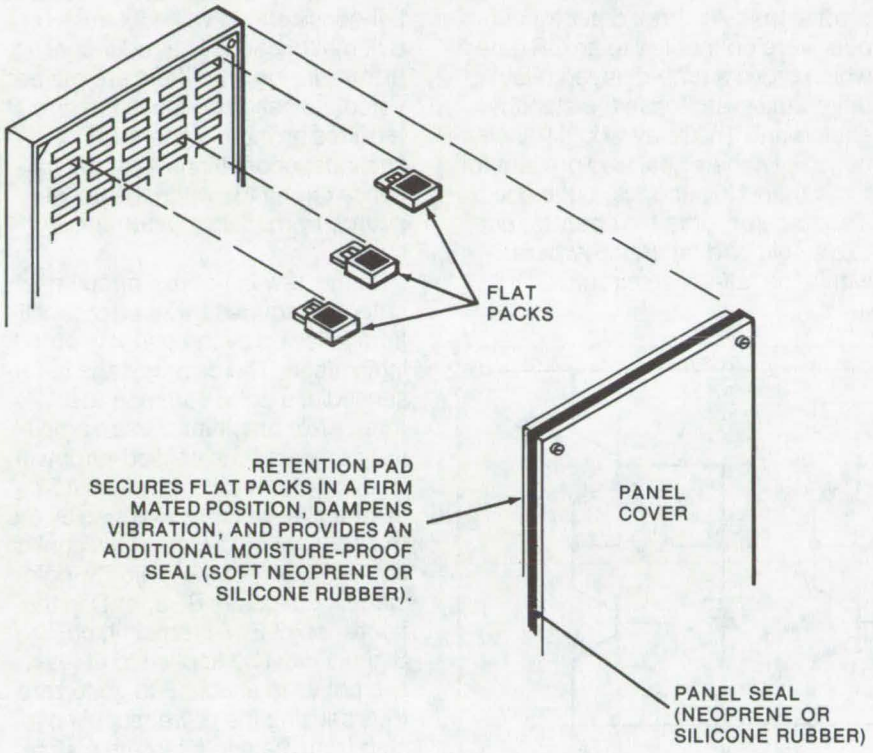

A new scheme proposes the use of preprogramed microelectronic circuit packs to perform the signal-routing function. The circuits are housed in a connector originally designed for flat-conductor cable (FCC) wiring. The concept is similar in design to that described in the preceding article (MSC-19455). The plug-in packs are instantly-replaceable.

The connectors are plugged into a selector panel which functions as a master patch panel. They are held in the board by a spring-loaded retainer panel. Signal leads from other equipment are terminated at an appropriate connector. When the plug-in pack is inserted it automatically determines signal route paths.

This work was done by Eugene J. Stringer of Rockwell International Corp. for **Johnson Space Center.** *For further information, Circle 22 on the TSP Request Card.*
MSC-19456

The **Microprogramable Module** is a small lightweight selective circuit/function panel that utilizes microelectronic circuits in flat packs to eliminate hard wiring and heavy-harness routing to various subsystems.

Present methods of selecting and interconnecting equipment groups are often implemented via a patch panel. The output of each instrument is terminated at its appropriate socket, and cables are used to route the signal-flow or order-of-equipment function. This is a time-consuming process, and it is complicated by socket and cable down-time for periodic maintenance and potential misrouting of cables during the initial cable plug-in.

Majority-Voted Logic Fail-Sense Circuit

A self-monitoring hybrid circuit reacts to both static and dynamic changes.

Caltech/JPL, Pasadena, California

The fail-sense circuit previously used in a portable high-reliability ac power inverter consisted of three single-channel detectors. These monitored overvoltage, undervoltage, and frequency shift. The overvoltage and undervoltage detectors were connected to the dc-regulated bus, the frequency shift detector was connected to the main ac bus, and detection was accomplished by using a tuned transformer. Its output was rectified to produce the required error signal. All three detector outputs were connected to an OR gate which drove a time-delayed relay driver and switched in the standby equipment. The relay would transfer normally if the signal was present for more than 1.5 seconds, but it could also transfer, or fail to operate, due to a single part failure anywhere within the fail-sense circuit.

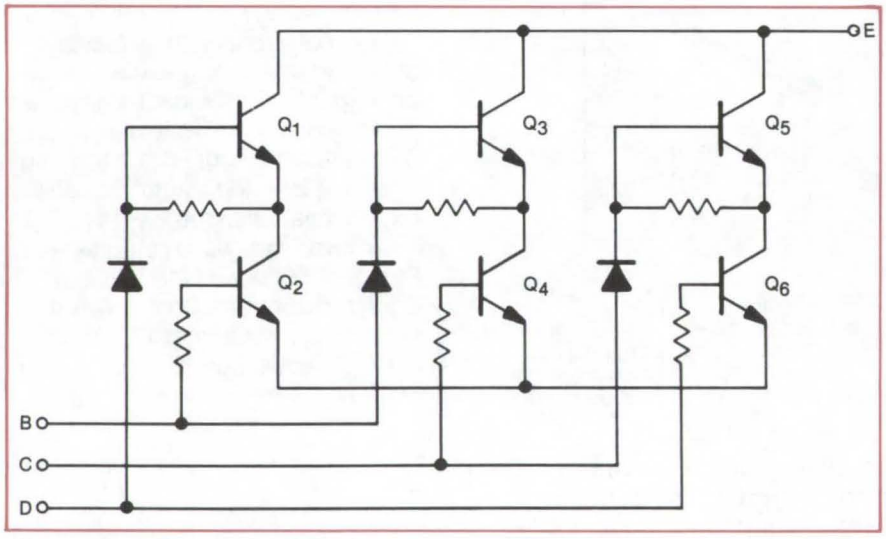

The **Majority-Voted Logic** component of the fail-sense circuit receives three error-voltage signals that are sensed at a single point by three error amplifiers. The error-amplifier outputs (B, C, and D) are weighed by the logic circuit. If a transistor shorts, only one signal is required to operate; if a transistor opens, two signals are required.

A single-part failure in an updated fail-sense circuit will not cause circuit malfunction. The redundant error-sensing amplifiers are majority voted, so called because the circuit requires an input signal to at least two independent inputs for the fail-sense circuit to switch the power source from main to alternate supply.

In the new fail-sense circuit each detector requires three error amplifiers followed by the majority-voted logic stage. The error voltage is sensed at a point common to all three error amplifiers. Each amplifier compares the sensed error with its own reference to produce its error signal which is weighed by the majority-voting circuit. If a signal is applied to any of the majority logic stage input points B, C, or D in the figure, point E will remain high. Signals must be applied to at least two points to enable E to go to zero, thus causing the power supplies to shift from main to alternate source. If any part fails, open-circuits or short-circuits, the circuit will still function normally.

This work was done by Colonel W. T. McLyman of **Caltech/JPL.** *For further information, Circle 23 on the TSP Request Card.*
NPO-13107

Hybrid Thin-Film Amplifier

A miniature amplifier for bioelectronic instrumentation consumes only about 100 mW.

Lyndon B. Johnson Space Center, Houston, Texas

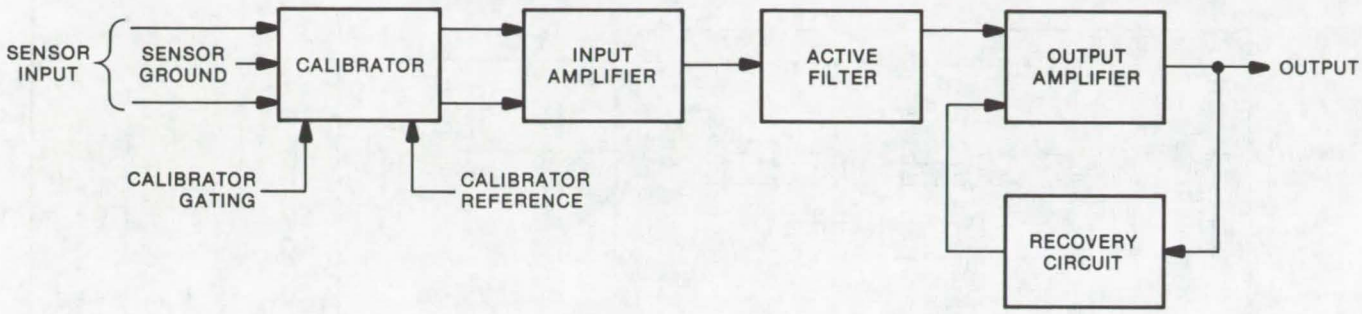

Hybrid Bioelectronic Instrument Amplifier has a frequency response flat to within 0.5 dB from 0.14 to 450 Hz. Five thin-film substrates contain, in total, eight operational amplifiers and seven field-effect transistor dice.

A hybrid bioelectronic signal amplifier/conditioner has been developed which consists of five thin-film substrates which contain, in total, eight operational amplifiers and seven field-effect transistor chips or dice. The amplifier/conditioner is calibrated via a gated voltage source. Calibrator switches, in series with the sensor input leads, transfer the amplifier input to the sensors or to a square-wave calibration gate voltage of 100 ms duration. The calibrate voltage is accurate to within ±0.1 percent. The voltage reference source is external to the amplifiers and may be simultaneously connected to several of the conditioners, each requiring a different calibration voltage level.

Amplifier/signal conditioner frequency response is flat within 0.5 dB from 0.14 to 450 Hz. The measured common-mode input signal rejection is 100 dB; input impedance is 40 MΩ in the common mode and differential modes. A block diagram of the amplifier is illustrated.

This work was done by Garry Cleveland of Lockheed Missiles & Space Co. for **Johnson Space Center.** *For further information, including a system schematic and parts layout, Circle 24 on the TSP Request Card.*
MSC-13975

Solid-State RF Switch

Consisting of NAND gates, the switch can be expanded to multipole input and can switch at frequencies up to 30 MHz.

Caltech/JPL, Pasadena, California

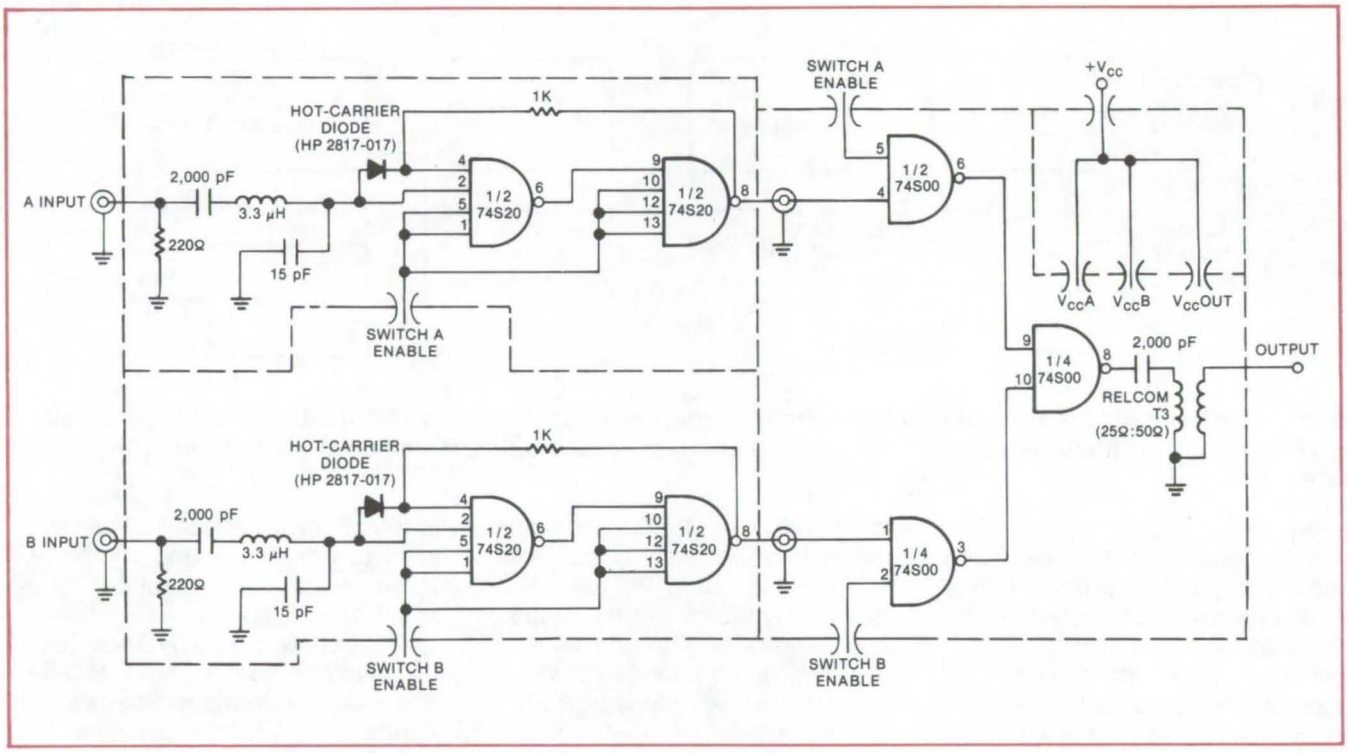

Solid-State Switch for RF is simple, inexpensive and offers high isolation [greater than 70 dB between the driven (on) input and the unused (off) input, or between inputs if both are off]. Temperature variation vs. phase is less than 0.1° /° C.

An RF switch uses digital integrated circuits (IC's) to provide isolation between inputs and between input and output ports. Switch isolation is greater than 70 dB between each of two unused input ports and between the unused input and the output port. Operating at 19.125 MHz, the dual-input switch as illustrated consists of three IC's with RF compensating circuits.

The inputs A or B are switched to the output by applying a +4-volt to +6-volt step to the appropriate switch-enable ports. Isolation between input and output is greater than 80 dB; the switch on/off ratio is greater than 90 dB. A nominal input level of +1 to +17 dBm is required to output a +12-dBm level for any input of the stated range.

Depending on frequency/power considerations, an appropriate line receiver could be used in lieu of the input filter network, which in some cases would give a significant increase in input sensitivity.

This work was done by Michael F. Hanna and Harry K. Detweiler of **Caltech/JPL.** *For further information, Circle 25 on the TSP Request Card.*

This invention has been patented by NASA [U.S. Patent No. 3,808,464]. Inquiries concerning nonexclusive or exclusive license for its commercial development should be addressed to the Patent Counsel, NASA Resident Legal Office-JPL [see page A8]. Refer to NPO-13081.

RAM Digital Filter

A sophisticated means of implementing recursive and nonrecursive digital filters.

Caltech/JPL, Pasadena, California

A newly-proposed digital filter is designed to store all possible combinations of filter coefficients in a random access memory (RAM). The filter has a very high speed and hence high cutoff frequencies. Based on this new design, low-order (7 or less) filters can be made at reduced cost.

The filter as shown includes an analog-to-digital converter (ADC), an X shift register, a memory, an accumulator, and a digital-to-analog converter (DAC). In operation the analog input signal is sampled. The samples are converted to their representation in radix (-2) and are serially fed to the X shift register which generates a memory address as shown. With each new bit a new word is selected from memory and is added to the accumulator. Following the addition, the accumulator contents are shifted left one bit and their sign is reversed. After J such cycles [J being the number of bits per sample in radix (-2)] the accumulator contents are transferred to a standard (radix 2) DAC which yields the sample of the filtered function (analog output). Next the accumulator is zeroed, and the construction of the next output sample starts.

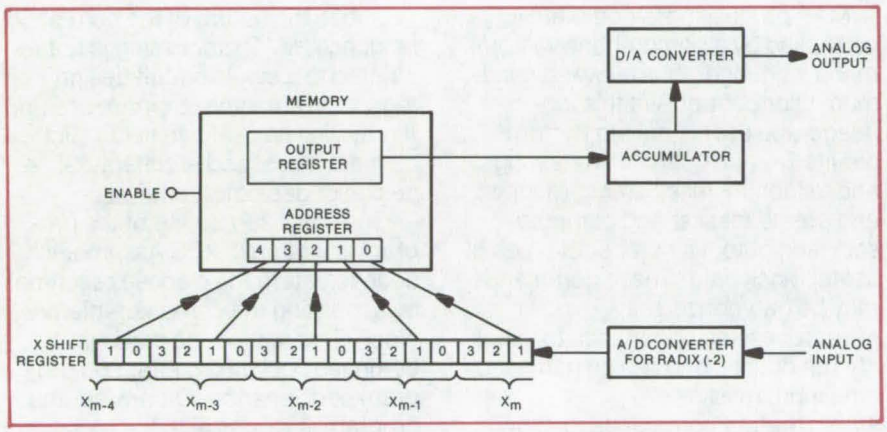

The **Nonrecursive RAM Digital Filter** shown above is a modification of a conventional digital counting filter. The register holding the filter coefficient in the digital counting filter is replaced with the much larger random access memory that stores all possible combinations of the coefficients. However, the counter and gates required there are eliminated in the RAM implementation.

The described configuration is a nonrecursive RAM digital filter. It should be noted, however, that the same basic shift register structure can also be applied to the recursive case. The feature of the RAM filter is that it achieves its speed by totally eliminating any computing to get the accumulator inputs. The closely related counting filters are characterized by a longer input-output delay because the accumulator inputs are computed in a pipeline structure. The RAM filter therefore has a definite advantage in applications requiring minimal delay. In low-order filters it also has a cost advantage over equal-speed counting filters.

This work was done by Shalhav Zohar of **Caltech/JPL.** *For further information, Circle 26 on the TSP Request Card.*
NPO-13659

Books and Reports

These reports, studies, and handbooks are available from NASA as Technical Support Packages (TSP's) when a Request Card number is cited; otherwise they are available from one of NASA's Industrial Application Centers or the National Technical Information Service.

Simplified Cut-Core Inductor

Data on the design of grain-oriented steel inductors

Moly-Permalloy powder cores are often the filter inductors routinely specified in high-frequency power converters and pulse-width-modulated switching regulators. The powder cores are convenient to use since they are analyzed in considerable detail in design literature offered by core manufacturers. However, the Permalloy powder core is not the optimum choice of inductor if size and weight are important.

There are significant advantages in using C-type cores and cut toroids fabricated from grain-oriented silicon steel. The grain-oriented core features greater design flexibility

(particularly in high-frequency inductors) since the airgap can be adjusted to any desired width and the relative permeability is high even at high dc flux density. Grain-oriented steels offer typical flux densities of 1.6 tesla with useful linearity to 1.2 tesla. Moly-Permalloy cores, when passing dc, have a flux density capability only to about 0.3 tesla.

A technical memorandum is available which describes the design of a linear reactor fabricated from grain-oriented steel. The memorandum consists of design charts and nomograms, and it illustrates the design of a grain-oriented inductor via a seven-step example. Typical values of core inductance, operating frequency, and coil current (dc and ac) are given.

The report includes a design procedure example. In step 1 of the example the energy stored in the inductor is determined. The value is used to find the area product of core window area times the effective iron area, a value necessary to complete step 2. In step 3 the wire size is determined by using wire-size tables found in the memorandum. The number of turns of wire is calculated in step 4, the resultant number of which is used in step 5 to determine the airgap dimensions. The effect of fringing flux on wound inductance is next considered; the number of turns may have to be recalculated to compensate for the fringing before proceeding. In step 6 the ac and dc flux densities are determined, and the final step of the procedure is the calculation of core loss.

This work was done by Colonel W. T. McLyman of **Caltech/JPL.** *To obtain a copy of the report, Circle 27 on the TSP Request Card.*
NPO-13600

Computer Programs

These programs may be obtained at very reasonable cost from COSMIC, a facility sponsored by NASA to make new programs available to the public. For information on program price, size, and availability, circle the reference letter on the COSMIC Request Card in this issue.

Mask Analysis Program

Efficient analysis of integrated-circuit masks and more general design problems

MAP (Mask Analysis Program) was developed to analyze masks from any circuit design technology. The program uses minimal core and time resources and performs the following analysis functions: artwork verification, device identification, nodal analysis, capacitance calculation, and logic equation generation. For data base simplicity, MAP processing operates on mask data which has been converted from its original form to orthogonal rectangles. This rectangular refinement process consists of breaking orthogonal polygons into rectangles, breaking non-orthogonal polygons into thin horizontal rectangular slices which approximate the shape with a degree of accuracy chosen by the user, and performing any necessary scaling or offsetting.

MAP processing is completely controlled by a comprehensive command language, thus allowing maximum user control. Via this language, the user is able to perform qualitative and quantitative testing and to identify mask areas, modify and create masks, and compute, sort, and output a number of types of useful mask data. These commands may be categorized as:

- Preprocessing commands to specify run options and assign names to the input masks,
- Input/output commands to allow the user to transfer data conveniently,
- Operational commands to direct the performance of a long list of single-mask and double-mask operations resulting in the creation of new masks,
- List-processing commands to direct several multiple-mask processes which require complex list-processing techniques,
- Dimensional-processing commands to initiate various dimensional calculations, and
- Control commands which allow the user to change position in the command string to construct loops and branches in processing.

Due to the nature of the command language, MAP processing is not restricted to a single circuit design technology or even to circuit design. It may well be useful in fields such as mechanical and architectural design or geological analysis.

One small subroutine of the program is written in XDS Assembler code to determine elapsed real time by accessing the computer internal clock. This subroutine can be dummied out with no affect on program performance. Otherwise, the program is written with the most basic and universal FORTRAN statements, thus minimizing modifications necessary for changing computers. A minimum of 180K bytes of core is required; however, the program is structured so that it may be readily overlaid, further reducing the core requirements.

FORTRAN IV
XDS SIGMA5

This program was written by Michael Martin of **Marshall Space Flight Center** *and Cheryl L. Mitchell of M & S Computing, Inc. For further information, Circle A on the COSMIC Request Card.*
MFS-23431

Electronic Systems

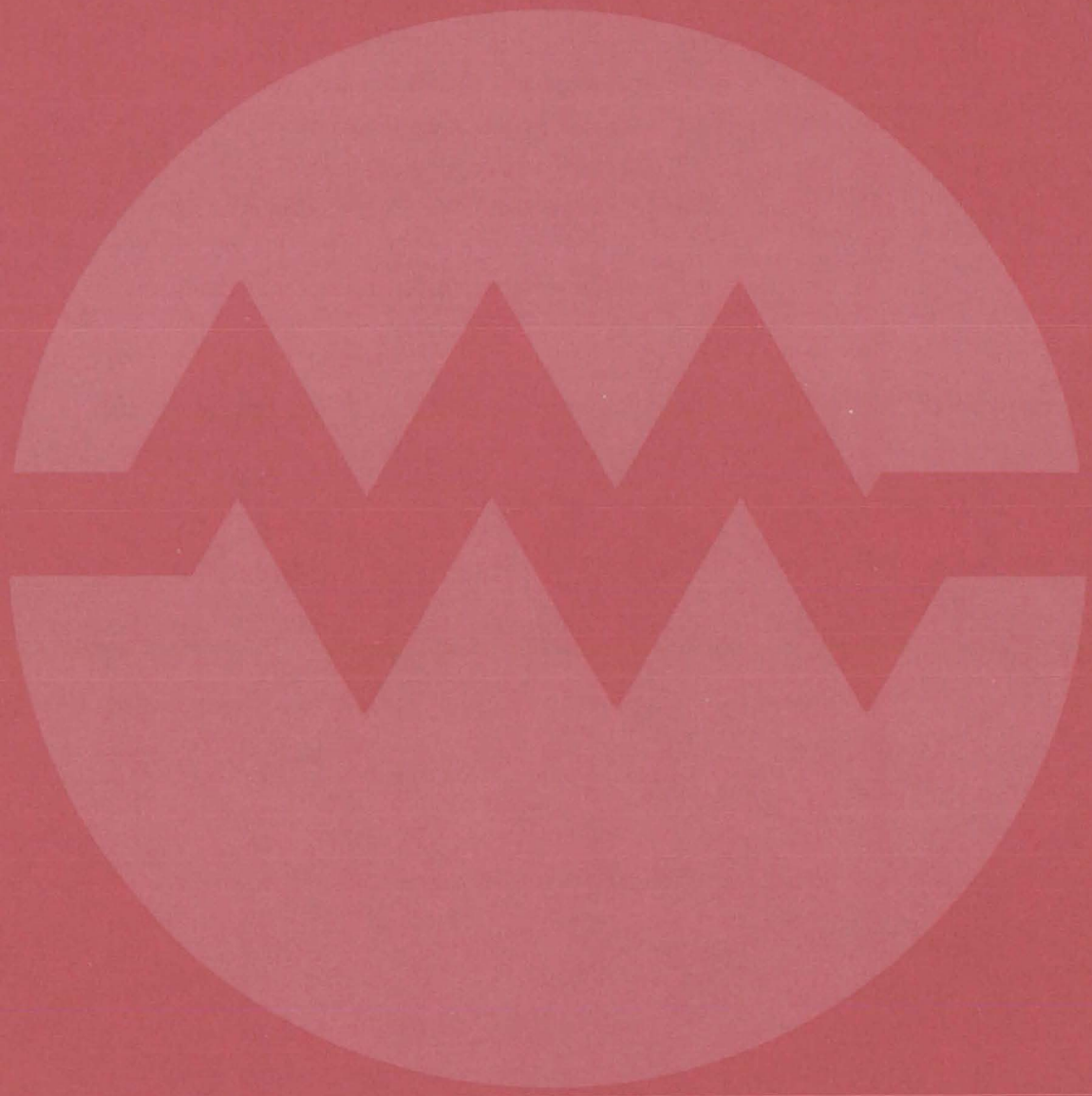

Hardware, Techniques, and Processes

Books and Reports

Manchester Transition Tracking Loop [MTTL]

Improved synchronizer
for biphase-L data

Lyndon B. Johnson Space Center, Houston, Texas

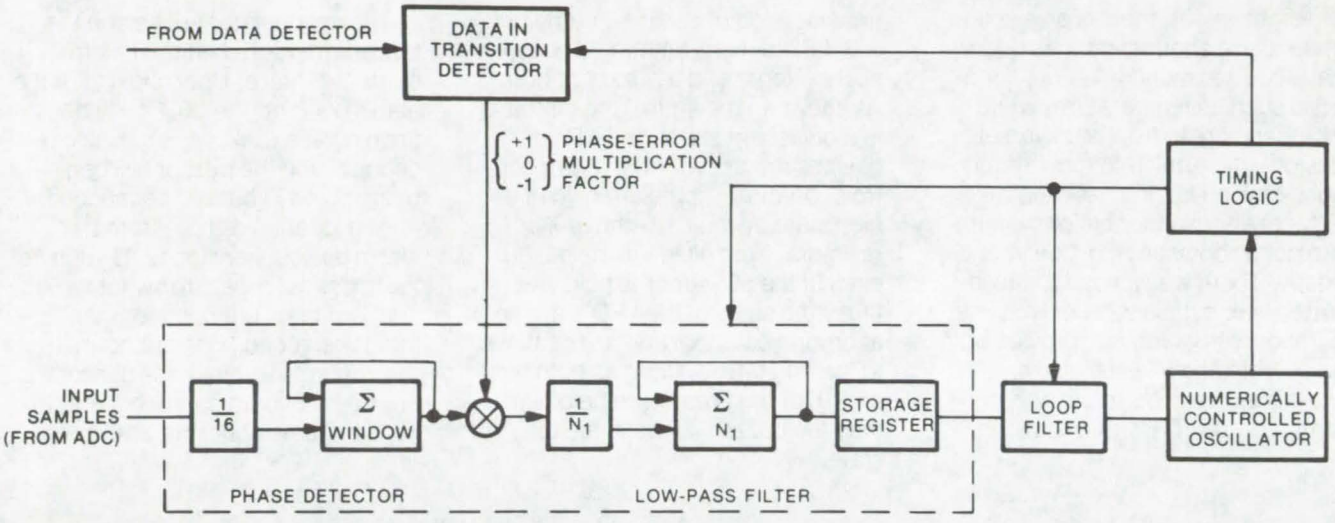

Phase Detector for Manchester-Coded Signals performs signal integration over a narrow window centered at estimated transition time. If transition occurs at mid-symbol, phase-error sample is multiplied by +1 or -1 to remove data dependency. The symbol synchronizer comprises a receiver front end, data recovery, phase-detection, and clock-regeneration circuits. The input broadband SNR is processed by an analog AGC circuit and then is sampled via a 4-bit parallel A/D converter. All subsequent processing is digital.

A symbol synchronizer optimized for Manchester-coded (biphase-L) digital data is used to lock the receiver onto the incoming binary codes in the proper time sequence. The synchronizer is a special-purpose computer which operates on sequential input samples of received data signals and is used to extract timing, data, and lock status information. Normally a digital transition tracking loop (DTTL) performs this function with a nonreturn-to-zero (NRZ) input. However, when Manchester-encoded signals are used with DTTL decoders, the biphase-L signal crosses from a high to a low value during the time interval of a single-bit symbol, and the DTTL may be unresponsive.

In the new tracking loop, a separate phase-detection algorithm is incorporated for acquisition; the programed acquisition-to-track sequence includes automatic bandwidth switching. Digital signal processing minimizes disturbing transients in this switching scheme. Additionally, the MTTL system has the most effective phase-detection signal-to-noise ratio (SNR) of any synchronizing processor. It can operate at any symbol rate by simply changing the master clock frequency; all system parameters, such as loop bandwidth and damping factor, remain constant.

Integration in the phase detector is performed over a narrow window centered at the estimated transition time. The resulting phase-error estimate is corrected for the sense (direction) of the data, which is determined in one of two manners.

If the transition over which the phase error was obtained occurs at mid-symbol, then a data-detection integration (matched to biphase-L) is performed over a full symbol time centered at that transition. A resultant decision of the data sense defines whether the phase-error sample is due to a rising or to a falling transition. The phase-error sample is then multiplied by +1 or -1 to remove the data dependency.

If the transition occurs between two symbols, then integrations are performed over full symbol times on either side of the transition. Both integrations are compared with zero to determine the data estimates. Then the phase-error sample is multiplied by +1, -1, or zero, depending upon the direction or existence of the deduced transition. That is, a between-symbol transition is rising if two successive data bits are 1's, falling if 0's, and nonexistent for the two other cases of 10 or 01.

All decisions in the data-aiding portion of the standard DTTL are made via integrations performed over a full symbol time. Results are 3 dB better than existing designs which integrate over half-symbol times. Unlike the DTTL, the MTTL phase detector fully utilizes the additional half-symbol information present in the biphase-L signal.

This work was done by Alfred Cellier, Lit Ning Ma, and Douglas Clayton Huey of TRW, Inc., for **Johnson Space Center.** *For further information, Circle 28 on the TSP Request Card.*
MSC-14842

Inexpensive Low-Voltage Solid-State Alarm

An audible and visual alarm for temperature, liquid-level, and pressure monitors

Lewis Research Center, Cleveland, Ohio

A lightweight, inexpensive solid-state alarm annunciator has been developed to monitor various functions such as temperature, liquid level, and pressure. Its universal design will permit it to monitor functions beyond its original intent.

Most alarm annunciator systems are quite sophisticated, bulky, and costly. There was a need for an inexpensive, simple system with few components which can provide both an audible and a visual alarm.

An inexpensive system was constructed from TTL (transistor-transistor logic) devices, combined with LED's (light-emitting diodes), pushbuttons, and a buzzer or horn. As shown in the figure, the circuit is in a quiescent state, and TTL devices are used for the alarm controls. All three inputs are held in a high state by their 1K-ohm pullup resistors. With all inputs held high, pin 3 of the 555 timer is held low, thus both sides of the LED's are held at ground potential and are confined to the off state. As long as both pin 1 and 16 of the buzzer are held high, then the buzzer will be in the off state.

The annunciator LED's and the buzzer are turned off until alarm contact closure. Upon closing of the alarm contact, the LED's will begin flashing at a rate of 1.5 pulses per second, and the buzzer will begin buzzing at 1.5 buzzes per second.

At a location remote from the alarm device, sensing units such as thermostats, pressure switches, or float switches are used for monitoring. When conditions are normal, the contacts within these sensors are open. Should operating conditions become abnormal, the open

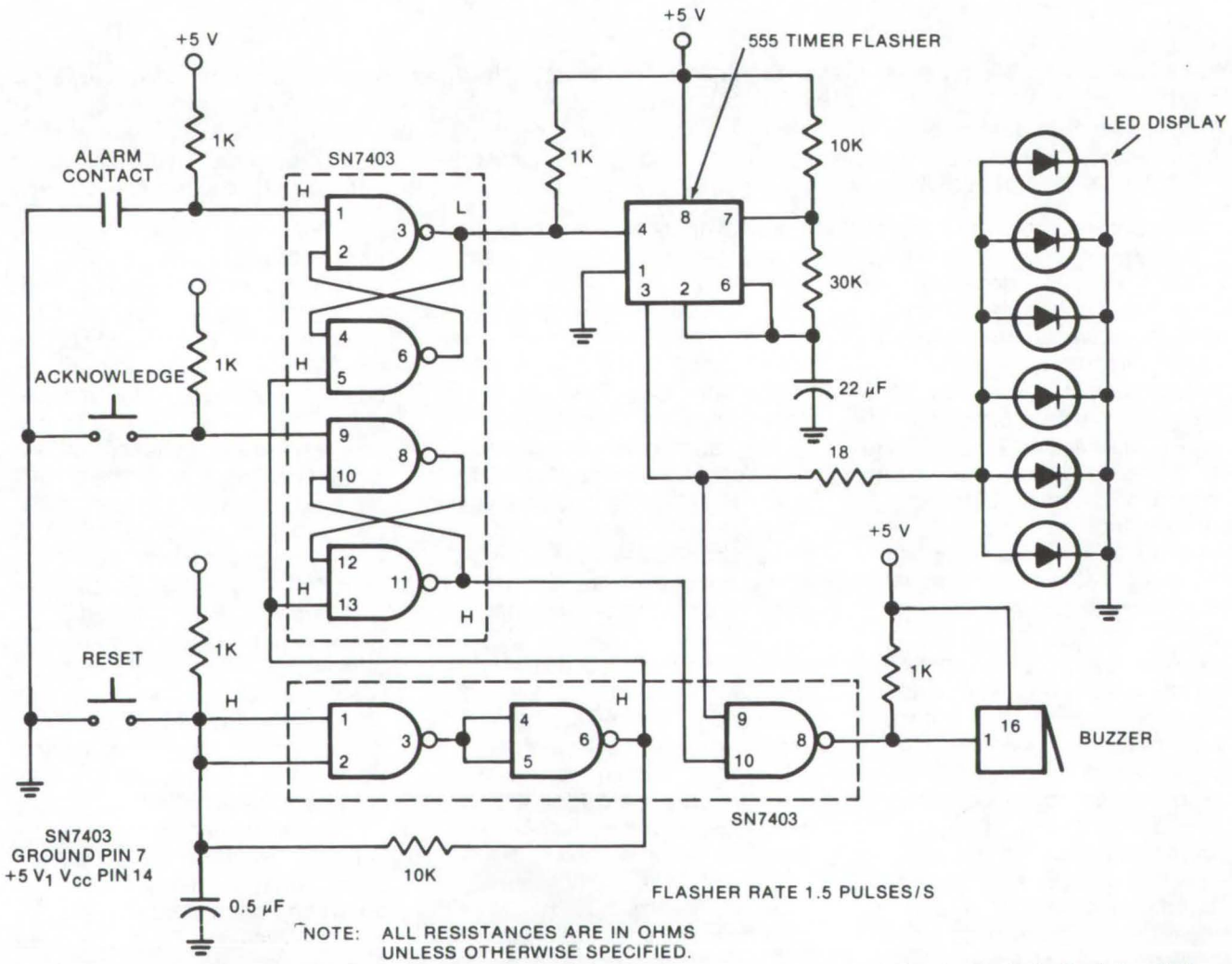

The **Solid State Alarm** is shown in a quiescent state. All three inputs are held high, and pin 3 of the 555 timer is low, keeping the LED's off. Upon closing of the alarm contact, the LED's will begin flashing.

contacts within the sensors will automatically close. The closed contacts activate the annunciator by emerging both the audible signal and the flashing LED's. A horn acknowledge button is used to stop the audible buzzer.

However, the LED's will continue flashing until the abnormal condition is cleared at the remote location, so that the alarm contacts in the sensing units again open in their normal position. The alarm reset button is then pressed which causes the alarm circuit to reset. If the alarm condition is not cleared, pressing the reset button will cause the audible alarm to return. Once the circuit is reset, the flashing LED's will turn off, the circuit will normalize, and the device will be ready for the next alarm.

This work was done by Donald H. Hardy of **Lewis Research Center.** *No further documentation is available.*
LEW-12544

Voltage-Offset Reduction in Data Transmitters

An inductor and a pair of diodes improve the pulse-to-pulse efficiency of a transformer-coupled data transmitter.

Lyndon B. Johnson Space Center, Houston, Texas

In transformer-coupled data transmitters, where complementary data pulses alternately drive a pair of identical output transistors, the currents flowing through both legs of the primary winding must be of identical amplitude and duration. If the mirror-image primary currents are not equal, the resulting asymmetric output, V_{out}, will contain an offset voltage, V_{os}. This offset may falsely trigger on a receiver connected to the output, if the level detection threshold voltage of the receiver is comparable with the V_{os}. Such asymmetry may be caused by input pulse imbalance (amplitude or duration) or by differences in the conductance of the output transistors.

A current source which consists of an inductor and two silicon diodes may be used to reduce output voltage offset and makes the circuit less sensitive to conductance differences in the output transistors. As illustrated the supply current, i_1 and i_2, flows through inductor L_1. The reactance of L_1 at the data pulse repetition rate (1 MHz in the prototype) is higher than the reflected load impedance; the current flowing through L_1 changes very little from pulse to pulse. The inductor, therefore, acts as a low-power-loss source which drives the output transistors with a current sufficient to saturate Q_1 and Q_2, thus retaining high-power efficiency.

The diodes (CR_1 and CR_2) limit the voltage drop across the inductor to approximately ±1 V during current buildup at the start of transmission and during gaps between pulses. After the direct current builds up, the ac voltage drop across L_1 becomes small (±0.3 V) and remains low as the inductor regulates current during successive pulses.

This work was done by C. Earle Theall of The Singer Co. for **Johnson Space Center.** *For further information, Circle 29 on the TSP Request Card.*
MSC-14933

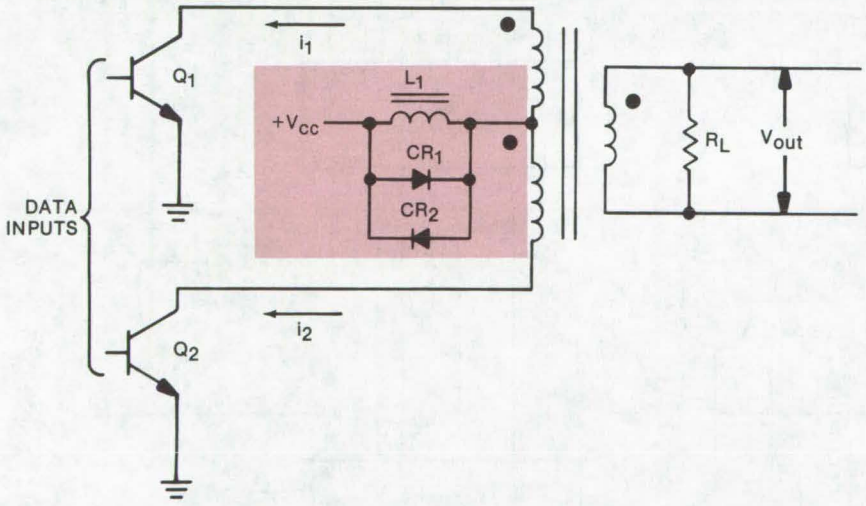

Voltage-Offset Reduction inductor and diodes are common components having an inductance of 250 μH and forward voltage drop of 0.6 V, respectively. At a pulse repetition rate of 1 MHz, choke reactance is 1,500 ohms; V_{out} is 15 V peak.

Binary/BCD-to-ASCII Data Converter

Easier to expand and troubleshoot
than ROM-implemented converters

Goddard Space Flight Center, Greenbelt, Maryland

A new digital data converter inputs multiple precision binary words, converts the data to multiple precision binary-coded decimal (BCD) data, and routes these data back to the computer. The converter accepts two computer words from a 16-bit minicomputer (32 bits total) and converts them to 80 bits of binary-coded decimal standardized (ASCII) data. Compared to previous data converters, this method reduces the required computer software, time, and memory.

The new converter can readily change its conversion base. Unlike prior converters which use a read-only memory (ROM) dedicated to base 10 only, the converter base can be readily changed without the need for a new gate structure for each base changeover.

Each decade of the converter, as partially illustrated, consists of a 7483 4-bit adder, a 74L95 4-bit parallel-in/parallel-out right shift register, and one-third of a 74H11 AND gate. The 7483 continually adds 3 to the contents of its associated shift register. If the contents are 4 or less, the most significant output bit is zero. If the contents are 5 or more, this bit is one.

The bit state controls the mode of the associated register. If the bit is one, then the sum of 3 plus the contents of the register is replaced but shifted one bit to the right. The least significant bit is either shifted in serially or loaded in parallel.

The support software has optional leading zero suppression and stores

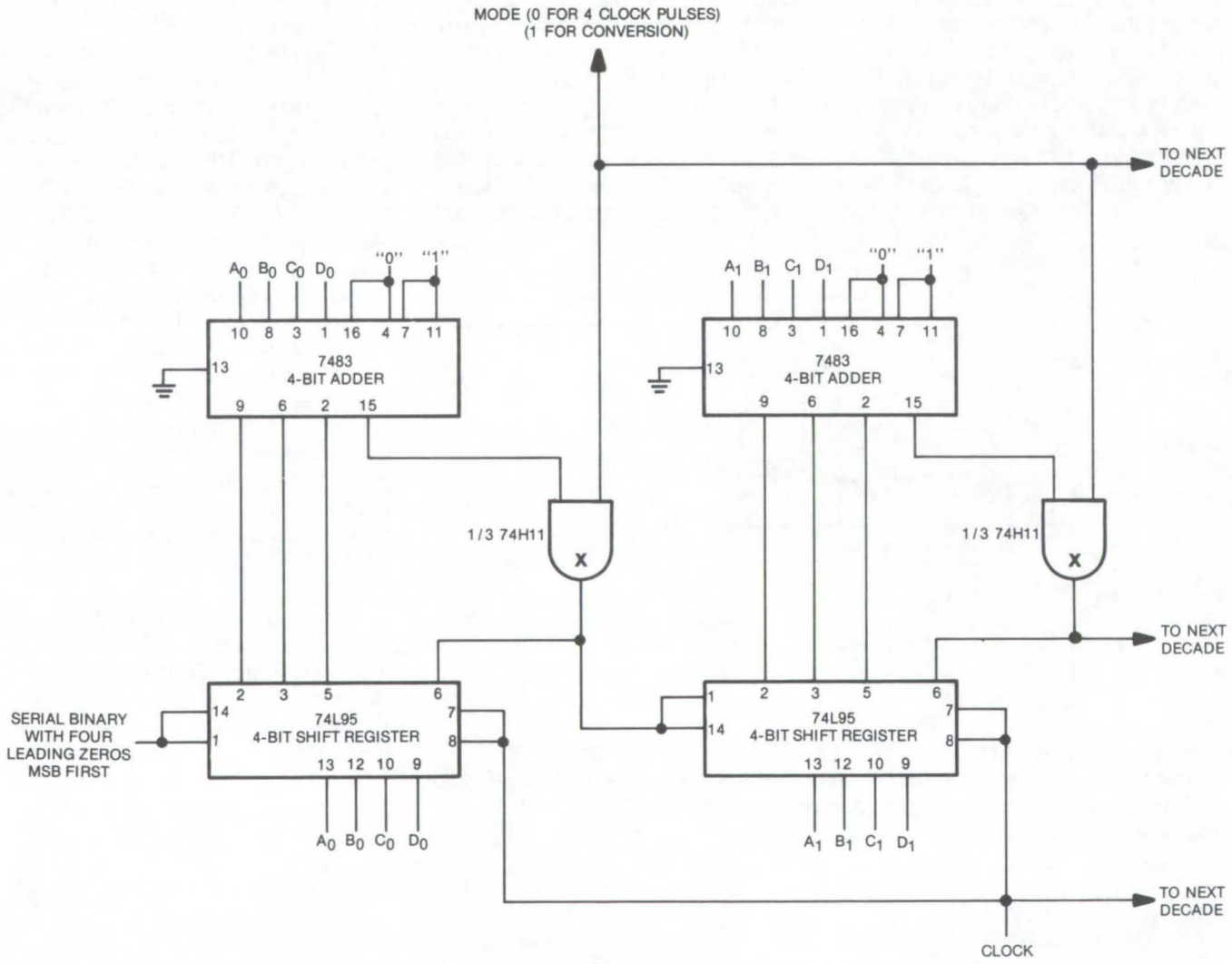

Two Decades of the Data Converter are shown to indicate how the 7483 controls the shift register in such a way as to be parallel loaded or shifted one place to the right.

the results where desired and requires approximately 100 locations of memory depending on the computer which is interfaced to this converter. The actual conversion time for 32 bits is 72 μs, and the range is zero to (2^{32}-1). The master clock frequency is 500 kHz, conversion time is 36 pulses of this clock. If clock frequency is increased conversion times (using faster registers) as low as 10 μs are possible. The total time to execute one complete passthrough and software for a 32-bit conversion and zero suppression is about 240 μs.

This work was done by Anthony J. Miller of **Goddard Space Flight Center.** *For further information, Circle 30 on the TSP Request Card.*

This invention is owned by NASA, and a patent application has been filed. Inquiries concerning nonexclusive or exclusive license for its commercial development should be addressed to the Patent Counsel, Goddard Space Flight Center [see page A8]. *Refer to GSC-12044.*

PN Ranging/Telemetry Transmission

Pseudonoise (PN) ranging and asynchronous binary data are transmitted simultaneously on the same frequency band.

Goddard Space Flight Center, Greenbelt, Maryland

Pseudonoise (PN) codes are currently being used in two-way ranging systems. The coded signal is transmitted from a base station to a remote station where a transponder retransmits the code. At the base station, the phase difference between the transmitted and retransmitted signals is compared to determine the distance between stations. At the same time it is often desirable to transmit information in the form of binary data on the same frequency band as the pseudonoise codes.

Methods previously considered for this either interfered with the ranging function or required that the binary-data rate be limited to about one-tenth the chipping rate of the PN code. (The chipping rate is the rate at which individual pulses in the PN code stream are derived. It is equal to the code repetition rate divided by the number of members in the code.)

A new system can transmit the range-indicating PN codes and simultaneously transmit auxiliary information as binary data at a rate at least on the order of the PN chipping rate. The PN code is modulated by a data stream with a relatively-low bit rate. An independent data stream with a relatively-high bit rate can be transmitted in the same frequency band as the PN ranging code.

The data link between the base and remote stations employs two suppressed-carrier waves. One is quadriphase modulated by both PN ranging codes and a binary signal with a bit rate an order of magnitude less than the PN code chipping rate. The other carrier is quadriphase modulated by a binary signal with a bit rate that is at least on the order of the chipping rate. The frequencies of the two suppressed carriers are relatively close to each other so that their frequency bands overlap.

The two suppressed-carrier waves are linearly combined and are transmitted to a receiving station. The amplitude of the carrier wave with the PN ranging is controlled so as not to degrade the detectability of the second (auxiliary-information) wave at the receiving station. The auxiliary information (high-bit-rate binary data) modulated on the second carrier is coherently detected to allow recovery of the two modulation signals. The lower-bit-rate binary signals on the PN ranging carrier are recovered by a pair of matched filters at the receiver. The filters include a means of deriving the transmitted pseudonoise codes.

The pseudonoise codes derived at the receiver are mixed with the received signal to increase the amplitudes of the two data sources modulating the PN ranging signal and to make its amplitude greater than that of the second (binary-data) signal.

This work was done by L. F. Deerkoski of **Goddard Space Flight Center.** *For further information, Circle 31 on the TSP Request Card.*

This invention is owned by NASA, and a patent application has been filed. Inquiries concerning nonexclusive or exclusive license for its commercial development should be addressed to the Patent Counsel, Goddard Space Flight Center [see page A8]. *Refer to GSC-12017.*

Receiver Performance Evaluator

Signal-to-noise ratio is estimated and bit errors in Manchester-encoded data streams are detected, using a microprocessor-based test set.

Caltech/JPL, Pasadena, California

A signal-to-noise ratio (SNR) estimator and a bit-error rate detector were created for testing the quality of a radio relay subsystem. In both circuits, Manchester-coded test signals are preprocessed to give an NRZ code prior to signal analysis, thus reducing the number of required computational steps.

Figure 1 illustrates the signal-to-noise ratio estimator, a part of the bit-error rate detector. The received signal is first fed to a X1 multiplier to decode the receiver data output and to provide a nonreturn-to-zero (NRZ) pulse-code-modulated (PCM) bit stream. The multiplier changes the output polarity if required, depending on that portion of the code being demodulated.

The multiplier output is a bit stream (signal) with noise; an integrating digital voltmeter (DVM) determines the average (or dc value) of each bit pulse with noise. In order to establish the noise level, the absolute value of the average of many pulses is recorded. The noise of a particular pulse is the difference between the value of that pulse amplitude and the average amplitude of many pulses. A general-purpose digital computer is used to store the absolute level of each pulse sampled.

After each reading, a signal is routed from the DVM via the computer to the SNR estimator. It integrates one bit; the peak value of the integration voltage is then stored long enough for the DVM to execute the proper conversion. Once enough bits have been integrated and their respective levels recorded, an estimation is made of the SNR.

The bit-error detector block diagram and its interface with the radio relay subsystem (RRS) are shown in Figure 2. A bit stream is generated in a test set and is fed to a uhf test transmitter. The receiver under test

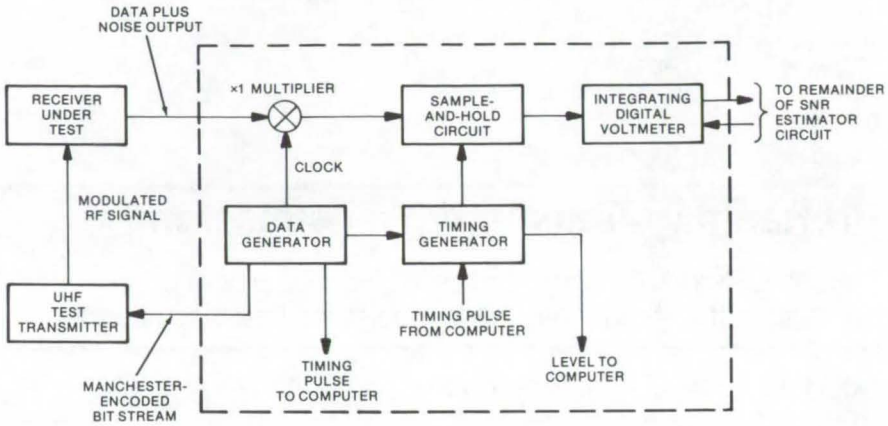

Figure 1. The **Signal-to-Noise Ratio Estimator** uses a X1 multiplier to extract a bit stream (signal) with noise. To determine the noise level, the absolute value of the average of many pulses is recorded. The noise on a particular pulse is determined by subtracting the absolute value of that pulse from the average amplitude of several pulses.

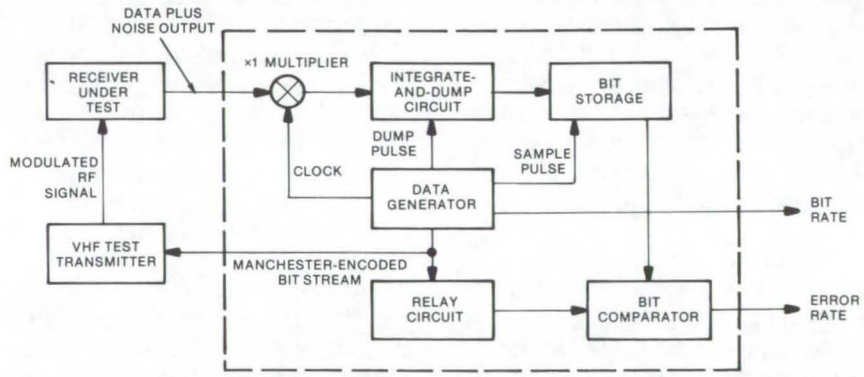

Figure 2. The **Bit-Error Detector** determines the degree of signal distortion of the Manchester-encoded data stream attributable to the receiver under test. The detector does not add any noise or further degrade the data-plus-noise signal.

detects the RF signal and demodulates the data. The bit-error detector first decodes the Manchester-encoded data to generate an NRZ bit stream via the multiplier. After processing, the data stream is fed to an integrate-and-dump circuit. It decides whether a particular bit with noise is logic high or logic low. The integrating time constant is approximately 10 times greater than the actual bit period; the integrator closely approximates a near-perfect bit-stream integration.

The integrate-and-dump circuit acts as a matched filter to recover the signal from the signal-plus-noise generated by the RRS. Once a bit has been recovered, it is stored and compared to a signal which corresponds to what the data should be.

This method determines the bit-error rate and thus the performance of the RRS.

The bit stream, once processed by the integrate-and-dump circuit, is fed to a bit-storage circuit which determines the polarity of the output of the integrate-and-dump at some point in the middle of the output pulse. The following circuit, a bit comparator, compares the received data, as interpreted by the integrate-and-dump, with the transmitted data. These data are delayed by a time equal to the delay in the received-data path. The bit comparator outputs a pulse only when compared pulses differ or if an error exists. Thus, counting the errors over a period of time and dividing by the number of bits transmitted over the same period yield the bit-error rate.

This work was done by Joseph A. Cusack and Harold R. Meyering of Motorola, Inc., for **Caltech/JPL.**
For further information, Circle 32 on the TSP Request Card.
NPO-13701

Concatenated Algebraic Decoder

A coding/decoding technique for manipulating information in digital data streams.

Lyndon B. Johnson Space Center, Houston, Texas

A new technique for manipulating digital data consists of mating two separate coding/decoding methods to produce a hybrid inner-code/outer-code system. The hardware to implement the technique has also been developed. Interactive digital circuitry is used to manipulate casually-related digital data.

The inner code consists of an (8,4) orthogonal code. This code may be regarded as a (7,4) Hamming Code augmented by an overall parity-check bit (the last bit in each word). Thus, to correct one error, the decoder need only determine the three-bit Hamming Code syndrome ($p_1p_2p_3$) from the first 7 code-word bits. If the syndrome is all zeros (000), either no errors have occurred or if the code word contains an odd number of "one's," the overall parity bit is in error (excluding, of course, the possibility of three or more errors). In either event, the information bits (bits 1, 2, 3, and 5) can be assumed to be correct.

If the syndrome is other than all zeros, it will uniquely identify the location of the error (again provided only one error has occurred). A logical combination of the syndrome bits can then be used as the error corrector. (If the error is not in an information bit, of course, no correction is required.)

Thus if the word contains no errors, no correction is made. If it contains either one or two errors, they are corrected. If the word contains three or more errors it is rejected. A total of 1/60th millisecond is available for carrying out the two steps needed to decode each of the inner code words. These decoded words then constitute the four-bit symbols of the outer code. These symbols are shifted serially in groups of 15 to the outer-code decoder shift register.

Since only erasures are to be corrected in the outer-code decoder, it can be made relatively simple. When the code word contains at most two erasures, it is always possible to shift the code word cyclically until one erasure appears at either the 4th or 9th symbol position and the other appears at the 10th, 11th, 12th, 13th, or 14th position. In the absence of either erasures or errors, any nine consecutive symbols of a (15,9) Reed-Solomon Code define the next succeeding symbol. If one of these nine symbols is an erasure, the tenth symbol then uniquely determines what these symbols must be. But this is precisely the situation when the code word is cyclically shifted as described above.

If the code word contains errors as well as erasures, of course, the corrected erasures may be in error. If the number of erasures plus errors is six or less, however, the distance properties of the code guarantee that the resulting corrected word will not be a code word and, hence, that some of the parity-checks must fail. This event can therefore be detected by shifting the code cyclically fifteen times (i.e., fifteen one-symbol shifts), and checking each time to see whether or not all the parity-check relationships are satisfied. Actually, while only six shifts are required, it is convenient to return the code to its original position.

Both erased symbols will be replaced by the time two complete cycles (30 shifts) have been completed. Then the corrected word is shifted fifteen more times. If any of the parity checks fail during this last step, or if more than two erasures are observed, the reject flip-flop is set and the decoded word is rejected. Otherwise it is accepted as a valid word. This completes the decoding operation. The decoded pair of command words can then be read out serially (or on a 4-bit byte basis) from the 9th column of a shift register. This can be done while the first nine symbols of the next code word are being read in.

This work was done by Raytheon Co. for **Johnson Space Center.**
For further information, Circle 33 on the TSP Request Card.
MSC-14058

Oral Annunciator With Programable Vocabulary

The basic vocabulary is 4 spoken words, expandable to 28.

Lyndon B. Johnson Space Center, Houston, Texas

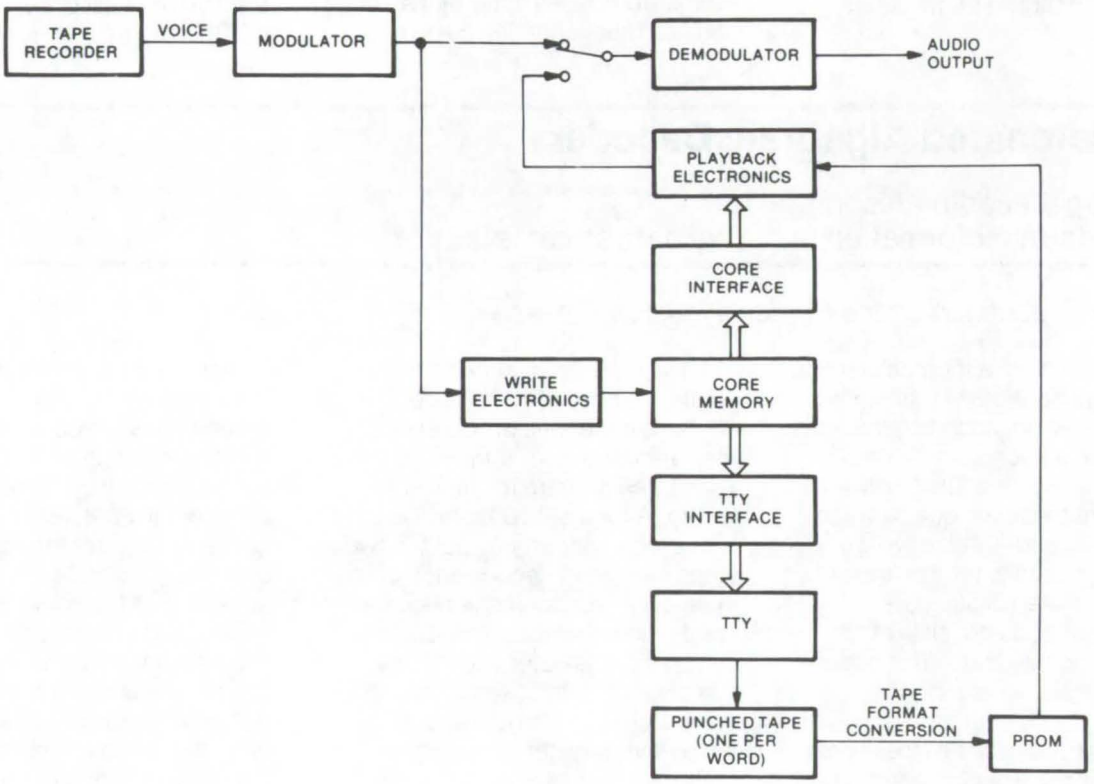

In the **Oral Annunciator,** a voice (analog) signal is converted to its digital equivalent and stored in a solid-state memory. Upon command, the memory becomes part of the annunciator system which includes other digital logic, a digital-to-analog converter, and an audio amplifier.

An oral annunciator system employing delta-squared modulation (D^2M) converts analog voice signals to an equivalent digital format and then stores the digital speech in a solid-state nonvolatile memory. The stored words are selectively reconstructed upon demand, using a delta-squared demodulator to reform the speech signals. The prototype annunciator has a basic vocabulary storage capacity of 4 spoken words, but the capacity can be increased to 28 words if a read-only memory (ROM), rather than the presently-used programable read-only memory (PROM), stores the digitized words.

A block diagram of the annunciator is illustrated. The process of word generation consists of:

1. Encoding the word waveform;
2. Storing the word bit stream in the core memory ("write electronics");
3. Playing back the stored-word bit stream from core via memory interface, ("playback electronics");
4. Dumping the digitized word through the teletypewriter (TTY) interface onto punched tape (either 4K or 6K bits long for the present vocabulary size);
5. Programing the solid-state memories for each word; and
6. Inserting the PROM's into the playback electronics for word testing.

The playback electronics implement the message selection by concatenating the bit streams representing each spoken word in the message and feeding the bits in a serial data stream to the demodulator. Control logic cycles the playback unit through 10 repetitions of any combination of 2-word messages by providing the timing signals that coordinate the logic functions. The logic functions include the PROM's, address, and counting logic.

This work was done by Don Paslay and Paul Wong of The Garrett Corp. for **Johnson Space Center.** *For further information, including a discussion of message synthesis techniques and breadboard development, Circle 34 on the TSP Request Card.*
MSC-14798

Signal Processing and Display for Electrochemical Data

A compact and inexpensive system automatically measures metabolic byproducts during micro-organism detection.

Langley Research Center, Hampton, Virginia

An electrochemical method for detecting micro-organisms, based on a linear relationship between initial cell concentration and time of molecular hydrogen (H_2) detection, was described in Tech Brief B73-10523, "Detecting and Measuring Metabolic Byproducts by Electrochemical Sensing." While the system described is very efficient and accurate, it does have drawbacks in routine general use: The recorder is expensive and bulky, and an operator must read and manually record the reaction end point.

A new, compact, and inexpensive, signal-processing and display apparatus alleviates these drawbacks. It automatically determines the reaction end point and displays the lag period in hours and minutes or directly in cell concentration. A multiplexed analog signal output, which is suitable for display on a strip-chart recorder or similar device, permits the operator to check out all channels and provides a permanent record of events. The unit can also be interfaced with a computer.

This system requires two electrodes, a standard pH reference electrode and a platinum cathodic electrode. Alternatively a combination redox electrode can be used in a container with a nutrient medium suitable for microbial growth along with the sample to be tested. The samples could be from a variety of sources where interest is in detecting and enumerating the number of micro-organisms (e.g., a sample of water for coliforms or a urine sample from a case of suspected urinary tract infection).

The electrodes are connected to an amplifier which provides the required high impedance electrode interface. The amplifier voltage gain is needed to drive the analog-to-digital (A-to-D) converter, the up/down binary counter, and the digital-to-analog resistance ladder. A clock provides operating pulses to the A-to-D converter at a rate slow enough to make the system immune to a noise spike. (This low operating rate forms a rudimentary digital filter.) The clock also drives an 80-minute timer that inhibits the threshold counter for the first 80 minutes of operation. This time period allows the A-to-D converter to capture and track the electrode voltage and also permits the electrode voltage to stabilize after insertion into the broth medium.

A special electronic circuit was designed to sense and record the end point. A counter determines the equivalent number of digital pulses that correspond to 10 mV of input voltage change. When this time is reached, the signal from the counter reverses the timer, which is started when the broth medium is inoculated with the sample; and the timer then runs backward until a count equivalent to 30 mV of electrode voltage is detected by the counter. At this time, the timer stops and displays a time equal to the length of time required for the inoculum to begin the production of measurable amounts of H_2 after inoculation.

The examination of a large number of strip-chart records reveals that the baseline (voltage level after stabilization) occasionally exhibits a slow, steady rise. Such a case can cause the 10-mV counter to reach its count earlier than it would with a flat baseline. To circumvent this problem, a circuit has been added that subtracts one digital count from the 10-to-20-mV counter often enough to prevent the observed nonsteady baseline from adversely affecting the correct detection of 10 mV and then 30 mV.

This work was done by Richard N. Young and Judd R. Wilkins of **Langley Research Center.** *For further information, Circle 35 on the TSP Request Card.*

Inquiries concerning rights for the commercial use of this invention should be addressed to the Patent Counsel, Langley Research Center [*see page A8*]. *Refer to LAR-11922.*

Design of Redundant Systems

An algorithmic approach aids the design of systems with multiple noisy inputs. It could be used with circuits, chemical processes, and machinery design. When transfer functions and parameter tolerances are known, the probabilities of failures for various designs may be determined.
(See page 417.)

Signal Processing and Display for Electrochemical Data

A compact and inexpensive signal processor and display have been developed for the electrochemical detection of metabolic byproducts. Two electrochemical electrodes provide the signals; the new apparatus automatically determines the reaction end point and displays the lag period in time or cell concentration. The apparatus can be used with a standard pH reference anode and a platinum anode or with redox electrodes.
(See page 351.)

Short-Range Biotelemetry System

A compact vhf transmitter will relay EKG, EEG, and EMG data to a receiver located over 25 feet away. The transmitter is an integral part of the biosensing electrodes and has two operating frequencies. It could be used to monitor postoperative patients without cumbersome wires.
(See page 400.)

Microprograming for Real-Time Data Acquisition

Microprogramed firmware asynchronously handles transmit and receive functions.

John F. Kennedy Space Center, Florida

A new microprograming (firmware) technique has a polling interval of 100 μs and satisfies the following requirements:

- It allows full data-bus duplex operation;
- Measurement data can be obtained by polling various hardware interface modules on a 1-megabit data bus;
- Polling functions are transparent to software operations;
- Polling is accomplished on a cyclic basis with a fixed interval between polls;
- Verification of the proper response is performed as part of the receive function;
- The transmit function is able to interrupt the receive function; and
- "Off-the-shelf" processors are utilized.

The firmware package is a trap-initiated microprograming technique that asynchronously handles a transmit-and-receive (T/R) function as shown in Figures 1 and 2. In addition, the microcode traps used to perform the assigned tasks require expansion of the computer direct-memory-exchange (DMX) trap capability to include recognition of a user-implemented trap.

This technique has several distinguishing features. For instance, the time-sequenced polling function can be performed while software tasks are executed in the processor asynchronously. The method also allows software to be used to institute tasks which must run interrupts inhibited for times that would perturbate the fixed polling interval. Finally, the addition of only one user-implemented trap for both operations allows the transmit function to trap out the receive function in order to maintain a prescribed polling interval.

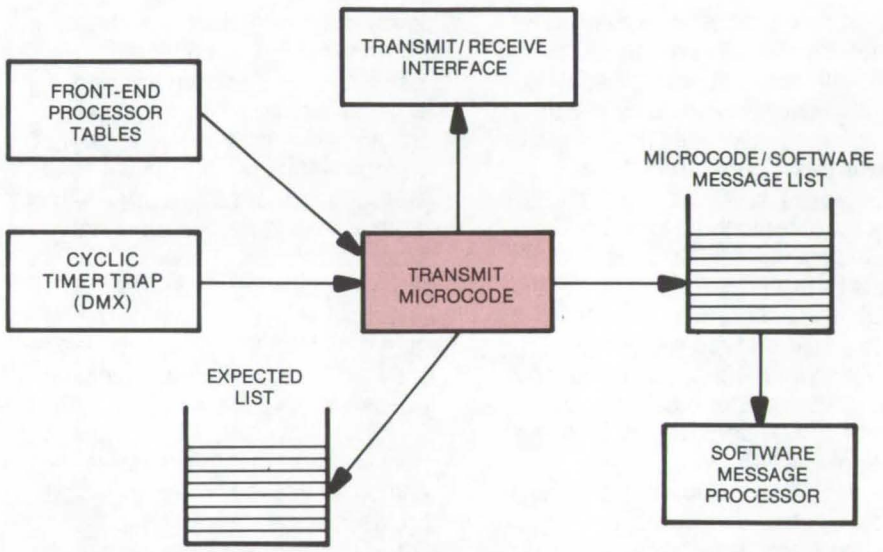

Figure 1. The **Transmit Microcode Trap Logic** is conditioned by a preset clock. A measurement request or issuance of a command is controlled by a set of software-initialized polling tables.

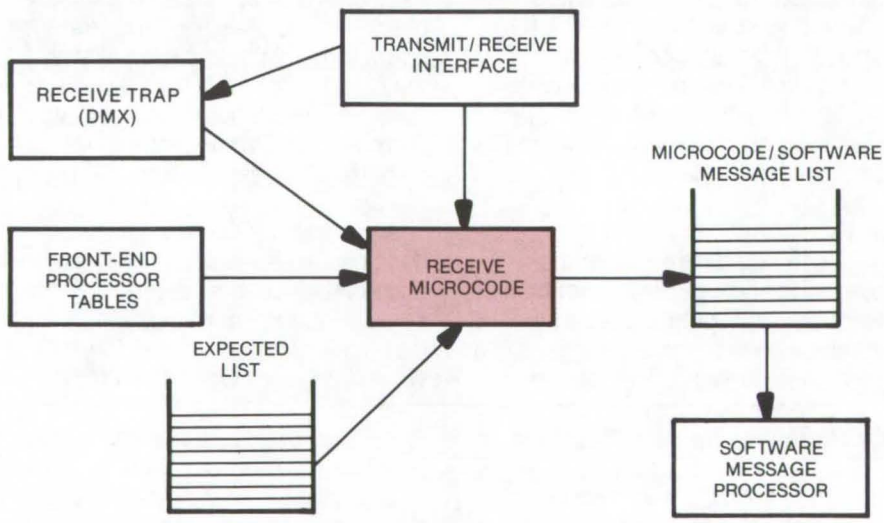

Figure 2. The **Receive Microcode Trap Logic** is conditioned by the transmit/receive hardware when a response is returned on the data bus.

The data bus is controlled by a transmitter/receiver which interfaces with the processor in control. The transmit microcode trap logic, as shown in Figure 1, is conditioned by a preset clock. The operations performed on the bus may be a request for a measurement or the issuance of a command. The sequence of these operations is controlled by a set of software-initialized polling tables. Multiple tables provide for a change of sampling rates.

The receive microcode trap logic, as shown in Figure 2, is conditioned by the T/R hardware when a response is returned on the bus. An input sequence acquires the data and performs certain validity checks. Any resultant errors from these operations are reported to software. Some of the errors, considered catastrophic, cause the microcode to inhibit all further operations on the bus.

This technique may be implemented on any computer system having a user-writable control store and microcode trap logic; it has been implemented in the GSE Front End Processor (FEP) for the Space Shuttle Solid Rocket Booster at the Kennedy Space Center.

This work was done by Frank J. Patella of IBM Corp. for **Kennedy Space Center.** *For further information, Circle 36 on the TSP Request Card.*
KSC-11027

Subcarrier Signal Combiner for Arrayed Antennas

Quadrature correlation for automatic signal phasing and variable delay is used to combine signals for improved signal-to-noise ratio.

Caltech/JPL, Pasadena, California

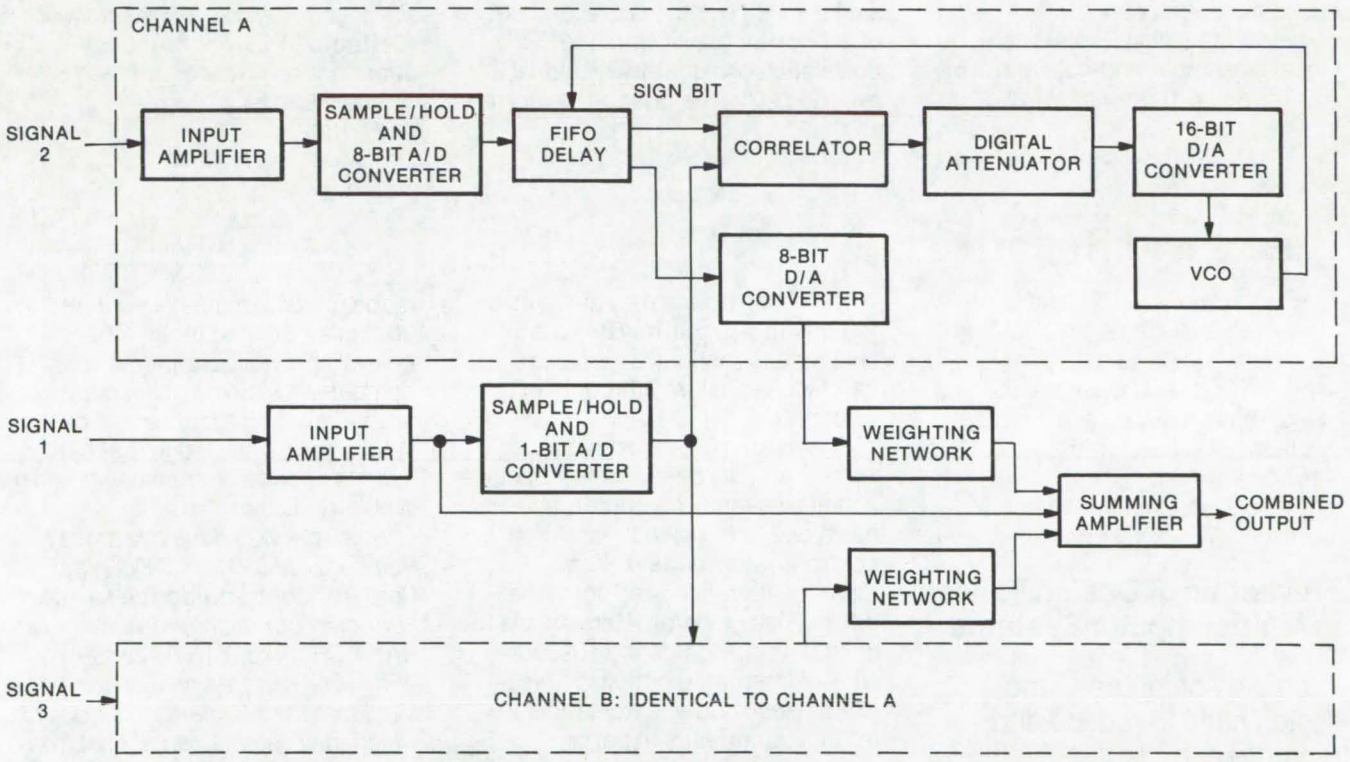

The **Signal Combiner** converts two incoming analog signals to a digital and then quadrature-correlates them against a third digitized signal used as a reference. A 16-bit D/A converter translates the correlation values into an analog voltage that is applied to the input of a VCO which determines the FIFO clock rate and phase-locks the signals to the reference signal. The FIFO output is combined in the summing amplifier to increase the signal-to-noise ratio.

The signal-to-noise ratio (SNR) of a received signal can be improved by receiving the transmission at more than one site and combining these received signals. Differences in transmitter source-to-site distances, however, cause the signal to arrive with a different delay at each station. Further delays, which are fixed but generally unequal, are incurred in relaying the signals to the common combining site. Since the

distance between receiving sites is small (compared to the distance from the transmitter to any one of the sites), the delay differences can be compensated for at the receiving site via a signal combiner with variable delay.

The signal combiner uses first-in/first-out (FIFO) memories to obtain controllable delays of the received signal and quadrature correlation for automatic signal phasing. The combiner adds the subcarrier signals, making synchronization requirements less severe than if received RF or IF signals were to be added. For a system with three receivers, the combiner compensates for the variable delays from each of two of the signals; they are locked in phase and combined with the first (reference) signal.

As shown in the figure, the most delayed signal (signal 1 from the baseband output of receiver 1) is converted to a digital reference signal by sample-and-hold and 1-bit ADC circuits. This signal always arrives at the combiner input later than the other two signals. At the combiner site the three baseband signals are fed to the input of the signal combiner, which delays the signals from receivers 2 and 3 by the amount required to synchronize them with the signal from receiver 1. Once properly phased, the signals are assigned a weighting factor according to their original SNR's and are combined in a summing amplifier. Weighting factors are chosen to optimize the SNR of the sum.

The baseband signals from receivers 2 and 3 are digitized by sample-and-hold and 8-bit ADC circuits. (The 8-bit converter minimizes signal quantization error.) Each is then correlated with signal 1 and then quadrature correlated.

Quadrature correlation is obtained by subtracting the correlation of signal 1 with signal 2 advanced 90° of subcarrier phase from the correlation of signal 1 with signal 2 retarded 90°. The quadrature correlation crosses zero when signal 2 agrees in phase with signal 1 and is therefore suitable as a control function for the delay. A 16-bit digital-to-analog (D/A) converter then translates the digital quadrature correlation values into an analog voltage which is applied to the input of a frequency synthesizer used as a voltage-controlled oscillator (VCO).

The VCO determines the FIFO buffer input clock rate in order to phase lock signal 2 to signal 1. Duplicate hardware locks signal 3 to signal 1. The 8-bit parallel outputs of the FIFO's are converted to analog and combined in the summing amplifier with the reference. In the three-receiver array using this combiner, with two 26-m antennas and one 64-m antenna, the signal-to-noise ratio was increased by 1 dB.

This work was done by Helmut C. Wilck and Robin A. Winkelstein of **Caltech/JPL.** *For further information, Circle 37 on the TSP Request Card.*
NPO-13723

Books and Reports

These reports, studies, and handbooks are available from NASA as Technical Support Packages (TSP's) when a Request Card number is cited; otherwise they are available from one of NASA's Industrial Application Centers or the National Technical Information Service.

Prevention of Design Flaws in Multicomputer Systems

Examples of failures, and design hints to reduce and repair generic faults.

A recent report summarizes research on failure-mode analysis for multicomputer systems where two or more computers may serve as a redundant set. Such systems are subject to generic design flaws that can result in failures throughout a system.

The report discusses failure modes such as data-bus monopolization by a faulty computer, shutdown due to transients, loss of control-system equalization, memory alteration, and software errors. Design parameters shown to be important include the susceptibility of integrated circuits to electromagnetic and electrostatic interference, interfaces of parallel redundant electronic strings, and software completeness.

Examples of types of failures are given, and recommendations are made for design measures to reduce and repair generic faults. The analysis provides a typical computer-switching philosophy for several existing systems and develops basic knowledge that can be used to analyze generic design-flaw problems further.

This work was done by James M. Romberg of McDonnell Douglas Corp. for **Johnson Space Center.** *Further information may be found in NASA CR-147657 [N76-23889], "Prevention of Design Flaws in Multicomputer Systems," a copy of which may be obtained at cost from the National Technical Information Service, Springfield, Virginia 22151.*
MSC-14920

Physical Sciences

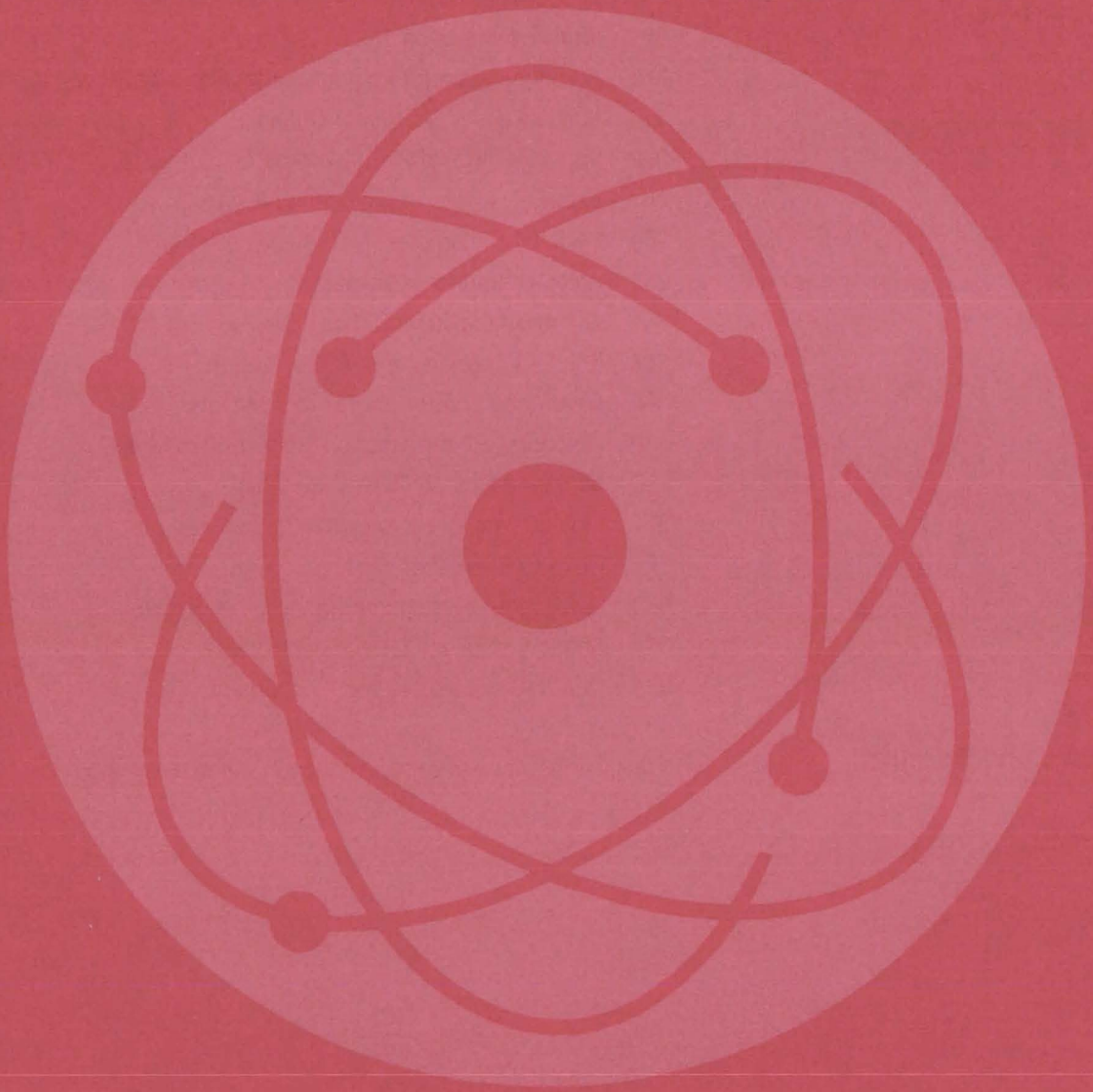

Hardware, Techniques, and Processes

Books and Reports

Computer Programs

Laser Particulate Spectrometer

An instrument with potential applications in air-pollution, clean-room, and particle-size monitoring

Lyndon B. Johnson Space Center, Houston, Texas

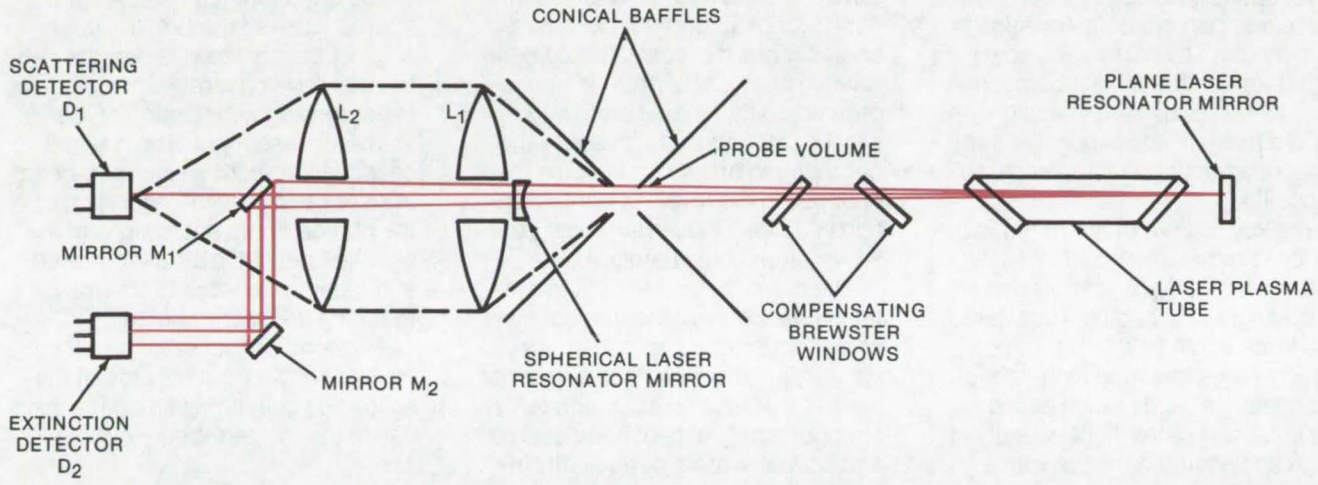

The **Spectrometer Sensor Head** has a laser beam passing through the holes in lenses L_1 and L_2 and onto the extinction detector. A hermetically-sealed laser tube and resonator mirror prevent corona discharge problems during chamber pumpdown.

A laser particulate spectrometer (LPS) has been designed to detect particulate fluxes. A hybrid laser scattering-and-extinction technique is used to measure particle diameters from 0.8 to 2.75 μm and speeds from 0.2 to 20 m/s. Operating pressures range from ambient to ultra-high vacuum, and temperatures range from 77 to 300 K.

Particles to be measured pass through the beam within the resonant cavity of the laser. The laser beam is constrained to operate in a "doughnut" mode (the beam cross section is a bright ring around a dark central spot). As the particles pass through the beam, light is scattered out of the beam thus reducing its effective intensity. Two photodiodes detect the amount of light scattered out of the beam and the reduction in intensity of the beam caused by the passage of the particles. Small particles tend to scatter light, but do not extinguish the laser action by a measurable amount. Large (over 10μm) particles, however, do perturb and extinguish the laser. Both of these effects are related to particle size, and electronic circuitry in the LPS extracts the size information from the photodiode signals.

The single He-Ne laser tube (see figure) is enclosed within a hermetically sealed housing to protect it over a wide range of temperatures and pressures. The laser beam exits through a double Brewster window to preserve beam alinement. The laser-cavity mirror is mounted concentrically in the first scattering-collection lens, and the photodiode detectors are located behind them. Thermostats and heaters embedded within the aluminum body of the housing and black anodize on the exterior surfaces control the temperature.

Data are collected and reduced by routing the signals from the LPS electronics to a multichannel analyzer and calculator. The instrument is calibrated by spraying known-size spherical particles and glass microbeads through the beam.

This work was done by Bruce A. Boyd, Rodney M. F. Linford, and Raymond J. Schmitt of McDonnell Douglas Corp. for **Johnson Space Center.** *Further information may be found in: NASA CR-144375 [N75-29407] "Particulate Contamination Spectrometer, Vol. I, Final Technical Report," a copy of which may be obtained at cost from the National Technical Information Service, Springfield, Virginia 22151. MSC-14969*

Economical Measurement of Particle Concentration

An optical-scattering meter determines particle concentration in liquids.

Goddard Space Flight Center, Greenbelt, Maryland

An optical-scattering meter measures particle concentration in a fluid medium by correlating scattering-angle effects with composition. Its relatively simple design should make it less expensive than present equipment with comparable capabilities.

The key feature of the meter is the ability to measure simultaneously, and in a liquid, light scattered at a small angle (2°) and light scattered at a large angle (90°). The meter distinguishes between high-refractive-index particles, such as inorganics, that scatter light strongly at large angles and particles with a lower refractive index, such as organics, that scatter light at smaller angles. Thus it is possible to detect relative amounts of organic and inorganic contaminants and, with proper calibration, to measure the contribution of various species to changes in the levels of contamination in a river, industrial waste outlet, or other liquid medium.

The meter has three optical systems (see figure). The first consists of pinhole spatial filters, a beam splitter, a calibrated neutral-density filter, and a laser-output monitor. A chopper wheel between the source and optical system periodically interrupts the emitted light. A light-source, passed through the upper edge of the chopper, is detected and used to develop a reference signal to synchronize the detection of the scattered laser light. The neutral-density filter reduces incident-beam irradiance to prevent saturation of the photoelectric detector, and the pinhole filters stop stray-scattered and multiply-reflected light from reaching the scattering cell.

A second optical system detects scattered light from the side of the scattering cell. It has an optical axis 90° to the incident-beam optical axis.

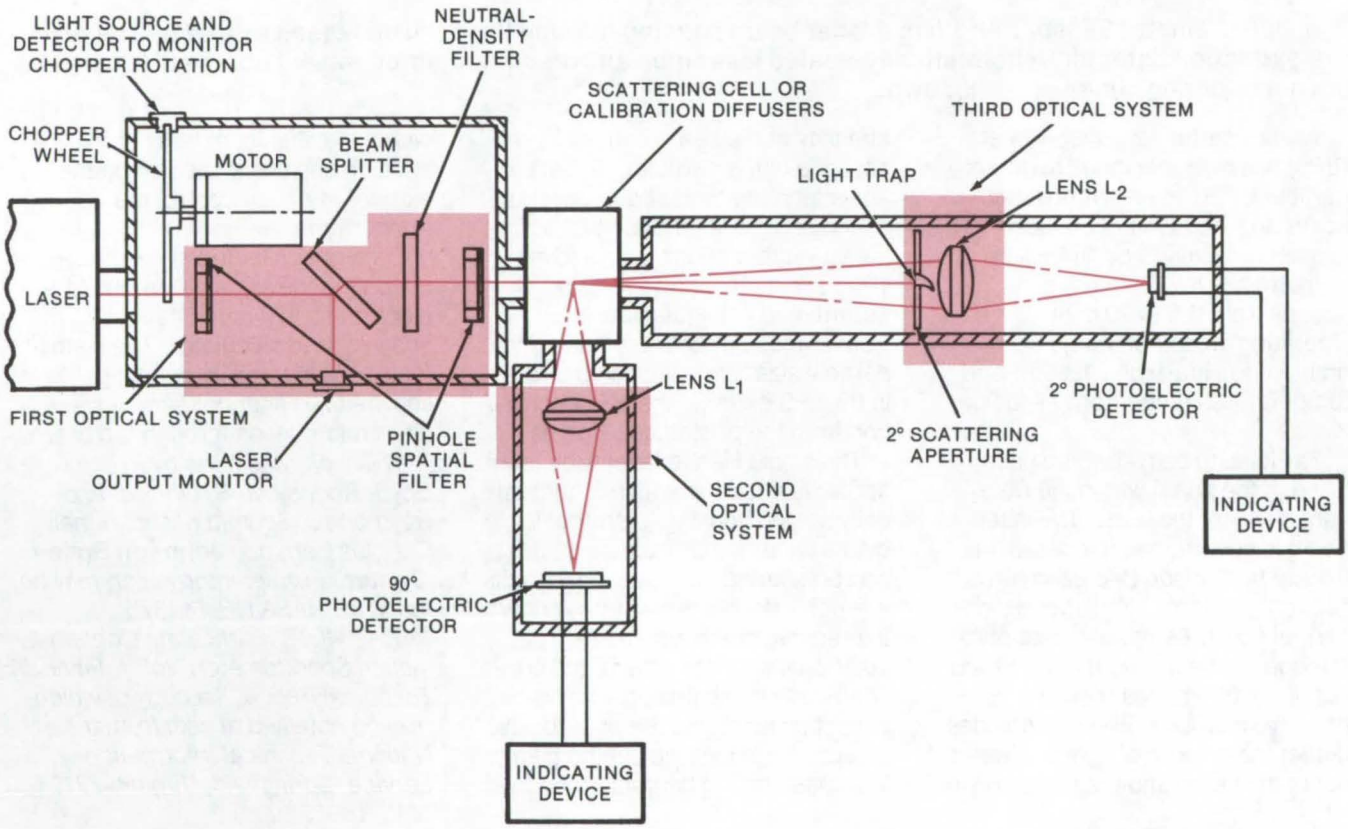

The **Laboratory Scattering Meter** utilizes three optical systems to detect light scattered (by particles in a hydrosol) at 2° and 90° simultaneously. The intensity of the scattered light will vary with its angular relationship to the optical axis of the incident beam. The light is detected by photoelectric detectors (silicon diodes) that generate an electrical signal proportional to the intensity of the light received. Light linearly transmitted by the hydrosol through the rear window is largely absorbed in a light trap. The light trap is a bent cone-shaped container having one open side and black internal walls.

A third optical system, consisting of a radiant-energy mask with a circular aperture and a focusing lens, detects the scattered light from the rear of the scattering cell and projects it through an annular aperture onto a focusing lens for imaging at a second photoelectric detector. The scattered rays from the aperture are at an angle of 2° to the incident beam.

The photoelectric detectors are connected with separate indicating devices. Each has a galvanometer for synchronously recording the amount of light received by the associated photoelectric detector. A Mie theory computer program was used to calculate the theoretical volume-scattering function for suspensions of latex spheres.

This work was done by W. R. McCluney of **Goddard Space Flight Center.** *For further information, Circle 38 on the TSP Request Card.*

This invention is owned by NASA, and a patent application has been filed. Inquiries concerning nonexclusive or exclusive license for its commercial development should be addressed to the Patent Counsel, Goddard Space Flight Center [see page A8]. *Refer to GSC-12088.*

Pinhole Diffraction Filter

A diffraction filter, analogous to an electronic attenuator, has many applications including use as a nondegradable UV filter.

Goddard Space Flight Center, Greenbelt, Maryland

A multistage diffraction filter consisting of a coalined series of pinholes on parallel sheets has been proposed as a nondegradable UV filter. Optical elements subject to strong UV radiation over a period of time degrade in transmission or reflection, thereby resulting in sensitivity degradation. The filter could be used to reduce the radiation flux to a low level and would not itself be degraded by the radiation.

A beam is attenuated as each pinhole diffracts the radiation in a controlled manner into a divergent beam, and the following pinhole accepts only a small part of that beam. As an alternative to pinholes, slits could be used to give finer control of the attenuation and color balance. Using the number of stages and d^2/l (where d is pinhole diameter and l is the distance between pinholes) as design parameters, the spectral shape and total attenuation at a given wavelength can be specified. More precise specifications can be met by varying hole diameters between stages or using slits.

Pinholes (controlled circular apertures) or slits are made by photoetching thin metal sheets. Holes down to less than 5 μm can be made in nickel sheets 5 μm thick. Plating can give a finer control on hole diameter, and sheets may be stacked in proper alinement by photoetching holes for dowel pin location. One hole and one slot per sheet would be a correctly constrained location, and the sheet may be clamped between two frames. The sheets in their frames are connected by doweling together the frames so that the pinholes lie in a straight line. A typical three-stage filter with 25 μm diameter apertures has a plate spacing of 0.5 cm. For n stages of attenuation, n+1 sheets are required.

Applications of such a filter would be as follows:

a. A means of reducing radiation flux levels in the selective observation of vacuum ultraviolet processes and for photon-counting instrumentation;
b. A calibration filter to calibrate photon-counting systems by comparison with standard detectors which operate in a current mode (diodes, ionization chambers);
c. A low-wavelength pass filter with little attenuation at a chosen wavelength and rapid cutoff at longer wavelengths (relatively large pinholes and many stages would be required); and
d. A color-balancing filter where a decrease of radiation flux to shorter wavelengths from a source is compensated for within a chosen wavelength range.

This work was done by Bruce E. Woodgate of **Goddard Space Flight Center.** *For further information, Circle 39 on the TSP Request Card.*

GSC-12120

A Forward-Scatter Polarimeter for Chemical Analysis

An instrument can be used for environmental, spectroscopic, and meteorological analysis.

Caltech/JPL, Pasadena, California

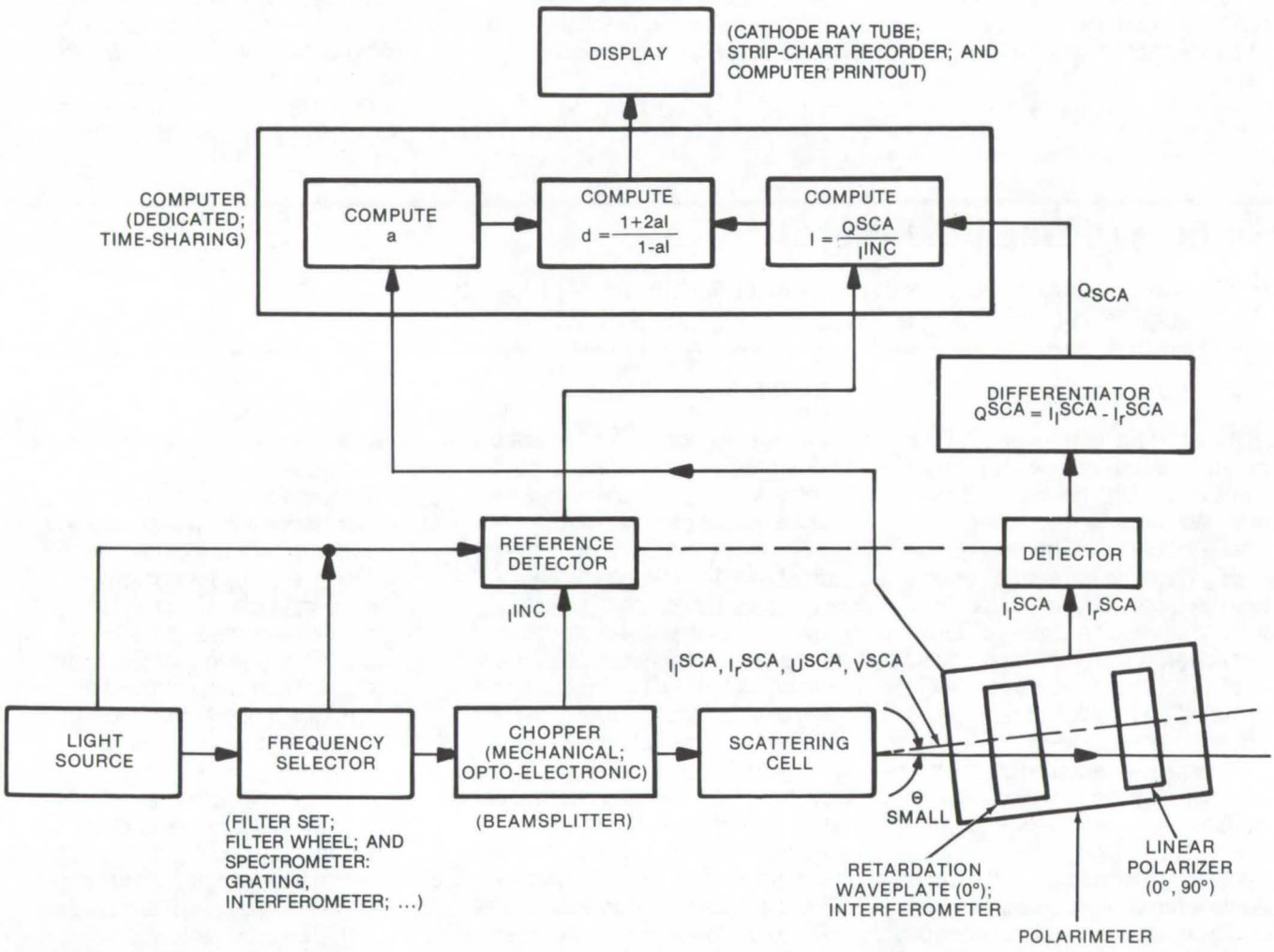

The **Forward-Scattering Polarimeter** measures two states of orthogonal polarization parallel and perpendicular to the scattering plane, defined by the directions of incident and scattering light, to determine the (effective) gaseous depolarization factor.

The properties (size and identification) of polluting atmospheric particles are determined from the scattering (in the near-forward directions) of light illuminating the particles. Particles are usually embedded in host gases that also scatter incident light along the same directions. Therefore particulate properties (refractive index and particle size) are not easy to determine. A new forward-scatter polarimeter can determine the physical structure of molecules and molecular systems in the presence of an arbitrary number of chemically-different scattering particulates. Once the properties of gases are known, their effects can be evaluated, and their contribution to forward-scattering light eliminated. No mechanical separation of the gases from the particles is required, and the instrument complements particle-size spectrometers and refractometers (based on the forward-scattering principle).

The depolarization factor of a gas embedded in a mixture of a number of different species of scattering particulates is determined. In the case of several different gaseous species, an effective depolarization factor describing the overall depolarization effects of all the gases is provided (independent of the similar factor for polluting particles).

A photopolarimeter (see figure) is used to evaluate two orthogonal states of polarization of scattered light. The differences between these two determinations (in the very near forward direction) normalized to the total intensity of incident light is essentially independent of the parti-

cles present and is determined from the ensemble-averaged depolarization factor of the host gases. The polarimeter, a differentiator, a computer, and a frequency band selector are used in the case of light of known intensity from a distant source. When a local source of unpolarized (natural) light is used with a sample cell, the chopper and the detector are used to measure the intensity of the local source.

This work was done by Alain L. Fymat of **Caltech/JPL.** *For further information, Circle 40 on the TSP Request Card.*

This invention is owned by NASA, and a patent application has been filed. Inquiries concerning nonexclusive or exclusive license for its commercial development should be addressed to the Patent Counsel, NASA Resident Legal Office-JPL [see page A8]. Refer to NPO-13756.

Stabilized Nd:YAG Laser Output

A feedback loop is used to control the optical path length in the cavity.

Goddard Space Flight Center, Greenbelt, Maryland

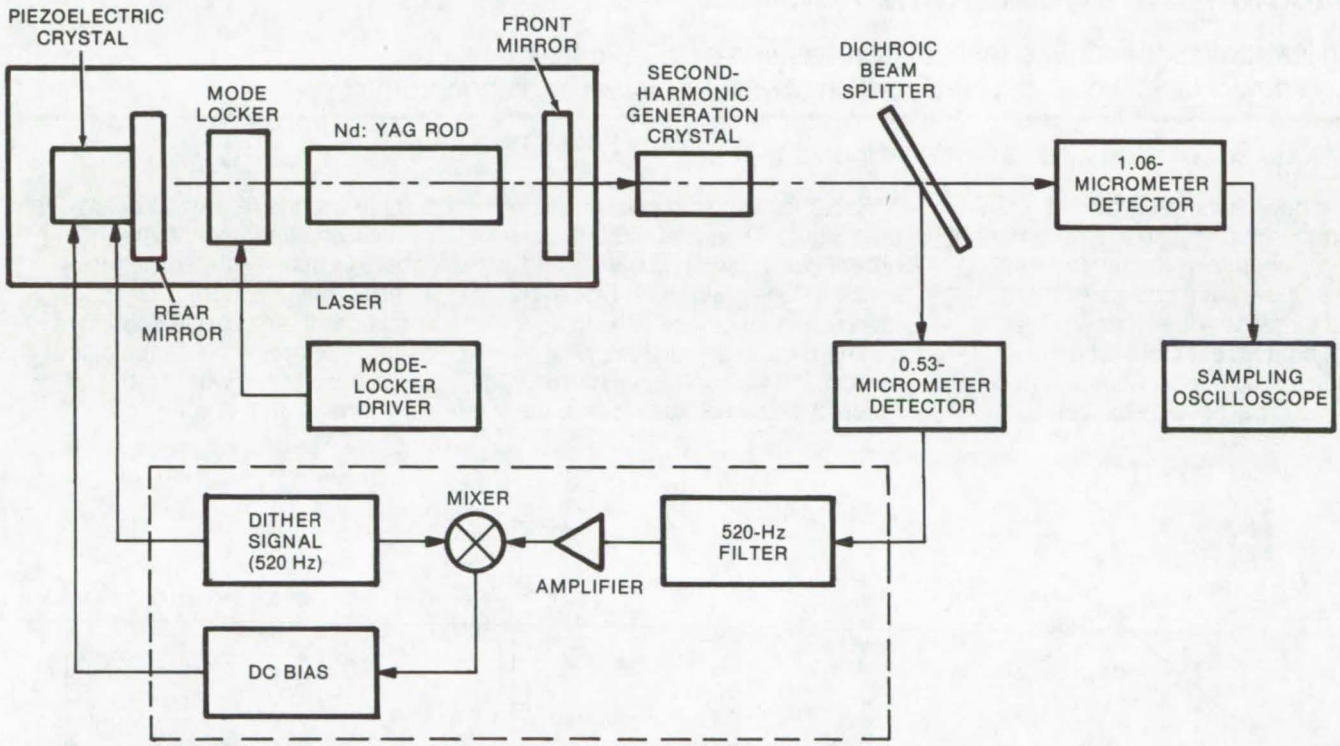

Stabilization System for Mode-Locked Nd:YAG Laser consists of a feedback-loop-controlled piezoelectric crystal attached to one of the reflectors to vary the optical path length within the laser cavity.

The stability of amplitude and repetition rate of mode-locked Nd:YAG laser pulses is of importance in pulsed laser communication systems. A way of stabilizing the amplitude and repetition rate has been developed by controlling the laser length through a feedback loop. The average second harmonic (of the fundamental 1.06-micrometer laser radiation) is detected by an integrating detector. The amount of second-harmonic power depends on the match between the optical length of the laser cavity and the mode-lock frequency. This length is controlled by a feedback loop.

The Nd:YAG laser (see figure) is in a double elliptical cavity and is operated in the TEM_{00} transverse mode. The rear mirror of the laser is mounted on the piezoelectric crystal. The fundamental 1.06-micrometer laser beam is externally focused into a barium sodium niobate crystal where it is partially converted into its second harmonic at 0.53 micrometer. The temperature of the barium sodium niobate crystal is maintained at its optimum second-harmonic phase-match point to within ±0.005° C, which eliminates any variation of power due to temperature changes in the crystal. The beam exits from the crystal, is collimated, and is then split by a dichroic beam splitter.

A small ac voltage (520 Hz) is applied to the piezoelectric crystal, causing the rear mirror to dither through a small change in length and resulting in a small ac variation in

the second harmonic. After filtering, the output of the second-harmonic detector is amplified and phase compared to the dither signal applied to the piezoelectric crystal. An error signal is fed back, changing the dc bias applied to the crystal and maintaining the laser cavity at a constant length, and stabilizing the mode-locked pulses.

An advantage of the technique is that relaxation oscillation noise is discriminated against by detecting the second-harmonic optical radiation power at the dither frequency rather than by detecting pulses at the mode-locked frequency. Furthermore, the frequency of the mode locker can be corrected to account for any frequency shifts, since the laser system is capable of retuning its length to match the new mode-locked frequency. Therefore, the receiver will continue to detect pulses at an unchanged frequency. The laser can also be stabilized immediately upon being turned on, thus eliminating power consumption during a warmup period.

This work was done by John Osmundson of **Goddard Space Flight Center.** *For further information, Circle 41 on the TSP Request Card.*

This invention is owned by NASA, and a patent application has been filed. Inquiries concerning nonexclusive or exclusive license for its commercial development should be addressed to the Patent Counsel, Goddard Space Flight Center [see page A8]. Refer to GSC-11571.

Vacuum-Ultraviolet Reflectometer

An instrument for surface reflectivity measurements — in fusion research, high-power laser work, and construction of spectrometers or monochromators

Lyndon B. Johnson Space Center, Houston, Texas

A new vacuum-ultraviolet reflectometer permits the measurement of hemispherical reflectance from 600 to 3,000 Å. At these wavelengths all but extremely-fine optical surfaces are diffuse reflectors, and measurement of the hemispherical reflectance is particularly difficult.

Radiation from a monochromator (see Figure 1) passes through an order filter, a radiation baffle, and a specially-designed three-blade rotating chopper before striking a platinum-coated, split spherical mirror. The split spherical mirror focuses the sample beam onto the sample and the reference beam onto the wall of a fluorescent integrating sphere [a stainless-steel sphere 4 in. (10 cm) in diameter that is sprayed with an opaque coating of barium sulphate reflectance paint and is overcoated with 3 mg/cm² of para-terphenyl, a fluorescing

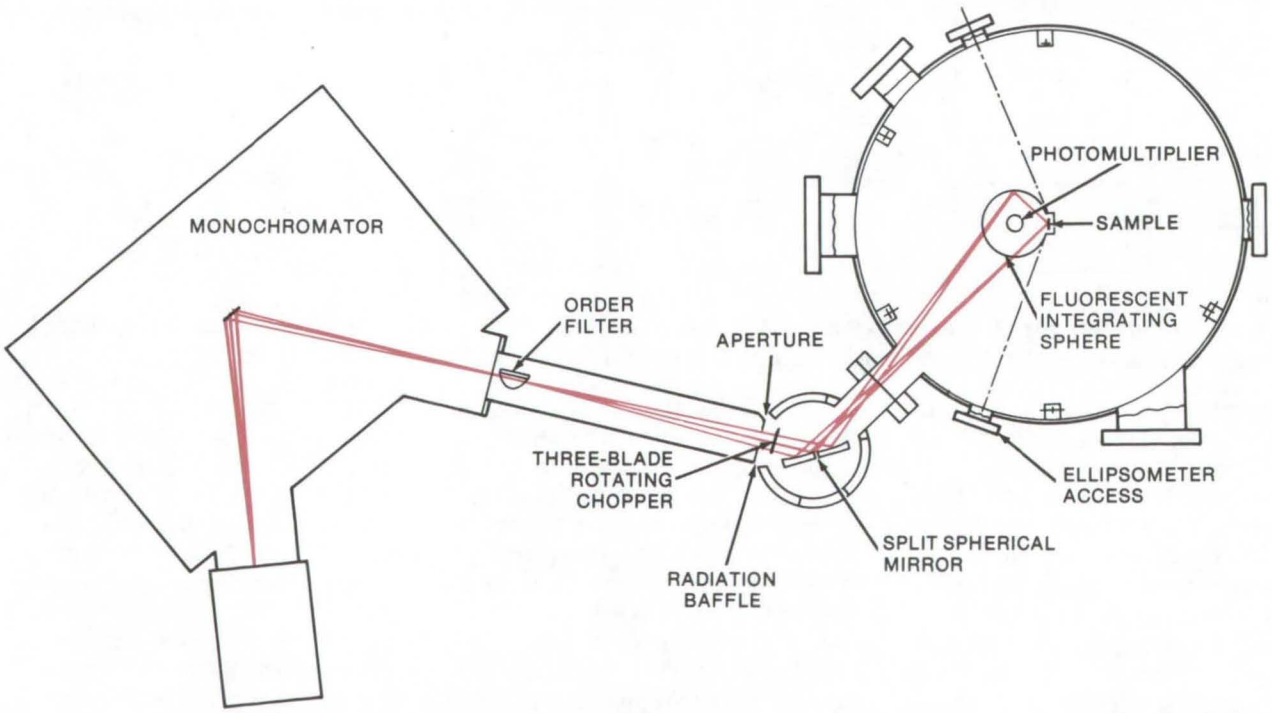

Figure 1. **Vacuum-Ultraviolet Reflectometer:** The baffle, three-blade chopper, and split spherical mirror transmit an alternating dual beam into the integrating sphere. The alternating beams (a reference beam and a sample beam) are detected by a high-gain photomultiplier and a modified logarithmic ratiometer (not shown).

material]. The alternating beams are detected by a high-gain photomultiplier, and the modified logarithmic ratiometer provides a reflectance analog output for this scanning system.

A key feature of this system is the alternating dual beam provided by the baffle, the three-blade chopper,

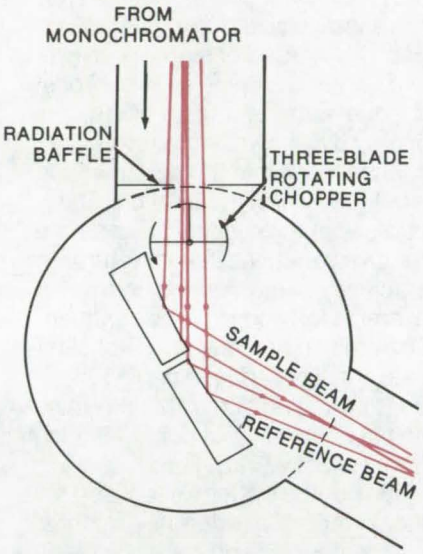

Figure 2. The **Key Elements of the VUV Reflectometer Optical System** which transmit a dual beam into the integrating sphere are the rotating chopper, spherical mirror, and radiation baffle.

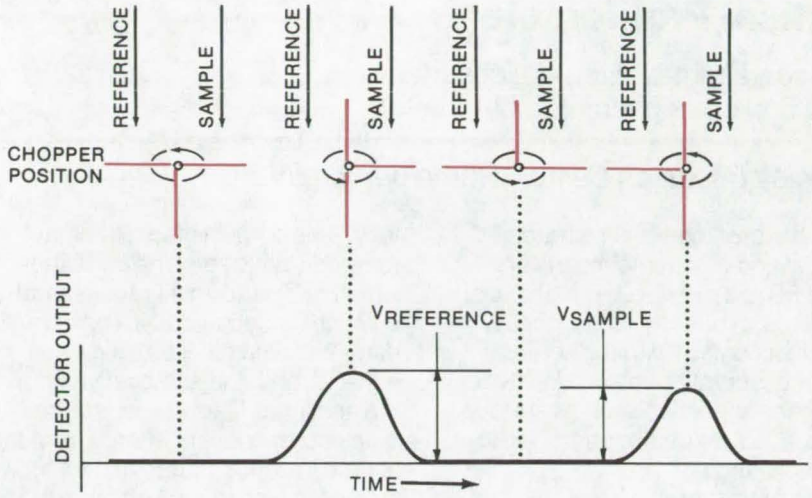

Figure 3. The **Output of the VUV Reflectometer System** is a reflectance analog output from a modified logarithmic ratiometer for each position of the rotating chopper.

and the split spherical mirror (see Figures 2 and 3). These components combine to provide a highly-efficient dual-beam system, using only one mirror in each beam. In the vacuum-ultraviolet region, especially below 1,200 Å, mirror coatings severely attenuate the available radiation; thus the number of such components must be minimized. This high degree of efficiency is essential when measurements of hemispherical reflectance are needed because an integrating sphere, an inherently low-efficiency optical device, is required in such a system.

The system is a fully-automatic, ratio-recording, scanning, vacuum-ultraviolet reflectometer capable of measuring hemispherical reflectance. It is easily adaptable for hemispherical transmittance measurements.

This work was done by Thomas H. Allen, Charles F. Dillow, and Rodney M. F. Linford of McDonnell Douglas Corp. for **Johnson Space Center.** *No further documentation is available.*
MSC-14995

External Heater for Cryogenic Vessels

A simple technique prevents icing of vessel walls.

Lyndon B. Johnson Space Center, Houston, Texas

Thermal insulation is usually applied to the exteriors of cryogenic storage tanks. External heaters can be used around the insulation to increase the tank-wall temperature and prevent icing of the walls by water or liquid nitrogen. The use of an external heating film prevents condensation and icing. When used in conjunction with a nitrogen purge system, this film increases the gas temperature, thereby preventing the gas from chilling the equipment to a temperature below acceptable levels. The technique may be useful for large cryogenic storage vessels such as those found in steel mills and hospitals. The proposed heater system includes a vacuum-deposited layer of gold sandwiched between two layers of Mylar. The Mylar acts as a carrier for the film and prevents damage.

This work was done by G. J. Wennagel of Grumman Aerospace Corp. for **Johnson Space Center.** *For further information, Circle 61 on the TSP Request Card.*
MSC-14056

Optical Profilometer

Noncontact measurement of surface area and other geometric parameters

Langley Research Center, Hampton, Virginia

In the profilometer illustrated, optical and electronic means are used to measure three-dimensional surfaces. It directly, and without physical contact with the surface under observation, determines various characteristics such as surface area, absolute depth, and point-to-point distance.

The optical profilometer, as shown, consists of an optical scanning subsystem, two light detectors with associated amplifiers, an analog divider, and an adjustable nonlinear function generator. The optical subsystem consists of a light source, a common lens, a scanning mirror, a movable sample platform, a sample light detector, a reference light detector, various beam splitters (to enable the use of coincident light paths), and apertures for the control of defocus sensitivity in the sample light detector. The output of the entire system is a voltage which is directly proportional to incident light on the sample and can be calibrated fully. This output is fed to a data recorder, a plotter, or a computer which can perform all required calculations automatically. The computer can also fulfill the purposes of either or both the analog divider or the nonlinear function generator.

In operation, light energy from the source is concentrated and imaged by the lens into a spot on the surface of interest. As the surface is moved away from perfect focus, the spot increases in size (defocuses) while the total energy in the spot remains virtually constant. Thus the energy density (watts/cm^2) decreases in the spot. The lens then reimages the spot in various degrees of defocus onto the two detectors, with the energy going to them divided by the beam splitter. This second pass of the energy through the lens further defocuses the spot, but as a result of the apertures in each light detector path, the amount of defocus for each is different.

Since the light detectors have a certain fixed size, the total energy they receive decreases as the spot increases in size due to defocus. Each light detector signal is amplified, and the sample channel goes into the numerator input of the analog divider while the reference channel goes into the denominator input to perform the division. The purpose of the division process is to remove variations in light return efficiency of the surface under examination due to slope variation. The division process does not eliminate sensitivity due to depth but does permit an accurate determination of depth without contamination from reflective variation.

In use, the system is focused onto the surface of a reference material. A lookup table is prepared by defocusing the reference material in incremental steps and recording the signal for each stop at zero deflection angle. The reference material is replaced with the sample surface to be measured and is positioned so

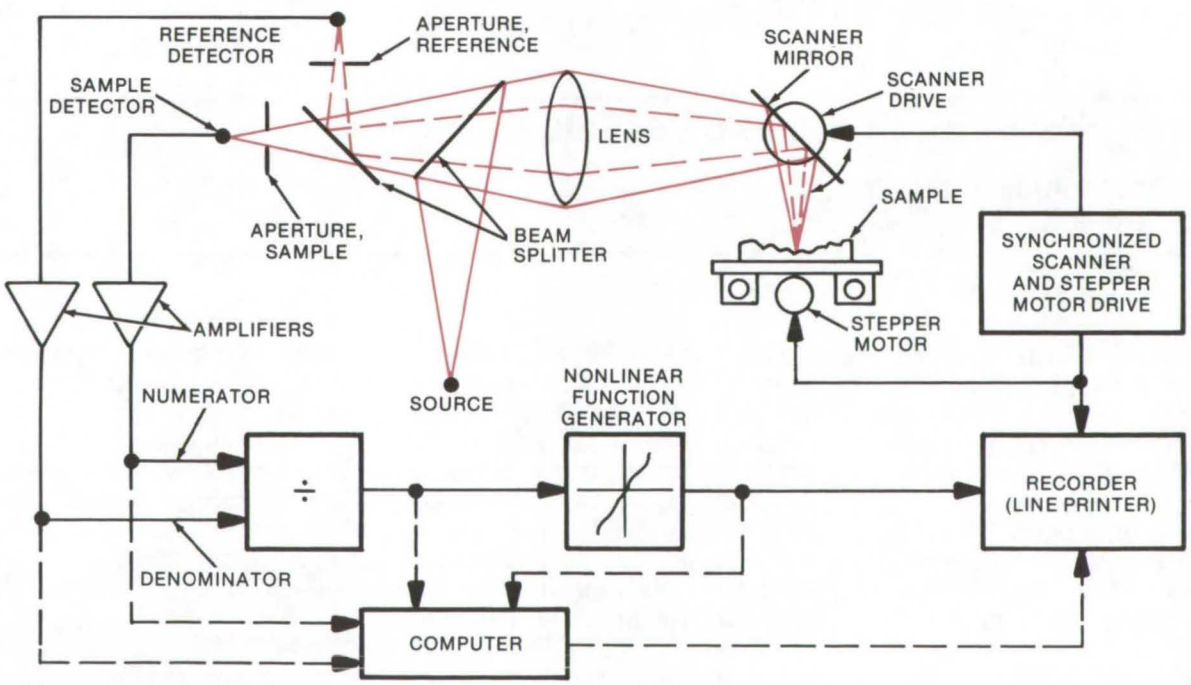

The **Optical Profilometer** is used to measure geometric characteristics of three-dimensional objects.

that the highest point of the sample is at the best focus.

The scanning mirror is started on the edge of the sample, and as the scanning mirror scans the image of the source across the sample, the ratios of the signals from the reference and sample channels are matched to the lookup table to determine the depth. An analog or digital compensation may be applied, which compensates for the difference between a surface of constant distance from the lens and a plane parallel to the sample table. This correction is expressed by $K(1 - \cos \Phi)/\cos \Phi$, where K is the lens-to-reference plane distance divided by calibration increment distance and Φ is the angle from normal to the reference plane.

The system can be modified to perform the same functions but in alternate methods:

- Detectors with different filters or wavelength responses, in lieu of mechanical apertures in the sample and reference channels, can be used in conjunction with separation of the lens area into various wavelength transmission bands (with the lens coated to transmit all wavelengths in a center area and only a band of wavelengths over the rest of its surface). The light detectors may then have filters placed over them to select the wavelength bands from a full aperture and only the center aperture of the lens.
- To eliminate the need for dual channels, retroflectors (microbeads) may be used to coat the sample surface, enabling the system to function without sensitivity to slopes.
- A laser could be utilized as the light source to modify the system sensitivity to depth as well as to allow the use of higher f-number optics.

This work was done by Ernest E. Burcher, W. Lane Kelly, IV, and Stephen J. Katzberg of **Langley Research Center.** *No further documentation is available.*

Inquiries concerning rights for the commercial use of this invention should be addressed to the Patent Counsel, Langley Research Center [see page A8]. Refer to LAR-11869.

Self-Calibrating Radiometer

An internal calibration surface need not be raised to the temperature of the external surface.

Ames Research Center, Moffett Field, California

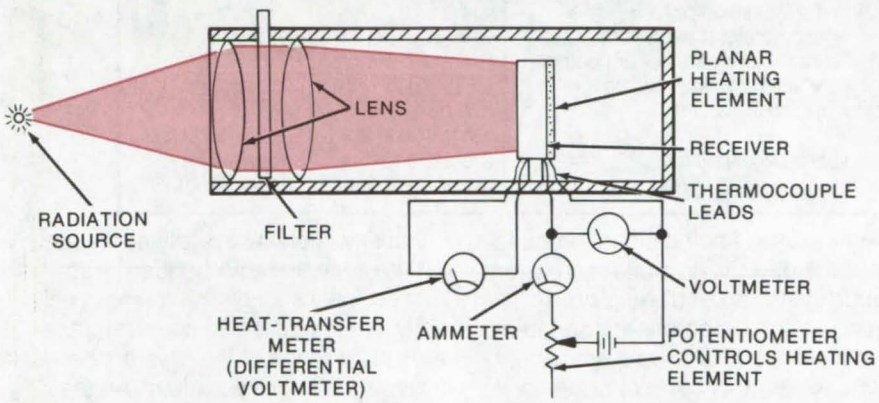

The Self-Calibrating Radiometer has differential thermocouples that measure the temperature on two sides of the receiver; one side is heated by absorbed radiation, the other by a resistance heater. By measuring the energy required to heat the back surface, the amount of energy absorbed on the front may be determined.

Radiometers are usually calibrated against a body of known temperature and surface emissivity. However, such calibrations require specialized high-temperature apparatus and are time consuming. Calibration has been simplified by a self-calibrating radiometer that includes a radiation receiver with a receiving surface that does not have to be raised to the temperature of a heat-emitting standard source.

As shown in the diagram, radiation flux from a source passes through two lenses and a filter before impinging on the receiver. The receiver consists of a block and pedestal fabricated from thermal insulating material; the front and rear surfaces have identical black coatings. A differential thermocouple on the receiver senses the difference between the front and rear surfaces. A planar heating element, energized by a power source, is embedded in the block at the rear.

The front surface of the receiver is heated by the radiation flux from the source, and the rear surface is heated by the planar heating element. The output of the heating element is adjusted by the potentiometer until the temperature of the rear surface is equal to that of the front surface. At this point, there is no heat transfer through the receiver, and the meter indicates a null or zero. The radiant energy impinging on the front of the receiver is equal to the energy applied to the heating element. The voltmeter and ammeter readings are a direct function of the energy used by the heating element.

This work was done by John Dimeff of **Ames Research Center.** *For further information, Circle 42 on the TSP Request Card.*

Title to this invention has been waived under the provisions of the National Aeronautics and Space Act [42 U.S.C. 2457(f)] to John Dimeff, Ames Research Center, Moffett Field, California 94035.
ARC-10811

Tunable Acoustical Optical Filter

Sensitivity and resolution in spectrometers are improved

Caltech/JPL, Pasadena, California

A new tunable acoustical optical filter increases the sensitivity and resolution of both passive and active spectrometers. The filter, which is capable of ranging through infrared and visible spectra, can be built as a portable device for field use. It is suitable for ecological surveying, for detecting pollution, and for onsite pollutant classification. The modified spectrometer may also be carried in an aircraft flying over stricken forest, farmland, or wilderness areas to "fingerprint" plant diseases. The cost of the modified spectroscope is about one-half that of similar devices of only conventional performance.

A block diagram of a passive spectrometer incorporating the crystal is shown in the figure. Incoming radiation is baffled and directed to the acoustical optical filter which is driven by an RF generator with the frequency varied via programed computer control. An analog transducer such as a photomultiplier tube may be used as the detector, but digital output detectors, such as CCD's, photodiodes, or Josephson junction devices, may also be used.

The computer sweeps the total band of filter output, stores information about spectral peaks detected by the transducer, and then reads and records this peak-response data within the total bandwidth of the filter for a specific time span. Since the filter is swept rapidly, near-real-time data may be obtained for the entire band. The rapid sweep also enables microsecond separation and evaluation of spectral input data.

In this class of instrument, sometimes called spectroscopic lidars, a computer controls both the frequency of emission from the laser (used to illuminate the scene at night) and the frequency transmitted by the filter. In two versions of active lidars, a tunable dye laser is directed at the target, with the return directed to the acoustical optical filter. One version uses analog signal processing; the other is its digital equivalent. Such systems used with photographic film detectors are capable of vastly simplifying image-processing requirements of camera and television pickup systems.

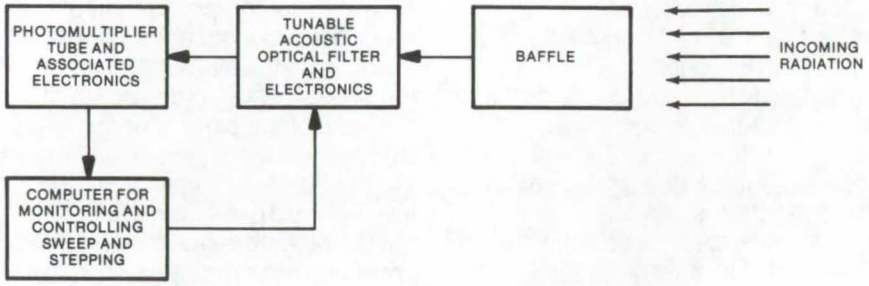

A **Simplified Passive Spectrometer System** as outlined above can achieve improved resolution using a tunable acoustical filter. The filter may also be used with active systems as described in the text.

Some Characteristics of the Tunable Optical Filters

Operational Characteristics:	Visible	Near UV
Free spectral range	4,500 to 7,500 Å	3,000 to 3,500 Å
Band-pass resolution		
Blue end	0.1 nm	0.04 nm
Red end	0.2 nm	0.07 nm
Time to scan full range	≈50 ms	≈40 ms
Time for transition of $\lambda_A \rightarrow \lambda_B$ (steady-state at each end)	≈30 μs	≈30 μs
Percent transmission for unpolarized light at saturated power level	35% (5W)	20% (4 W)
Modulation capability	0% to 100% dc to 150 kHz	0% to 100% dc to 150 kHz
Multiplexing capability	Possible for 3 wavelengths	Possible for 3 wavelengths

The new filter is a solid-state device which has an active crystal element. It is vibrated acoustically by a piezoelectric transducer bonded to it. The transducer is driven by an RF signal source. The crystal, when excited by a particular RF frequency, is tuned to act as a medium for controlled rotation of the polarization plane, enabling light to pass through it. Linear polarization crystals, which are located at the entrance and the exit of the tunable crystal, are adjusted to be precisely orthogonal in their transmission vectors.

In the absence of RF energy, transmission is severely attenuated. With a single radio frequency applied, only a single wavelength of light in the total free spectral transmission range of the crystal passes through the exit polarizer. As the radio frequency is swept via the computer, different wavelengths exit the filter. Characteristics of the tunable optical filters are listed in the table.

This work was done by Arthur L. Lane of **Caltech/JPL.** *For further information, Circle 43 on the TSP Request Card.*

This invention is owned by NASA, and a patent application has been filed. Inquiries concerning nonexclusive or exclusive license for its commercial development should be addressed to the Patent Counsel, NASA Resident Legal Office-JPL [*see page A8*]. *Refer to NPO-13640.*

Efficient Copper-Vapor Pulsed Laser

A special vessel replenishes the copper vapor at supersonic speeds.

Caltech/JPL, Pasadena, California

High-gain high-efficiency pulsed lasers have been developed, using copper vapor as laser material. These lasers generate 5,106-Å and 5,782-Å outputs with pulse durations extending to 65 ns, but a high average output power cannot be maintained without constantly replenishing the copper vapor.

In the new system, a high-velocity flow is attained by expanding a heated mixture of copper vapor, argon, and helium through a supersonic nozzle (see figure). As shown, an arc heater, operated on an argon/helium mixture, supplies the energy to vaporize the copper and to produce a high-temperature supersonic flow of the gas/vapor mixture. Copper powder is injected into the mixing chamber by an auxiliary flow of helium. The hot gas and entrained copper particles then impinge on a packed bed of tungsten pieces where the copper is vaporized. After passing through the packed bed and a plenum chamber, the mixture is accelerated through an uncooled "two-dimensional" graphite nozzle with throat dimensions of 20 by 0.55 cm.

Located 11.5 cm downstream of the nozzle throat are two parallel electrodes separated vertically by 5 cm. The lower electrode is formed by one edge of a copper strip, 1-mm thick 20-cm long, that is placed perpendicular to the flow direction. The upper electrode consists of the tips of 19 wires that are equally spaced on a line parallel to the lower electrode. The impedance of the wires is sufficient to distribute the discharge without resistive loading. The current is supplied by a 0.1-μF capacitor charged to 10 kV and discharged with a spark gap and an associated triggering device.

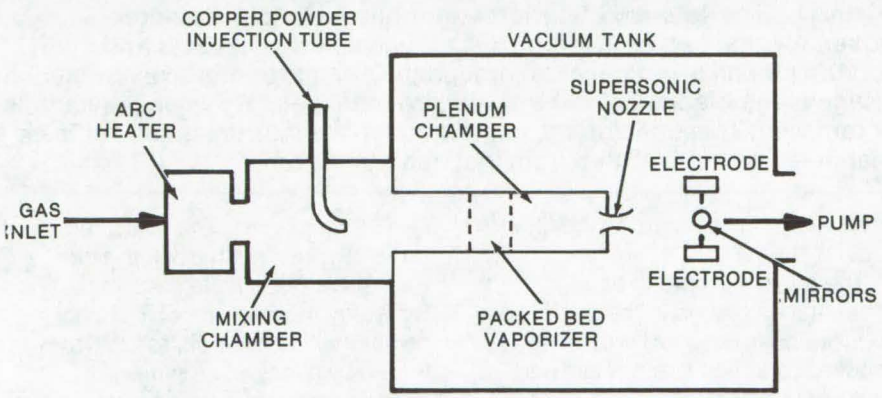

The **Supersonic Copper-Vapor Laser** utilizes a pulsed discharge transverse to a supersonic flow of copper vapor, argon, and helium.

The optical cavity consists of two mirrors placed 75 cm apart, with the cavity axis perpendicular to the current and flow directions. The cavity is a cylinder defined by the 2-cm mirror aperture and the lasant occupies a 20-cm length as defined by the 20-cm discharge length. Appropriate mirror coatings are used to vary the cavity transmittance from 3.8 to 48 percent for individual and simultaneous oscillation at 5,106 and 5,782 Å.

Typical tests show that the pulsed power density is 1.5 W/cm^3 and that the measured energy density is 0.18 μJ/cm^3. For both wavelengths (5,106 and 5,782 Å), the delay time between initiation of the current and the lasing-pulse peak power varies from 220 to 250 ns, and the pulse width varies from 110 to 185 ns. In addition, doubling the copper-powder injection rate at either a cavity pressure of 2 or 8 torr (265 or 1,065 N/m^2) doubles the output energy. The maximum energy density measured to date is 2.5 μJ/cm^3 with both lines oscillating simultaneously. The efficiency at this rate is 1.5 percent.

This work was done by Gary R. Russell, Nobel M. Nerheim, and Thomas J. Pivirotto of **Caltech/JPL.** *For further information, Circle 44 on the TSP Request Card.*

This invention has been patented by NASA (U.S. Patent No. 3,906,398). Inquiries concerning nonexclusive or exclusive license for its commercial development should be addressed to the Patent Counsel, NASA Resident Legal Office-JPL *[see page A8].* *Refer to NPO-13449.*

Measuring Scatter Angle From Mirrors

The scatter angles of UV and visible light are measured with an intensity or an amplitude scatterometer.

Marshall Space Flight Center, Alabama

For optical systems performance the scatter close to the specular beam is important. Also of concern is scatter from surface irregularities produced by aspheric figuring techniques. Millimeter-size irregularities can produce significant scatter within arc-minutes of the specular beam.

To measure the light scatter angle from mirrored surfaces, two different instrumentation systems are used. An intensity scatterometer makes small-angle (order of 10 arc-minutes) measurements, and an amplitude scatterometer (utilizing an interferometric principle for scatter measurements) measures smaller angles on the order of 10 arc-seconds. Both scatterometers use laser sources and can measure wavelengths into the ultraviolet (0.325 micron).

The intensity instrument (see Figure 1) has a diffraction-limited optical performance, with angular limitation being determined by the pinhole detector configuration at the final focal plane. Three laser lines are employed from a helium-cadmium and helium-neon laser for measurement in the UV/visible region. The laser beam is chopped by an all-reflecting chopper to modulate the light and to provide a synchronous reference signal 180° out of phase with the scattered light. A reflecting surface, M_1, produces a focused spot at the input focal plane. The system is symmetrical around the optical axis, and an arc of constant radius from the optical axis will be perfectly imaged at unit magnification as an arc in the final focal plane.

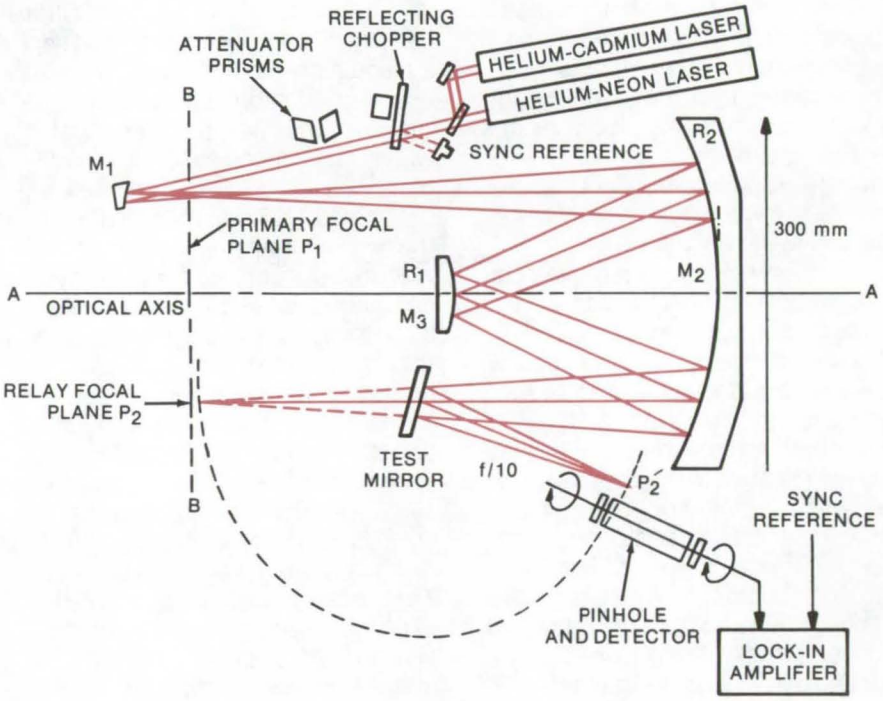

Figure 1. The **Intensity Scatterometer** has a pinhole/detector assembly that can be rotated 180° around a horizontal axis and then rotated around a vertical axis through the sample center to examine the image plane irradiance at the conjugate focal point P_2 when the sample is removed. This enables the scatter due to the instrument mirror to be measured and subtracted from that due to the sample.

The mirror sample to be measured is placed in the final focused beam and redirects the focused radiation to a pinhole and phototube detector assembly, mounted on an arm so it can pivot around the center of the scattering mirror. The pinhole size determines the smallest angle to specular that can be measured. The scattered radiation passing through the pinhole into a glass knife edge is detected by the phototube. The chopped signal from the phototube is detected by a lock-in amplifier.

The scatter-measuring interferometer (see Figure 2) consists of a Twyman-Green interferometer, with the reference mirror being oscillated along the optical axis by a piezo-

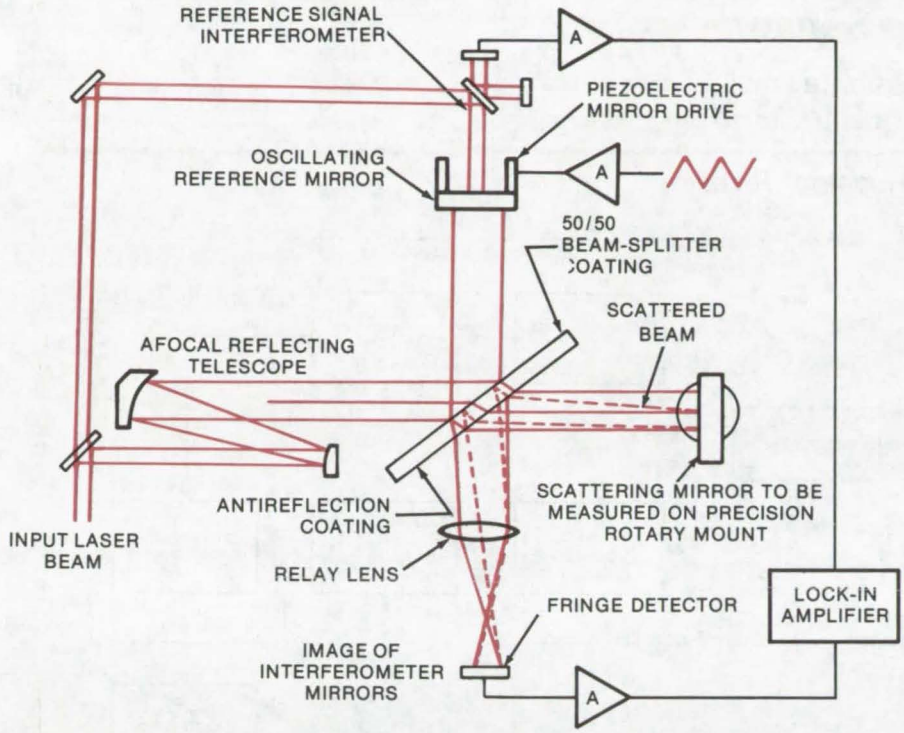

Figure 2. In the **Amplitude Scatterometer** the reference and sample specular beams are represented by dc terms in the phototube output current and the signal due to diffracted and scattered light as a current modulated at the frequency $f = 2v/c$ (where v is the mirror velocity in waves per second).

electric drive. A collimated laser beam is expanded by an all-reflective afocal telescope and is divided into the two arms of the interferometer by a beam-splitter coating. The reflected reference beam from the vibrating mirrors and the beam from the sample mirror with scatter to be measured are combined at the beam splitter, and the resulting interference pattern is detected by a photomultiplier placed at an image of the two interferometer mirrors. The angular resolution of this interferometer is about λ/D, where D is the diameter of the reference beam.

The interferometric scatterometer can measure much closer to the specular beam than the diffraction-limited intensity scatterometer. However, the latter instrument has the flexibility of being able to measure both narrow-angle and wide-angle scatter.

This work was done by The Perkin-Elmer Corp. for **Marshall Space Flight Center.** *For further information, Circle 45 on the TSP Request Card.*
MFS-23421

Hologram-Reconstruction Signal Enhancement

Heterodyne detection enhances holograms by combining the object beam with the reconstructed virtual-image beam.

Marshall Space Flight Center, Alabama

A new technique has been developed to enhance the output of a holographic memory. The principle of heterodyne detection is used to combine the object beam and the reconstructed virtual-image beam.

In the usual method of reconstructing a holographic memory, all the light valves in the page composer are closed (equivalent to blocking the object beam), and the virtual image of the stored-bit pattern is projected on a detection plane. In this system, all the light valves in the page composer are opened, and the virtual-image beam is allowed to interfere with the light from the valves. The amplitude of the detected signal for a single bit will be

$$A_S = (I_r/k)^{1/2} + (\eta I_r)^{1/2} \cos\omega t$$

where

$k = I_r/I_O$ is the beam ratio when the hologram is made,
I_r is the reference-beam intensity,
I_O is the object-beam intensity,
$\eta = I_S/I_r$ is the efficiency of the hologram,
I_S is the reconstructed virtual-image beam intensity, and
$\cos\omega t$ is the amplitude modulation of the reference beam.

The detected intensity will then be

$$I_S = A_S A_S^* = I_r/k + \eta I_r \cos^2\omega t + 2(\eta/k)^{1/2} I_r \cos\omega t$$

The first two terms are due to the object and image waves alone. The last term is the enhanced signal. The enhancement factor compared to a signal with a blocked object beam is then $G = 2/(\eta/k)^{1/2}$. Typical values are: $\eta = 10^{-3}$, $R = 4$, and $G = 33$. The analysis is similar in the case of a multibit array. Because the light valves are open, there will be an enhanced signal at frequency ω at those locations where there is a stored bit. At all other points there will not be two beams for constructive interference, and the signal will not be enhanced. Simple electrical filters can then be used to discriminate between stored bits and elements of the array.

This work was done by R. S. Mezrich of RCA Corp. for **Marshall Space Flight Center.** *For further information, Circle 46 on the TSP Request Card.*
MFS-23104

Miniature Carbon Dioxide Sensor

Precision optical elements make possible a small spectrometer for measuring CO_2 concentration in air.

Lyndon B. Johnson Space Center, Houston, Texas

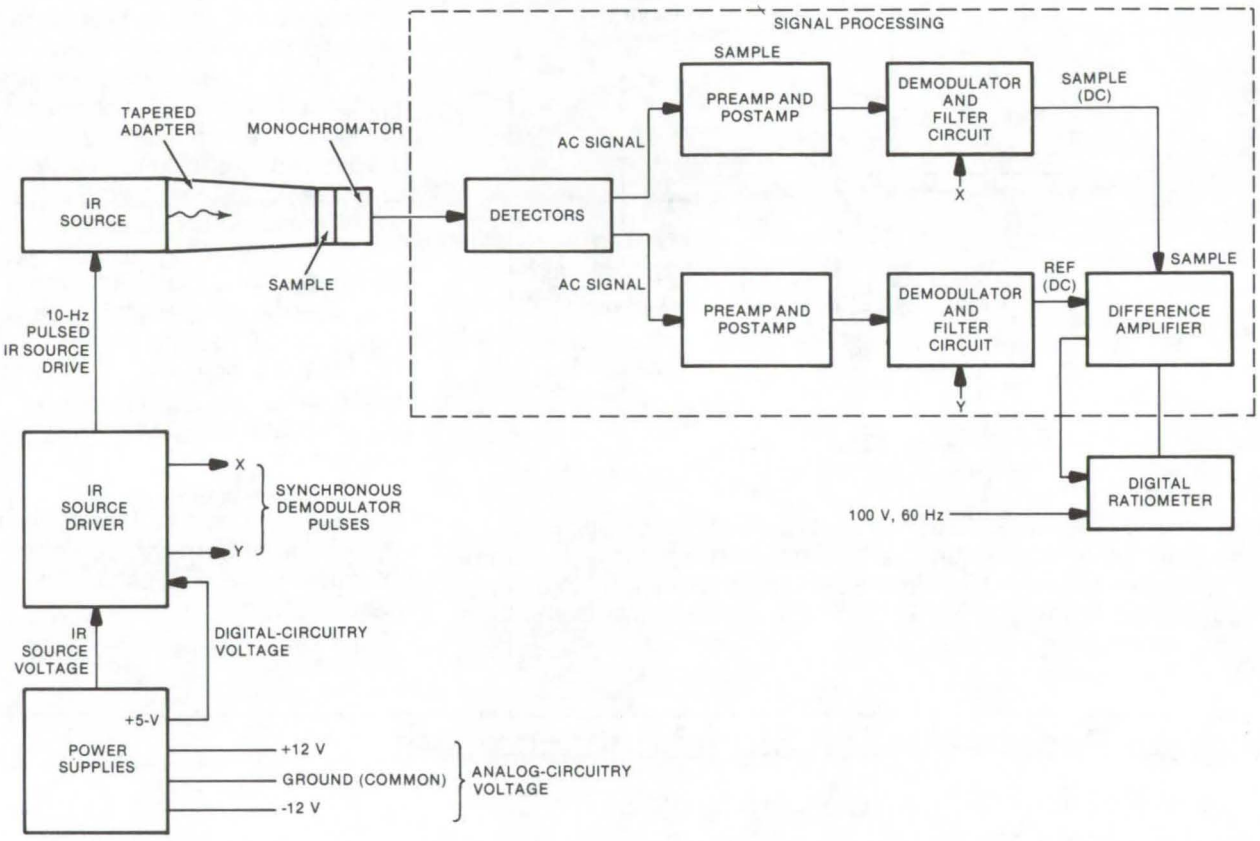

The **Carbon Dioxide Sensor** spectrophotometrically determines the CO_2 concentration in the sample cell. The IR source is optically coupled to the sample cell and monochromator by a tapered, reflective adapter.

A small infrared (IR) absorption spectrometer with a dual-wavelength monochromator has several valuable features:

- Size — 3.4 by 1.6 by 1 in. (8.7 by 4 by 2.5 cm)
- Accuracy — ±5% from 0 to 30 mm Hg
- Response Time — instantaneous and independent of temperature
- Specificity — effects of 0_2 and N_2 negligible and effect of H_2O vapor less than 0.5%
- Power Consumption — 2.5 W
- No Moving Parts
- Range — 1.5 to 30 mm Hg CO_2

The basic components of the system (see figure) are an infrared source, the optics including a dual-wavelength monochromator, detectors, and the associated electronics. The concentration of CO_2 is determined from two measurements: a sample measurement at 4.25 μm (an IR absorption band unique to CO_2) and a reference measurement at 4.0 μm (where there is no absorption from CO_2 or other gases likely to be present in a closed ecological system).

The IR source requires 1.8 W (average) of power. It is optically coupled to a sample cell and monochromator. The monochromator is a scaled-down Ebert-type instrument designed to separate 4.00-μm and 4.25-μm spectral images. The detector assembly consists of two pyroelectric detectors with outputs fed to two FET-input operational amplifiers (preamplifiers). The postamplifiers are noninverting current amplifiers. The demodulator and filter circuits produce a dc signal related to changes in the peak-to-peak values of the ac inputs (sample and reference signals). The difference circuitry produces a single output proportional to the difference between the reference and sample signals. Finally, a ratio circuit with a digital readout converts the difference signal to a display of CO_2 concentration.

This work was done by Jean Bordeaux and Billie D. Henderson of Beckman Instruments, Inc., for **Johnson Space Center.** *Further information, including a detailed description of the system optics, electronics, mechanical structure, and performance, may be found in NASA CR-144508 [N75-33375], "Final Report, Carbon Dioxide Sensor," a copy of which may be obtained at cost from the National Technical Information Service, Springfield, Virginia 22151.*
MSC-16009

Monitor for Optical-Window Contamination

Attenuated total reflection is used to monitor contamination on optical windows.

Ames Research Center, Moffett Field, California

Optical contamination on an optical window can be monitored by measuring the attenuation of light that is reflected from the interior surfaces of the window at angles slightly larger than the critical angle. The monitoring system uses the window itself as the principal element of the well-known attenuated total reflection (ATR) technique frequently used for spectroscopic analysis of thin films. As indicated in the diagram, a light-emitting diode (LED) is used as an energy source, and the window is notched and polished to form a "beam splitter" that allows part of the nearly collimated light from the LED to pass on to a reference detector (not shown in the diagram). The "beam splitter" directs the remaining part of the light at angles slightly greater than the critical angle at the interface, so that it will be reflected without loss from the interior surfaces of a clean window. After a number of reflections from the parallel surfaces of the window, the light is transmitted to a detector by a fiber-optic bundle or a sapphire rod. When the outer surface of the window becomes contaminated, the critical angle of incidence for perfect reflection is much larger, and lossless reflection is no longer possible because light penetrates the interface.

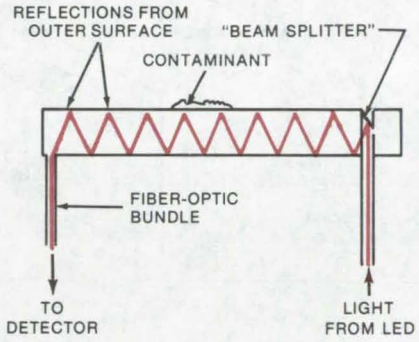

The Optical Contamination Monitor includes a notch in the monitored window; it acts as a beam splitter to reflect a portion of the light at less than the critical angle and causes total internal reflection.

In tests using a helium-neon laser as a light source, it has been shown that the absorption of light can be nearly total for contaminant films of water, oil, degreasers, and the like. However, since solid particles such as dust or aluminum oxide powder, cannot make good optical contact with the outer surfaces of the window, they are not detected by the monitor.

In an alternative system for monitoring contamination, the interior and exterior surfaces of the window are not parallel, and the outer surface of the window is carefully alined to reflect some of the light of an LED source into a detector. When the outer surface of the window is clean, about 7 percent of the outgoing light is reflected back into the detector; as the surface becomes contaminated, the return is decreased. A separate reflection from the clean inner surface of the window may be used to monitor the output of the LED.

This work was done by Laurence N. Harnett of TRW, Inc., for **Ames Research Center.** *For further information, Circle 47 on the TSP Request Card.*
ARC-10947

Color to Black-and-White Converter

A PLZT filter, and two polarizers, pass color or monochrome images, depending on filter voltage.

Lyndon B. Johnson Space Center, Houston, Texas

A lanthanum-modified lead zirconate titanate (PLZT) ceramic plate, when sandwiched between a pair of conventional light polarizers, forms an electrically-controlled color to black-and-white converter for a TV camera. The plate/polarizer system is fastened to the camera lens and (depending on the voltage applied to the PLZT plate and polarizer orientation) is used as a neutral density filter, a selective-color filter, or a camera-pickup-tube light shutter. The assembly can be used with a TV camera at a remote site to enable the camera to transmit a color or a black-and-white signal on command.

A typical solid-state electro-optic color filter (SSEF) developed for TV applications is illustrated. The three basic elements, consisting of the two polarizers and the PLZT wafer, are shown respective to the optical axis. The PLZT surfaces contain a deposited-electrode pattern for the application of control voltages. Initially unpolarized light is linearly polarized by polarizer 1 at an angle of 45° to the X reference axis. This light passes through the PLZT wafer and impinges on polarizer 2.

In the absence of an electric field, the PLZT plate is isotropic and does not affect the polarization of the light. Because the polarization axis of the second polarizer is at an angle of 135° to the reference, the two crossed polarizers block the light. This is the off state for the filter.

An electric field, applied to the electrodes implanted within the plate, causes the PLZT to become birefringent. When the potential is adjusted to provide half-wave retardation, the resultant output from the plate is linearly polarized at 90° to the plane of the polarizer axes. In this case maximum transmission is achieved, and the filter is in the on state. Increasing the potential beyond the on state permits selective-color filtering.

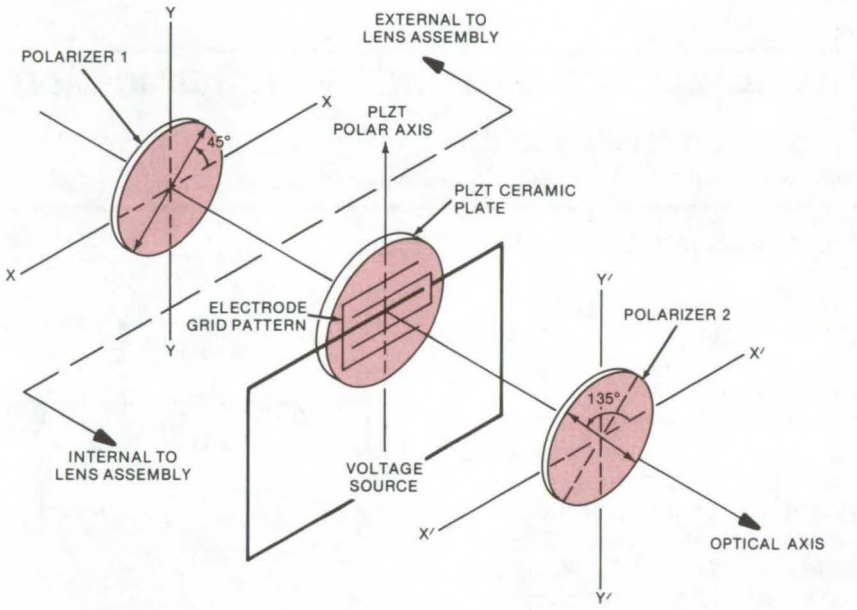

The **PLZT Optical System,** when installed before a TV camera lens, can be used as a neutral density filter, a selective-color filter, or a light shutter. When the optics are set up as a selective-color filter in a field-sequential color-TV system, deactivating the system renders a black-and-white video signal from the camera.

The system may be made to act as a neutral density filter by controlling the potential applied to the PLZT plate, and thus the polarization angle of light passing through the plate. The maximum light intensity through the system is determined by its geometry and by the strength of the electric field applied to the PLZT.

This system may be conveniently used as a light shutter by turning the electric field on or off. By increasing the electric field strength beyond the voltage which maximizes light transmission, the device acts as a wavelength-dependent retardation plate (e.g., the optical system becomes useful as a selective-color filter).

The PLZT plate and the second polarizer are both alined along the optical axis of the television pickup tube. No optical effect occurs to light passing through the combination of only the plate and a single polarizer, with the exceptions of polarization of the light and a possible loss in light intensity. Without the first polarizing device in position along the optical axis of the optical system, it is effectively deactivated.

This work was done by William E. Perry of **Johnson Space Center.** *For further information, including a description of the system optics, Circle 48 on the TSP Request Card.*

This invention is owned by NASA, and a patent application has been filed. Inquiries concerning nonexclusive or exclusive license for its commercial development should be addressed to the Patent Counsel, Johnson Space Center [see page A8]. *Refer to MSC-12618.*

Low-Light-Level Integrating Video System

Digital data from a low-dispersion spectrograph via an integrating TV camera are stored and displayed in near real time.

Marshall Space Flight Center, Alabama

An astronomy-grade video system, as illustrated, is mated to a low-dispersion spectrograph for low-light-level applications. Spectral information in the range of 400 to 750 nm (4,000 to 7,500 Å) is derived in a computer-type memory and is stored via magnetic tape for later analysis. The storage system incorporates an A/D converter which digitizes the analog video signal to a 6-bit equivalent.

Second-order operation allows simultaneous coverage of a 140-nm (1,400-Å) band, selected by grating tilt throughout the 350-nm (3,500-Å) range. Spectral resolution obtainable is on the order of 0.6 nm (6 Å).

The two-section 25-mm vidicon camera pickup tube uses an electrostatically-focused diode image section and a magnetically-focused and deflected readout section. A planoconvex fiber-optic faceplate is coated with a photocathode having an S-20 (420 nm, peak) response deposited on its inner surface. The tube target has an Al_2O_3 supporting membrane, followed by an aluminum signal electrode upon which is deposited a thick, highly porous layer of KCl.

The photoelectrons dissipate their energy in the KCl by generating secondary electrons which are trapped in the vacuum voids between the KCl particles. The positive potential applied to the signal electrode establishes an electrical field across the KCl layer (the surface of the KCl being maintained essentially at gun cathode potential by the read beam).

The secondary electrons migrate toward the signal electrode, leaving the KCl target surface positively charged with a spatially distributed image, the intensity corresponding to the optical image. The variations in charge pattern result in a corresponding current variation in the neutralizing read beam as it is scanned by the deflection mechanism across the target. The effective capacitance across the target couples this current fluctuation to the signal electrode, and the video analog voltage is developed across a load resistor to ground.

The camera logic circuit permits timed, sequential camera control and low-light-signal integration. An expose command initiates target preparation, which consists of a selected number of expose/read cycles. The target is flooded with diffuse light and is read off to insure uniformity. Then, a number (again, selected) of read-only cycles are performed to reduce the residual charge level on the target.

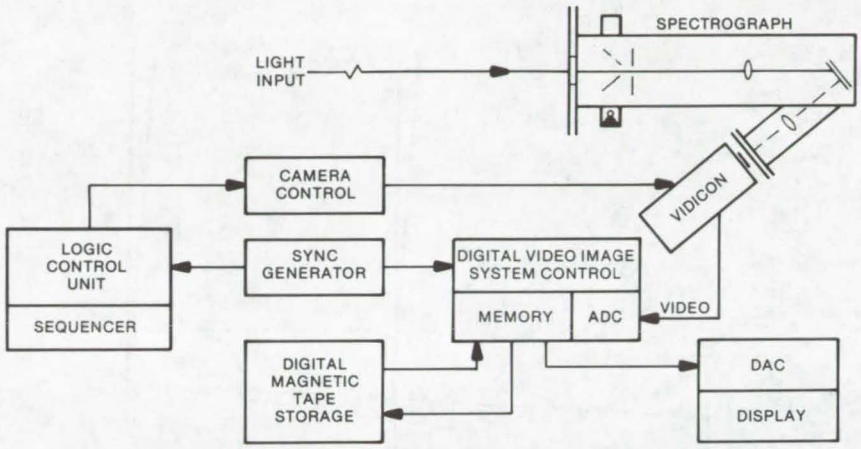

The **Low-Light-Level Integrating Video System** consists of a TV camera using a 25-mm SEC vidicon, a low-dispersion spectrograph, and a digital video image system (DVIS) used for buffer storage of video data during tube readout scanning. A 6-bit ADC converts video to digital data which are stored on magnetic tape for future evaluation.

Following target preparation, the filament is turned off and allowed to cool down for a selected period. A command turns on the high voltage, and the unknown image is integrated onto the target. The readout beam is blanked during integration and, during a selected warmup period for the filament after integration, is terminated by turning off the high voltage. A logic signal then unblanks the readout beam and transfers the single frame of video analog information to the recorder.

This work was done by B. J. Duncan, T. D. Fay, E. R. Miller, and W. Wamsteker of **Marshall Space Flight Center** *and R. M. Brown and P. Neely of Computer Sciences Corp. For further information, Circle 49 on the TSP Request Card.*
MFS-23288

Shadow Mask for X-Ray Spectrometer

Masking improves
spectral/spatial resolution.

Goddard Space Flight Center, Greenbelt, Maryland

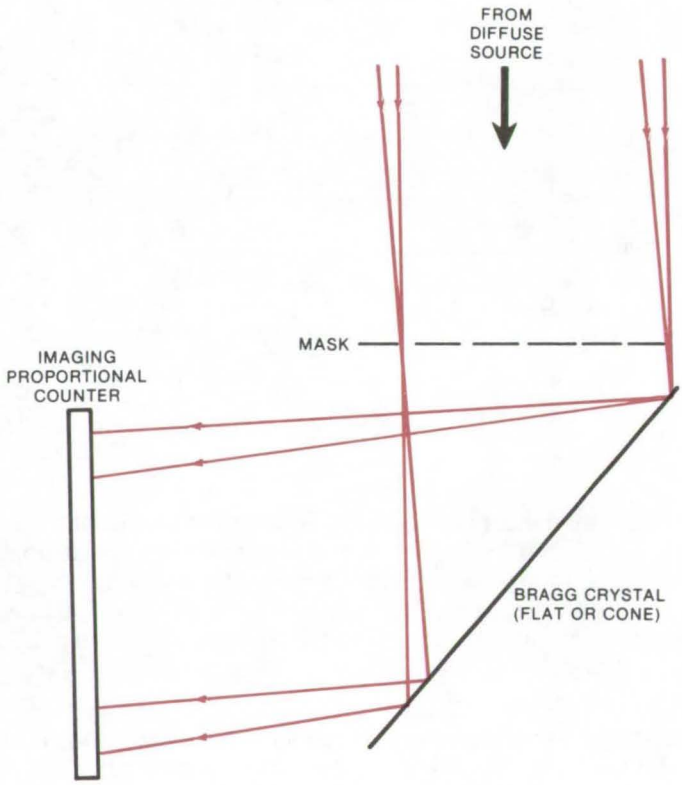

Figure 1. The **Shadow Mask** is used with a Bragg crystal spectrometer where it is placed in front of the crystal.

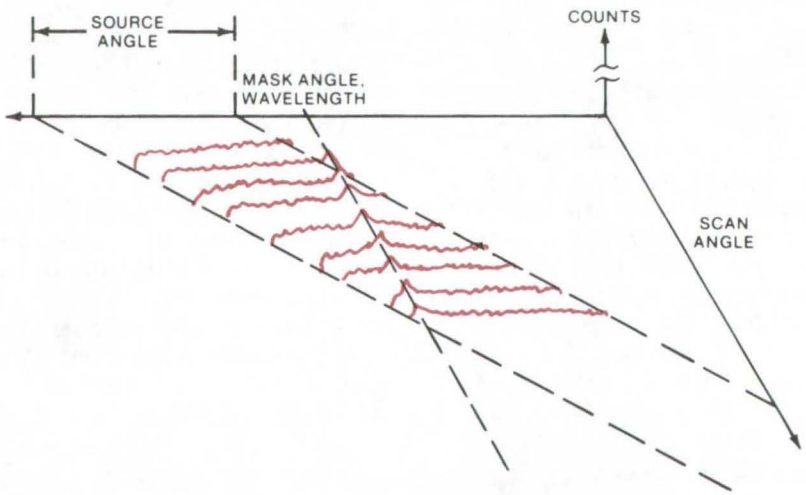

Figure 2. The **Direction of the Line and the Continuum** from an extended source can be determined, using the shadow-mask technique. This information allows the spectral line to be detected and the source to be mapped spatially.

An easily-implemented shadow-mask technique removes much of the confusion between spectral and spatial information in Bragg X-ray crystal spectroscopy. The mask-shadow imaging may be used in series with flat or conical Bragg crystals to separate the spatial/spectral convolution obtained when the spectrometer is scanned across an extended source emitting at more than one wavelength.

The masking technique is illustrated in Figure 1. The shadow of the mask placed in a beam of parallel X-rays is reflected by the Bragg crystal onto the imaging detector. The Bragg condition will be satisfied for a wavelength range corresponding to the angular diameter of the source. However, the mask pattern will move across the detector for different parts of the source. The arrival direction of an individual photon cannot be determined, as it can for true focusing; but the arrival direction of a statistical ensemble can be found. The accuracy of this process is limited by the background noise present.

Figure 2 illustrates the function of the mask as it is used to identify the direction of the continuum and the line radiation from an extended source. The technique improves discrimination, allows the line radiation to be detected, and provides data for spatial mapping of the source.

This work was done by Bruce E. Woodgate of **Goddard Space Flight Center.** *For further information, Circle 50 on the TSP Request Card.*
GSC-12131

Quartz-Crystal-Oscillator Hygrometer

A fast, small, accurate, and easy-to-use instrument measures dewpoint.

Goddard Space Flight Center, Greenbelt, Maryland

A new technique for measuring the dewpoint of water vapor in a gas employs a piezoelectric-crystal oscillator, supportive circuitry, temperature regulators, and readout. An electrically stimulated crystal is used to determine the dewpoint, from which both relative and absolute humidity may be determined. Currently, the most accurate dewpoint hygrometers detect condensation by optically monitoring changes in a reflecting surface. This new device eliminates the complex and expensive optical components by electronically sensing the condensation of moisture on a vibrating crystal.

Water condensing on the crystal surface changes the frequency of oscillation. When the crystal is at a temperature above the dewpoint of the ambient environment, only a very small amount of water adheres to the surface due to surface effects; and a state of equilibrium exists between the water in the atmosphere and the moisture on the surface. As the crystal is cooled, the amount of moisture on the surface changes slightly until the temperature reaches the dewpoint. Then there is a dramatic increase in surface water on the crystal, and a significant change in the oscillation frequency occurs (e.g., a cessation of oscillation).

The oscillation is monitored by a frequency meter, and the temperature of the crystal is controlled by a fluid at a temperature below the dewpoint. The fluid is passed through the mount to which the crystal is attached and cools it below the dewpoint. The device is warmed above the dewpoint by regulating the fluid flow and/or applying heat. When the frequency rate of change increases severely, the temperature of the crystal is equal to the dewpoint.

Some advantages of this technique are:

- The crystal is rugged and can be used in adverse environments.
- Crystal sensitivities can be greater than existing devices and can be more accurate.
- The system is simple in that only the crystal, an oscillator and readout, a temperature controller, and a temperature measurement are needed.
- The device can be smaller than existing instruments, with the entire device (except for power supplies and readout) occupying volume of 1 by 2 by 2 cm.
- The unit can be relatively inexpensively produced.

This work was done by Raymond Kruger of **Goddard Space Flight Center.** *No further documentation is available.*
GSC-12153

Books and Reports

These reports, studies, and handbooks are available from NASA as Technical Support Packages (TSP's) when a Request Card number is cited; otherwise they are available from one of NASA's Industrial Application Centers or the National Technical Information Service.

Terrestrial Photovoltaic Measurements Workshop

Proceedings on solar-cell measurement techniques

The proceedings are now available covering the Terrestrial Photovoltaic Measurements Workshop held recently at the NASA Lewis Research Center, Cleveland, Ohio. The workshop was jointly sponsored by the Energy Research and Development Administration (ERDA) and the National Aeronautics and Space Administration (NASA).

The purpose of the workshop was to review basic solar-cell measurement techniques and to decide upon an interim method for terrestrial solar-cell measurements in order that results may be correlated between organizations doing solar-cell research. The workshop was divided into three separate sessions: (1) solar intensity and spectrum conditions for terrestrial photovoltaics, (2) terrestrial Sunlight simulators, and (3) methodology for measurements and calibration of solar cells.

Several recommendations were made by the workshop for an interim period of 1 year. In the area of solar-cell measurements, it was agreed that measurements of solar-cell performance in natural Sunlight are the most acceptable. For laboratory measurements, a broadband-spectrum, filtered, artificial light source, such as a xenon arc lamp, was recommended.

Several performance measurement conditions were specified in order to put terrestrial solar-cell measurements on a common basis. Two of the performance measurements specified were solar-cell temperature of 301±2 K (82.4°±3.6° F) and 100 milliwatts per square centimeter intensity for the solar simulator.

Other workshop recommendations were as follows:

- An absolute spectral-response measurement technique which is applied to all types of solar cells should be developed;
- For theoretical calculations, a standard air-mass 2 solar spectral distribution curve should be used; and
- A centralized national laboratory should be established to perform reference photovoltaic measurements, to issue calibrated solar cells, and to perform the research and development to support the measurements program.

This work was done by **Lewis Research Center.** *A copy of the proceedings, NASA TM-X-71802 [N76-71615], "Terrestrial Photovoltaic Measurements — Workshop Proceedings," may be obtained at cost from the Technology Application Center, University of New Mexico* [see page A7]. *LEW-12643*

Computer Programs

These programs may be obtained at very reasonable cost from COSMIC, a facility sponsored by NASA to make new programs available to the public. For information on program price, size, and availability, circle the reference letter on the COSMIC Request Card in this issue.

WING

Calculating lightning-induced voltages in electrical circuits within an aircraft wing

A computer program (WING) utilizes a model of a generalized aircraft wing to calculate the resistive and inductive transfer impedances relating lightning current flowing through the wing to a voltage induced in a conductor within the wing. A wing was modeled because experimental measurements had shown the most severe induced voltages to be in circuits inside aircraft wings.

When lightning stroke currents flow through an aircraft, rapidly changing magnetic fields and structural voltage drops are created which cause transient voltages to arise in internal electrical wiring. Even if the aircraft is metallic, its noncylindrical geometry and finite structural resistivity result in hazardous voltages being induced into aircraft electrical systems. Before protective measures can be applied, the amount of possible induced voltage in each critical circuit must first be determined.

Simulated lightning test techniques have been developed to measure possible lightning-induced voltages in existing aircraft. However, during the aircraft design phase, the WING program may be used to evaluate the susceptibility of candidate electrical circuits to induced voltages, thus permitting the optimization of electrical circuit design and the incorporation of appropriate protective measures.

The reduction of previous experimental data has shown that voltages induced in a typical circuit are related to the lightning current by the basic expression

$$e_{oc} = R_S i_L(t) + M \frac{d(1-e^{-at}) i_L(t)}{dt}$$

where

e_{oc} = induced voltage appearing across open circuit terminals,

R_S = the effective structural resistance,

M = an effective transfer inductance between the lightning current and the particular electrical circuit,

$i_L(t)$ = lightning current (a time-varying function), and

a = the reciprocal of the time constant of current penetration into the aircraft skin.

The program is based on the Biot-Savart and Faraday laws. It also takes into account various geometric configurations. R_S is determined from material resistivity properties.

The computer program accepts wing dimension and conductor location parameters. It prints out the transfer resistance and the transfer inductance as well as the flux density at the conductor location. Comparisons between the model and actual test results have been favorable.

BASIC
GE TSS

This program was written by J. Anderson Plumer of General Electric Co. for **Lewis Research Center.** *For further information, Circle B on the COSMIC Request Card.*
LEW-12108

Materials

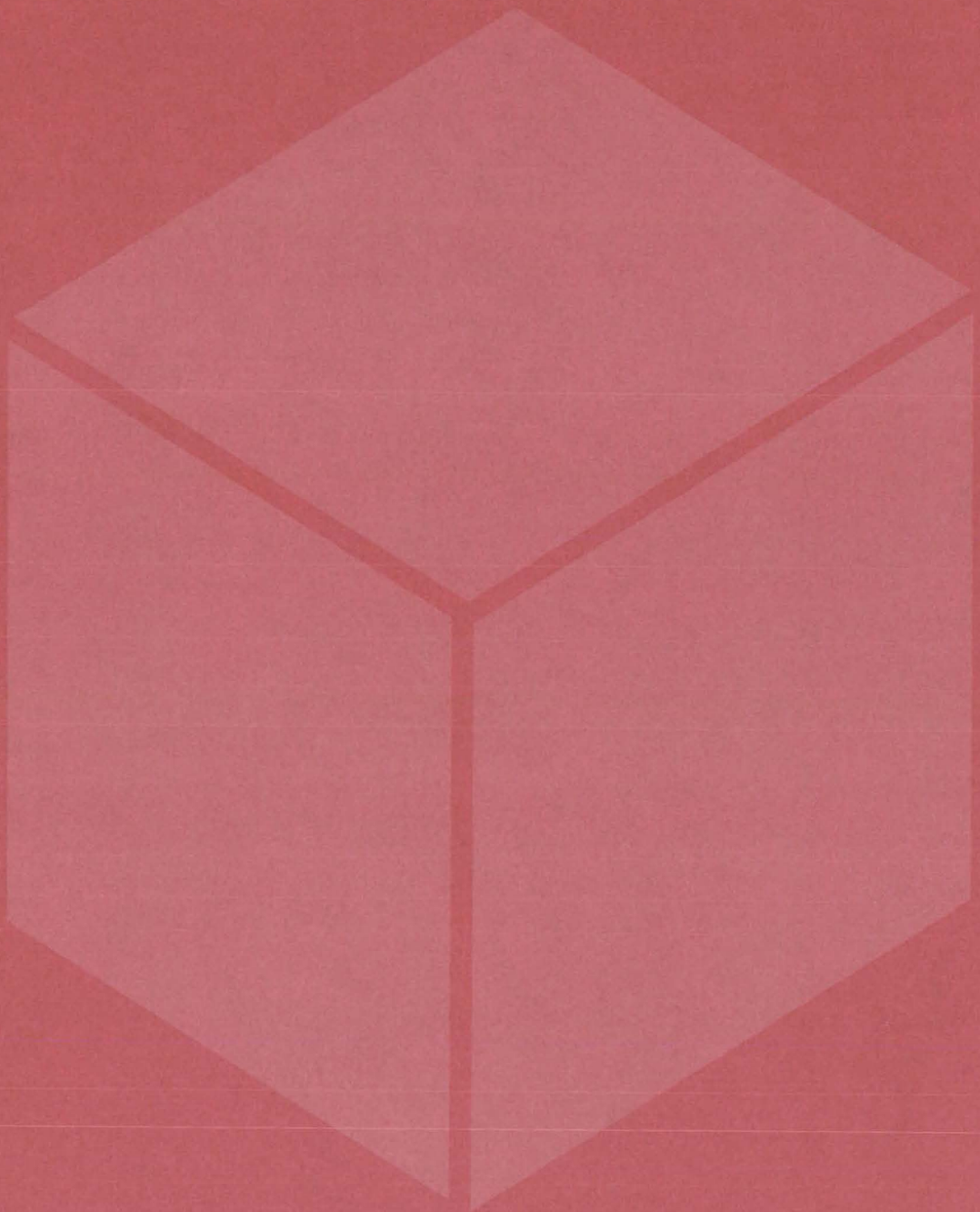

Fraction Collector for Electrophoresis

A rotating jet of eluting buffer reduces the effects of convection during particle separation.

Marshall Space Flight Center, Alabama

In electrophoresis, dissolved chemical species or suspended particles (e.g., proteins, bacteria, or blood cells) are removed from a liquid by subjecting them to an electric potential gradient. The particles or molecules will migrate through the field at different rates, depending on their mobilities and charge. A major interfering process in this procedure is convection in the fluid, caused by temperature or concentration gradients, Joule heating, and other factors.

This convection must be stabilized in such a way not only to enhance separation but also to facilitate physical collection of the separated species. A new technique, rotating-seal fraction collection, is designed for rotating-tubular or concentric-tubular electrophoresis devices that reduce convection effects. A thin jet of eluting buffer is directed across the electrophoresis medium (the lumen) in a direction perpendicular to the electrophoretic flow. Complete elution is achieved by rotating the jet and/or lumen with respect to one another.

A typical application of the technique is shown in Figure 1, a simplified version of a rotating-seal fraction collector used with a rotationally-stabilized electrophoresis tube. Here, the jet is stationary, and the electrophoresis tube rotates. The rotating seal, shown in detail in Figure 2, has a stationary half through which the jet of buffer is directed. Since the buffer is the same as the electrophoresis buffer, it will not alter the composition of the medium.

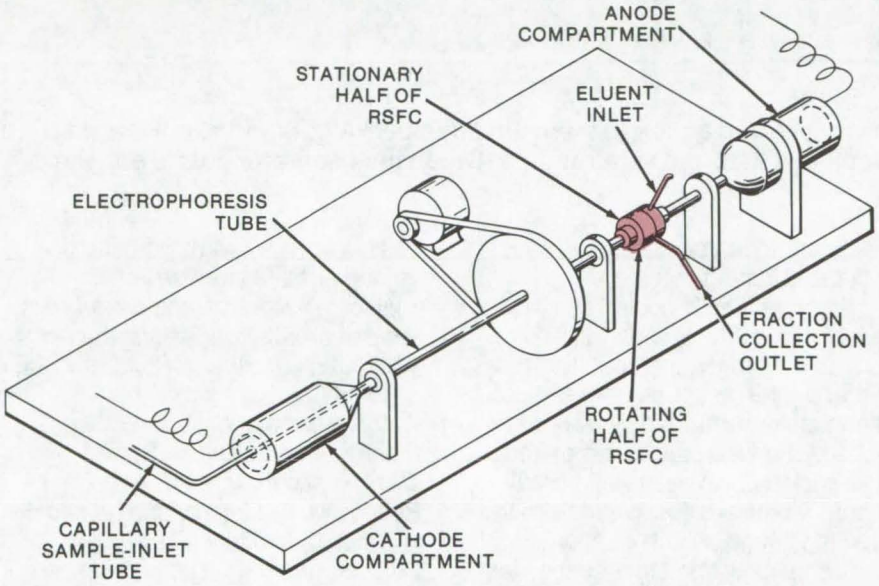

Figure 1. A **Horizontal-Tube Electrophoresis Device** is shown with the rotating-seal fraction collector (RSFC). The cathode compartment, which is filled with buffer solution, is connected to the electrophoresis tube. Also connected to the tube is the rotating half of the RSFC. These three components are rotated slowly during the electrophoresis process. The other half of the RSFC, a short section of tube, and the anode compartment are fixed and do not rotate. The mating halves of the RSFC are wet with buffer to effect a seal, and eluent is directed through a port in the rotating half. As the tube and rotating half of the RSFC turn, the separated species is swept out of the tube through an outlet from which it may be collected in a test tube.

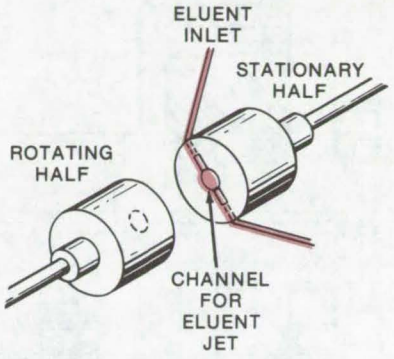

Figure 2. The **Rotating-Seal Fraction Collector** consists of two mating holes made of glass, Teflon, or a similar material. In this version, a slot in the stationary half provides a path for the eluent jet. The rate of eluent flow depends on the electric field and ion mobilities. Typical operating data are: flow of 0.01 to 0.2 ml/min for a tube diameter range of 0.1 to 0.5 cm and an electric field of 5 to 30 V/cm.

As each zone of constituent passes through the tube, it will be effectively swept out of the tube by the eluent jet. Fractions can be monitored visually, by UV, or by other conventional techniques. The general principle as illustrated here can be applied to a variety of electrophoresis devices, including concentric-tube systems, effectively to collect separated samples.

This work was done by Milan Bier of the Veterans Administration Hospital, Tucson, Arizona, for **Marshall Space Flight Center.** *For further information, Circle 52 on the TSP Request Card.*

Inquiries concerning rights for the commercial use of this invention should be addressed to the Patent Counsel, Marshall Space Flight Center [see page A8]. Refer to MFS-23459.

Molecular Beam Generator

A research tool for generating heavy-organic-molecule beams may have applications as a coating device.

Lyndon B. Johnson Space Center, Houston, Texas

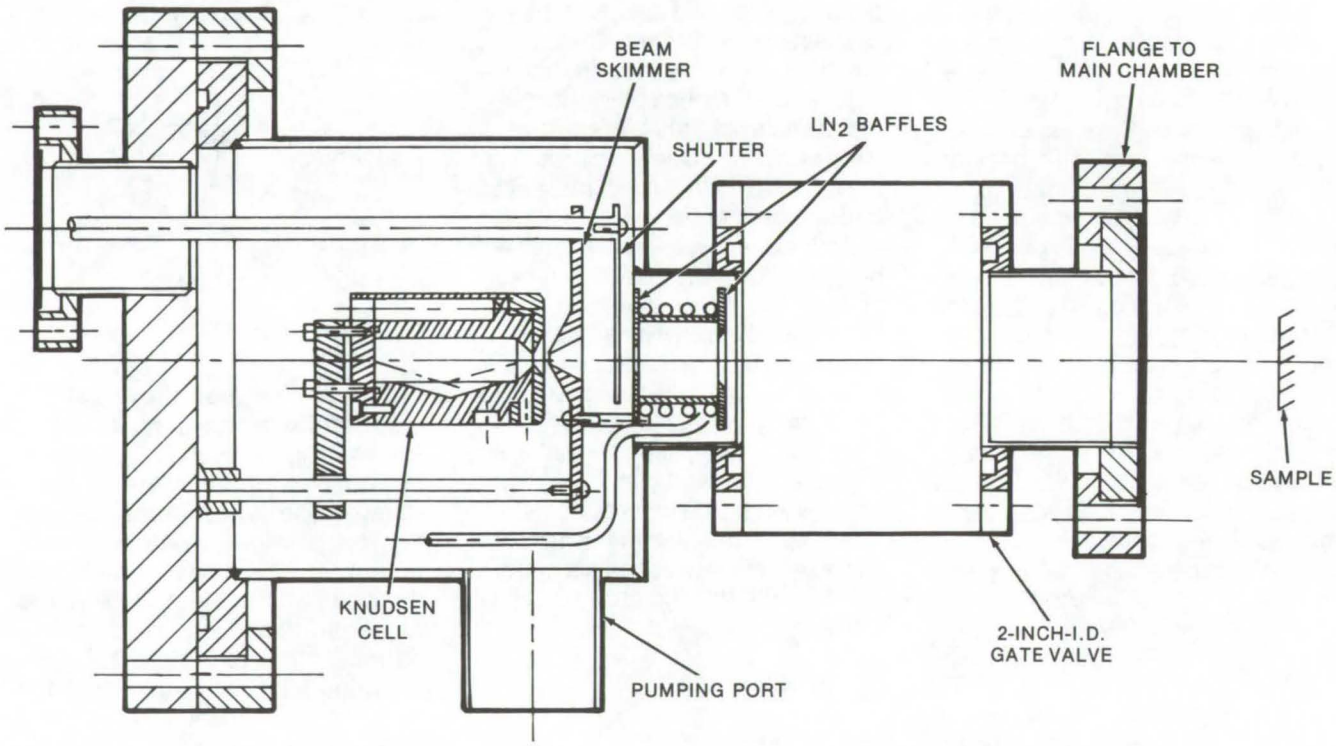

The **Molecular Generator** is housed in an isolated annex to the main chamber. A gate valve, connecting flanges, and liquid nitrogen baffles result in a 21.6-cm separation between the generator nozzle and the sample to be contaminated.

Until recently, vacuum-deposition coating techniques have been limited to metals, oxides, and certain dielectric compounds. Now these techniques have been adapted for studying the kinetics of molecular contaminants.

A heated source (see figure) generates organic vapors which pass through a specially designed nozzle in order to direct a beam of organic molecules at the sample. To limit the field angle of the molecular beam, a single-orifice nozzle and aperture system is used. A combination of three apertures limits the beam cross section to the diameter of the sample. The beam skimmer deflects the outer portions of the beam to facilitate their immediate removal via the pumping port.

A cryogenically cooled collimator further limits the beam area and reduces the stray molecular flux from entering the main chamber. Deposition time is controlled by a shutter located between the skimmer and the cooled collimator. All internal components are supported from the sealing flange, which is mounted on slides to allow complete access for cleaning and recharging the source. The source is instrumented for temperature measurement and control of the heater currents.

Data from a calibration run of the molecular beam generator with diffusion pump oil show deposition rates ranging from 6 to 15 Å/min.

Although the system has been designed primarily for use with high-molecular-weight organic materials, it can with slight redesign be used with other gases, such as ammonia, nitrogen, and oxygen.

This work was done by Robert G. Richmond of **Johnson Space Center** *and Thomas H. Allen, Rodney M. F. Linford, and James E. Wittman of McDonnell Douglas Corp. Further information may be found in NASA CR-144376 [N75-29135], "Evaluation and Study of Advanced Optical Contamination, Deposition, Measurement, and Removal Techniques," a copy of which may be obtained at cost from the National Technical Information Service, Springfield, Virginia 22151. MSC-14996*

Catalytic Oxidation of Waste Materials

A soluble salt, introduced upstream, is converted to a catalyst inside the reactor.

Lyndon B. Johnson Space Center, Houston, Texas

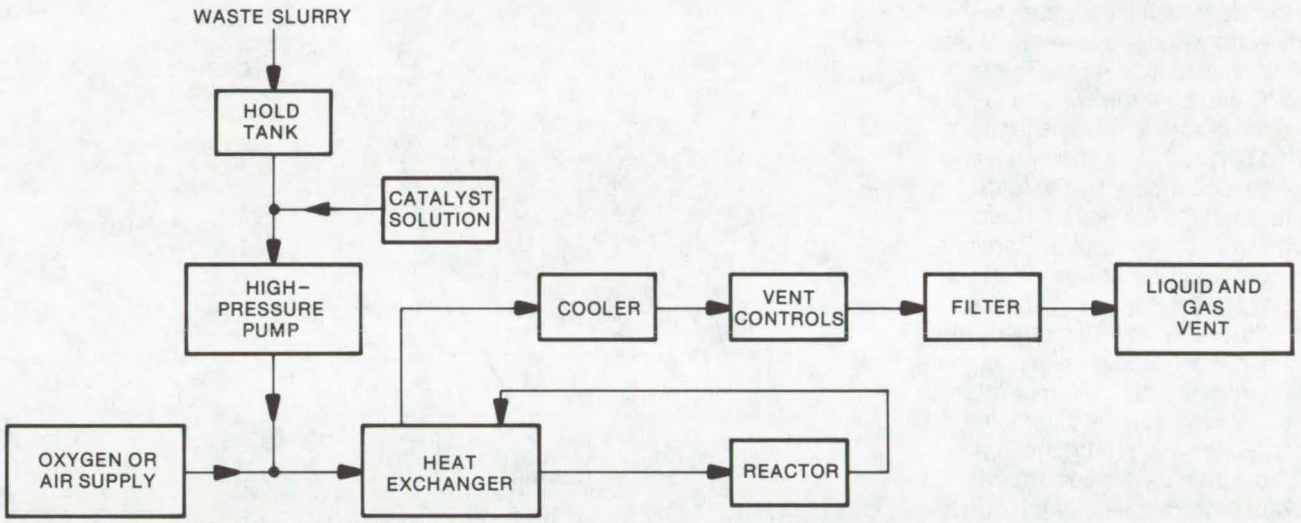

A **Wet Oxidation Reactor** utilizes ruthenium black, an effective catalyst, to reduce human wastes. Ruthenium trichloride is added to the waste stream, heated to reactor temperatures (≈550° F), and on decomposing, ruthenium metal will deposit itself on the internal walls of the reactor vessel. After a short "pickling" time, the addition of ruthenium trichloride can be discontinued except for periodic repickling periods.

A method for the treatment of waste-product streams is based on forming catalytically active surfaces from soluble ruthenium salts ($RuCl_3$). The aqueous stream of human waste is mixed with soluble ruthenium salts (a wet oxidation process) and is introduced into a reactor at a temperature where ruthenium black (a known effective catalyst) forms on the internal surfaces of the reactor. This provides a catalytically active surface to convert the oxidizable waste materials into more-easily-handled breakdown products such as water and CO_2.

The amount of ruthenium salts that must be dissolved in the input feed material containing the waste products will vary, depending upon the amount of waste products to be oxidized, the size and configuration of the reactor, and other factors. The reaction is maintained in the reaction vessel in the presence of an oxygen-containing gas for a time sufficient to oxidize at least a portion of the waste material. When the desired amount of oxidation has occurred, the reaction product containing the oxidation products of the waste material is removed from the reaction vessel. The temperature in the reaction vessel is about 175° F (80° C) or greater, and sufficient pressure is maintained to prevent substantial vaporization of the aqueous liquid medium.

One advantage of this technique is that should the ruthenium black catalytic surface lose its activity due to attrition from the reactor surfaces, poisoning, temperature upsets, or other factors, a fresh catalytic surface can be supplied without emptying the reactor, as would be required for a solid charge of catalyst in the reactor. Soluble ruthenium salt can be added to the reactant vessel while the reaction is in process, and by adjusting the temperature conditions to the proper range, the catalytically-active ruthenium black will be deposited on the reactor walls. Alternately, the reaction could be terminated for a period of time sufficient to resurface the walls of the reactor by using a separate liquid medium containing the dissolved salt.

Unlike soluble catalysts (which can also be introduced upstream from the reactor), ruthenium does not exit the reactor with the processed sewage. Most of it will be deposited on the walls and remain inside. Thus waste streams can be treated without creating products that damage the environment or create health hazards.

This work was done by Robert Bruce Jagow of Lockheed Missiles & Space Co., Inc., for **Johnson Space Center.** *For further information, Circle 53 on the TSP Request Card.*

This invention is owned by NASA, and a patent application has been filed. Inquiries concerning nonexclusive or exclusive license for its commercial development should be addressed to the Patent Counsel, Johnson Space Center [see page A8]. *Refer to MSC-14831.*

Composite Laminate Warpage

Prediction of warpage in composite laminates is made simple by a set of predictive equations.

Lewis Research Center, Cleveland, Ohio

Fiber composite laminates at times warp when they are removed from the fabrication mold. This warping can be large enough to make the laminate useless for its intended purpose. The laminate warping is caused mainly by the following two factors: (1) nonuniform fiber-volume content through the laminate thickness and (2) fiber misorientations. The presence of either or both of these factors combined with the lamination residual stresses, resulting from the curing temperature, produce combinations of bending and twisting which force the laminate to assume a warped surface.

Exact determination of the curvature of the warped laminate requires the solution of coupled fourth-order partial differential equations. Solutions to the coupled partial differential equations, or to approximate equations, for predicting laminate warpage as a result of bending nonsymmetries and residual stresses are not available in the literature.

Simple equations have been derived which can be used to predict the corner deflection resulting from laminate warping. These equations are based on the schematics illustrated in Figures 1 and 2. The resulting equation is:

corner deflection $= \delta = \delta_X + \delta_Y + \delta_{XY}$

where $\delta_X = R_X(1 - \cos \Theta_X)$;
$\delta_Y = R_Y(1 - \cos \Theta_Y)$;
$\delta_{XY} = R_{XY}(1 - \cos \Theta_{XY})$ and

where $R_X = 1/\varkappa_{XX}$; $R_Y = 1/\varkappa_{yy}$;
$R_{XY} = 1/\varkappa_{XY}$;
$\Theta_X \cong \sin^{-1}(a/R_X)$;
$\Theta_Y \cong \sin^{-1}(b/R_Y)$;
$\Theta_{XY} \cong \sin^{-1}(a/2R_{XY})$.

The notation used in these equations is evident from the schematics in Figures 1 and 2; $\varkappa$ is the local curvature determined from the well-known laminate theory.

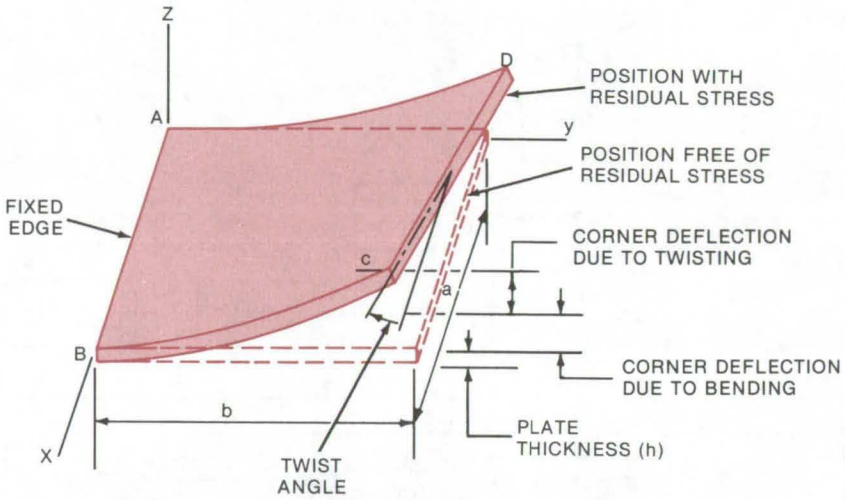

Figure 1. The **Effects of Residual Stress** are illustrated in this schematic of a deformed nonsymmetric angle-plied laminate with residual stresses.

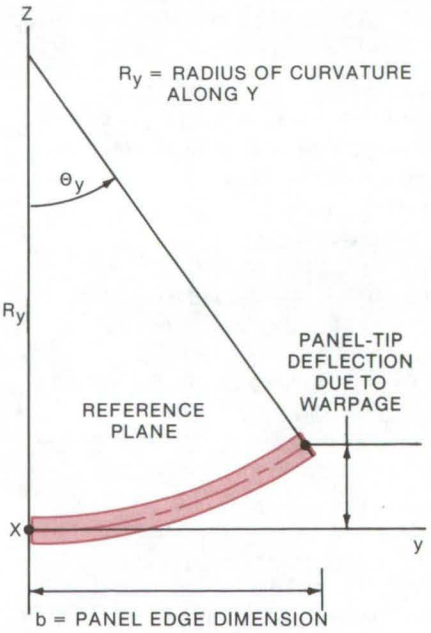

Figure 2. **Corner Deflection** is analyzed, using the geometric relationship between the corner-deflection panel-edge dimension and the radius of curvature.

Linear laminate theory is used in conjunction with the moment-curvature relationship without solving the coupled fourth-order partial differential equations of the plate or laminate. The micromechanics and macromechanics of composite materials are used in conjunction with laminate theory to assess the contribution of factors such as ply misorientation, fiber migration, and fiber and/or void-volume ratio nonuniformity on the laminate warpage.

Using these equations, it was found that a 1° error in the orientation angle of one ply was sufficient to produce an end deflection equal to two laminate thicknesses in a 25.4- by 25.4-cm (10- by 10-in.) laminate made from eight-ply MOD-I/epoxy. This example is illustrated graphically in Figure 3. Using a sensitivity analysis on the governing parameters, it was found that a 3° fiber migration or a void-volume ratio of 3 percent in some plies is sufficient to produce laminate corner deflection equal to several laminate thicknesses.

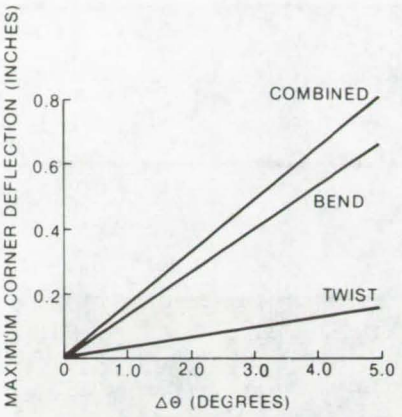

Figure 3. The **Predicted Maximum Warpage** corner deflection (point C in Figure 1, a = b = 10 in.) is shown due to residual stress in a (0_2, $+30$ $+\Delta\theta$, -30, ∓ 30, 0_2) laminate from MOD-I/ERLA-4617 composite at 0.5 fiber-volume ratio and ΔT = -300° F.

These equations should be of considerable practical value to both fabricators and designers. For example, the fabricator could use the equations to obtain an a priori assessment of the warp resulting from factors which may be difficult to control accurately during laminate fabrication. The designer, on the other hand, could use the results to specify tolerances which would minimize warp-producing nonsymmetries, or he could use the results to design the laminate with warp-compensating nonsymmetries.

This work was done by Christos C. Chamis of **Lewis Research Center.** *Further information may be found in NASA TM-X-71619 [N75-11048], "A Theory for Predicting Composite Laminate Warpage Resulting from Fabrication," a copy of which may be obtained at cost from the New England Research Application Center [see page A7].*
LEW-12615

Determination of Trace Amounts of POF_3

The extinction coefficient required for spectroscopic measurements is determined from an isosymmetric molecule.

Lewis Research Center, Cleveland, Ohio

Quantitative measurements of trace amounts of phosphorous oxyfluoride (POF_3) are often made by spectroscopic measurements that require a knowledge of the extinction coefficient of POF_3. (The extinction coefficient is a measure of the absorption of light by a dissolved substance. It is given by the formula

$$\varepsilon = \frac{1}{cd} \cdot \log \frac{I_0}{I}$$

where I_0 and I are the intensities of the incident and transmitted light, respectively, in a solution d centimeters thick of molar concentration c.)

In particular, the phosphorus-oxygen bond-stretching frequency of POF_3 has a very large extinction coefficient, and its absorption peak at 1,420 cm^{-1} can be employed to determine trace concentrations of POF_3. However, it is very difficult to obtain phosphorous oxyfluoride of purity well enough defined for direct measurement of the extinction coefficient.

An alternative approach takes advantage of the fact that the phosphorous oxyfluoride and phosphorous oxychloride ($POCl_3$) both belong to the same molecular symmetry group (C_{3v}) and should have extinction coefficients that are approximately the same. The extinction coefficient of reagent-grade phosphorous oxychloride was measured, and this coefficient was employed to calculate phosphorous oxyfluoride concentrations. This technique was found to permit quantitative determination of trace concentrations of POF_3 in unknown solutions and thus provides the analytical chemist with an additional tool for use on a problem not amenable to current analytical techniques.

This work was done by J. N. Foster of Rockwell International Corp. for **Lewis Research Center.** *No further documentation is available.*
LEW-10577

Flame-Resistant Elastomeric Polymers

Elastomeric compounds lead to useful products for automotive, textile, upholstery, and paint industries.

Lyndon B. Johnson Space Center, Houston, Texas

Several new fluorinated elastomers, urethanes, and neoprenes are flame resistant and produce very little smoke in environments containing as much as 100 percent oxygen. They were developed as resilient materials for scaling, vibration damping, cushioning, and restraining. Other possible applications for these flame-retardant elastomers include camera lens caps, helmet linings, packaging foams for instruments, coated fabrics, and other uses requiring the high elongation and recovery properties of rubbers.

The series of formulations, based on fluorinated rubber, is easily processed, chemically stable, and has other desirable physical properties. The effectiveness of additives, such as smoke suppressants and nonhalogenated flame retardants, was investigated. The most-flame-resistant formulation developed is shown in Table I. This formulation has a limiting oxygen index (LOI) of 95 to 100. When tested at 10 psia (69×10^3 N/m^2), under 31 percent O_2 and 69 percent N_2, using the silicone igniter, the material burned for only 50 seconds, and only 1 inch (2.5 cm) was consumed. It generated a heavy white smoke.

The formulation exhibiting the optimum balance of flame resistance and low smoke is shown in Table 2. This formulation has an LOI of 50. When evaluated, using the silicone igniter flame source in an atmosphere of 31 percent O_2 and 69 percent N_2 (10 psia), the material burned for 90 seconds (consuming 1 inch) and produced a relatively small amount of smoke.

Table 1. Flame-Resistant Formulation

Ingredients	Parts by Weight	Function
fluoroelastomers (based on the copolymer of vinylidene fluoride and hexafluoropropylene)	100	elastomer
lead oxide	15	curing agent
maleimide	4	curing agent
benzoyl peroxide	4.5	curing agent
decabromobiphenyl oxide	100	flame retardant

Table 2. Flame-Resistant and Low-Smoke Formulation

Ingredients	Parts by Weight	Function
fluoroelastomers	100	elastomer
lead oxide	15	curing agent
rubber accelerators (used to vulcanize fluoroelastomers and polyacrylate elastomers)	5	curing agent
hydrated alumina	50	flame/smoke retardant
ammonium polyphosphate	50	afterglow retardant

This and other formulations developed have been made into a wide range of useful products. For example, they have been:

- Extruded through a multifilament die to produce five-mil diameter elastic fibers and through a tubing die to produce excellent tubing and hose;
- Calendered to produce film and embossed sheeting;
- Compression molded to produce camera lens caps and ribbed constructions; and
- Dissolved in solvent to produce cements, paints, spread coatings, and saturating solutions useful in providing flame-resistant coatings, laminates, and impregnated foams.

This work was done by John T. Howarth, Suresh G. Sheth, and Kenneth R. Sidman of Arthur D. Little, Inc., for **Johnson Space Center.** *Further information may be found in NASA CR-144362 [N75-29264], "Flame Resistant Elastomeric Polymer Development," a copy of which may be obtained at cost from the National Technical Information Service, Springfield, Virginia 22151.*
MSC-16078

Enamel for High-Temperature Superalloys

New refractory passive thermal coatings are shock resistant and have desirable optical properties at high temperatures.

Marshall Space Flight Center, Alabama

Low-temperature, white, industrial porcelain enamels are largely designed for adhesion to extra-low-carbon steels and irons, with or without a primer coat (also termed ground coat). The linear thermal-expansion values of such substrates are 10 to 20 percent lower than for the high-temperature nonferrous superalloys. Typically, enameling glasses (frits) have a lower thermal expansion than substrate metals. Thus, the expansion mismatch is exaggerated by the use of the superalloys. The use of high-fusion-temperature glass, in order to exploit the high-service-temperature potential of superalloys, generally requires a glass composition with low thermal expansion. As a result, there are often unacceptable tradeoffs between enamel service temperature and thermal shock resistance (resulting from enamel-to-metal thermal-expansion mismatch).

Further property tradeoffs are required to obtain the requisite optical reflectance in the solar wavelength region, 0.2 to 2.5 μm. In this regard, conventional titania-opacified white enamels reflect about 65 percent of the solar wavelengths, in contrast to a minimum of 80 percent for a white thermal-control coating. The enameling of superalloys at high temperatures introduces increasing amounts of interfacial oxides. Because the oxides are black and are prone to diffuse into the enamel, high opacification is more difficult to attain in thin coatings.

Opacity proves to be the parameter which controls the design of this white refractory enamel. However, its primary components, the frit and the mill-added pigment, must provide a compatible combination which yields good basic enameling qualities on superalloys at service temperature extremes. Thus, at 1,000° to 1,200° C, fusion to a smooth, adherent, and coherent coating with well-distributed pigment should occur. It is most important that gas evolution be eliminated from this enamel as fired up to 1,200° C, whatever the source. For this reason, the composition of fluxing materials designed into the frit is critical.

The desired optical and high-temperature enamel properties have been obtained with glasses prepared from the system: Li_2O-ZrO_2-nSiO_2. Molar compositions range from n = 4 to n = 1.3, to which are added minor amounts (less than 5 to 7 mole percent) in varying combinations of alumina, alkali fluorides, boric oxide, alkali oxides, and alkaline earth oxides. These glasses are designed to be postprocessed into glass ceramics containing well-dispersed, submicron zircon and/or zirconia crystallites at a content of the order of 20 to 35 percent by weight.

The crystallized glass is blended with a submicron, disperse phase of cubic-stabilized ZrO_2 and is fired at 1,000° to 1,200° C to yield the white, refractory enamel. At a fired coating thickness of 0.0165 cm on Hastelloy X, such a zirconia enamel exhibits a solar absorptance (a_S) of 0.22. Initial coating adherence is good and is retained after repeated thermal soak and shock from 900° C to room temperature. These enamels, as coated on superalloy foils (less than 0.005 in. thick) and thin sheets, have high-temperature applications in industrial hardware (turbines, rockets, and jet engines) and in consumer hardware (ovens, ranges, and the like).

This work was done by H. Levin and W. E. Lent of Hughes Aircraft Co. for **Marshall Space Flight Center.** *For further information, Circle 54 on the TSP Request Card.*

Inquiries concerning rights for the commercial use of this invention should be addressed to the Patent Counsel, Marshall Space Flight Center [see page A8]. *Refer to MFS-22804.*

Improved Bonding of Honeycomb Panels

Large honeycomb panels are joined with metal braces, avoiding the wear points created when bolts or rivets are used to join the panels. The angular metal braces are bolted together and then bonded to the edges of the panels. The technique reduces fabrication time and costs and improves the strength and reliability of the finished product.
(See page 459.)

Signal Processing and Display for Electrochemical Data

A compact and inexpensive signal processor and display have been developed for the electrochemical detection of metabolic byproducts. Two electrochemical electrodes provide the signals; the new apparatus automatically determines the reaction end point and displays the lag period in time or cell concentration. The apparatus can be used with a standard pH reference anode and a platinum anode or with redox electrodes.
(See page 351.)

Low-pressure Low-Temperature Molding Process

A rubber mandrel is used to bond graphite/epoxy parts. The parts may be cured in an oven, making the process less expensive than those requiring autoclaving. The mandrel is a silicone rubber piece with a controlled expansion rate that is limited by a two-piece aluminum mold. Curing is at 350° F.
(See page 457.)

Second-Generation PMR Polyimides

New techniques for in situ polymerization of monomer reactants extend their useful life.

Lewis Research Center, Cleveland, Ohio

The excellent processing and elevated-temperature properties of the class of polyimides known as PMR polyimides (developed at the NASA Lewis Research Center) have made it possible to realize much of the potential of fiber-reinforced high-temperature resin matrix composites. Prior work has demonstrated the versatility and advantages of the polyimides prepared using the Lewis-developed PMR (in situ polymerization of monomer reactants) approach (see references NASA TM-X-67803 and TM-X-71616). PMR polyimides can be processed by either compression or autoclave molding techniques, and the addition reaction involved yields laminates with very low void content.

In the PMR approach, the reinforcing fibers are impregnated with the PMR polyimide solution, which consists of a mixture of monomers dissolved in a low-boiling alkyl alcohol such as methanol or ethanol. The first-generation PMR monomer mixture consists of the appropriate stoichiometric quantities of the following: (a) dialkyl ester of an aromatic tetracarboxylic acid, (b) an aromatic diamine, and (c) monoalkyl ester of an alicyclic dicarboxylic acid. The molar ratio of a:b:c is n:(n+1):2. Mixtures of various diester-diacids (monomer a) and aromatic amines with more than two amino groups can be used with proper adjustments made with respect to stoichiometry.

Commercially available PMR polyimides based on first-generation technology use the following monomers: dimethyl ester of 3,3′,4,4′-benzophenonetetracarboxylic acid (BTDE), 4,4′-methylenedianiline (MDA), and 5-norbornene-2,3-dicarboxylic acid monomethyl ester (NE). This combination of monomers at a stoichiometry such that the formulated molecular weight is equal to 1,500 was found to provide the best overall balance of processability and retention of mechanical properties after 500 hours of exposure in air at 589 K (600° F) (see reference NASA TN-D-6877). Several major suppliers are now producing PMR polyimide prepreg materials, and a number of jet engine and aircraft parts are being made from them and evaluated.

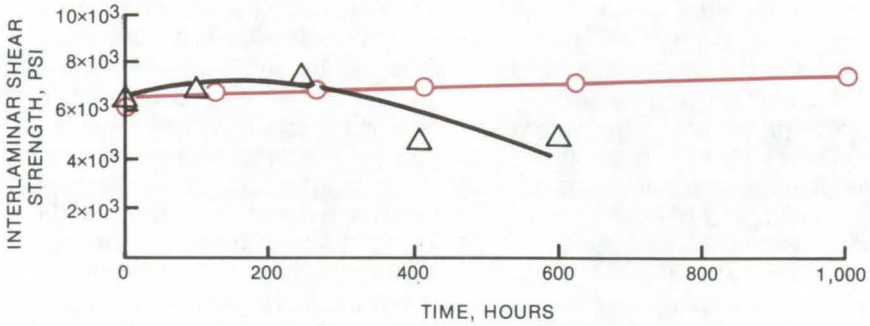

The **Interlaminar Shear Strength** of PMR Polyimide/HTS graphite-fiber composites at 600° F (589 K) is maintained longer for the second-generation formulations.

Continuing research has resulted in the development of PMR polyimides with improved thermo-oxidative stability at 589 K (600° F) (see references NASA TM-X-71894 and TM-X-71816). The newly developed PMR polyimides, which are referred to as "second-generation" PMR polyimides, are based on the dimethyl ester of 4,4′-(hexafluoroisopropylidene)-bis(phthalic acid) (HFDE) and p-phenylenediamine (PPDA) and NE. The useful life at 589 K (600° F) of fiber-reinforced composites made with currently available and with second-generation PMR polyimides are compared in the figure. Tests were conducted at 589 K (600° F) after exposure in air at 589 K (600° F) for various time intervals. It can be seen in the figure that the useful life of the second-generation PMR polyimides is at least twice that of the earlier PMR polyimides.

This work was done by Tito T. Serafini and Raymond D. Vannucci of **Lewis Research Center** *and William B. Alston of the U.S. Army Air Mobility R. & D. Laboratory. Further information may be found in:*

NASA TM-X-67803 [N71-23367] "Thermally Stable Polyimides from Solutions of Monomeric Reactants,"

NASA TM-X-71616 [N74-34960] "Tailor Making High Performance Graphite Fiber Reinforced PMR Polyimides,"

NASA TN-D-6877 [N72-29598] "Addition Type Polyimides from Solutions of Monomeric Reactants,"

NASA TM-X-71816 [N76-11289] "PMR Polyimides with Improved High Temperature Performance," and

NASA TM-X-71894 [N76-21337] "Second Generation PMR Polyimides."

Copies of these reports may be obtained at cost from the New England Research Applications Center *[see page A7]**.*

LEW-12738

Purity Test for Copper-Plating Solutions

Overvoltage at the cathode indicates the presence of impurities.

Marshall Space Flight Center, Alabama

Impurities in acidic copper-plating baths can cause deposits to be brittle, rough, discolored, and streaky. They can also cause poor plating adhesion. Knowledge of the impurity levels of plating solutions is important for quality control, and can be determined by a simple test based on the measurement of polarization voltage.

The ideal relationship between the polarization voltage (V_p) in an acid copper bath and the applied current is described by

$$V_p = a - b \log I$$

where a and b are constants and I is the applied current. However, in a contaminated bath, impurities block parts of the electrode surface, and this leads to greater (more negative) polarization of the cathode. This effect is used in the experimental arrangement shown in Figure 1 to measure the impurities in a copper-plating solution.

A constant current is applied to the electrodes A and B. The polarization voltage, V_p, is measured between the Cathode A and a third, unpolarized, electrode (C). At an applied current density of 10 mA/cm², the value of V_p after 3 hours is between -80 and -100 mV in a clean bath; but it is between -110 and -180 mV in a contaminated bath. A current density of 10 mA/cm² is used because it is in the range at which the value of V_p is most sensitive to contamination.

Figure 2 compares the variation of V_p with time for clean and contaminated plating baths. Usually 15 minutes is sufficient to distinguish between the two cases.

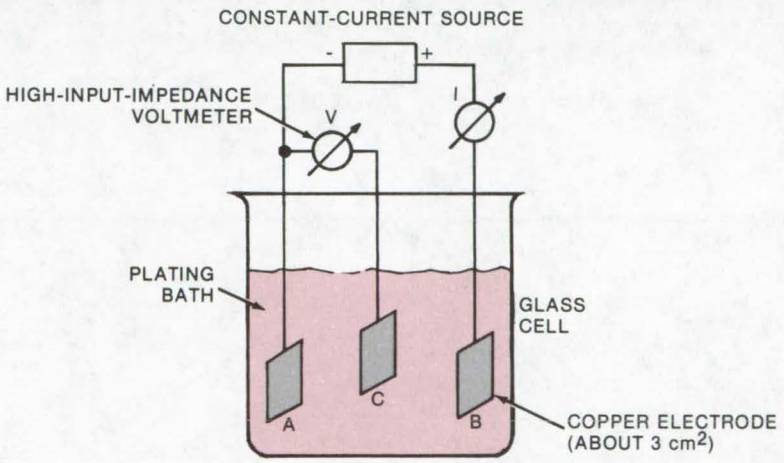

Figure 1. The **Electrode Configuration** shown above can be used to measure the extent of impurities in an acid copper-plating solution. It can be inserted into any plating tank and will show whether the bath is clean or contaminated, within 15 minutes.

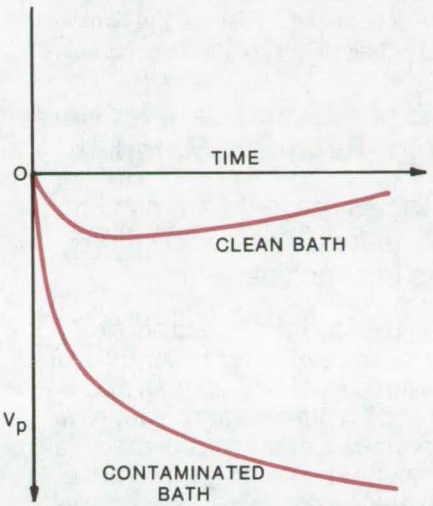

Figure 2. A plot of **Polarization Voltage Vs. Time** shows how impurities in the solution cause greater negative polarization of the cathode.

This work was done by Florian B. Mansfeld of Rockwell International Corp. for **Marshall Space Flight Center.** *For further information, Circle 55 on the TSP Request Card.*
MFS-19298

Books and Reports

These reports, studies, and handbooks are available from NASA as Technical Support Packages (TSP's) when a Request Card number is cited; otherwise they are available from one of NASA's Industrial Application Centers or the National Technical Information Service.

Experimental Data for New Fire-Retardant Materials

Tables present flammability data for polymeric coatings, foams, and textiles.

The flammability and physical properties of 24 upholstery and furnishing materials, such as those used in commercial aircraft, have been evaluated and published in a report. Flammability properties of materials commonly used prior to 1968 were compared with those of new fire-retardant materials. Results indicated that pre-1968 materials ignited easily, allowed the fire to spread, produced large amounts of smoke and toxic combustion products, and were capable of supporting flash fires causing major damage. The new fire-retardant materials were found to restrict fire propagation, to decompose rather than ignite, and generally to resist combustion. Less smoke was produced, and lower concentrations of toxic combustion products and lower resulting environmental temperatures were noted.

Physical properties, such as strength, flexibility, and abrasion resistance, were determined mechanically in the laboratory. Other data presented include degradation upon heating, limited-oxygen indices, smoke generation, flammability afterglow, and char length. Thermogravimetric (TGA) tests were used to determine thermal-degradation profiles. The weight loss of each material as a function of increasing temperature was recorded along with the temperature at which degradation began (which was also taken as the point at which the high rate of potentially toxic offgassing occurred). Other offgassing analysis and toxicity tests were also conducted.

Smoke generation was measured by heating the material in a chamber and measuring the loss of light transmittance through the chamber. The limited-oxygen index (refers to minimal volume fraction of oxygen in a slowly-moving oxygen/nitrogen atmosphere that will support flaming combustion) was measured by suspending the material in a chamber and igniting it at the top. The test is a reproducible measure of the intrinsic flammability of material.

This work was done by Daniel E. Supkis of **Johnson Space Center.** *Further information may be found in NASA TM X-58165, "Refurbishment of NASA Aircraft With Fire-Retardant Materials." Copies of this report may be obtained at cost from the National Technical Information Service, Springfield, Virginia 22151. MSC-16022*

Life Sciences

Hardware, Techniques, and Processes

Computer Programs

Measuring Mandibular Motions

A simply-mounted quickly adjusted system measures motion in three dimensions.

Ames Research Center, Moffett Field, California

Dental health can often be determined by the static and dynamic relationships between the maxilla and the mandible. However, border profiles of mandibular movements have been difficult and costly to measure, because of inadequate techniques or because of the effects of the required patient preparation.

An improved system overcomes many of the prior problems. Mandibular motion along three axes is measured by three motion transducers on a floating yoke that rests against the mandible. The system includes electronics to provide a variety of outputs for data display and processing.

A head frame is strapped to the test-subject's skull to provide a fixed point of reference for the transducers. The head frame also supports a yoke, or facebow, that is attached to the mandible. Two transducers are located over the ears, and one is supported near the forehead. Motions of the facebow are communicated to the transducers by rigid couplings.

The transducers are low-friction, infinite-resolution cermet potentiometers that are activated by the axial motion of the terminal end of a small-diameter rod and by its angular disposition from a fixed point of reference central to the transducer. Output signals from the transducers can be processed to provide corrections for small errors in positioning relative to the hinge axis. Additionally, the signals are conditioned to provide simultaneous monitoring of various movements or combinations of movements for display or for computer processing of data.

The electronic stability of the system permits displacements of the order of 0.03 mm to be measured for vertical displacement of the facebow, left-to-right motion, and forward motion. However, overall stability may be limited by the way in which components are mounted and coupled to maximize rigidity but minimize discomfort to the test subject.

This work was done by John Dimeff and Salvatore Rositano of **Ames Research Center** *and Robert C. Taylor of the University of California. For further information, Circle 56 on the TSP Request Card.*
ARC-10956

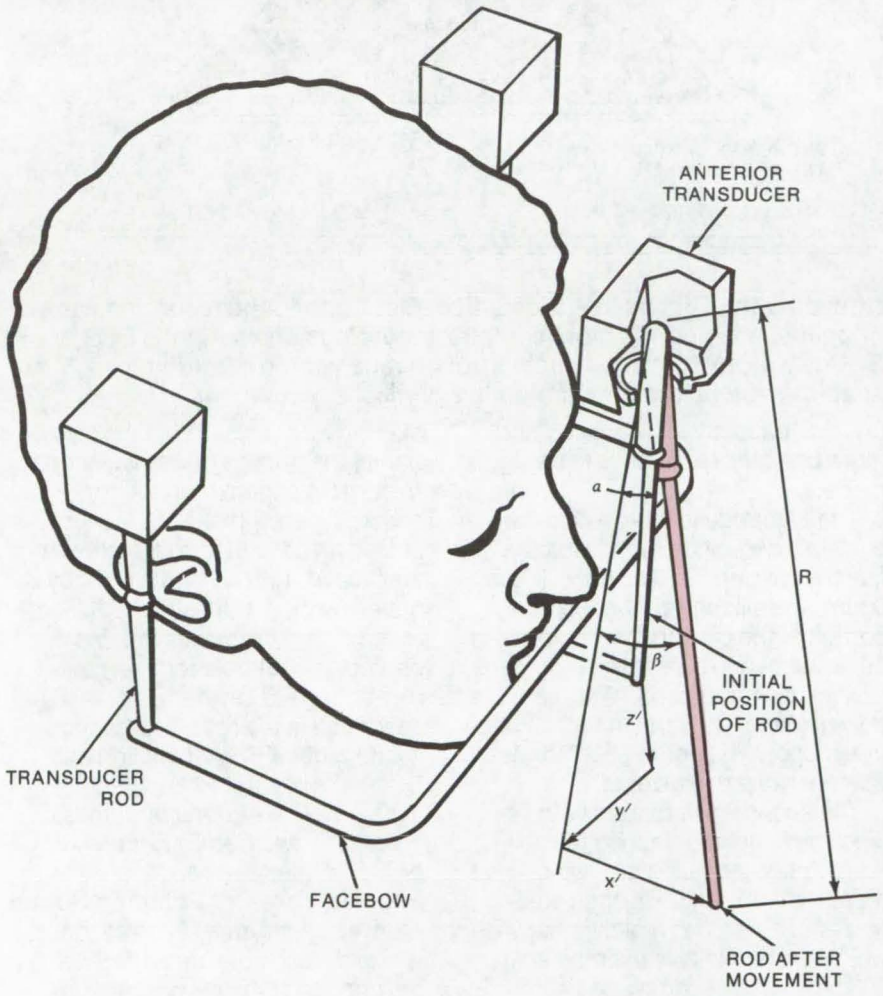

Transducer Operation is illustrated for the anterior transducer. The position of the measuring rod after movement of the mandible is shown in color. Extension and angular displacement are exaggerated for clarity. Motion of the rod is detected in spherical coordinates, where α and β are angular displacement and R (the extension) is the radial variable. The data may be transformed to x,y,z Cartesian coordinates.

Disposable Biomedical Electrode

Lower patient EEG (or EOG) monitoring costs by using throwaway electrodes which snap into a stretchable, reusable recording cap.

Lyndon B. Johnson Space Center, Houston, Texas

A reusable recording cap equipped with compressible snap-on bioelectronic electrodes is worn by a patient to allow remote monitoring of his electroencephalogram (EEG) and electro-oculogram (EOG) waveforms. The electrodes can be attached to the inside surface of a stretch-textile cap at 12 monitoring positions and at one or two ground positions.

The cap can be stretched to accommodate some variation in head size, and the use of three or four basic cap sizes allows most any head size to be fitted. Because the electrodes are prepositioned, they can be placed by the patient without the help of a skilled technician.

This updated recording cap/electrode system is more cost effective than previous versions. An earlier model, described in NASA Tech Brief B72-10642, was a stretch-textile cap with a group of three electrodes permanently attached to the inside surface. For sanitary purposes the cap/electrode was disposed of after only one wearing, a fairly expensive procedure since the major costs incurred in fabricating the system — and particularly the expensive cap — could not be lowered through repeated use. In the new system the recording cap is fitted with snap-on recording electrodes. After each wearing, the cap is cleaned and stored for further use; only the electrodes are disposed of. The new system has an estimated materials costs of one-tenth that of the disposable version.

The new cap/electrode is also more versatile. Previously the number of electrodes (two EEG channels and one EOG channel) limited use mainly to monitoring patients while asleep. In the new system the electrodes may be located at any of the 12 monitoring positions as standardized by the International Federation of Societies for Electroencephalography and Clinical Neurophysiology. This increased capacity allows faster and more complex recordings to be made.

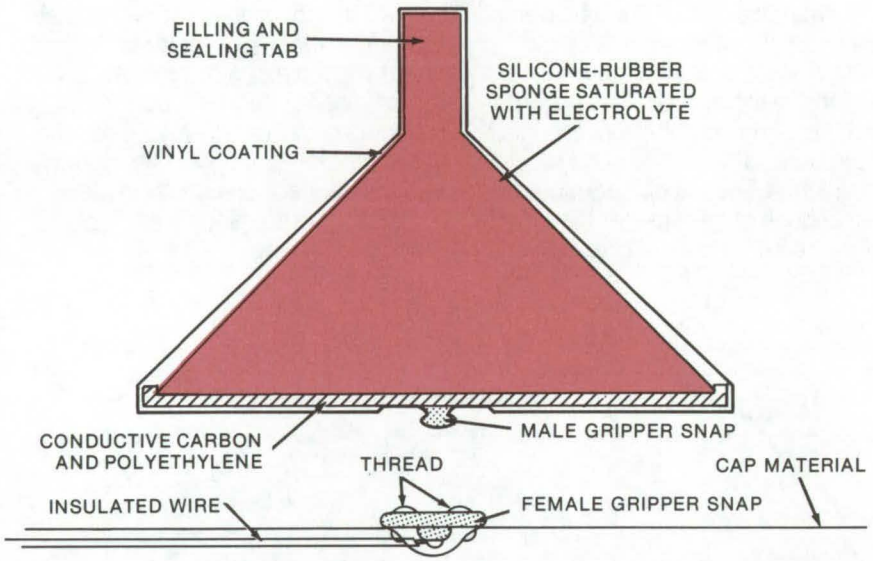

Attaching the **Disposable Biomedical Electrode** to the recording cap via gripper snaps permits more complex recordings of a patient's EEG or EOG waveform. Lowered costs through reuse of the recording cap enables system implementation in a clinical environment.

The electrode is attached to the cap via a two-piece metal clothing fastener or gripper. As shown in the figure, the silicone-rubber sponge portion of the electrode is molded and attached to a base of 30 percent lampblack carbon and 70 percent polyethylene, as is the male half of the gripper. The entire assembly is coated with a thin layer of vinyl.

The sponge is saturated with electrolyte gel by injecting the solution through a sealing tab, which is resealed with vinyl. Finished electrodes are stored in a plastic bag in which the humidity is maintained at 100 percent by adding a slight amount of water before sealing. The assembly is used by fitting electrodes to the cap grippers and cutting off the electrolyte-seal on each tab, permitting electrolyte to flow out of the electrode. The cap, when worn by the patient, automatically positions the electrodes and causes the escaping electrolyte to moisten the wearer's scalp. An insulated wire, soldered to the female half of the gripper, feeds waveforms to suitable patient monitoring/recording equipment.

Because the electrodes are prepositioned, they can be placed by a patient without the help of a skilled technician. This makes the cap particularly suitable for a remote monitoring EEG system, as described in the article following: "Automated EEG Acquisition and Display" (MSC-16111).

This work was done by James D. Frost, Jr., and Carl E. Hillman, Jr., of The Methodist Hospital of Houston, Texas for **Johnson Space Center.** *For further information, which consists of a more detailed description of the new recording electrode, Circle 57 on the TSP Request Card.*

This invention is owned by NASA, and a patent application has been filed. Inquiries concerning nonexclusive or exclusive license for its commercial development should be addressed to the Patent Counsel, Johnson Space Center [see page A8]. Refer to MSC-14623.

Automated EEG Acquisition

With this portable unit, minimal training is required to conduct EEG's in the field.

Lyndon B. Johnson Space Center, Houston, Texas

Electroencephalography (EEG), a means of monitoring brain functions, is essential to the diagnosis of certain neurological diseases. Despite a rising demand for EEG in routine practice, applications remain relatively rare because of its expense and complexity and the scarcity of highly skilled operators.

The availability and routine use of EEG could be extended by a newly-developed and tested EEG acquisition and display unit. This automated self-contained portable device, shown in Figure 1, can be used by technicians with minimal training. Data acquired from the patient at a remote site are transmitted to a centralized interpretation center, using conventional telephone equipment. There, the diagnostic information is analyzed, and the results are relayed back to the remote site. Consequently, high-quality EEG diagnostic services, formerly possible only in some large medical centers, are made widely available. The components and functions of both the data acquisition and display unit and the centralized processing center are shown in Figure 2.

Data Acquisition and Display Unit

The recording cap, a key part of the overall system, contains 14 snap-in electrodes: 12 recording electrodes connected in eight different pairs and 2 ground electrodes. The cap eliminates the need for careful and time-consuming measurements in placing electrodes. The cap and the electrodes are described in the preceding article, "Disposable Biomedical Electrode" (MSC-14623).

The electronic circuitry includes a preamplifier attached to the recording cap. Signals from the eight electrode pairs are amplified initially in the cap to reduce extraneous electrical signals and artifacts due to the subject's movement. In the unit itself, the signals are further amplified and pass through a band-rejection filter (60 Hz, 40 dB). Overall, a $\pm 10\ \mu V$ signal at the preamplifier input is boosted to ± 1.414 V.

Each of the eight amplified signals is phase-modulation coded in a separate voltage-controlled oscillator. The oscillator outputs are multiplexed to form a composite audio-frequency signal for transmission over a telephone line.

Special circuit features include a built-in calibration signal and an electrode test circuit. The calibration signal allows the central facility to check overall gain to insure accurate interpretation of EEG amplitude signals. The electrode test circuitry checks the adequacy of electrode-to-scalp contact by determining the resistance between the 12 recording and the 2 ground electrodes.

Central EEG Interpretation Facility

Functions at the central facility include:

- Recognition, decoding, and display of received signals
- Advice and assistance to the remote site
- EEG interpretation
- Transmission of the EEG report

After normalization and decoding, the received signals are displayed on a graphic recorder for visual analysis. This allows real-time review of the signals by experts who can discuss results with remote-site technicians over the voice communications channel.

The central facility also includes automated EEG analysis to assist professionals in interpreting the incoming signals. First-order electronic analysis is performed in a special unit that detects period or wavelength, peak-to-peak amplitudes, and spikes, and interfaces to the second-order analysis system. The second-order analysis occurs in a minicomputer and is the central analysis component. It is an online real-time system that collates information from the first-order system and obtains additional information from the EEG signals. The third-order system, a full-sized computer facility, is currently utilized only for bulk storage of data. Future plans are to expand this role to statistical analysis of EEG signals.

Figure 1. The **Data Acquisition and Display Unit** for EEG includes: a recording cap, an eight-channel cap-mounted preamplifier, automatic electrode-testing circuitry, final amplification and band-pass filtering, eight-channel magnetically-coupled telephone telemetry, a voice communication channel and alarm circuit, and a decoder and printer.

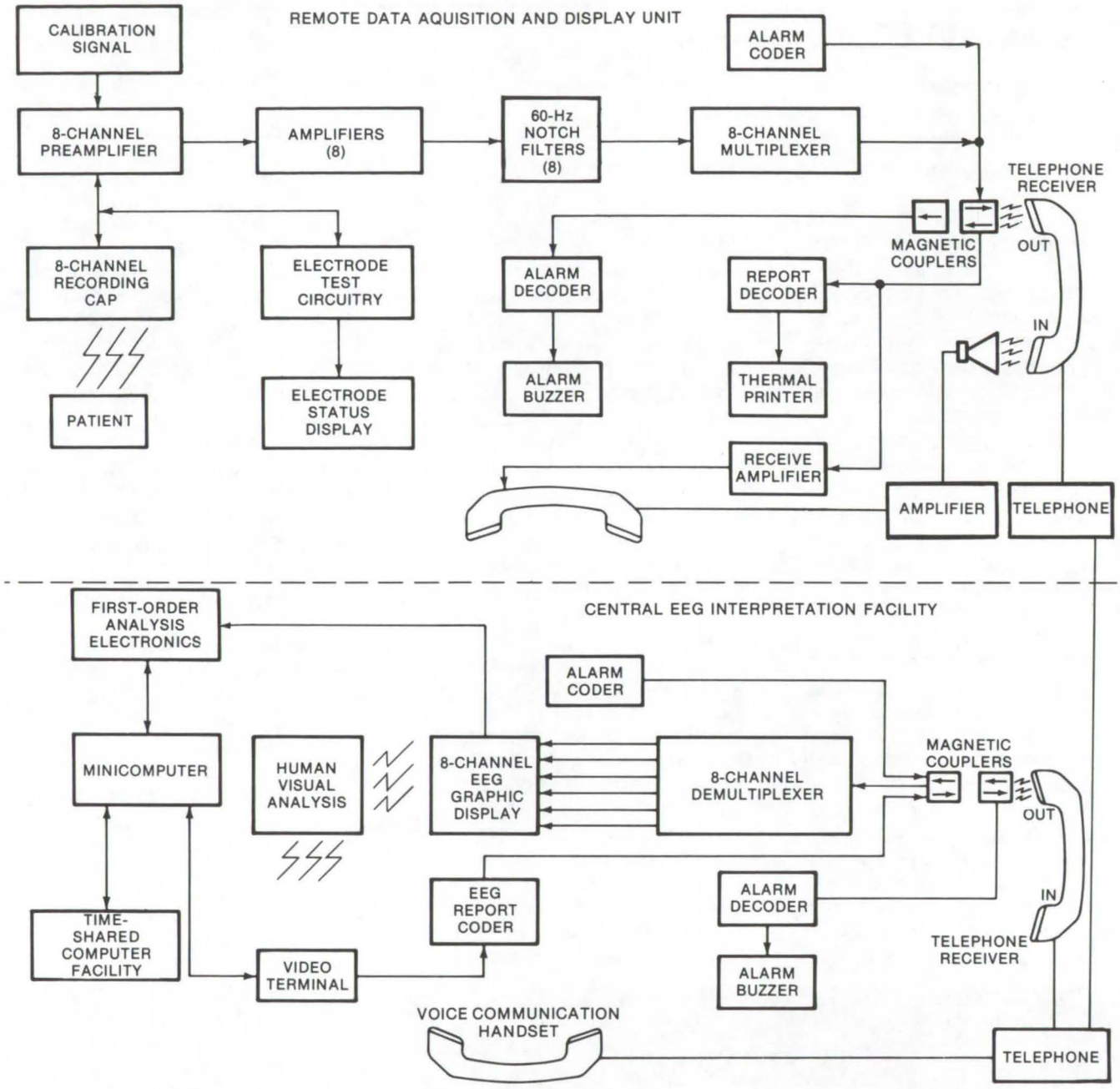

Figure 2. In the **Remote-Site EEG Analysis System,** The EEG Data Acquisition and Display Unit (Figure 1) is used to relay EEG signals to a centralized facility over conventional telephone lines. The highly trained specialists, using computers, analyze the signals and send information back to the remote site on a real-time basis. An audible alarm can be used to interrupt EEG transmission for voice consultation between the two locations.

The results of the first-order and second-order analyses are displayed on a terminal and compared, by the electroencephalographer, to the results of his own visual analysis. A final report is sent back to the remote site where it is reproduced on a printer.

System Test and Evaluation

The entire system has been tested and evaluated under laboratory and remote conditions. The quality of transmitted signals was found to compare favorably with directly monitored EEG's. The system presently has an upper frequency limit of 40 to 50 Hz, due to telephone line restrictions. Although 100 Hz is the recommended upper limit for EEG, most known abnormalities can be identified from the lower frequency signals.

The system as it now stands has proved valuable in specific situations, such as the long-term monitoring of epileptic subjects. In this case, where the type of abnormality expected is specified beforehand, the automated analysis agrees quite well with human evaluation.

This work was done by James D. Frost, Jr., and Carl E. Hillman, Jr., of The Methodist Hospital for **Johnson Space Center.** *Further information may be found in NASA CR-147554 [N76-22888], "Automated Electroencephalography System and Electroencephalographic Correlates of Space Motion Sickness." A copy may be obtained at cost from the National Technical Information Service, Springfield, Virginia 22151.*

Inquiries concerning rights for the commercial use of this invention should be addressed to the Patent Counsel, Johnson Space Center [see page A8]. Refer to MSC-16111.

Remote Water-Monitoring System

Water samples are obtained, analyzed, and stored, while data are transmitted to a receiving station.

Langley Research Center, Hampton, Virginia

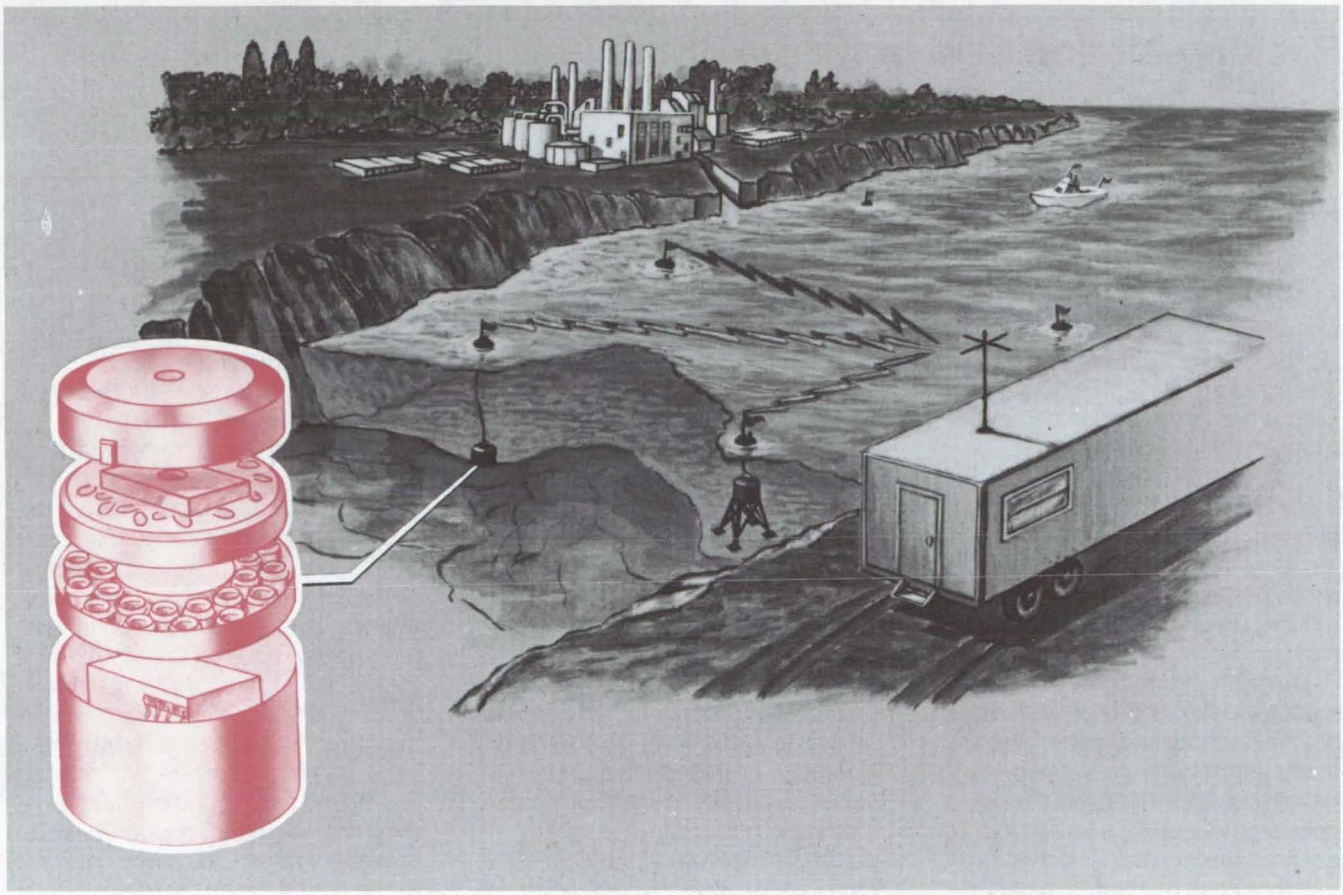

The **Coliform Bacteria Monitor** consists of a floating buoy, which contains the transmitting and receiving antenna, connected to a submerged unit. The submerged unit contains, basically, an intake valve and delivery tube for conducting the sample to the container where measurements are taken.

A general-purpose, remote water-quality sampling system (see illustration) detects micro-organisms in water. It integrates sampling, sample preservation, and sample analysis and allows remote operation and data handling. The system has been designed to overcome difficulties previously experienced in the interpretation of remote measurements from aircraft and spacecraft. These difficulties were primarily in measuring changes in water quality, mainly problems of correlating surface measurements with remote measurements. While this system is used in the sampling and analysis of coliform bacteria, the concept could be applied to other types of water analysis.

The sampling apparatus is sterilized and remains sealed against outside contamination, both before and after sampling intake. Samples may be obtained at any depth through adjustment of the intake valve length. Coliform bacteria are enumerated by measuring the amount of hydrogen produced during the consumption of the nutrient by the bacteria. The number of organisms is directly proportional to the time required for this electrochemical process to produce a measurable voltage level. The time interval between inoculation and voltage rise (lag time) is electronically processed and transmitted to a remote receiver station.

Sampling occurs after a command signal transmitted to the sampler platform initiates, simultaneously, operation of the flight sensors and the remote sampler platform systems. The platform system obtains and analyzes the sample. Although the concept has been demonstrated for the remote detection of coliform bacteria, the operating principles can be extended as well to a variety of physical or chemical measurements. The command signal can also activate a navigation device to determine the precise geographical location of the sampler platform.

This method offers better data correlation and minimizes human error in the handling of samples and instrumentation. Sampler platforms can be positioned and made operationally ready long before needed, eliminating rendezvousing problems. Data can be taken by the monitoring system over extended periods of time and relayed to remote stations as it is obtained. Samples can be stored in a natural environment for later laboratory analysis.

This work was done by David C. Grana and David P. Haynes of **Langley Research Center.** *For further information, Circle 58 on the TSP Request Card.*

Inquiries concerning rights for the commercial use of this invention should be addressed to the Patent Counsel, Langley Research Center [*see page A8.*] *Refer to LAR-11973.*

Rocking-Motion Sensor for the Blind

A feedback system notifies the wearer when specific types of body motion occur

Lyndon B. Johnson Space Center, Houston, Texas

Some body motions (such as rocking motions) are unconscious and often unwanted phenomena exhibited by congenitally blind people. To cope with this difficulty, a motion sensor has been used that incorporates an audible biofeedback signal to warn a blind person that he is rocking and records occurrences for behavior analysis. The recorder and motion sensor (with a remote body-mounted accelerometer for sensing motion) are separate body-mounted units.

The system can operate in three modes independently of each other or simultaneously: sensing, feedback, and refractory. In the sensing mode (see figure) a counter counts pulses produced by a transducer (an accelerometer used to monitor rockings) and compares the accumulated count with a presettable timer to determine if a threshold has been reached within a time frame. If, when the time interval has passed, an insufficient number of pulses has been counted, the counter is reset to zero; and a new time frame is initiated. However, if the number of pulses is greater than the preset number, the threshold is exceeded; and the system produces timing control signals and an alert signal and will switch into the second or feedback mode.

In the feedback mode the alert signal is produced upon the occurrence of each monitored pulse. A recorder is turned on (by a timing control signal) to record an indication corresponding to the alert signal. The system will stay in the feedback mode until no further pulses are detected for a desired time interval after the last detected pulse, and then a control signal shifts the system into a third or refractory mode. In this mode a final signal is recorded, and the recorder is turned off, switching the system back to the sensing mode.

The sensor (an accelerometer that can be mounted on a pair of eyeglasses) detects forces due to acceleration and gravity and is normally oriented to sense forward accelerations. Coupled to the transducer is a signal-conditioning amplifier which has a variable gain adjustment that can be used to vary the rocking required to produce a rock signal. The overall system is preprogramed to discriminate rocks from normal movement by varying three parameters: the amplitude of the motion required to produce a rock, the number of rocks required to reach a threshold, and the time frame during which rocks are counted. The system is timed by a clock that also produces the tone

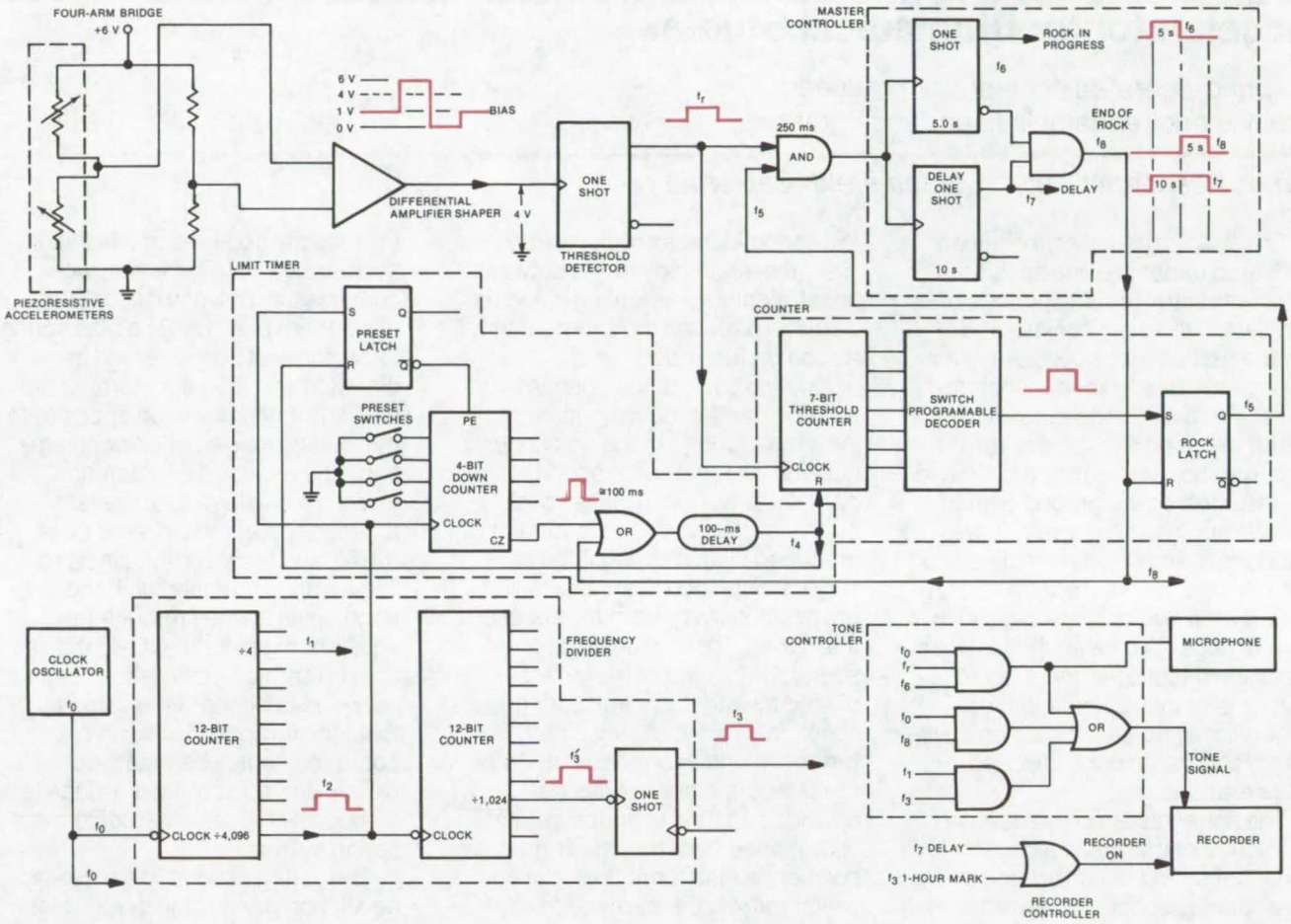

The **Rocking-Motion Sensor System** generates signal f_6 after a rocking motion has been detected. Signal t_0 (an input to the tone controller that places a distinct tone on the tape recorder for each event) is gated to the microphone each time that signal f_r (the rocking pulse) arrives within a 5-second time span created by f_6. Signal f_6 turns on the recorder whenever a rock has been detected, and signal f_7 holds on the recorder an additional 5 seconds after f_6 falls to zero. Signal f_3 turns on the recorder 3 seconds each and every hour. At the end of a rock motion, signal f_8 causes a strip of f_0 to be recorded as an end-of-rock tone.

signals for recording. Control signals are derived from multivibrators and logic networks.

This work was done by Arthur Mandell of **Johnson Space Center** *and Joseph E. Morgan and John T. Polhemus of Martin Marietta Corp. For further information, Circle 59 on the TSP Request Card.*

This invention is owned by NASA, and a patent application has been filed. Inquiries concerning nonexclusive or exclusive license for its commercial development should be addressed to the Patent Counsel, Johnson Space Center [see page A8]. Refer to MSC-14805.

Accelerator for Biomedical Studies

A spring-operated accelerator produces precise and repeatable linear accelerations.

Ames Research Center, Moffett Field, California

Small biological specimens can be tested under precise accelerations, repeated for long periods of time, with an easily constructed device that employs constant-force springs to provide linear accelerations. The basic parts of the accelerator are shown in the diagram. The fixed base permits the device to be mounted on the ground or in a vehicle such as an aircraft; it also supports the spring assemblies and the carriage tracks (rods). The test load is attached to and moves with the carriage. Typically, the test load consists of test specimens and cameras or instrumentation for observing or acquiring data on specimen responses to the imposed accelerations.

The spring assembly at each end of the track consists of a constant-force flat spring coiled around a free-running spool. The assemblies can be easily removed so that springs of different strengths and configurations can be installed. The free end of each spring is fixed to hooks on the carriage. The force applied by either spring is proportional to the cross-sectional area of the spring in the transition region (i.e., the section of spring between the straight segment lying along the carriage path and the segment fully wound on the spool).

One, or both, of the springs is of two constant-force magnitudes. With the carriage in the equilibrium position, the two-force spring is partially unwound from its spool, such that a greater spring force is produced by this spring if the carriage is displaced from its equilibrium position away from the spool of this spring, thereby unwinding the spring, than if the carriage is displaced toward this same spring spool, in which case the spring is further wound upon its spool. Thus, the two spring assemblies are arranged so that when the carriage is displaced from the equilibrium position, a bias force is produced which returns the carriage toward the equilibrium position.

To operate the linear accelerator, the carriage is initially displaced from its equilibrium position and released. The bias spring force produced accelerates the carriage toward the equilibrium position. With the velocity acquired in this initial accelerated travel, the carriage continues its movement past the equilibrium position. The bias spring force is thereupon reversed in direction and then accelerates the carriage in the direction opposite to the initial spring-applied acceleration. The reversed acceleration slows the carriage to an instantaneous halt at the extreme of its travel; and then the velocity is reversed and increased until the carriage again passes through the equilibrium position, where the applied spring acceleration is again reversed to become the same as that initially applied. This cyclic operation continues until it completely degrades or the carriage is stopped by means external to the spring system.

The spring assemblies may also be supported near the center of the path so that only one spring is in a force-producing relationship to the carriage at a given time. In this latter configuration, a spring with two force magnitudes is not required.

By using a vertical arrangement, gravity in combination with a spring system of one or two spring assemblies may be used to produce the required force to accelerate the carriage toward the equilibrium position. The guide tracks or rods may not be necessary.

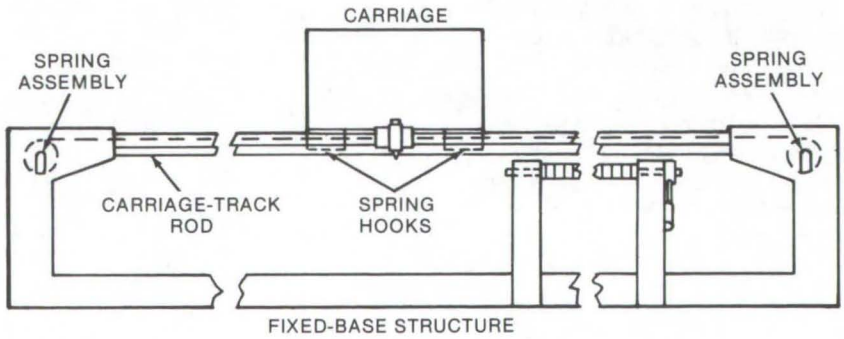

The **Spring-Operated Accelerator** consists of a fixed base, two spring assemblies, a carriage, and a test load.

This work was done by George L. Shillinger, Jr., of **Ames Research Center.** *For further information, Circle 60 on the TSP Request Card.*

This invention is owned by NASA, and a patent application has been filed. Inquiries concerning nonexclusive or exclusive license for its commercial development should be addressed to the Patent Counsel, Ames Research Center [see page A8]. Refer to ARC-10898.

Multiposition Rescue Litter

A very lightweight stretcher locks into several configurations, including one for compact storage.

Lyndon B. Johnson Space Center, Houston, Texas

By utilizing four multiposition locking hinges and folding supports (see Figures 1 and 2), a new rescue litter has a wide range of applications in emergency situations. The stretcher can be set up in a chair-carrier position, or it can be folded to one-third its length. Adjustable support positioners (see Figure 3) can hold plasma and provide limb support and end-tilt positions. The special hinges and supports eliminate the need for separate accessory items and save weight and storage space; the compact one-third length folded position permits easier handling in rescue.

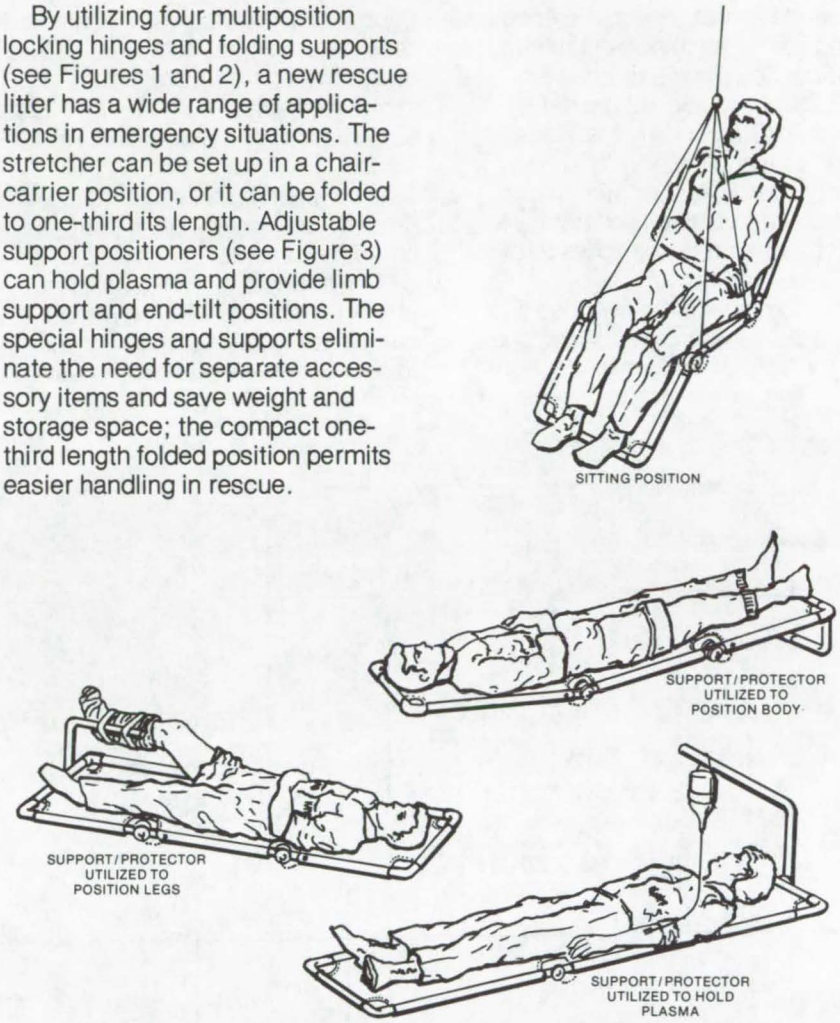

Figure 1. The **Rescue Litter** can be set up in several positions, and the tubular end support can be positioned on the frame for limb or plasma support or for end-tilting support.

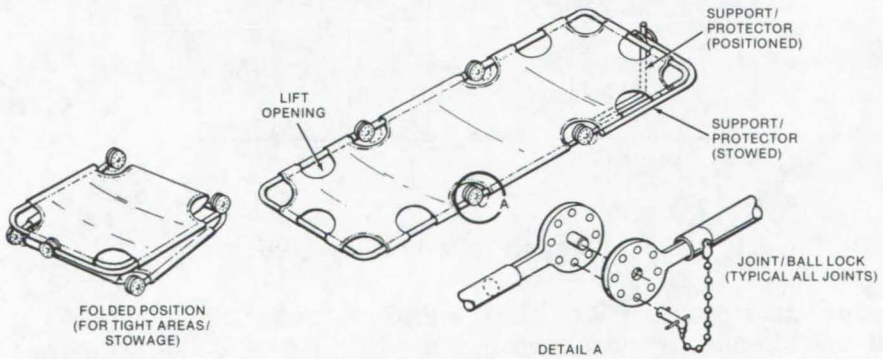

Figure 2. A **Multiposition Locking Hinge** can be locked in several positions, enabling the litter to be folded.

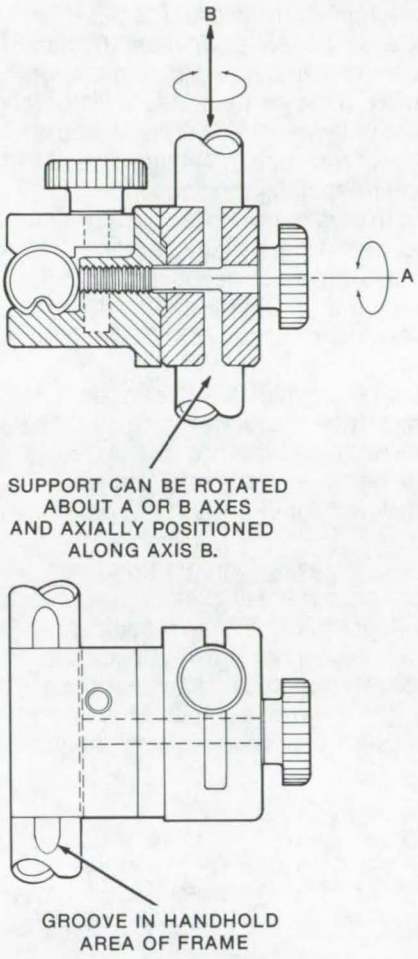

Figure 3. The **Adjustable Support Positioner** can be positioned on the litter frame to hold objects. The positioner can be rotated about the A or B axis and axially positioned along axis B.

This work was done by Richard L. Robbins of Rockwell International Corp. for **Johnson Space Center.** *No further documentation is available.*

Inquiries concerning rights for the commercial use of this invention should be addressed to the Patent Counsel, Johnson Space Center [see page A8]. Refer to MSC-16148.

Short-Range Biotelemetry System

Monitor medical patient's vital signs, using implantable vhf equipment

Lyndon B. Johnson Space Center, Houston, Texas

A miniaturized vhf transmitter relays a patient's biotelemetric data to a receiver located 25 or more feet away. It is constructed as an integral part of the electrode sensors and is one of two such transmitters used, one transmitter per sensor pair. Each crystal-controlled battery-powered transmitter is assigned one of two carrier frequencies: 157.55 MHz and 172.05 MHz. Signals from electrocardiogram (EKG), electromyogram (EMG), and electroencephalogram (EEG) electrodes frequency-modulate the carrier. The transmitters have two gain settings; the higher is used for EEG signals, the lower for EKG and EMG data inputs.

A three-stage integrated-circuit (IC) instrument amplifier boosts sensor signals prior to modulating the transmitter. The IC chosen can convert from a balanced-input to a single-end mode output. Since the amplifier is used to process unequal-amplitude sensor inputs, a compensating gain adjustment is built into the amplifier. The electrodes are capacitively coupled to the data amplifier. Direct current flow between sensors and skin (from the battery source) is thus eliminated. Inductive and capacitive filters are used between the electrodes and data amplifier inputs.

The companion receiver has two tuning units (each of which matches one transmitter frequency). The double-conversion crystal-controlled receiver amplifies, demodulates, and processes the biotelemetry signal for display. A phase-lock-loop IC demodulates the amplified RF signal.

The system is likely to find greatest use in monitoring post-operative patients. For example, a patient recovering from a heart attack could be monitored without cumbersome wires (presently used to connect the monitor instrumen-

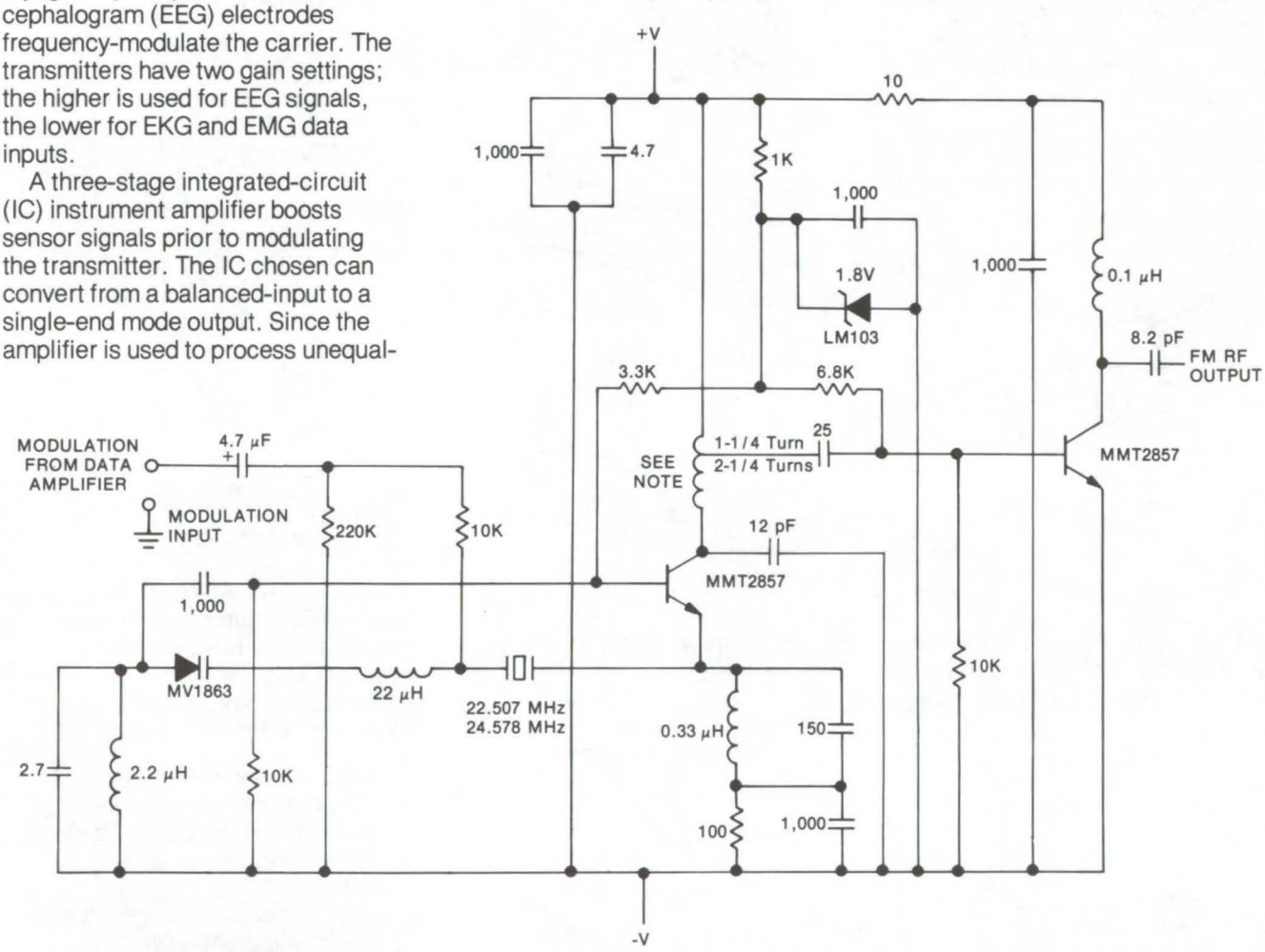

NOTE: ALL RESISTANCES ARE IN OHMS

NOTE: COIL 3-1/2 TURNS 22 AWG ON 8-32 COIL

The **Biotelemetric VHF Transmitter** relays vital signs from EEG, EMG, or EKG electrodes, depending on which is connected to the data amplifier. The frequency-modulated crystal-controlled oscillator, buffered by a final broad-tuned amplifier, feeds 157.55 MHz or 172.05 MHz to an untuned antenna.

tation to the patient) getting in the way. The vital signs of ambulatory patients can be transmitted via the biotelemetry links which can be used to gather data while the patient participates in therapeutic excercise (e.g., running, playing tennis, and the like).

This work was done by R. Lorenz of Southwest Research Institute for **Johnson Space Center.**

Further information may be found in NASA CR-144640 [N76-14474], "Short Range Miniaturized Biotelemetry System," a copy of which may be obtained at cost from the National Technical Information Service, Springfield, Virginia 22151.
MSC-16011

Miniature Carbon Dioxide Sensor

A small IR absorption spectrometer with a dual-wavelength monochromator measures carbon dioxide concentration. The IR source is at two wavelengths: one absorbed by CO_2 and the other not. Electronics convert the absorption ratios at the two wavelengths to concentration data.
(See page 370.)

Atmosphere-Generating System

A new life-support system stores a breathable atmosphere as hydrazine and water. These are chemically converted to an oxygen/nitrogen atmosphere. The system consists of modular electrolytic gas generators and distribution and control subassemblies. A system of 12 modules will provide sufficient air for 12 men. The modules are mounted on rails in a cabinet, allowing ready installation and removal. Each component is sealed and has its own internal manifolding.
(See page 424.)

Fraction Collector for Electrophoresis

A new version of a rotating-tube electrophoresis apparatus employs a rotating jet of eluting buffer to reduce the effects of convection during particle separation. Designed for electrophoretic separation of micro-organisms and biological species, the system combines gravity/gradient compensating rotation of the lumen with a buffer flush at the fraction outlet to increase separation efficiency.
(See page 379.)

Computer Programs

These programs may be obtained at very reasonable cost from COSMIC, a facility sponsored by NASA to make new programs available to the public. For information on program price, size, and availability, circle the reference letter on the COSMIC Request Card in this issue.

DAM — Detection and Mapping

Landsat mapping of natural resources

A new software system, DAM, provides up-to-the-minute maps of surface water (and other resources) at a variety of scales, sheet formats, and tick intervals. Onboard each orbiting Landsat is a multispectral scanner (MSS) which provides repetitive digital "pictures" of the Earth every 18 days. The DAM (detection and mapping) package is an integrated set of manual procedures, computer programs, and graphic devices which process these MSS data into precisely registered and formatted maps. Users communicate with programs in the DAM package in ordinary English, either by punched cards or from a conversational remote terminal.

The detection and mapping procedure is divided into five steps:

1. *Acquire Data* — The purpose of this step is to assemble the Landsat imagery and data tapes, maps, meteorological data, and Landsat data catalogs required for implementation of the procedure.
2. *Establish Control Network* — The purpose of this step is to select a network of ground control points identifiable on both the Landsat data and corresponding maps. These are used to tie the two data types together to insure a computer-generated map which is accurately scaled and registered for correlation with a conventional map. The registration process is accomplished by a series of steps performed on each set of four Landsat digital tapes corresponding to a 100-by-100-nautical-mile scene for the area to be analyzed. The data are preprocessed, and potential control points are selected and evaluated.
3. *Determine Spectral Limits* — The DAM package requires a set of spectral limits which defines the reflectance characteristics in the Landsat channels of the material to be detected and mapped. Predefined spectral limits for water are provided for in the DAM package.
4. *Specify Computer Map Characteristics* — Each Landsat scene covers almost 35,000 square kilometers. Hundreds of conventional maps, in a variety of

scales and formats, ranging from 7.5-minute quadrangles (150 square kilometers) to 1°-by-2° sheets (10,000 square kilometers), may be required to cover this area. Employing simple, English-like commands, the user specifies (individually or by map series) the characteristics for as many as 999 maps within one Landsat scene.

5. *Generate Computer Maps* — This processing step occurs in a single computer run (typically batch), and user input is comprised of control network (on cards or disk), Landsat MSS digital data (on tape), classification specifications (on cards), and computer map characteristics (on cards). This processing results in computer-generated line printer output showing the location of each point classified as water at the specified scale.

The types of data required for processing images are as follows:

- Landsat MSS positive film transparencies at a nominal scale of 1:1 million for all four MSS channels and each covering approximately a 100-by-100-nautical-mile ground scene;
- System-corrected MSS digital data on CCT's, four for each Landsat scene;
- Landsat data catalogs and microfilm sets for use in the selection of Landsat images and tapes;
- Map indexes;
- Small-scale maps for reference purposes;
- Topographic quadrangle maps of the U.S. Geological Survey 7.5-minute or 15-minute series, for control network establishment; and
- Meteorological data.

Computer System Requirements — The computer programs in the DAM package are designed for use on any UNIVAC 1100-series computer system with the following minimum characteristics:

- EXEC VIII operating system,
- Twenty thousand words of user core storage,
- Two million words of user mass storage,
- One tape drive (two if tapes are to be duplicated),
- One card reader,
- One line printer,
- One remote terminal (optional), and
- One pen plotter (optional).

Programing Language — The DAM package contains approximately 200 subroutines. Over 90 percent of the subroutines are written in UNIVAC FORTRAN V, and the remainder, in Assembler and EXEC VIII control language. Familiarity with programing languages is not required.

This program package was written by the Earth Observations Division of **Johnson Space Center.** *For further information, Circle D on the COSMIC Request Card.*

MSC-16096

Mechanics

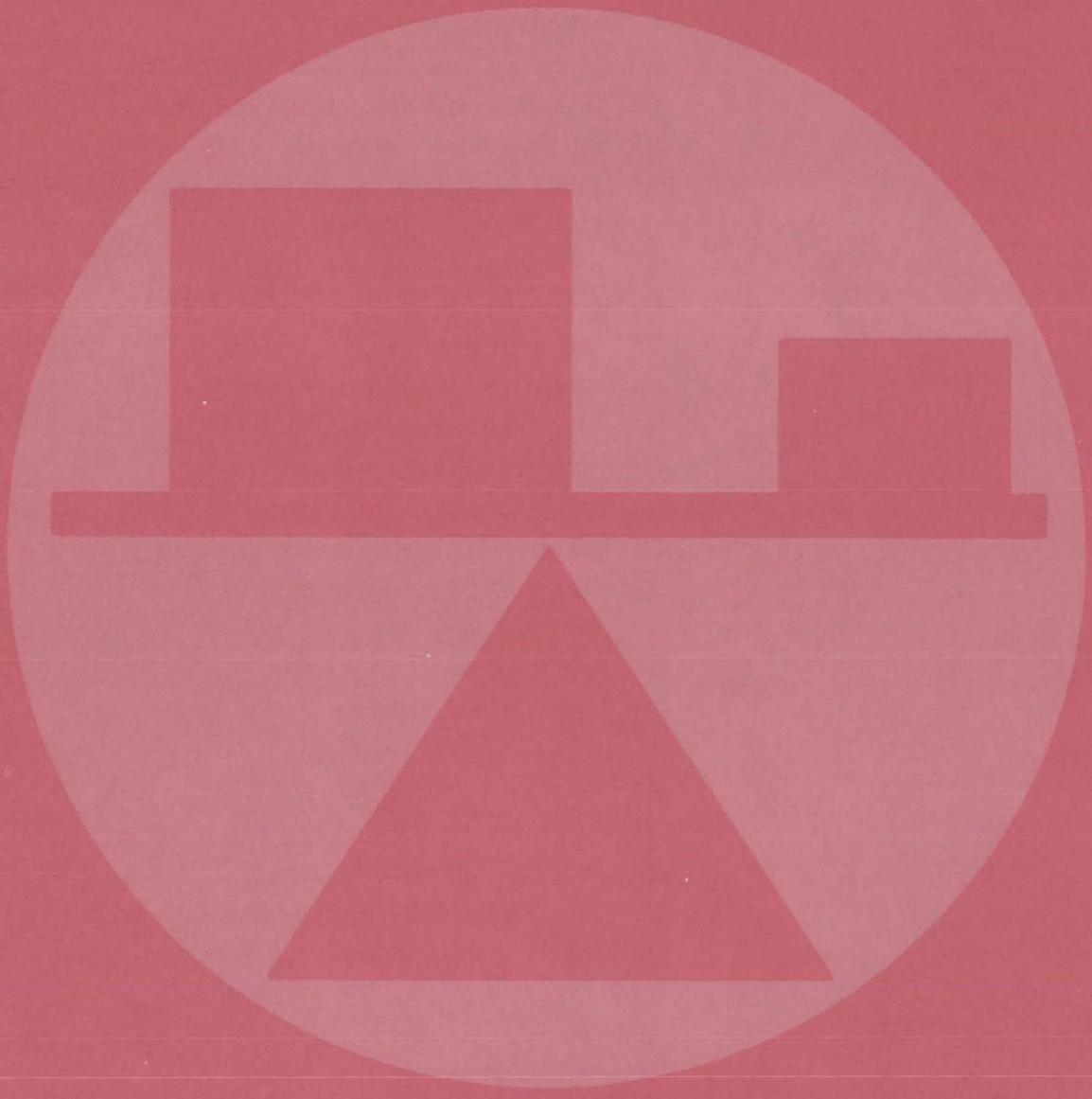

Hardware, Techniques, and Processes

Books and Reports

Computer Programs

Flexible-Pile Thermal Sealant

A brushlike thermal seal effectively insulates a gap that changes dimensions during use.

Lyndon B. Johnson Space Center, Houston, Texas

A pair of fiberglass textile fibers, woven in a weave-and-tuft strip, are used to insulate a surface gap which is exposed to severe thermal stress. The strip is fabricated as a continuous, fibrous-pile composite which has low thermal conductivity, a working temperature range of from -454° to 2,000° F (-270° to 1,090° C), low load compressibility, and good inhibition of plasma flow.

The fibers are arranged in a brushlike orientation normal to the base. The sealant (Figure 1) consists of pile-woven yarns and filler yarns which form a mesh in one direction. Warp yarns, used as a backing, are looped around the filler yarns and pile yarns and form a mesh in a second direction. A binder prevents yarn separation in the backing and is secured to one of the fixed edges of the gap. The pile yarns contact the other gap edge (which is free to expand and contract while undergoing thermal stress). Fiber strip construction can be varied, depending on the type, density, and height of the fiberglass yarns used.

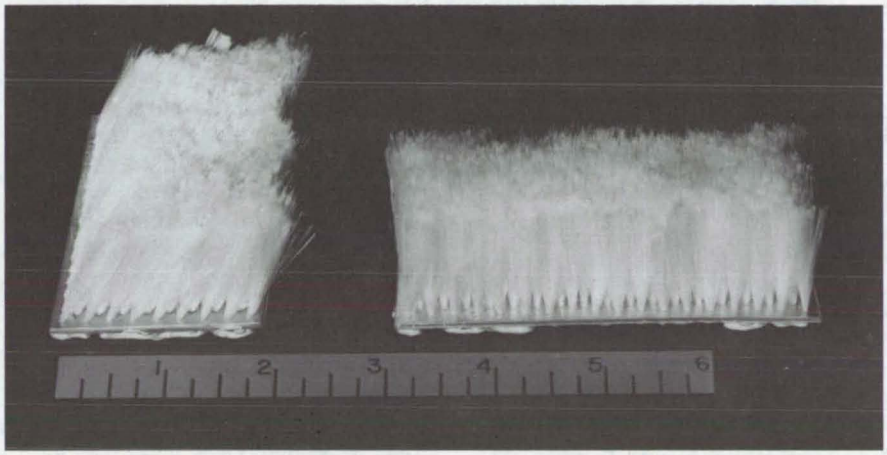

Figure 1. The **Thermal Sealant** is fabricated as a continuous, fibrous pile composite. The composite is effective at temperatures up to 1,400 ° F (760 ° C); another fiberglass yarn used to form the pile is effective up to 2,300 ° F (1,260 ° C).

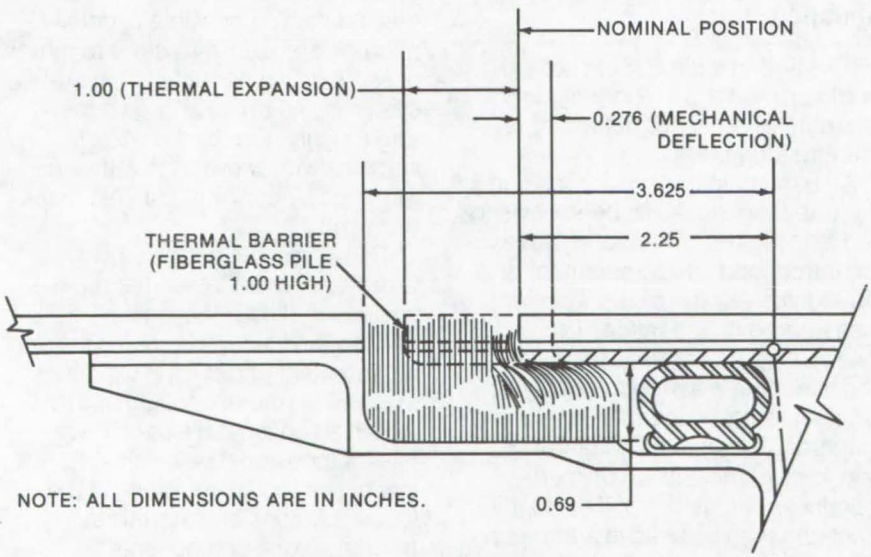

Figure 2. A **Flexible-Pile Sealant** is used to insulate a variable-width gap where severe thermal conditions are encountered. It can be seen that, although the gap distance changes, an effective thermal seal is retained.

The yarns and stuffers are fabricated from either a composition fiber formed of 65 percent silicon dioxide, 25 percent aluminum dioxide, and 10 percent manganese dioxide, or a quartz fiber having a composition of 99.9 percent silicon dioxide. The composition fiber is effective up to 1,400° F (760° C); the quartz, up to 2,300° F (1,260° C). After weaving, a binder of silicone rubber is applied to form an integral backing section. Pile density (excluding the backing) can vary from 9.5 lb/ft³ (152 kg/m³) to 27 lb/ft³ (432 kg/m³).

Figure 2 illustrates an application of the pile sealant. The pile, pointing upward, is attached to a stationary frame. A thermally actuated surface contacts the pile fibers. As the plate is warmed, it expands, thus varying the gap width. The pile, however, continues to insulate the gap thermally.

This work was done by George E. Anderson, Donald M. Fell, and Jerry S. Tesinsky of Rockwell International Corp. for **Johnson Space Center.** *For further information, Circle 62 on the TSP Request Card.*

This invention is owned by NASA, and a patent application has been filed. Inquiries concerning nonexclusive or exclusive license for its commercial development should be addressed to the Patent Counsel, Johnson Space Center [see page A8]. *Refer to MSC-19568.*

Ultrasonic Measurement of Fracture Toughness

An inexpensive nondestructive method ranks materials by fracture or crack toughness.

Lewis Research Center, Cleveland, Ohio

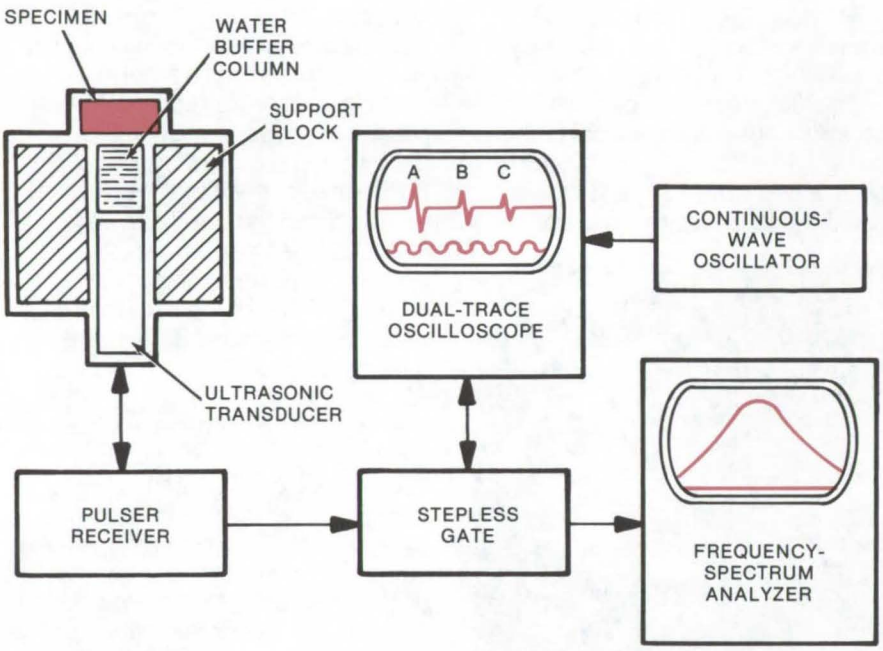

Ultrasonic Ranking of Fracture Toughness may be carried out by using the equipment shown above. Properties of the material under test may be determined from oscilloscope tracer similar to the example shown, where A represents the front-surface (water interface) echo, B represents the first back (free) surface, and C represents the second back (free) surface. The intervals between echoes are used to calculate velocity. Echoes B and C are electronically gated for frequency-spectrum analysis for calculating attenuation.

Current methods for measuring the fracture or crack toughness of materials can be time consuming and expensive. The methods for obtaining valid plane-strain fracture-toughness (K_{IC}) values for metallic materials often involve massive specimens and test equipment. Consequently, it can become costly to make sufficiently large numbers of K_{IC} measurements to satisfy statistical requirements or to cover an adequate range of material types. It is desirable to have a simple, inexpensive, and nondestructive method for ranking fracture toughness both for research and for production or field use. Although it would not completely replace mechanical destructive testing, the ultrasonic method would provide a corroborative and alternative means for determining fracture toughness.

An ultrasonic method for ranking fracture toughness has been devised and investigated. Ultrasonic waves are introduced into a specimen, and ultrasonic velocity and attenuation measurements are made. The measured data are used in an equation to estimate a proportionality coefficient for the material investigated (generally a metal) by comparison with known (measured) fracture-toughness values (K_{IC}). The coefficient can then be used in a formula for determining unknown fracture-toughness values.

Ultrasonic velocity and attenuation measurements are made by using a water-buffered pulse-echo method involving the apparatus depicted in the sketch. (The specimen thickness and density are determined in prior tests.) The velocity is determined from measurements of the period between ultrasonic echoes within the specimen on the basis of the continuous-wave oscillator signals. Velocity values for the specimens are combined with density values to obtain acoustic impedances used to calculate the reflection coefficient. This coefficient is used to determine the attenuation coefficient of the specimens from data produced by frequency-spectrum analysis of the first two back-surface echoes, B and C, from the free surfaces of the specimens. By using special broadband ultrasonic transducers, the frequency spectra that are obtained will cover a wide range, say from 5 to 50 MHz. Using these spectra, it is possible to determine the variation of attenuation coefficient relative to ultrasonic frequency for each specimen. From these data, it is possible to determine differences in fracture toughness. It is also possible to calibrate a system to automatically give fracture toughnesses by the use of samples with known K_{IC} values determined by conventional test measurements.

This ultrasonic method involves an advancement in nondestructive evaluation (NDE) technology. In conservative use, this method would be important in reducing expenses involved in fracture-toughness testing. In an advanced embodiment, this method could be a valuable inspection tool in determining the local variations of materials in fracture-prone components.

This work was done by Alex Vary of **Lewis Research Center.**
Further information may be found in:
NASA TM-X-71769 [N75-29241], "The Feasibility of Ranking Material Fracture Toughness by Ultrasonic Attenuation Measurements," and
NASA TM-X-71889 [N76-21319], "Correlations Among Ultrasonic Propagation Factors and Fracture Toughness Properties of Metallic Materials."
Copies of these reports may be obtained at cost from the New England Research Application Center [see page A7].
LEW-12642

Wingtip Smoke Generator

Generator produces low-density nontoxic smoke.

Ames Research Center, Moffett Field, California

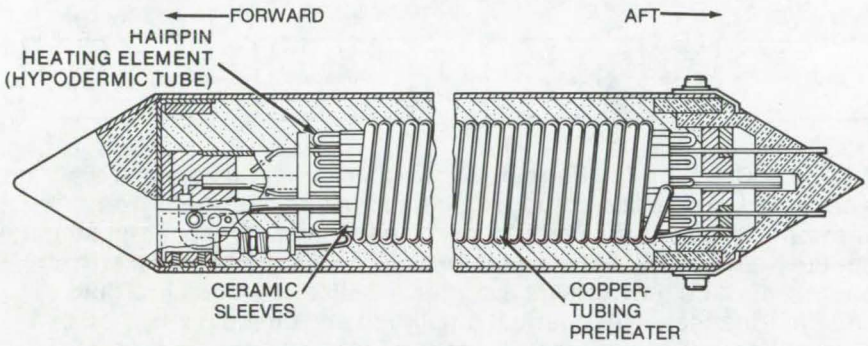

The **Smoke Generator** prototype is contained in a stainless-steel canister about 50 cm long and 8 cm in diameter. Five 2.44-meter lengths of 1.6-mm (O.D.) hypodermic tubing, electrically insulated by ceramic sleeves, are formed into hairpin heating elements. About 12 meters of 4.8-mm (O.D.) copper tubing are wrapped around the assembly (chamber, elements, and insulator) as a preheater.

The investigation and study of aircraft wingtip vortexes in flight require the wake to be visible. This can be achieved by injecting smoke into the vortex. Thus a chase plane, instrumented with a hot-wire anemometer, can fly into the wake and measure the vortex characteristics. A number of smoke generators have been designed, but some produce a smoke that could contaminate the fine-wire probes of the anemometer; others are too large and could create their own wakes as well as generate a toxic smoke with a high particle density.

A new wingtip smoke generator produces a nontoxic smoke of low particle density. As indicated in the diagram, stainless-steel hypodermic tubing is used as a heating element and as a passageway for oil which is to be vaporized. Voltage is applied across the ends of the tubing to generate heat so that the oil flowing through the tubing becomes hot and vaporizes just before leaving the tubing. The superheated vaporized oil emerges as smoke when it hits the cooler air. The pattern of the smoke is determined by the ceramic nose cone of the generator.

The smoke generator can be dimensioned according to available current and oil capacity. As shown in the diagram, one end of each of the five hypodermic tubes is connected to a center chamber, and the other ends are terminated in a brass electrical bus which is insulated from ground. One end of the copper-tubing preheater terminates in the center chamber, and the other is connected to the oil source (pump and reservoir). Design allowances are made for expansion of metal as well as electrical and heat insulation.

An electrical current of 60 to 70 amperes is used to heat the elements and also to provide electrical power to a solenoid shutoff valve. Oil temperature is controlled by a thermostat and a relay that controls the current. Monitoring and control functions are performed in the cockpit.

This work was done by James R. Rogers of **Ames Research Center.**
For further information, Circle 63 on the TSP Request Card.

This invention is owned by NASA, and a patent application has been filed. Inquiries concerning nonexclusive or exclusive license for its commercial development should be addressed to the Patent Counsel, Ames Research Center [see page A8]. Refer to ARC-10905.

Measuring Trace Dispersants in Gas Streams

Phase shift of acoustic waves is used to measure the amount of gas on a sorption sensor.

Ames Research Center, Moffett Field, California

Gaseous substances present in gas streams can be detected and measured at concentrations as low as parts per trillion by a highly-sensitive, selective, and easily-miniaturized acoustic technique. The detection system utilizes the phase shift of acoustic waves to indicate the amount of material sorbed on a sensor surface.

As shown in the block diagram of Figure 1, the sorption sensor consists essentially of a very stable electronic oscillator, an acoustic transmission line, and a phase comparator. Because the three subsystems are separated (unlike prior similar devices for determining adsorbed masses), it is possible to optimize stability and to achieve low phase-noise levels. The transmission line is treated so that it will become an efficient adsorber (or possibly an absorber). To enhance sensitivity, the line is long compared to acoustic wavelengths; however, to keep physical size small, it is operated at 10 to 1,000 MHz. For maximum sensitivity to adsorbed mass, line vibrations should have a motional crest at the surface. The most appropriate mode is a surface mode on a surface-acoustic-wave line (e.g., guided or unguided Rayleigh waves) or a torsional mode on a slender rod.

When the detector is operated in a gas stream, the ac signal from the oscillator is converted to acoustic energy (buffered coupling) by the first transducer and is applied to the transmission line (see Figure 2). As the line propagates acoustic energy along its length, the energy is damped in amplitude and shifted in phase in proportion to the amount of

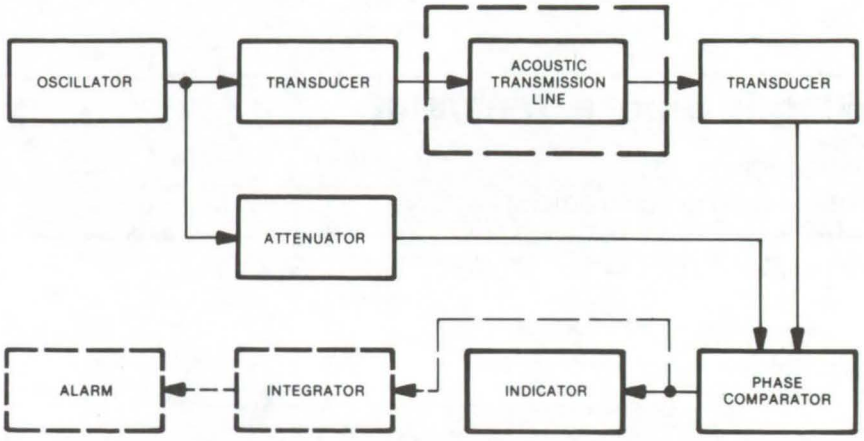

Figure 1. The **Sorption Sensor,** shown as a generalized block diagram, is designed to detect a sorbate dispersed in a fluid stream. The electronic output of the oscillator is transduced to an acoustic signal input to the acoustical transmission line, an elongated body with an external surface that acts as a sorber. The line is placed in a fluid medium. Changes in acoustical amplitude and phase on the transmission line are proportional to changes of sorbate on its surface.

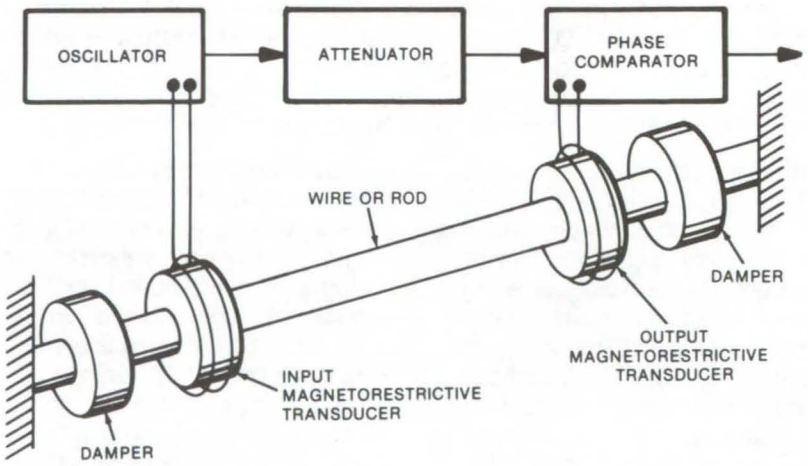

Figure 2. The **Acoustic Transmission Line** can be made from a length of wire or rod, subjected to axial tension or compression. The rod is coated with a sorbent film. The dampers acoustically isolate the output portion of the wire by preventing torsional vibrations of the wire from being reflected from the mounts.

material sorbed on its treated surface. As the concentration of the sorbable substance in the gas surrounding the line changes, the quantity retained by the treated line surface also varies to maintain sorption equilibrium conditions. The altered acoustic energy is converted to a corresponding electrical signal by the second transducer, and then its phase is compared with that of the oscillator signal. The difference between the input and output acoustic energy is indicative of the concentration of sorbate in the gas stream. If the amount of the sorbate is small, the phase-shift output is essentially a linear indicator of the sorbed mass.

This work was done by Otis L. Updike of the University of Virginia for **Ames Research Center.** *For further information, Circle 64 on the TSP Request Card.*

This invention is owned by NASA, and a patent application has been filed. Inquiries concerning nonexclusive or exclusive license for its commercial development should be addressed to the Patent Counsel, Ames Research Center [see page A8]. Refer to ARC-10896.

Noise Suppressor for Turbofan-Jet Engines

A lightweight suppressor does not reduce thrust unduly and has no moving parts.

Ames Research Center, Moffett Field, California

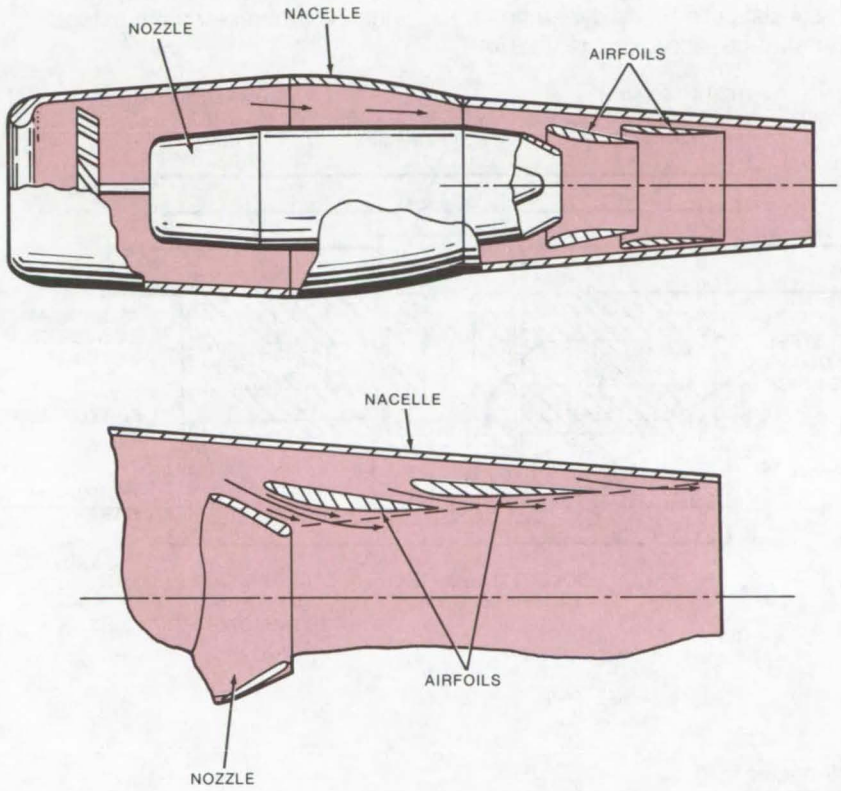

In the **Noise Suppressor for Turbofan-Jet Engines,** a nozzle is used to elongate and shape the jet exhaust into a conical configuration. A nacelle confines engine-fan air around the cone and has its outlet end on the conical surface. With the engine operating at a power setting of 92 percent, indicated noise reduction is about 0.89 dB.

A specially-designed exhaust nozzle equipped with bypass separators is the basis of a new noise suppressor for jet engines. The illustration shows the noise suppressor installed on a fan-jet engine and an enlarged view of the primary feature of the suppressor: a short, thick-lipped nozzle that elongates and shapes the jet exhaust into a conical configuration. This configuration induces the formation of a pair of vortexes in front of the nozzle.

The nacelle confines engine fan air around the conical configuration and has its outlet end on the conical surface where the radial velocity component is zero. Bypass air is deflected inward for admixture with the hot exhaust gases, and the shear between the relatively-hot higher-velocity jet gases and the relatively-cool fan air is minimized. The results of tests on a model of the suppressor, weighing only about 50 kg, have indicated noise reduction of about 0.89 dB per percent of thrust with the engine operating at a power setting of 92 percent.

This work was done by Dah Yu Cheng of the University of Santa Clara for **Ames Research Center.** *For further information, Circle 65 on the TSP Request Card.*

This invention is owned by NASA, and a patent application has been filed. Inquiries concerning nonexclusive or exclusive license for its commercial development should be addressed to the Patent Counsel, Ames Research Center [see page A8]. Refer to ARC-10812.

Air-Suspended Dynamometer Table

Improves the accuracy of fractional-horsepower testing

Caltech/JPL, Pasadena, California

A circular dynamometer table used to test motors is mounted on a shaft supported by compressed air. Seals used to maintain air pressure under the thrust-air bearing are implemented via a ferrofluidic compound which is activated by a large permanent magnet. Only motor bearing friction is read on the force gage used to record the motor reaction force (torque). Low dynamometer bearing friction is also aided by the use of a tachometer which consists of an optoelectronic scanning disk clamped to the shaft of the motor under test.

Dynamometers which derive torque-vs.-speed and torque-vs.-current curves of fractional-horsepower electric motors must contribute minimal bearing friction to the tests for accurate real-time curve plotting. The quest for high dynamometer accuracy is, however, offset by the need to test fractional motors of varying weights, shaft speeds, and torque values ranging over four decades upward from tenths of an ounce-inch.

The low-friction table as illustrated consists of a round dynamometer surface, approximately 12 in. (30.48 cm) in diameter, with a 12-in. moment arm from the center of rotation to the point of application of the force transducer. It is suspended on the thrust-air bearing, and the bearing is contained in a close-tolerance housing.

A motor under test is mounted in a fixture which is mounted, in turn, on the round dynamometer table. An inertia wheel is fixed to the motor mount, and an optically coupled tachometer is used.

The air thrust bearing, into which the dynamometer shaft extends,

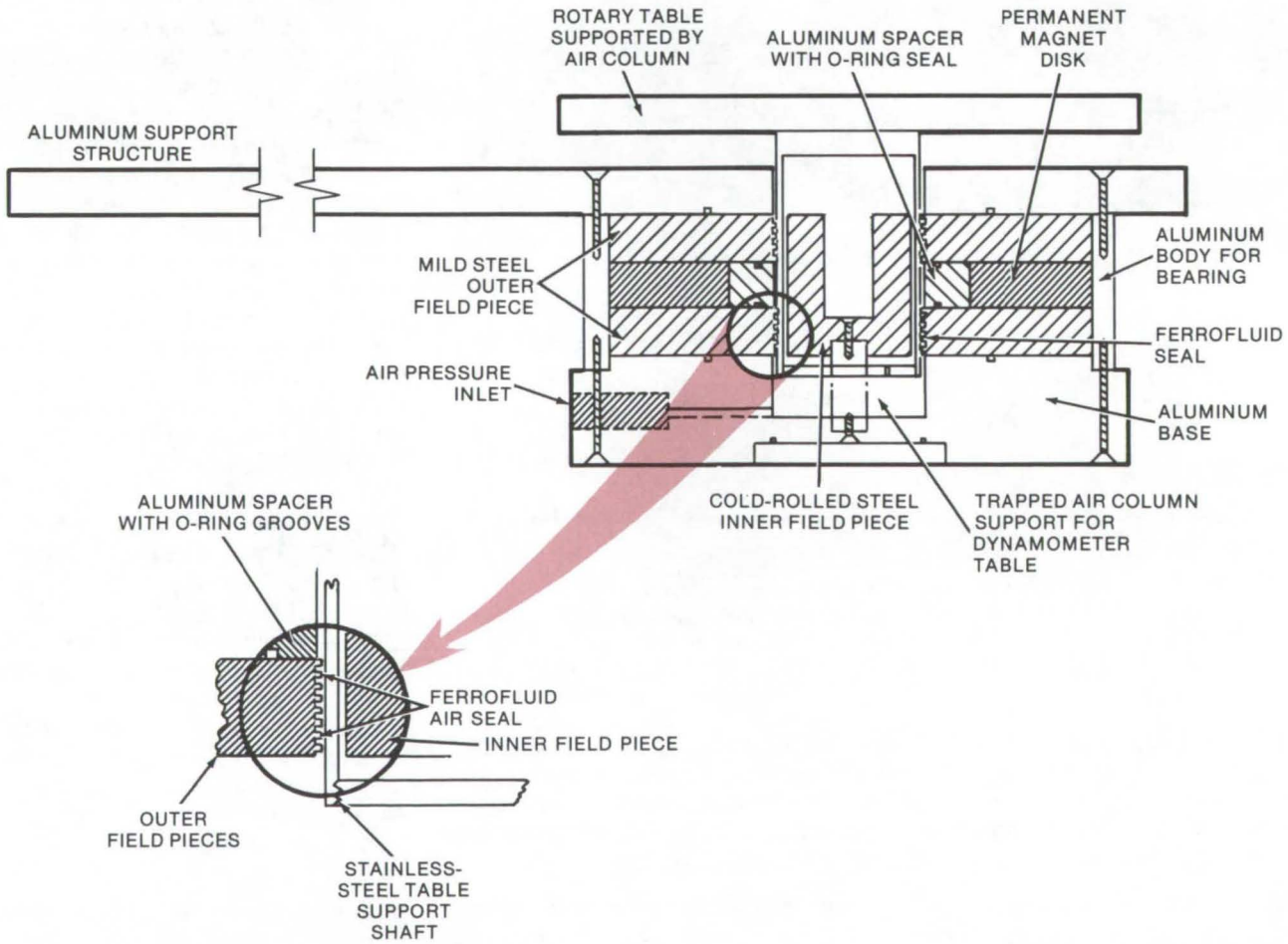

The **Air-Suspended Dynamometer Table** is used to test fractional-horsepower motors. The test motor is mounted to the table, and an inertia wheel, in turn, is attached to it. An optoelectronic-encoded tachometer disk is fixed to the motor shaft; output signals are processed in a pulse counter to indicate shaft speed.

consists of magnetic polar rings separated by a spacer. Ferrofluidic material, retained by the spacer, acts as an air seal between the rings and the shaft hub to maintain the compressed-air pressure. A set of permanent magnets is used to damp the movement of the dynamometer table (in combination with the fluid sealant) when larger motors are tested.

Torque measurement from approximately 0.01 to 1,000 oz-in. (7×10^{-5} to 7 joules) can be accommodated. Instrument bearings can also be evaluated by using rundown techniques, a method which tests the change in torque as the bearing races decrease in speed. Resultant torque-vs.-speed and torque-vs.-current curves are plotted in real time on an x-y plotter.

This work was done by Theodore A. Casad of **Caltech/JPL.** *For further information, Circle 66 on the TSP Request Card.*
NPO-13794

Time-Domain Reflectometry for Cable-Fault Isolation

Faults at multiple-cable splices can be located

John F. Kennedy Space Center, Florida

Existing multiple-cable fault isolation techniques include measuring cable mutual capacitance, exciting the line with pulse tones, and resistance-bridge measurements. Most problems with multiple cables escape accurate fault location whenever the cable failure is a high-resistance open circuit, a high-resistance to ground path, or an adjacent conductor short. Time-domain reflectometers (TDR's), which are commonly employed to provide impedance profiles of constant-impedance cables, can be used in an unorthodox new manner to isolate the fault at a specific multiple-cable splice location.

TDR's have not normally been utilized in long-distance high-loss cables because the amplitude and shape of returning waveforms have been distorted; however, for many applications this problem is not significant. If the multipair cable under investigation displays classical lumped-circuit characteristics (as shown schematically in the figure) on the TDR cathode-ray screen, the procedure may be followed. Cable inductance and resistance parameters remain constant over cable length; capacitance and conductance (C and G) parameters, however, change at each spliced location.

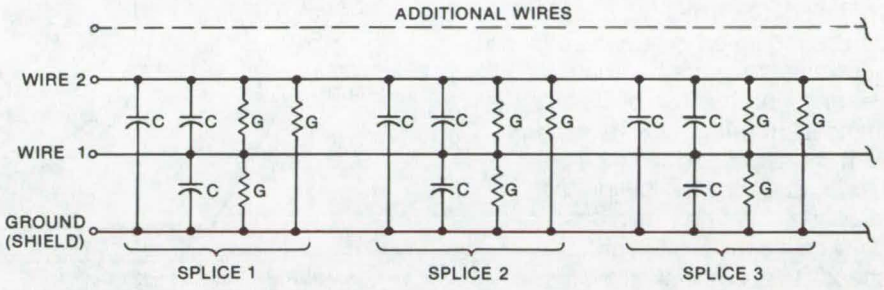

A **Spliced Multipair Cable** can often be reduced to the circuit shown above. If TDR is used in a mode in which the deflection sensitivity of the return display unit is increased, small perturbations of the splices will fill a significant portion of the vertical graticule, allowing the position of the discontinuities to be determined.

If the approximate distance to any splice location is known, a functional wire in the bundle can be used to establish corresponding TDR length. The actual distance to the break is known when the wire containing a faulty splice is displayed. A second technique is used if the splice distances are unequal. The TDR display will reveal unequal perturbation distances which can be used as a splice identification locator.

This work was done by Ken D. Wood of IBM Corp. for **Kennedy Space Center.** *For further information, Circle 67 on the TSP Request Card.*
KSC-10741

Fluid-Film Bearing Damper

Damper for rotating machinery has a noncircular support that allows changes in dynamic properties.

Lewis Research Center, Cleveland, Ohio

A fluid-film bearing damper has been developed and tested for use as a bearing support when installed as an integral part of the machine frame of a small, lightweight turbomachine. This newly developed bearing damper can be controlled for either manually or automatically altering its stiffness and damping properties without interrupting the operation of the rotating equipment.

The fluid-film bearing damper can be regulated to have a stiffness equivalent to or greater than the bearings, or they can be flexible (as in most aircraft turbine machinery) with stiffness less than those of the bearings. These flexible or "soft" supports serve two functions: (1) They cause the system critical speeds to occur well below the operating speed range, and (2) they can reduce the forces transmitted to the bearings and thereby dramatically extend bearing life.

Once support flexibility is introduced, however, it becomes necessary to provide a damping mechanism. Flexibility without damping can produce a system sensitive to shock, as in the case of suddenly applied unbalance loads.

The dynamic properties of a fluid-film bearing are altered when the pressure in the film or the thickness of the film is changed. Properties such as stiffness and damping have a direct effect upon the natural frequencies of the bearing supports and thereby the rotating system. By regulating the pressure of the supporting fluid film, it is possible to change its stiffness. By changing the thickness of the film, it is possible to change its damping characteristics. This means that both the threshold frequency of nonsynchronous whirl and the amplitudes of motion at synchronous whirl can be controlled.

This newly-developed noncircular bearing support with dynamic properties that can readily be changed makes it possible to operate a rotor with a greater magnitude of unbalance by "detuning" the system, i.e., varying either or both stiffness and damping, and thereby changing either the amplitude of resonance or the frequency at which resonance occurs.

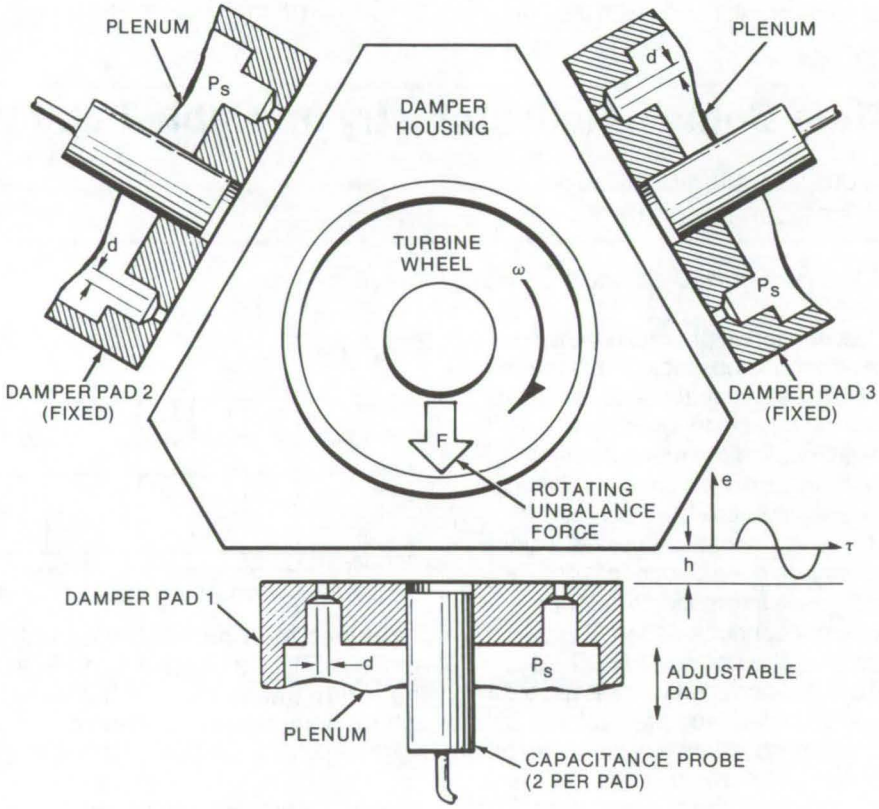

The **Test Apparatus** for the measurement of stiffness and damping obtainable with an air film includes a three-pad air squeeze-film damper. The clearances and air supply pressure were manually adjusted in the test apparatus, but could be readily adjusted by automatic controls. A type of feedback loop could incorporate sensing elements, such as noncontacting displacement probes, force transducers, and accelerometers, making the system fully automatic. The damping device itself will work with either journal or ball bearings.

A test apparatus was used to measure the magnitudes of stiffness and damping that could be obtained with an air film. As shown in the schematic drawing, the device consists of a triangular-shaped damper housing having three precision-ground and lapped faces located by three externally-pressurized air film damper pads. The damper pads are actually hydrostatic gas bearings having multiple feed holes in their faces. Two of the pads are rigidly attached to a baseplate, while the third is mounted on a micrometer slide permitting adjustment of the clearances in all three damper pads. Each pad has its own air supply which can be regulated independently. The housing is supported vertically by a pocketed externally pressurized thrust bearing.

During tests, an unbalanced air-driven turbine wheel was mounted on the inside of the circular cavity in the housing, with its plane of rotation perpendicular to the damper pad faces. The rotating turbine wheel produces a harmonic exciting force acting normal to each air film damper surface. This force is resisted by the vector sum of the air film stiffness and damping forces. Tests conducted at different clearances and supply pressures showed that both stiffness and damping could be controlled.

This work was done by Robert E. Cunningham of **Lewis Research Center.** *Further information may be found in NASA TN-D-7987 [N75-25192], "Experimentally Determined Stiffness and Damping of An Inherently Compensated Air Squeeze-Film Damper," a copy of which may be obtained at cost from the New England Research Application Center* [see page A7].

Inquiries concerning rights for the commercial use of this invention should be addressed to the Patent Counsel, Lewis Research Center [see page A8]. *Refer to LEW-11158.*

All-Nickel Hot-Wire Probe

For high-temperature applications in supersonic and hypersonic wind tunnels

Ames Research Center, Moffett Field, California

A new hot-wire probe body is machined from 99.5 percent nickel into a cylindrical shape with a chisellike point at one end that forms the taper-edge faces shown in the figures. The body is bored out close to the tip, and the electrode holes at the leading edge are shaped at the angles shown by EDM techniques to a depth of about 2.5 mm. A V-groove is cut at the leading edge to accommodate the probe wire. The 0.2-mm supporting wire electrodes are also 99.5 percent nickel; before insertion, they are baked in air for 2 hours at 900° C to form an insulating and adherent oxidation coating approximately 0.01 mm thick. After the electrodes are inserted (slip fit) into the EDM holes, the assembly is baked to form an oxidation layer on the hole surfaces.

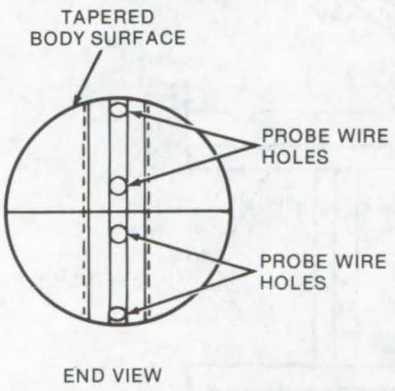

Figure 1. From the **End View of the Anemometer,** it may be seen that it has a circular cross-section. The forward end is ground to a tapered, streamlined shape so that air flows smoothly over the body. Four cylindrical holes, machined into the nickel probe body, receive two pairs of probe wire conductors.

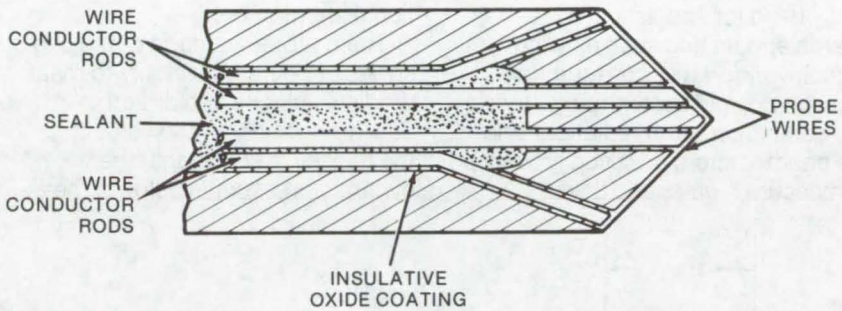

Figure 2. **Probe Wires** are secured to the outer ends of the probe body and are encapsulated to protect against vibration. The encapsulant is applied as a paste; then it is heat treated at an elevated temperature until cured. The individual probe wires are installed so that they are tangent to the edge faces of the probe body.

The probe wire, 90 percent platinum/10 percent rhodium and 10 μm in diameter, is set so that it just emerges from the V-groove, and then it is spot welded to the exposed ends of the electrodes. Subsequently, the V-groove is filled with a ceramic adhesive that covers about one-half the circumference of the probe wire; the adhesive is cured for 8 to 24 hours at 120° C. The main cavity of the probe is filled with a ceramic insulator that embeds the electrodes. The probe operates satisfactorily in a wind tunnel at temperatures of 700° to 760° C, where the hot-wire sensor is at red heat.

This work was done by Fred R. Lemos of **Ames Research Center.** *For further information, Circle 68 on the TSP Request Card.*

This invention is owned by NASA, and a patent application has been filed. Inquiries concerning nonexclusive or exclusive license for its commercial development should be addressed to the Patent Counsel, Ames Research Center [see page A8]. *Refer to ARC-10911.*

Velocity Sensor for Slow Flows

An easily-made inexpensive device could measure flows from 0.2 to 20 ft/s.

Langley Research Center, Hampton, Virginia

An inexpensive sensor for flows with extremely-low dynamic pressure is essentially an "inside-out" hot-wire anemometer. Hot-wire anemometers measure air velocity by measuring the temperature rise, power consumption, and heat-transfer coefficient of a hot wire, rod, or sphere. From this data, the Nusselt number and the Reynolds number are calculated to determine the air velocity.

Hot-wire anemometers are generally used for sophisticated research and testing such as wind tunnel work. Power consumption must be corrected for thermal inertia, conduction, and radiation; and the anemometers are usually used to measure high-speed flows.

The new inside-out anemometer measures the temperature rise in the fluid instead of in the wire. As air flows through a small channel in a heated insulated metal slug, the inlet and outlet air temperatures are monitored. The exterior shape of the sensor is especially chosen to create a two-dimensional flow that is relatively independent of the Reynolds number. This makes determination of the flow velocity rather easy, compared to a conventional anemometer.

The major advantage of the sensor is, of course, its ability to measure flow velocity and direction in cases where either the velocity or the density is so low that the dynamic pressure is below a measurable range. Futhermore, the device, as shown in the figure, is inexpensive and easily constructed. The air passages are copper tubing that may be curved to achieve the proper length. Differential thermocouples measure the temperature difference between the air at the inlet port and the heated slug and the temperature difference between the air at the outlet port and the slug. Because of the design of the sensor, the velocity of the air within the channel may be determined simply from the log of the ratio of the measured temperature differences.

To relate the flow within a channel to a free-stream velocity, the field driving the channel flow is created by two-dimensional flow around a

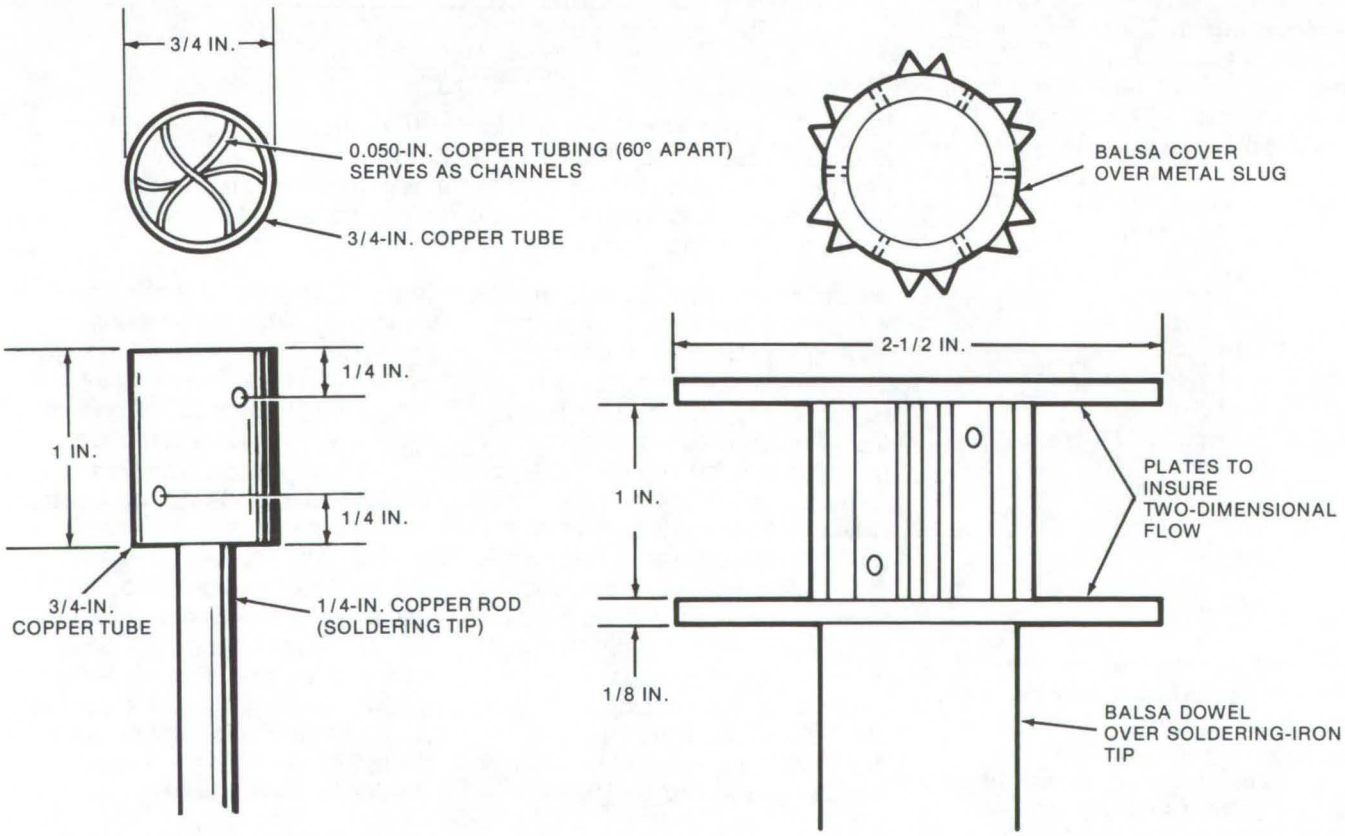

The **Metal Slug for the Slow-Flow Velocity Sensor** is a single piece of copper tubing, inside of which small-diameter channel tubes are placed. The 3/4-in. tube is then filled with solder. A soldering iron is used to heat the slug, and thermocouples are placed at the inlets and outlets of the channels. Finally, the slug is fitted with ribs and top and bottom plates to direct the airflow.

sharp-edged concave polygon. The channel velocity will be proportional to the free-stream velocity times a function of the stream direction. The proportionality constant and the stream-direction function are determined by calibration in a known flow. Several channels (three or more) are used for redundant determination of velocity and direction. This device could be made into an inexpensive hand-held instrument for measuring ventilation and air-conditioning flows or, with some modification, to measure liquid flow.

This work was done by Wayne E. Simon of Martin Marietta Corp. for **Langley Research Center.** *For further information, Circle 69 on the TSP Request Card.*
LAR-11785

Improved Gas-Pressure Transducer

Resonant-frequency coupling is used to measure the intensity of radiation-induced pressure variations.

Ames Research Center, Moffett Field, California

An optically-selective, acoustically-resonant, gas-detecting transducer has been developed for use with nondispersive infrared gas analyzers that require the detection of periodic pressure fluctuations within the gas sample being analyzed (see NASA Tech Briefs B72-10198, B74-10243, and B75-10082). Improvements in sensitivity and immunity to background noise are attributed to the use of a diaphragm which has a mechanical resonance frequency equal to the acoustic resonance frequency of the reference-gas chamber in the analyzer.

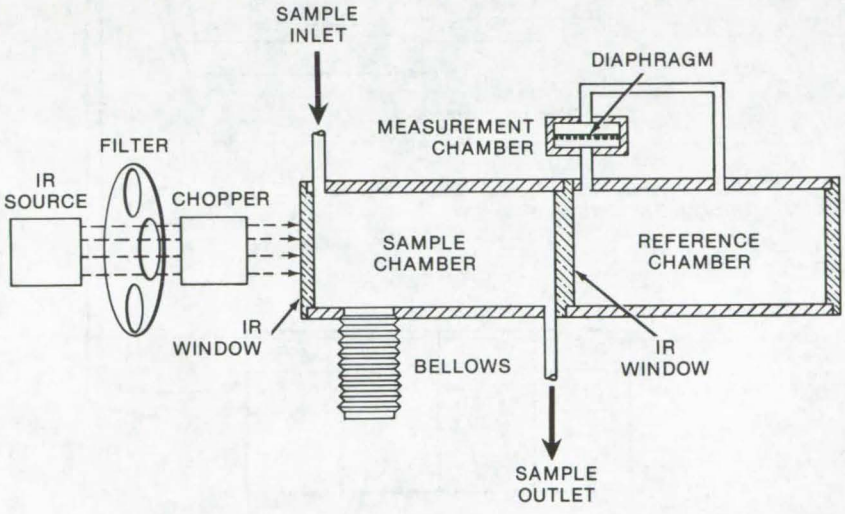

The **Pressure Transducer** has three gas-filled chambers. The acoustic resonant frequency of the reference chamber is equal to the mechanical resonant frequency of the diaphragm, the chopper frequency, and the bellows modulation frequency. Radiation-induced pressure fluctuations in the reference chamber depend on the amount of radiation absorbed in the sample chamber, and thus on the sample-gas concentration.

In the diagram, the transducer with the diaphragm is shown coupled to the reference-gas chamber. The acoustic resonant frequency of this chamber is the same as the resonant frequency of the diaphragm and the chopping rate of the chopper. The gas to be analyzed is led into the sample-gas chamber via the upper inlet. The density of the gas in the sample chamber is modulated by the bellows attached to the chamber. The modulation frequency is identical to the acoustic resonant frequency of the reference-gas chamber.

Infrared radiation from the source is filtered and chopped before passing into the gas chambers. Any radiation not absorbed by the sample gas causes pressure fluctuations in the reference-gas chamber and in the upper chamber of the transducer, forcing the diaphragm to vibrate. The vibration of the diaphragm is amplified, filtered, and recorded; its displacement is inversely proportional to the concentration of the gas in the sample chamber.

This work was done by John Dimeff of **Ames Research Center.** *For further information, Circle 70 on the TSP Request Card.*
ARC-10639

Contamination Monitoring of Fluids

An in-line system is applicable to medical technology, environmental pollution control, and food technology.

John F. Kennedy Space Center, Florida

A passive and automatic method for determining contamination levels in dynamic fluid systems is based on an electro-optical instrument consisting of a laser and an array of photodiodes. It was designed as an online monitor to measure contamination in the oil in a hydraulic system. However, its increased speed, particle-size detection range, and accuracy make it suitable for processing industries, pollution control, medical technology, and many other areas. As shown in Figure 1, the main components include:

- A light source
- A test section
- A photodiode array
- Signal-processing circuitry
- Particle-sizing logic
- A minicomputer and display

The instrumentation will detect particles from 5 to 100 microns in size. For the design application, a typical residence time for a particle in the viewing area is 10 μs with 80 μs between particles. (These particle and speed requirements are not compatible with conventional instruments and were a major motivating factor for the development of this new apparatus.)

Laser light passes through the sample fluid onto the photodiode array. As particles in the moving fluid transverse the light source, their shadows are magnified and focused on the light-sensitive photodiodes. The light-sensor outputs are directed to a minicomputer where they are interpreted and processed. Results are displayed on a graphics terminal as a histogram showing the distribution by size of contaminating particles.

The system optics are shown in Figure 2. The power output of the He-Ne laser is 3.5 mW at a fluid-transparent wavelength that also coincides with the maximum sensitivity of the photodiode array.

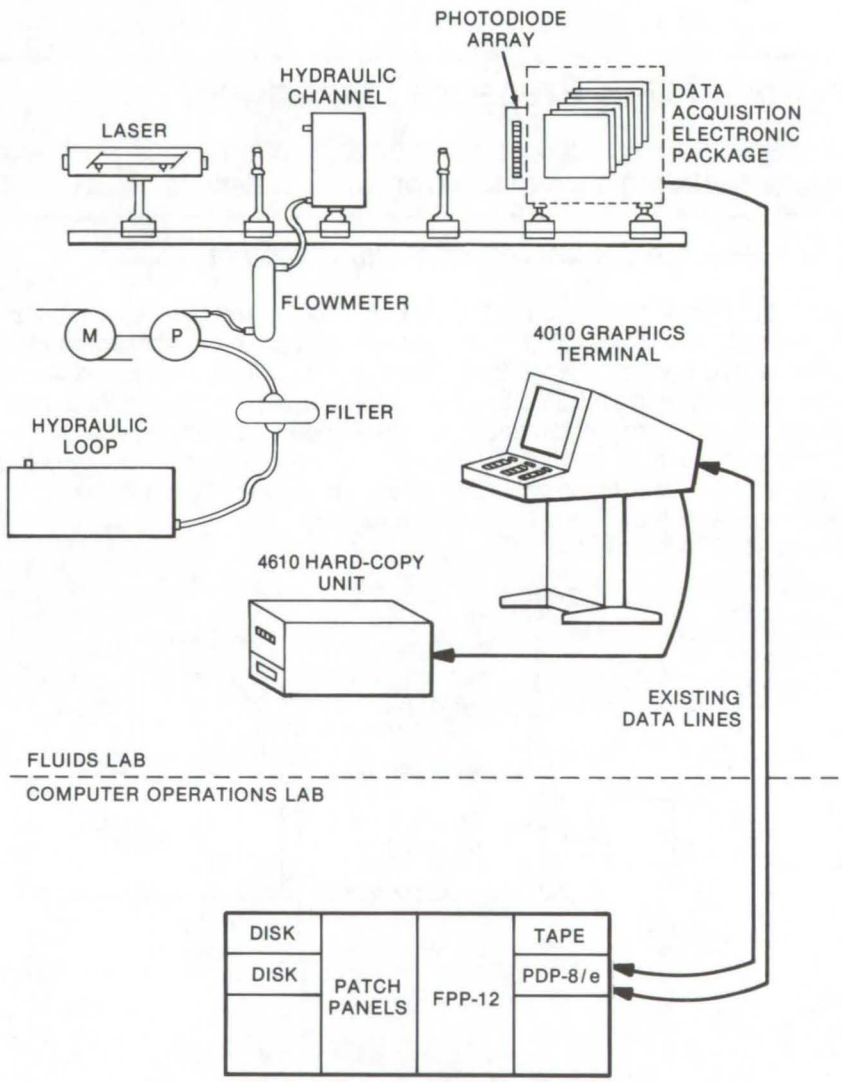

Figure 1. The **Online Detection System** was designed to measure contamination in the oil in a high-pressure hydraulic system. The computer is a general-purpose minicomputer with a 12-bit word length, a 1.2-microsecond basic machine-cycle time, and a memory of 32,768 words. The disk operating system (DOS) permits extremely rapid assemblage, execution, and debugging of programs. The DOS, in conjunction with a floating-point processor, expedites FORTRAN IV execution by a 30-to-1 margin over a system without a floating-point processor. The graphics terminal has a maximum data-transfer rate, from the computer, of 9,600 baud, and it operates in two modes: alphanumeric and graphic.

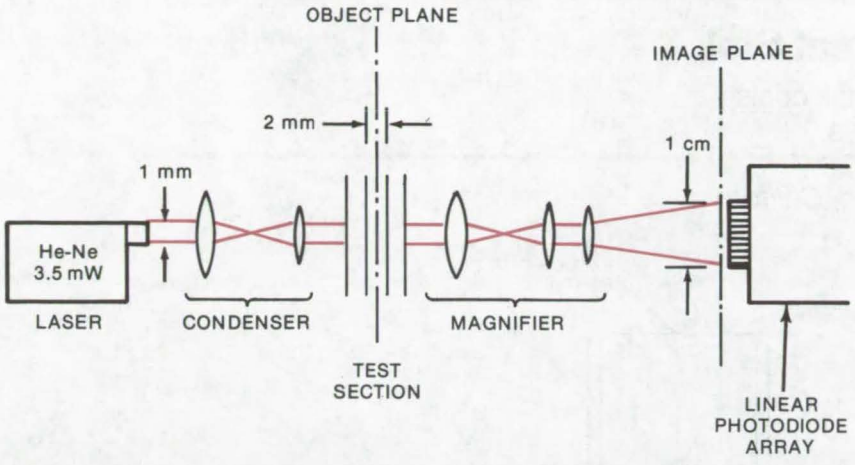

Figure 2. The **Contamination-Monitoring Optical System** has a condenser designed for a magnification of 20X. At this magnification a 0.5-mm-diameter beam will fully illuminate the photodiode array and will increase the intensity by a factor of 4. Condensation is obtained by using two singly-convex lenses with a focal-length ratio of 2. The lens with the larger focal length is nearer the laser, and the lenses are separated by a distance equal to the sum of their focal lengths. The beam diameter is condensed by a factor of 2. It remains collimated, and no additional beam divergence is introduced.

Ordinary glass lenses are employed in the condenser and magnifier, and fused quartz windows are used for the remaining optics without significant absorption losses. To maintain a parallel light source, a doublet lens system is used to condense the laser beam and to reduce its diameter so that maximum advantage can be made of the laser power.

Particles flowing in the fluid at the object plane appear as sharp shadows on the image plane. The channel thickness is 2 mm so particles may physically be at a distance of ±1 mm from the object plane. Magnification determines the number of photodiodes shadowed by particles of a particular size. A quantization error occurs due to rounding the particle size to the nearest number of photodiodes. The smaller particles shadow the smallest number of photodiodes, and therefore the maximum quantization error occurs in sizing these particles. A magnification of 80X is used to size small particles; therefore, a 10-μm particle shadows four photodiodes and has an acceptable 25-percent quantization error. An 80X magnification is used for counting small particles in the range 10 to 50 μm, and a 20X magnification, for particles in the range 50 to 100 μm.

This work was done by Ronald D. Bonnell, Robert O. Pettus, Curtis A. Rhodes, and Irving F. Stowers of the University of South Carolina for **Kennedy Space Center.** *For further information, Circle 71 on the TSP Request Card.*

Inquiries concerning rights for the commercial use of this invention should be addressed to the Patent Counsel, Kennedy Space Center [see page A8]. *Refer to KSC-11037.*

Design of Redundant Systems

A method for analysis of systems with noisy inputs is applicable to circuits, chemical processes, and machinery.

Lyndon B. Johnson Space Center, Houston, Texas

A procedure for the design and analysis of redundant systems is especially useful when there are multiple noisy inputs and when the outputs are required in terms of statistical quantities and probabilities of signal excursions beyond desired levels.

The analysis is an algorithmic approach with system outputs described in terms of joint probability densities associated with the output random process time series. The outputs are determined by system transfer functions, random process inputs (described in terms of power spectral densities), and by uncertainties in the system parameters. Results are expressed in a form suitable for user-oriented software that serves as a routine design tool.

The system was originally created for the analysis of a three-element redundant sensor system. It considers correlations between supposedly "random" noise effects, static errors, and dynamic errors due to signal levels and changes in signal levels. Power spectral densities are derived and expanded in terms of the system parameters, about their nominal values. These expressions are transformed from the frequency domain to the real-time domain to serve as correlation functions for signal differences.

Using the correlation function, variances and covariances are calculated to define joint normal probability distributions. Finally, parameter values are selected for the derivation of explicit probability density functions that are used for the probability of failures.

The approach and the algorithms are applicable to many types of systems, such as chemical process control, circuits, mechanical and electromechanical systems, and other systems with known transfer functions and parameter tolerances.

This work was done by Louis F. Doty of Honeywell Inc. for **Johnson Space Center.** *For further information, Circle 72 on the TSP Request Card.*

MSC-16026

Sublimator/Evaporator Heat Sink

An economical self-regulating heat sink cools by drawing liquid through porous tubes.

Ames Research Center, Moffett Field, California

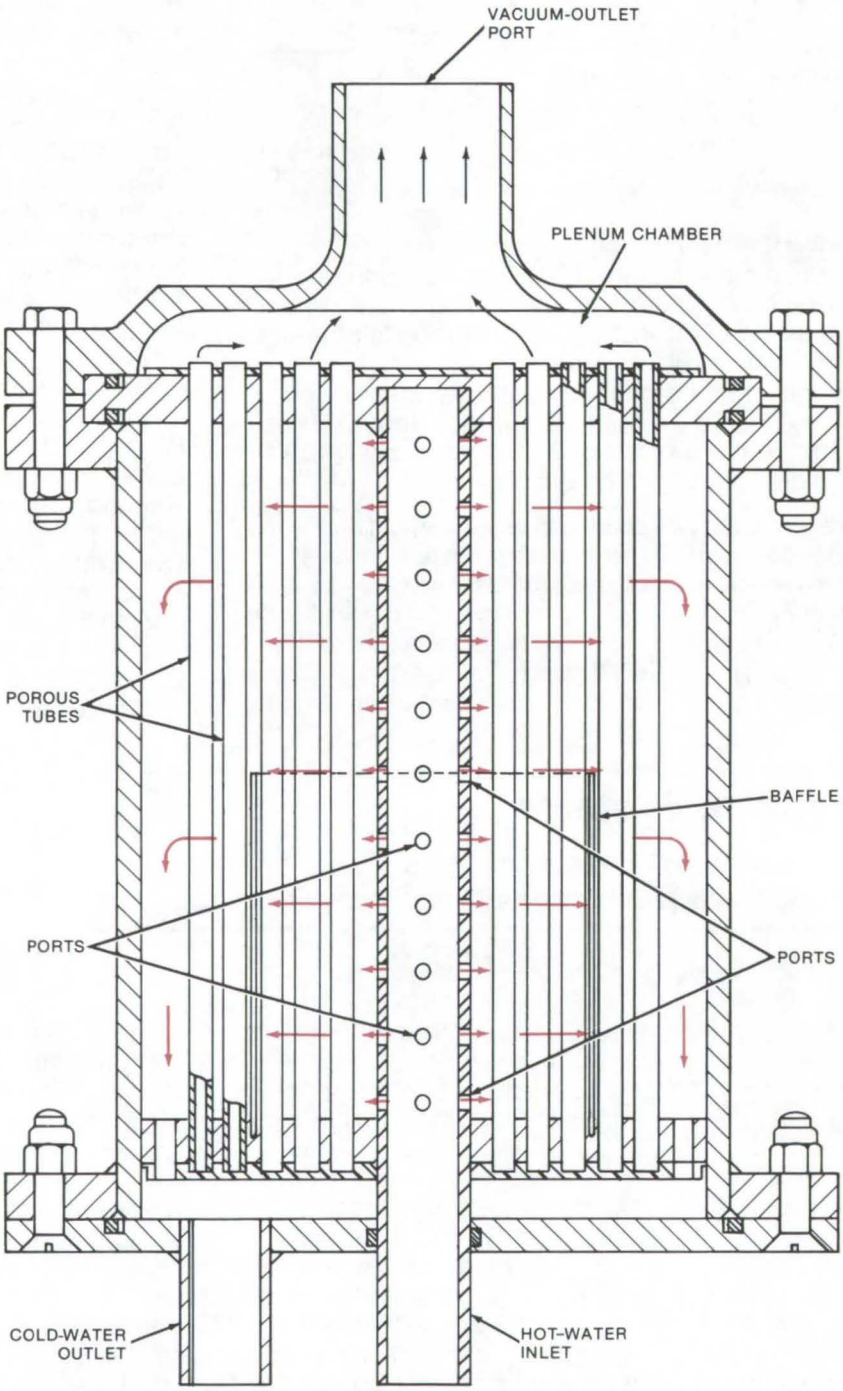

The **Permeable-Tube Heat Sink** removes heat from liquids by vaporization or sublimation. Hot liquid flows outward from the inlet, around the porous pipes where it is evaporated and cooled, and to the housing wall where it is channeled through the outlet pipe. The demonstration version shown above is approximately 13 cm long and 8 cm in diameter and weighs about 0.7 kg when wet. It was designed to remove from 120 to 600 J/s (400 to 2,000 Btu/h) with output liquid temperature in the range 0° to 10° C.

An easily maintained "refrigerator" for cooling liquids removes heat by evaporating a portion of the liquid through a bundle of porous tubes. This technique, which is characterized by a high rate of heat transfer and structural simplicity, utilizes the heat of vaporization (or sublimation in some cases) to cool the porous tubes, which in turn cool the liquid.

The core of the tubular evaporator/sublimator shown in the diagram contains a bundle of evacuated porous tubes that are sealed at one end and are open to a vacuum chamber at the other end. The tubes can be constructed of a membrane material, a porous metal, or a foam supported by a screen. They are surrounded by a housing with a central hot-water inlet and a cold-water outlet.

Hot water enters through the central inlet and is evenly distributed by suitably placed ports. At maximum heat load, the unit functions as an evaporator because the pressure drop and sonic, choked flow effect in the vapor flowing out through the porous tubes is sufficient to maintain the saturation pressure at the tube walls above the triple point of water. At lower heat loads, the vapor pressure in some of the tubes may drop below the triple point, and ice may form on part of the porous tube walls. These tubes then function as a sublimator. The wall temperature of these tubes will drop sufficiently to cause the formation of ice on the coolant side, but because of the tube spacing, this does not prevent the circulation of fluid within the container.

This work was done by Bruce W. Webbon of **Ames Research Center.** *For further information, Circle 73 on the TSP Request Card.*

This invention is owned by NASA, and a patent application has been filed. Inquiries concerning nonexclusive or exclusive license for its commercial development should be addressed to the Patent Counsel, Ames Research Center [see page A8]. *Refer to ARC-10912.*

Low-Onset-Rate Energy Absorber

Controlled deceleration rates without amplifying system loads

Lyndon B. Johnson Space Center, Houston, Texas

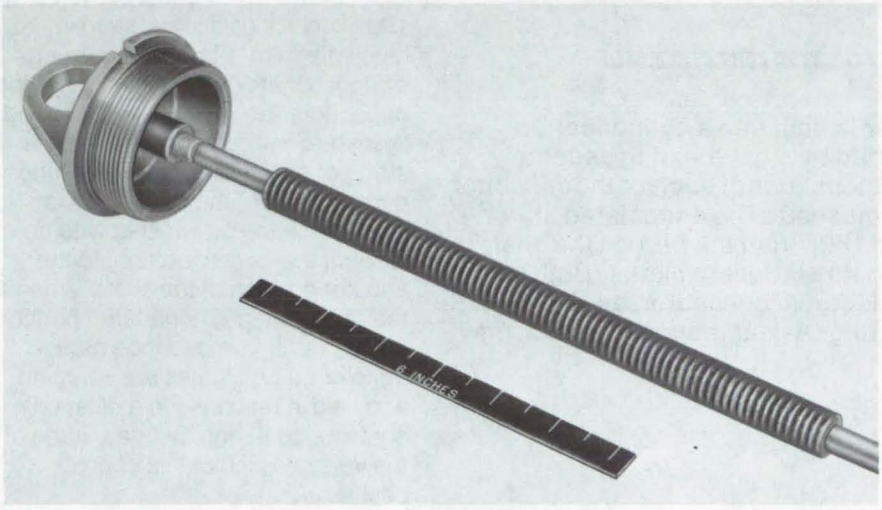

The **Low-Onset-Rate Energy Absorber** uses an Inconel shaft with stainless-steel washers to decelerate a moving mass at a controlled rate. A dry-film lubricant is sprayed on the shaft area which contacts washers.

The low-onset-rate energy absorber shown in the figure is used to decelerate a moving mass at a controlled rate without amplifying loads through the system. The absorber dissipates the energy of motion through the heat of friction and is 22 times more efficient than automobile brakes.

A uniform-diameter Inconel rod and a series of fully-annealed stainless-steel washers are the major absorber components. The washers are pressed onto the rod and are spread apart. The inside diameters of the washers are made 0.25 mm (0.01 in.) smaller than the rod diameter, forcing the washer material to yield when the washers are pressed on the rod. Energy is absorbed by stroking these washers along the rod. As each washer is picked up, the load increases by a small amount. The loading is thus spread over a significant length of time.

Dry-film fluorocarbon lubricant is sprayed over all stroking portions of the rod. The type and amount of lubricant are very important for maximum system effectiveness.

This work was done by William H. Keathley and Clarence J. Wesselski of **Johnson Space Center.** *Further information may be found in NASA-TM-X-64444 [N70-35706], "Low Onset-Rate Energy Absorber", a copy of which may be obtained at cost from the National Technical Information Service, Springfield, Virginia 22151.*

This invention has been patented by NASA (U.S. Patent No. 3,603,433). Inquiries concerning nonexclusive or exclusive license for its commercial development should be addressed to the Patent Counsel, Johnson Space Center [see page A8]. Refer to MSC-12279.

Capacitive Shaft-Angle Encoder

The analog output voltage, proportional to the input shaft position, is derived from a precision dc source.

Ames Research Center, Moffett Field, California

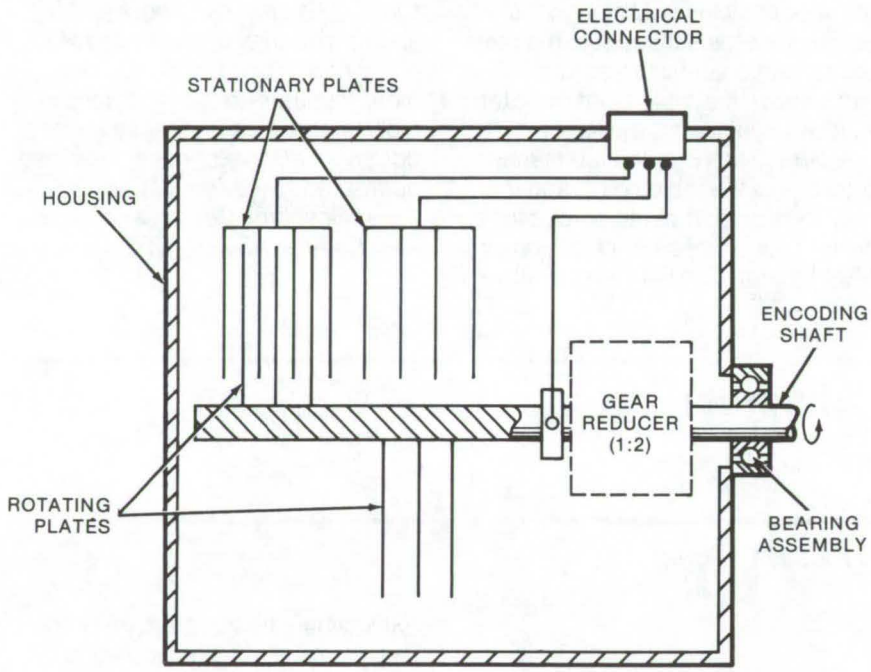

Figure 1. The **Capacitive Transducer** is built into a cylindrical housing. The encoding shaft, supported by a ball-bearing assembly, supports two sets of half-spherical rotor plates of each of the capacitor sections. The first set of rotors is enmeshed in its associated stator plates, while the second set (located 180° from the first on the shaft axis) offers minimum interaction with its stationary plates. Both sets of stationary plates are wired to an electrical connector, as are the rotors via the encoding-shaft pickup ring. A gear reducer or a cam may be used to drive the rotors.

A new capacitive-potentiometric shaft-angle encoder is less expensive and less subject to wear than conventional resistive-potentiometer devices. Two identical 180° stator-rotor variable capacitors, electrically connected in series and ganged on a common input shaft, form the sensing element of the shaft-angle encoder. The rotor plates of each capacitor (Figure 1) are connected to the encoder shaft: one set covers 0° to 180° and the other set covers 180° to 360° of shaft angle. The capacitance of each section of the sensing element varies linearly with a change in the angular position of the shaft, but the sum of the two capacitances is constant for all angular positions.

A control signal generated by a 10-kHz clock oscillator, seen in the block diagram (Figure 2), operates switches that alternately connect the capacitors to a dc power supply and then the center tap of the series string of capacitors to a measuring circuit. Each of the capacitors is charged by the power supply to an amount that is proportional to the angular position of the shaft. When their center tap is connected periodically to a high-impedance measuring circuit, voltages are sampled and held in response to a delayed control signal, and the magnitude of the voltage is indicative of shaft position.

Molecular Beam Generator

A molecular beam generator for heavy organic molecules may be used as a laboratory instrument or to deposit organic coatings. The generator has a nozzle and aperture designed especially for beams of heavy organic molecules. Deposition rates are from 6 to 15 Å/min.
(See page 380.)

Low-Cost Pressure-Data Encoder

An electronic encoding altimeter has a pulsed output with a pulse width proportional to altitude. It is a digital replacement for an electromechanical system previously used. The inexpensive encoder converts a pressure-proportional input voltage to a digital signal that may then be routed to monitoring or display equipment.
(See page 325.)

Controlled Linear Clamper/Loader

A pneumatic fixture can be used to clamp odd-shaped parts to non-uniform surfaces. It consists of a rubber bladder (enclosed in a housing) and movable blocks through which the clamping force is applied. The concept can be implemented in most any size or shape, depending on the desired application.
(See page 463.)

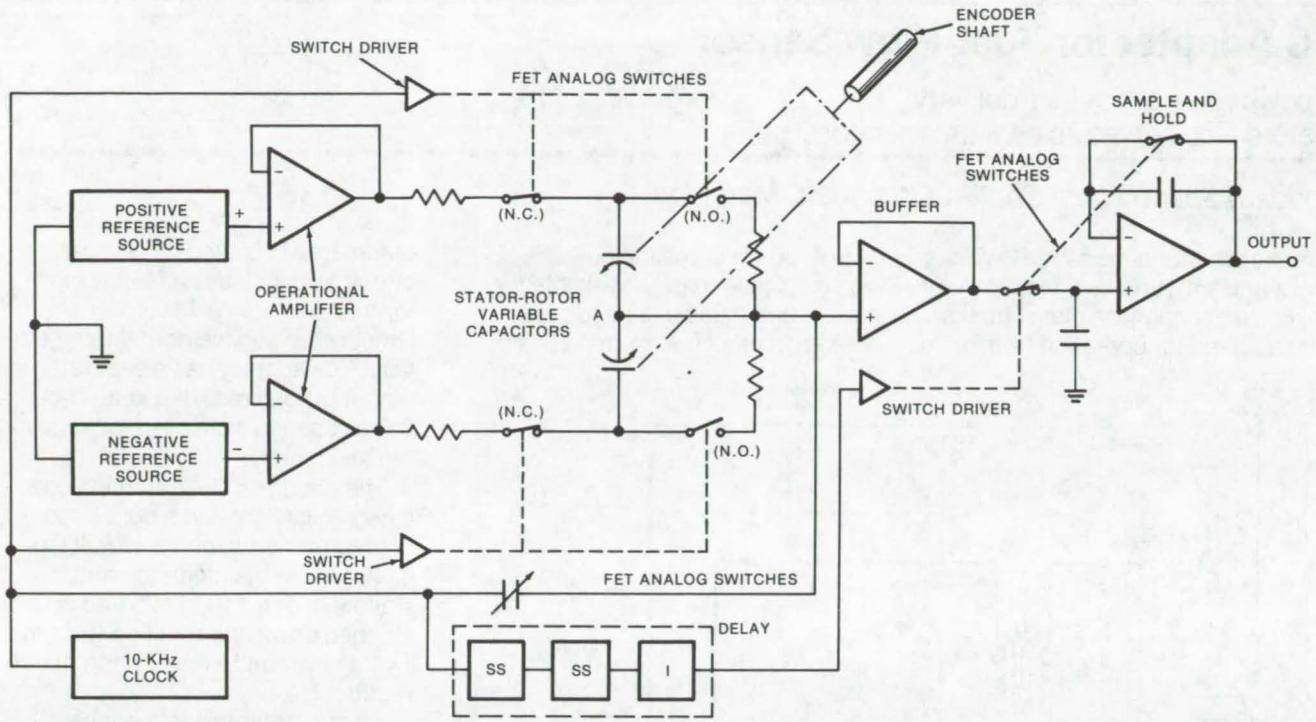

Figure 2. The **Shaft Encoder** consists of two dc voltage reference sources, three pairs of FET analog switches, and the two-section capacitive transducer. When the N.O. switches are closed, the capacitors (charged via the reference sources) are discharged via the resistors. The clock control signal alternately couples the capacitor to a charge circuit, then a discharge path. A FET-input operational amplifier buffers the common-point (A) output voltage and sources it to the sample/hold circuit. It responds to a delayed clock signal and holds the voltage appearing at point A after the capacitors are charged. The sample/hold output is directly proportional to the encoder shaft position.

This work was done by Ronald J. Hruby and Robert L. Wilson of **Ames Research Center.** *For further information, Circle 102 on the TSP Request Card.*

This invention is owned by NASA, and a patent application has been filed. Inquiries concerning nonexclusive or exclusive license for its commercial development should be addressed to the Patent Counsel, Ames Research Center [see page A8]. Refer to ARC-10897.

Purity Test for Copper-Plating Solutions

A simple test, based on the measurement of polarization voltage, indicates the level of impurities in a copper-plating bath. Impurities in the bath contaminate the cathode when electrodes are immersed in the bath. This contamination makes the cathode polarization voltage more negative. A three-electrode arrangement and a constant-current source are used to monitor polarization voltage and to determine impurity levels.

(See page 387.)

Catalytic Oxidation of Waste Materials

A new technique for catalytic oxidation of waste materials employs a soluble ruthenium salt that is introduced upstream from the reaction chamber. In the reaction chamber, heat causes the soluble salt to be deposited as an insoluble ruthenium black catalyst on the internal surface of the reactor. Thus no soluble catalyst exits the reactor to contribute to pollution of the treated water. Because the soluble salt is introduced external to the reactor, the system may be "recharged" while the purification is in process.

(See page 381.)

Terrestrial Photovoltaic Measurements Workshop

The proceedings of a recent workshop on basic solar-cell measurement techniques discusses methods of correlating solar-cell research results by different organizations. Areas covered included solar intensity and spectrum conditions, Sunlight simulators, and measurement and calibration methods. Sunlight was agreed upon as the most acceptable source for solar-cell measurements, with a xenon arc lamp or other broadband filtered source for laboratory measurements.

(See page 375.)

AC Adapter for Fuel-Flow Sensor

A power source for fuel-delivery meters also serves as a failure monitor.

Goddard Space Flight Center, Greenbelt, Maryland

An ac adapter allows the 12-Vdc fuel quantity meters designed to maximize economy on diesel trucks to be adapted for operation from a 115-V, 60-Hz domestic power supply. These readily-available fuel meters can thus be used to aid in conservation of fuel oil in homes or commercial buildings. The adapter circuit also includes a failure monitor that activates a visual warning light and an audible horn if the meter fails. The adapter has a separate output to solenoids that keep bypass valves open in case of a blockage in the fuel meter.

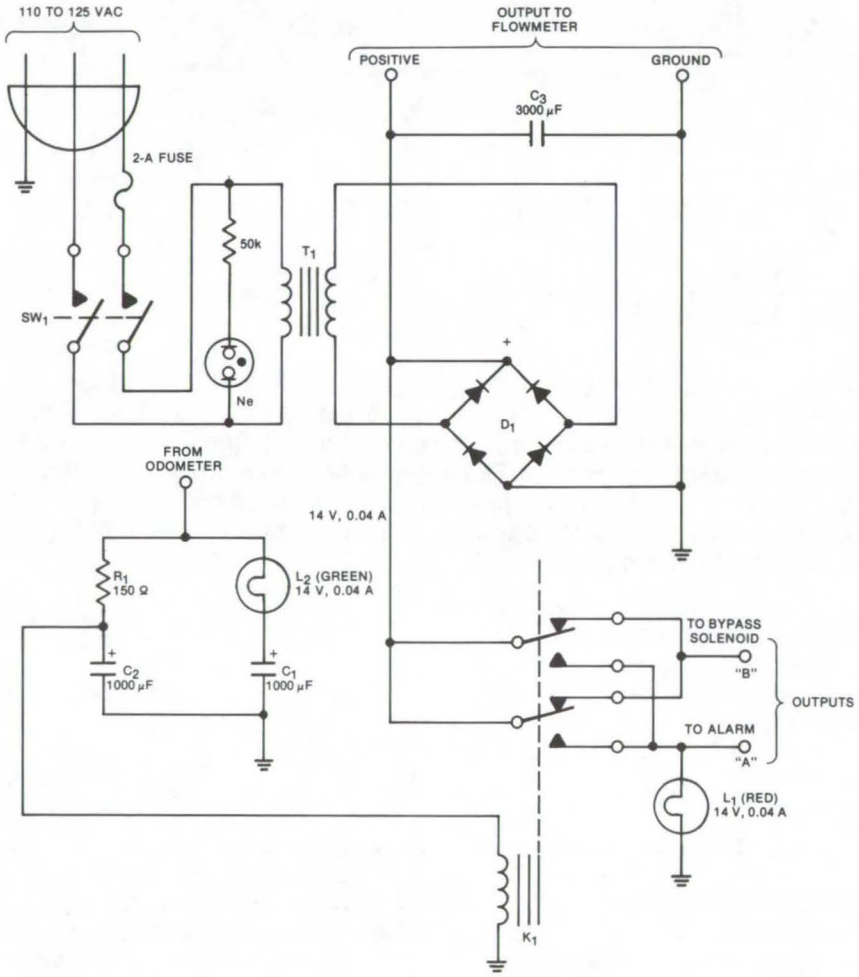

The **AC Adapter for Battery-Operated Fuel Meters** converts domestic ac power to the 11 to 14 Vdc needed to operate the fuel meter. Additional outputs operate solenoids controlling meter-bypass valves and an audible failure alarm.

The circuit as illustrated includes a neon pilot light and a double-pole double-throw switch for circuit isolation during maintenance and installation. The 110 to 125 Vac is stepped down and rectified to 11 to 14 Vdc by transformer T_1 and bridge rectifier D_1.

An odometer inside the fuel-quantity meter provides a short pulse [0.5 s, 11 V, 100 mA (maximum)] every time a unit of fuel is delivered. This pulse charges capacitor C_1 and turns on light L_2 twice (once while C_1 charges and once during discharge), but provides insufficient current both to charge C_2 and raise the voltage at K_1 enough to activate it.

When the internal reservoir in the fuel meter falls below a certain level, the odometer output becomes a steady 11-Vdc signal that will saturate capacitors C_1 and C_2 and activate relay K_1. The result is a visual warning and an audible warning such as a horn or bell.

This work was done by Lester L. Millman of **Goddard Space Flight Center.** *For further information, Circle 74 on the TSP Request Card.*
GSC-12037

Paddle-Pin Alinement Test

A segmented alinement bar speeds up patch distributor paddle-pin tests

John F. Kennedy Space Center, Florida

Paddle-pin alinement of multidistribution electrical panels requires that all cables and modules routed to the rear of the distributor panel be removed before servicing. This can mean handling as many as 60 cables to prepare for an alinement test. During the connection/disconnection process, it is very easy to damage a connector pin or puncture a connector insert, requiring possible distributor rework, cable replacement, or cable retermination.

The present method of paddle-pin testing is to insert an L-shaped machined test bar in a slotted jig which is placed in the area of the removed patch board. The bar is positioned so that it touches each pin in the distributor, 40 pins at a time. A battery-driven buzzer/connector probe determines pin electrical continuity with the bar.

However, this method has its drawbacks. The bar is uninsulated from the distributor frame, which itself is grounded. Since some of the pins connect to grounded wires, more than one pin in a row can go to this common point. To make certain that the pins are alined, there must be no electrical contact between individual pins. This is done by removing all cables from the distributor.

A new alinement method eliminates the need to disconnect cables or to remove the distributor. A segmented, insulated test bar is substituted for the steel bar. Each portion of the bar touches only one pin, and it is insulated from the frame of the distributor. The bar segments are connected to individual indicator lamps. Probing each test point with this insulated bar energizes a specific light only if the pin under test is making contact with its related portion of the bar.

The test bar, shown in the photo foreground, is machined from a block of Micarta which then has holes drilled in it and brass studs inserted. The studs are machined to close tolerance to get a fixed distance from the stud centerline. This enables alinement testing since all pins are required to touch the block once it is in position. By machining the other side of the stud to a different fixed distance from center, a no-touch test can be performed. In this position any pin probed that turns on a light is out of tolerance and must be corrected. A printed-circuit cable and connector reduce the weight on the bar, further adding to tester portability.

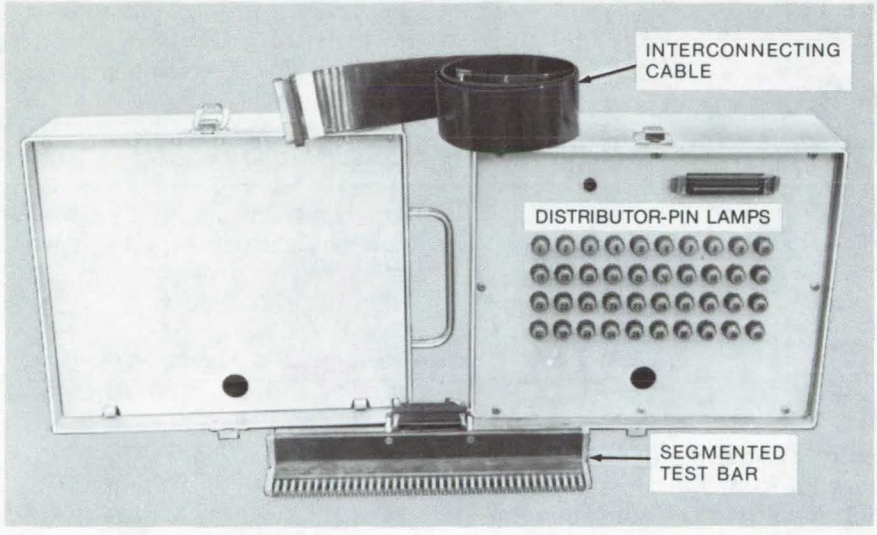

The **Paddle-Pin Alinement Test Set** uses a segmented bar that touches only one pin at a time.

This work was done by David M. Gilliam and James A. Foster of **Kennedy Space Center.** *For further information, Circle 75 on the TSP Request Card.*
KSC-10740

Atmosphere-Generating System

Stored hydrazine and water are converted to a life-support atmosphere.

Lyndon B. Johnson Space Center, Houston, Texas

A new concept in storing a breathable atmosphere requires less heavy equipment than high-pressure or cryogenic storage techniques. A nitrogen/oxygen atmosphere is stored as hydrazine and water in low-pressure tanks. These chemicals are then converted by electrolysis to gases for breathing.

The system consists of a set of modular units for electrolytic gas generation, distribution, and control. Several of the subassemblies, such as the fluid/gas holding-and-control unit and the combination pump and bubble separator, may also be useful in other fluid-handling systems.

The hydrazine and water electrolysis system is designed as a series of self-contained modules: individual hydraulic assemblies with no electrolyte connections. Each is completely sealed with its own internal manifolding for the electrolyte circuit. The modules are mounted on rails in a cabinet, for easy installation and removal. All modules are cooled by a common cold plate that interfaces with a module when it is installed. The cabinet contains individual replaceable electronic assemblies for each module, water-conditioning equipment, and monitoring equipment. A system of 12 modules will provide sufficient air for 12 men and requires 7,020 watts of power.

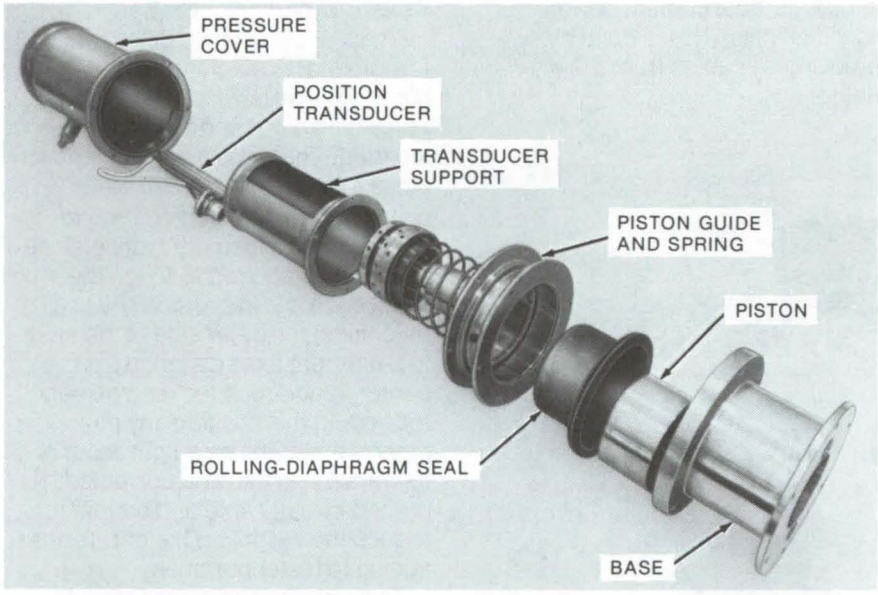

Figure 1. The **Electrolyte Reservoir** controls system pressure and supplies the high/low electrolyte safety-shutdown signals and the water and hydrazine feed-control signals. A piston that interfaces the gas and electrolyte uses a rolling-diaphragm seal for reduced friction. Torque generated by compression or release of the spring is isolated from the seal by a ball radial/thrust bearing. The position transducer is a differential-transformer piston which supplies cell control, safety, and feed signals.

The major components in the system are:

- A 22-cell electrolysis stack having a hydrophilic matrix within each cell to improve its resistance to gas/liquid differential-pressure fluctuations.
- An electrolyte reservoir that includes controls for the water and hydrazine feed rates, the operating pressures, and the volume (Figure 1).
- A combination pump and bubble separator that circulates the electrolyte and removes gas bubbles entrained in the electrolyte loop (Figure 2).
- A baseplate that contains internal manifold and routing passages for the electrolyte loop, interfaces for the liquid-loop components, and structural supports for the assembly.

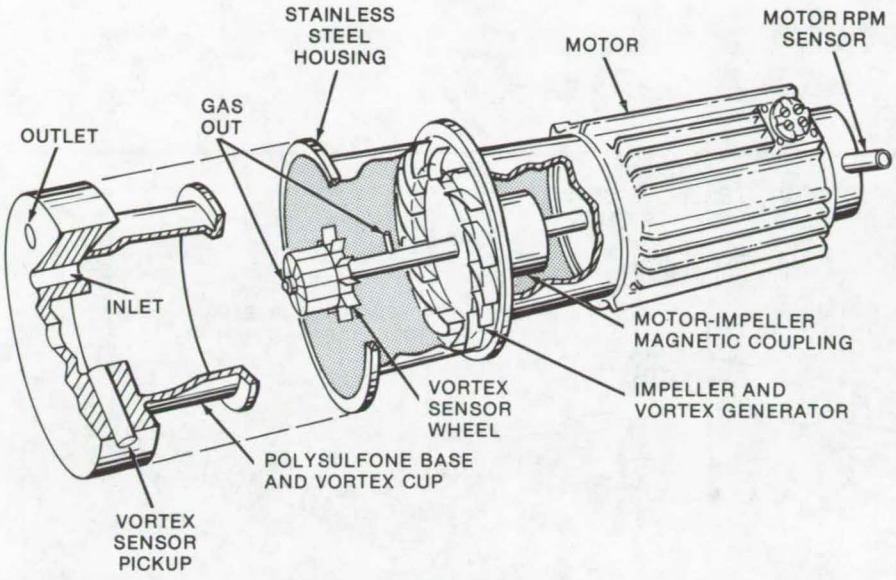

Figure 2. The **Pump and Bubble Separator** circulates electrolyte and removes gas bubbles dissolved in the feed water. It is a magnetically-coupled centrifugal pump with a single impeller that creates a force field sufficient to concentrate gas bubbles along the center of the pumping chamber. The gas is vented through a nonrotating shaft. The gas, as it is trapped in the unit, grows in a cylindrical shape. As the diameter of this gaseous cylinder increases, the free-floating impeller slows, and an rpm sensor triggers a solenoid valve to discharge gas, thus decreasing the diameter of the gaseous cylinder until the sensing impeller picks up speed and causes the rpm sensor to close the valve.

This work was done by Ralph E. Mahan and Phillip A. Wagner of Lockheed Missiles & Space Co., Inc., and Warren J. Conner of Fluid Dynamics Corp. for **Johnson Space Center.** *Further information may be found in NASA CR-134390 [N74-31581], "The Development of Non-cryogenic Nitrogen/Oxygen Supply System," a copy of which may be obtained at cost from the National Technical Information Service, Springfield, Virginia 22151. MSC-14713*

Economical Measurement of Particle Concentration

A relatively simply-designed, optical scattering meter measures particle concentration in fluids. The meter correlates scattering-angle effects with composition. It measures simultaneously light scattered at a small (2°) and at a large (90°) angle. By measuring the refractive index, it can be used to measure the relative amounts of organic and inorganic particles and the contribution of various species to changes in contamination levels in such applications as monitoring rivers or industrial waste outlets.
(See page 358.)

Composite Laminate Warpage

A set of simplified equations predicts the warpage of fiber composite laminates that often occurs upon removal from the fabrication mold. The equations predict corner deflection and are based upon the micromechanics and macromechanics of composites, as well as laminate theory. Factors considered include ply misorientation, fiber migration, and void/volume ratio nonuniformity. The equations could be used to obtain an a priori assessment of factors that are difficult to control during fabrication, to design warp-compensating nonsymmetries, or to specify tolerances to reduce warping.
(See page 382.)

Self-Calibrating Radiometer

A simplified self-calibrating radiometer has a radiation receiver with a receiving surface that need not be raised to the temperature of the heat-emitting source. The front surface of the radiation receiver is heated by energy from the heat source; the rear surface is heated by a resistance heater. The heater is adjusted until the front and rear of the radiometer are at the same temperature, and the energy required by the heater to maintain this isothermal state will be equal to the energy absorbed by the front of the receiver.
(See page 365.)

Manual Trash Compactor

Hand-operated ratchets
compress trash in the bag.

Lyndon B. Johnson Space Center, Houston, Texas

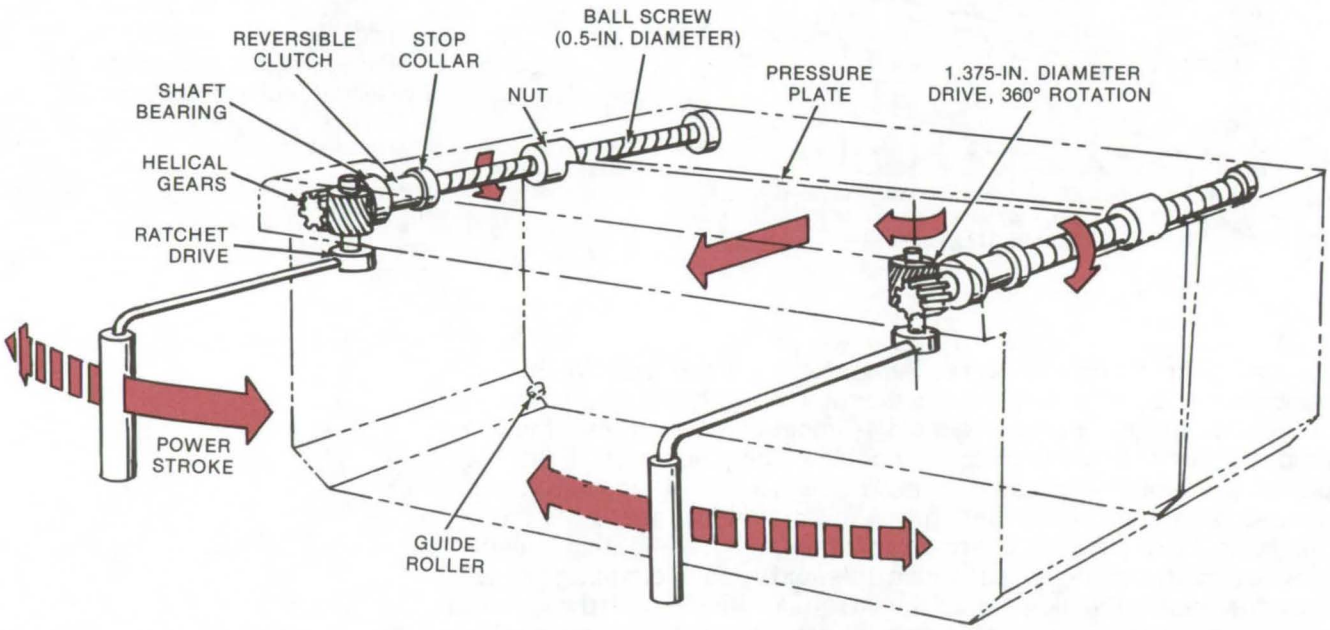

The **Manual Trash Compactor** has a compressive force 2,000 pounds (907 kilograms), which exceeds the yield strength of food cans. The compactor size is 2 cubic feet (0.05 cubic meter) in volume and weighs 30 pounds (13.5 kilograms).

A small hand-operated trash compactor may prove useful where space is at a premium or where there is no power for an electrical compactor. The trash compactor would eliminate the need for individual trash bags and disposal containers. Because it is hand operated, this type of compactor may prove less expensive to manufacture and use than powered compactors.

The compactor, as shown in the figure, consists of a housing with front-loading door, trash compactor bag, and drive ratchets. Material placed in the bag is crushed; when the bag is full of compressed trash, it is removed from the compactor and is then disposed. Ratchet-type handles transmit the force exerted on them to a gearset which drives a pair of ball screws. The ball screw nut is attached to a pressure plate which moves when the screw turns. As the screw turns, the pressure plate moves and compresses the bag. When the bag is full, an empty bag is inserted into the compactor, and the pressure plate is returned to its starting position by reversing the hand-operated ratchets.

This work was done by G. E. Stevenson of Nelson and Johnson Engineering, Inc., for **Johnson Space Center.** *For further information, Circle 76 on the TSP Request Card.*
MSC-16039

Books and Reports

These reports, studies, and handbooks are available from NASA as Technical Support Packages (TSP's) when a Request Card number is cited; otherwise they are available from one of NASA's Industrial Application Centers or the National Technical Information Service.

Time-Domain Aircraft Model

Fourier transformation improves aerodynamic coefficients.

A mathematical technique transforms aerodynamic coefficients in the frequency domain into a time-domain model. Aerodynamic-coefficient pairs are expanded in a series and are represented as even-order curve fits. A least-squares technique is used to demonstrate the validity of such a curve fit. The force terms are replaced by time-dependent terms (due to mathematical properties of Fourier transform), with new differential equations added for each term replaced in the force and moment equations.

These new equations are solved for the highest ordered derivative of each dependent variable. The result is a more complete set of aerodynamic force and moment equations incorporating frequency-dependence coefficients.

This work was done by David K. Scharmack of Honeywell Inc. for **Johnson Space Center.** *For further information, Circle 77 on the TSP Request Card.*
MSC-16018

Fundamentals of Fluid Sealing

A textbook for a course on fluid sealing

A text covering the fundamentals of fluid sealing, including seal operating regimes, has been published as an outgrowth of a course taught by NASA personnel at several technical society and university seminars. The text provides the background necessary for a fundamental understanding of fluid sealing in general and of specific seal types in particular.

Fluid sealing, as other branches of engineering, draws on the experience and knowledge of many other disciplines and fields. The engineering of seals can involve tribology (lubrication science), fluid mechanics, heat transfer, structural and solid mechanics, thermodynamics, chemistry, physics, materials science, and dynamics, as well as other fields.

The fundamentals of fluid flow are important to understanding various sealing devices. The text discusses those fundamentals as they apply to seals. Basic principles of incompressible (liquid) and compressible (gas) sealing flows are studied. The mechanism of film pressure generation between moving surfaces is described. Fundamental friction and wear concepts, various seal-lubrication operating regimes, and surface topography effects are also presented.

General fluid-flow equations governing liquid and gas sealed fluids and laminar and turbulent flow are developed. These equations are applicable for many seals. Included in the text are seal performance parameters and seal operating regimes. Also discussed are geometry effects, surface deformations, rotation, pressure balancing, the concept of flow function, the mechanisms of seal surface separation, fundamental friction and wear concepts applicable to seals, seal materials, and pressure/velocity criteria. These fundamentals enhance the understanding of various sealing devices and permit more in-depth study of specific seals, including positive-contact seals, close-clearance seals, and fixed-geometry seals.

This work was done by John Zuk of **Lewis Research Center.** *A copy of the textbook, NASA TN-D-8151 [N76-19462], "Fundamentals of Fluid Sealing," and a second, related report, NASA TM-X-71851 [N76-17399], "Dynamic Sealing Principles," may both be obtained at cost from the New England Research Application Center.* *[see page A7].*
LEW-12683

Astronautic Structures Manual

A three-volume reference work on aerospace strength analyses

A detailed reference work on methods for strength analysis, as used throughout the aerospace industry, is presented in an extensive three-volume (2,450 pages) set. This is possibly the most thorough and complete single source of information on structural analysis available today. Most of the analysis methods can be carried out by hand, are general enough to cover many types of structures, and are sufficiently sophisticated for accurate estimates of expected strengths. This compendium is not only a catalog of analysis techniques for elastic and inelastic stress ranges not usually available elsewhere but also serves as a reference source on the background and development of the methods.

The information is a condensation of published journal articles, industry and university publications, textbooks, and government documents. Illustrative examples are included to clarify techniques, and tables and curves are included where necessary. The manual includes eight sections:

A. General Methods — Volume 1
B. Strength Analysis — Volumes 1 and 2
C. Structural Stability — Volume 2
D. Thermal Stresses — Volume 3
E. Fatigue and Fracture Mechanics — Volume 3
F. Composites — Volume 3
G. Rotating Machinery — Volume 3
H. Statistics — Volume 3

Section A, a general introduction of methods, includes discussions of loads, combined stresses, and interaction curves. An in-depth discussion of the use of the metric system includes many conversion tables.

In the section on strength analysis (B), analysis techniques, tables, and data are presented on joints and fasteners (mechanical, welded, and brazed), lugs and shearpins, springs, plastic bending, beams under axial loads, lateral buckling of beams, shear beams, frames, rings, thin shells, torsion, plates, and holes and cutouts. Section C covers the stability of columns, plates, and shells, and it includes information on the analysis of local instabilities that lead to buckling and wrinkling.

Section D, on thermal stresses, presents techniques dealing with thermoelasticity, the strength of materials solutions, inelastic effects, and thermal shock. Fatigue and fracture mechanics are covered in section E. Factors influencing fatigue strength, low-cycle fatigue, and cumulative fatigue are analyzed. Fracture mechanics topics include stress-intensity factors and flaw growth.

Section F discusses composites and laminated composites; rotating machinery and statistical methods are given a brief treatment in sections G and H.

This work was done at **Marshall Space Flight Center.** *To learn how to obtain a copy of the manual, Circle 78 on the TSP Request Card. MFS-23547*

Cavitating Performance of Pumping Machinery

A simplified technique for predicting performance

A four-volume publication has been released which contains extensive cavitation data and a simplified technique for predicting cavitation performance of pumps. The cavitation data developed consist of pressure and temperature measurements within fully-developed hydrogen and nitrogen fluid cavities, and were acquired for venturi, hydrofoil, and three sizes of quarter-caliber ogive shapes.

Over the past 30 years, much confusion in the cavitation literature is attributable to the failure to recognize clearly and/or categorize cavitation data. The presence of dissolved gases, minerals, and particulate matter adversely affects the cavitating performance of equipment and simultaneously complicates analysis and data correlation. All data treated in these reports are considered to be virtually free of these effects, an advantage of cryogenic test fluids.

To design liquid-handling equipment such as pumps and flowmeters, the designer must determine whether cavitation will occur and frequently the extent of such cavitation. Since the formation and collapse of vapor cavities alter flow patterns, cavitation may reduce the efficiency of pumping machinery, produce vibrations, cause flow instabilities, and reduce the precision of flow measuring devices. The collapse of these vapor cavities can also cause serious erosion damage to pump blades, flowmeter vanes, and the like. A designer usually attempts to avoid cavitation but not always successfully; also, cavitation can sometimes be beneficial. For these various reasons, therefore, it is desirable to predict the cavitating performance of equipment.

Liquid hydrogen and liquid nitrogen were chosen as test fluids both to acquire sufficient knowledge to permit intelligent design of pumps for near-boiling liquids and also because predictive analyses indicated that the physical properties of hydrogen and nitrogen make them particularly desirable test fluids. The objectives of the study were: (a) to determine experimentally the flow and thermodynamic conditions required to induce incipient and developed cavitation on various hydrodynamic bodies, (b) to improve existing correlation expressions for the prediction of cavitating performance of hydraulic equipment, and (c) to establish, if possible, a technique for predicting the fluid-handling capability of dissimilar cavitating equipment, using different fluids.

The analysis of convective heat-transfer and mass flux-limiting processes resulted in improved correlative/predictive expressions applicable to pump design and operation. Extensive data with developed cavitation were acquired for stationary hydrodynamic bodies immersed in a flowing cryogenic liquid. These data were satisfactorily correlated, using the improved semiempirical correlative expressions. These expressions were extended to predict cavitating pump performance, with the only similarity requirement being a constant ratio of the cavitating-to-noncavitating pump head rise.

NASA liquid-hydrogen pump data were used to demonstrate the adequacy of this extension. It was shown that the ability to predict cavitating performance of pumps can be significantly extended. The extension of semiempirical correlating expressions from stationary bodies to pumping machinery was substantiated.

This work was done by Jesse Hord, Lowell M. Anderson, and William J. Hall of the National Bureau of Standards for **Lewis Research Center.** *Further information may be found in:*

NASA CR-2054 [N72-24363] "Cavitation in Liquid Cryogens, I — Venturi";
NASA CR-2156 [N73-16255] "Cavitation in Liquid Cryogens, II — Hydrofoil";
NASA CR-2242 [N73-28153] "Cavitation in Liquid Cryogens, III —Ogives"; and
NASA CR-2448 [N74-34704] "Cavitation in Liquid Cryogens, IV — Combined Correlations for Venturi, Hydrofoil, Ogives, and Pumps."

Copies of these reports may be obtained at cost from the New England Research Application Center *[see page A7]*. *LEW-12423*

Solar Heated and Cooled Office Building

A working system is providing useful data for future solar-energy systems.

A new office building at the NASA Langley Research Center in Hampton, Virginia, is equipped with a solar heating and cooling system designed as a joint project with the NASA Lewis Research Center. This installation will be a full-scale working test-bed facility to test flat-plate solar-energy collector systems for heating and cooling buildings.

The office building is a single-story structure containing 4,923 square meters (53,000 square feet) of floor space for 350 engineering personnel. A 1,393-square-meter (15,000-square-foot) solar collector area, located adjacent to the building, will provide between 80 and 100 percent of the heating and cooling requirements during the late fall, winter and early spring months, and between 50 and 60 percent of the cooling requirements in the summer. The solar collector system will be capable of accepting up to 16 different types of solar collectors simultaneously, thus serving as a full-scale test bed for both state-of-the-art and advanced solar collectors.

The building heating and cooling system operates on 344 to 378 K (160° to 220° F) hot water generated from solar energy or from a steam utility system. The building energy requirements were determined by using the U.S. Post Office Department's Equipment and Energy Consumption Analysis Computer Program. Activated charcoal filters reduce the ventilation air requirements by 75 percent which reduces the air-conditioning load by about 10 percent. The solar energy available was determined by weather bureau data from recording stations near the Langley area. The amount of solar energy that can be captured depends upon the angle of incidence and the thermal efficiency of the collection system. For the southern Virginia area latitude, an incident angle of 30° is considered near optimum. The thermal efficiency of the solar heating system was determined to be between 30 and 50 percent because the efficiency of the solar collectors to be tested will vary. Using the building energy requirement and the solar energy available, it was determined that a solar collector area of 1,393 square meters (15,000 square feet) would be required to demonstrate operation of the solar heating and cooling for all modes of operation. Since there usually is a difference between the amount of energy needed and the amount of energy available for any particular day, both hot-water and cold-water storage is provided to even out these differences.

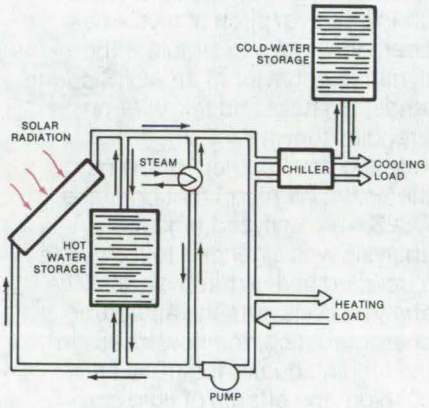

The **Solar Heating and Cooling System** installed at a Langley Research Center office building supplies a major portion of the heating and cooling requirements.

The solar-energy system (shown schematically in the figure) uses an absorption-cycle (lithium bromide/water) air-conditioner, which can operate with hot water supplied by solar heat or conventional means. Heat is supplied by conventional hot-water baseboard convectors.

Arrangements to inspect this solar heating and cooling system during normal working hours, may be made by writing to the Technology Utilization Officer at Langley Research Center. See page A4 for the correct address.

This work was done by William L. Maag of **Lewis Research Center.** *Further information may be found in NASA TM-X-71615 [N74-34541], "Solar Energy to Heat and Cool a New NASA Langley Office Building," a copy of which may be obtained at cost from the Technology Application Center, University of New Mexico [see page A7].*

LEW-12512

Computer Programs

These programs may be obtained at very reasonable cost from COSMIC, a facility sponsored by NASA to make new programs available to the public. For information on program price, size, and availability, circle the reference letter on the COSMIC Request Card in this issue.

GEODYN

Orbital and geodetic parameter estimation

GEODYN was written for applied research in satellite geodesy, specifically for the calculation of orbit and geodetic parameter estimates. Two previously-existing computer programs used in satellite geodesy research were merged and enhanced, resulting in the more capable, accurate, and versatile GEODYN program. GEODYN is capable of estimating that set of orbital elements, station positions, measurement biases, and a set of force model parameters such that the orbital tracking data from multiple arcs of multiple satellites best fit the entire set of estimated parameters.

Cowell's method of numerical integration is used for the satellite equations of motion and the variational partials for force model parameters which are to be adjusted. Cowell's method, as implemented in GEODYN, uses

predictor/corrector formulas for the equations of motion and corrector formulas only for the variational partials. Optional orders may be selected for the integration process along with optional variable-step integration processes for highly elliptic orbits. Although GEODYN is primarily an Earth-oriented program, it has also been used for translunar and interplanetary trajectories.

Since measurements generally occur at times not coincident with the integration steps, GEODYN uses an interpolation scheme for computing the instantaneous satellite position and velocity vectors. This scheme is a variation of the integration corrector formulas and maintains the same level of accuracy as the integrator.

The Bayesian least-squares estimation process is used by GEODYN for solving the geodetic parameter estimation problem. Bayesian estimation is used because of its utilization of a priori information. Consequently, GEODYN requires the input of a priori estimates and uncertainties of all parameters to be determined in the solution.

Due to the multiarc nature of the GEODYN estimation process, a partitioned solution of the normal equations is performed. Partitioning of the normal matrix allows the inclusion of a virtually unlimited number of arcs to the solution. Each arc contains information about only one satellite (or two satellites when satellite-to-satellite tracking is involved) and spans some user-specified period of time.

GEODYN provides default values for most of the parameters affecting the solution and allows all of the values to be altered on option. A large set of support programs is included to reduce the data and analysis problems of the user. They can be described generally as data-handling programs, analysis and plot programs, and auxiliary estimation programs. The GEODYN program was developed to be utilized on a large-scale computer with 400K bytes of user-accessible core.

FORTRAN IV
G or H Compiler
IBM 360

This program was written under the direction of Barbara Putney of **Goddard Space Flight Center.** *For further information, Circle E on the COSMIC Request Card.*
GSC-12014

Air-Cushion Landing Systems

A computer-implemented, detailed heave/pitch analysis

A mathematical model for heave/pitch analysis of air-cushion landing systems (ACLS) is based on a fundamental analysis of the body dynamics and fluid mechanics of the aircraft/cushion/runway interaction. A computer program based on this heave/pitch analysis has been developed to simulate the dynamic behavior of an ACLS during landing impact and taxi over an irregular runway.

In the development of the model the heave (vertical) motion of the ACLS was analyzed, and the analysis was extended to formulate a coupled heave/pitch model. The analysis considers the air source characteristics, the flow losses in the feeding ducts, the trunk and cushion, the effects of fluid compressibility, and the dynamic trunk deflections including ground contact. The computer program simulates the dynamic motion of an ACLS-equipped aircraft caused by landing impact and taxi over an irregular runway. Input to the program includes data such as cushion and trunk geometry, aircraft weight, fan characteristics, and runway surface profile.

The execution sequence of the program after the input data are read in is: (1) the initial geometry is calculated, (2) the static characteristics are computed and printed, (3) the initial conditions for the dynamic simulation are determined, and (4) the state equations are numerically integrated to determine the time history of ACLS pressure and motion following landing impact. The main capabilities of the program are:

- To determine static ACLS characteristics, to aid in fan selection, and to determine allowable limits for equilibrium cushion loading;
- To evaluate dynamic landing and taxiing performance, including the vibration caused by runway irregularities; and
- To determine optimum values of design parameters for improved dynamic performance.

The program can easily be adapted to run on any computer with a FORTRAN compiler. The storage requirements for this program are 64K octal 60-bit words.

FORTRAN IV
CDC 6000 Series, Run Compiler

This program was written by Khushroo M. Captain, Ashok Boghani, and David N. Wormley of Foster-Miller Associates Inc. for **Langley Research Center.** *For further information, Circle F on the COSMIC Request Card.*
LAR-11783

Analysis of Axisymmetric Shell Structure

Stress, vibration, and buckling characteristics of general shells of revolution

A system of six compatible computer programs for structural analysis of axisymmetric shell structures applies to a common structural model but analyzes different modes of structural response. The structures may be classified according to their function into three groups, designated as the 100, 200, and 300 series. In particular they are:

- Linear static response under asymmetric loads,
- The buckling of linear states under asymmetric loads,
- Nonlinear static response under axisymmetric loads,
- The buckling of nonlinear states under axisymmetric loads,
- Imperfection sensitivity of buckling modes under axisymmetric loads, and
- Vibrations about nonlinear states under axisymmetric loads.

These programs treat branched shells of revolution with an arbitrary arrangement of a large number of open branches but with at most one

closed branch. Current dimensioning allows for seven branch points, each of which may have as many as five branches emanating from it. Branches which close at the axis of revolution (i.e., dome closures) are not considered to be closed branches. A maximum of 23 dome closures or other shell edges is allowed.

At each meridional station, the shell wall may consist of as many as five orthotropic layers, in each of which elastic properties may vary only in the meridional direction. At each material point, the shell is assumed to possess orthotropic principal axes in meridional and circumferential directions. All geometric and mechanical properties of the structure are assumed to be axisymmetric, but may have arbitrary meridional variation.

A continuous reference surface arbitrarily located within or near the shell wall is treated. The shell may be stiffened by:

- Up to 34 discrete isotropic rings,
- Stringers with stiffness circumferentially distributed, or
- An elastic foundation attached to the shell wall.

The effects of thermal loads and live pressure fields are included.

FORTRAN
CDC 6000 Series
FORTRAN Compiler

This program was written by Wendell B. Stephens of **Langley Research Center** *and Gerald A. Cohen and Raphael T. Haftka of Structures Research Associates. For further information, Circle G on the COSMIC Request Card.*
LAR-12059

SPAR

Structural-Performance Analysis and Redesign

Finite element techniques, in which airframes and other complicated structures are mathematically modeled as assemblages of beam, plate, and similar elements, have emerged in recent years as probably the single most important class of methods used in theoretical analyis of aerospace structures. The strong feature of the finite element technique is its suitability for accurately characterizing extremely complicated structures for which the determination of exact analytical solutions is impossible.

The problems encountered with this method are primarily the accurate and efficient input and handling of the large quantities of numerical data. The SPAR system of processor programs was developed to perform stress, buckling, and vibrational analysis of large linear finite element systems in excess of 50,000 degrees of freedom, while minimizing processing cost, execution time, central memory storage, and secondary data storage requirements, through the use of sparse matrix solution techniques and other computational and data management procedures designed for problems of very large size.

A data base comprised of automatically-maintained direct access libraries (DAL's) is used to provide a means of information exchange between an array of totally-independent absolute programs (processors). The DAL's are generated, serviced, and interrogated, using a system of routines collectively called IMSYS (information management system). IMSYS is written almost entirely in FORTRAN and operates nearly identically on UNIVAC and CDC systems.

An arbitrary number of data sets may be entered in a DAL, using IMSYS. A data set already in a DAL may be replaced by using IMSYS to enter into the DAL a new data set having the same name. Among other services, IMSYS provides the ability to interrogate DAL's to determine their contents, to delete data sets, selectively to copy data sets from one DAL to another, and to copy (and subsequently retrieve) entire DAL's from disk or drum to tape. Through IMSYS, DAL's can be created and utilized in a wide variety of ways, without concern for DAL internal format, or for the procedure implemented by IMSYS routines in actually executing the data transmissions.

The crucial factor in implementing the DAL approach was to minimize the input/output activity required by IMSYS without using an excessive amount of core storage for directories and without restricting DAL generality (e.g., the form and number of data sets in a single DAL or the number of separate DAL's simultaneously activated). The method used in IMSYS, which involves dynamic swapping of segments of DAL tables of contents between secondary storage and a small in-core directory area, has shown excellent performance. In SPAR applications most DAL operations have been observed to require a single input or output access.

Other significant features include:

- The computer execution costs achieved by the basic static solution routines are very close to the minimum that can possibly be attained by using direct solution procedures, generally affording substantial savings when compared with the costs associated with constant or variable-width band matrix, "active column," or partitioning solution methods used in other programs. A number of run-time comparisons with other well-known finite element programs have been made. In no case has any other program been found to execute as fast as SPAR, even for structures ideally suited to band matrix or active column methods; and in large problems very substantial differences in run time (e.g., factors of 10 or more) have often been observed.
- SPAR attains its low execution costs through the use of a solution technique based on a direct elimination procedure which (unlike band matrix and active column techniques) avoids virtually all unnecessary arithmetic operations by recognizing, in essentially complete detail, the sparsity characteristics of network stiffness matrices.
- The element repertoire includes a very general class of beam elements and 3-node and 4-node plate/shell membrane and bending elements (isotropic, orthotropic, or aeolotropic). Beam elements may include the effects of shear center/centroid offsets, transverse shear

deflection, and nonuniform torsion. Section properties (such as moments of inertia, area, shear deflection constants, torsion constants, principal axis orientation, and shear center location) may be input directly, or the program will compute them for many types of sections (wide flanges, boxes, tube, angles, zees, channels, and tees), given only the section dimensions as input.

- Plate/shell membrane and bending-element formulations based on "hybrid" variational methods are included, providing substantial improvements in the accuracy of displacements and stresses. Only flat two dimensional elements are presently available. Three-dimensional elements are planned for the near future.
- Loadings include point forces and moments at joints, pressure loads, nonzero specified joint motions (in "oblique" directions, if required), and thermal loading. Oblique joint restraint is allowed.
- The data input apparatus is designed to minimize the amount of manual effort required to prepare data decks for large-scale applications. Extensive use is made of "libraries" of beam and shell section properties, material constants, and the like in generating problem definitions. This method usually reduces greatly the amount of manual effort (and probability of error) in preparing data decks for large structures. For example, the section properties of a beam are "defined" by referring to the applicable set of data in one of the libraries. Accordingly, the detailed definition of each unique section appears in the input data only once, regardless of how many elements have that particular section.
- Multidimensional "network generators" of input data for element definitions, position coordinates, constraint, applied loading, and the like are provided.

For most SPAR executions, $20{,}000_{10}$ to $30{,}000_{10}$ words of central memory are sufficient.

FORTRAN IV, Assembler Coding
CDC 6000/CYBER Series
[LAR-12062]
UNIVAC 1100 Series
[MFS-23182]

This program was written by W. D. Whetstone of Lockheed Missiles & Space Co., Inc., for **Langley Research Center** *and* **Marshall Space Flight Center** *and Larry Kiefling of* **Marshall Space Flight Center.** *For further information, Circle H [CDC 6000/CYBER Series] or Circle S [UNIVAC 1100 Series] on the COSMIC Request Card.*
LAR-12062/MFS-23182

Math Model of 3-D Aircraft Configuration

Curved surfaces of an aircraft are defined in surface-patch equation form.

A new computer program can be used to construct surface equations for aircraft configurations. The numerical model of the input configuration is assumed to be symmetrical about the XZ plane (positive Y side) and may include any combination of components. The configuration is usually positioned with its nose at the origin and with the length of the body stretching in the positive X direction. The coordinate system used for this program is a right-handed Cartesian-coordinate system. Since the modeling technique expects to approximate a smooth surface, sufficient input data points with no abrupt changes in curvature should be supplied. The geometry input section of the program can be easily replaced with a different form so that the program could be useful for any three-dimensional object or objects.

A three-dimensional parametric cubic-spline technique is used for the patch boundary curve definitions in which the coordinates are expressed as cubic functions of one variable. A series of adjacent polynomial segments between each given point is used to represent the curve. The length of each segment is used as the parameter and is later normalized to one. Linear segments are used when a line consists of less than three points.

The X, Y, and Z coordinates of a surface patch are each single-valued cubic functions of two parameters. The coefficients of these cubics are expressed in terms of end points and partial and cross derivatives with respect to the parameters. The result is a parametric bicubic representation of three-dimensional surfaces.

Orthographic projections are created by applying the three-dimensional rotation equations directly to the patch equations describing the body surface for plotting the object at any desired viewing angle. The rotated patch equations are projected into the two-dimensional patch form of the paper plane. An enriched surface may be obtained from the rotated and projected patch equations by holding one parameter constant and varying the other.

The orthographic plotting routine also includes a hidden line option where the normal vectors are computed from the rotated and projected form of the patches. A positive normal vector indicates that the point is visible, and a negative normal vector indicates that the vector points away from the viewer and thus is not visible. Another routine computes and plots the surface coordinates of a cross section through the body at any desired orientation. The calculations consist of the simultaneous solution of the patch equations and the equation of a plane.

FORTRAN
CDC 6000 Series
SCOPE 3

This program was written by Charlotte B. Craidon of **Langley Research Center.** *For further information, Circle J on the COSMIC Request Card.*
LAR-12029

Transient Thermal Analysis of Fluid Systems

An efficient program for evaluating small thermal networks

Because general-purpose thermal network computer programs are inefficient for evaluating small networks (under 200 nodes), a more efficient program has been developed to perform transient thermal analysis on networks of 2 to 200 nodes. The program performs a transient analysis of the hydraulic system, listing fluid and component temperatures, heat gains or losses, water boiled (if any), and pressure drops. Component and property curves are built into the program through easily-accessible data blocks.

By reading in several blocks of data, the built-in values may be changed, including environmental heat inputs and temperatures, heat exchange/evaporator controls, and initial conditions. All the network flows are then set, and the heat generated by the fluid flow is calculated, including the pump heat input. All the temperature equations are solved and iterated until a heat balance is obtained. The equations are implicit to allow a large calculation interval and are solved in a "forward" direction, using a 1.3 overrelaxation factor.

The heat generated by the fluid flow, called "flow work," is obtained from the flow and pressure drop with a factor in the equation to account for external work. The film coefficient is calculated as fully developed laminar or turbulent according to the Reynolds number. The laminar equation is also used for stagnent fluid. The film coefficient equations are standard empirical equations. For laminar flow the Hausen equation is used. The turbulent film coefficient equation is the empirical Dittus and Boelter equation. The program calculates the pressure drop for a particual node at a given flow.

The program may be used to model any 2-node to 200-node thermal network which transports heat by fluid flow convection. It can also be modified to add conduction along tubes and radiation.

IBM 360
FORTRAN G Compiler
IBM 360/370
FORTRAN IV Compiler

This program was written by Gorden D. Chandler and Ronald D. Trust of Rockwell International Corp. for **Johnson Space Center.** *For further information, Circle K on the COSMIC Request Card.*
MSC-19502

Determining Aircraft Stability and Control Derivatives

Three programs determine stability and control derivatives from flight data.

A system of three computer programs was developed for automating the preparation of large amounts of flight data, calculating estimates of the coefficients of the differential equations of motion that result in a good fit with actual data, and plotting predicted vs. flight-determined derivatives. A modified Newton-Raphson or quasi-linearization minimization technique is used for estimating aircraft stability and control derivatives. The three component programs are SETUP, MMLE, and SUMARY. The SETUP program is a preprocessor for automating much of the data preparation necessary for input to the MMLE component.

The MMLE (Modified Maximum Likelihood Estimation Program) is the basic program of the package and, as its name implies, obtains maximum likelihood estimates from flight data. Input to the program consists of the measured values contained in time histories of a flight maneuver on cards, tape, or disk; information on the flight condition of the maneuver; values of pertinent characteristics of the aircraft; a set of starting estimates of the derivatives; and option instructions. Output is available in three basic forms: printed, plotted, and punched cards. The basic output is always printed, with additional information optional. The plotted output is in the form of time history or derivative plots, and the punched cards are in the format required by the SUMARY associate program.

The SUMARY program reads a set of predicted and flight-determined derivatives and plots specific groups of the data as instructed. The same predicted derivative card deck used for the SETUP program may be used as input, or predicted derivatives may be omitted. The punched output from MMLE is input to SUMARY. The printed output includes the header cards for all flight points and a summary of the plot instructions. Additional informative messages are provided if no predicted derivatives or flight data are available at a requested condition. Plots are scaled for centimeter grid paper, with confidence levels indicated by vertical bars. Predicted derivative data are identified by small symbols at the beginning and end of each curve.

This program can be run on most large computers and is overlaid to reduce the core requirements to $52{,}000_8$ words (including all buffers and system routines for I/O). In unsegmented form the program requires $74{,}000_8$ words.

The programs have been used successfully on more than 3,500 maneuvers obtained from 30 different aircraft. These aircraft range from the smallest to the largest in existence, and the maneuvers were obtained over the altitude and Mach number ranges encompassing the limits of today's aircraft.

FORTRAN IV Compiler/Modification
SCOPE 3.4 OS
CDC 6000 Series

This program was written by Kenneth W. Iliff and Richard E. Maine of **Dryden Flight Research Center.** *For further information, Circle L on the COSMIC Request Card.*
FRC-10109

Swept Wing Aerodynamics

Analysis of viscous/potential flow interaction for swept wings

A method has been developed for the analysis of the viscosity-dependent aerodynamic characteristics of multielement infinite swept wings in incompressible flow. The method includes procedures for calculating the boundary layer development over infinite yawed wings and terms for normal pressure gradient and longitudinal curvature. These lead to improved predictions of the performance of multielement airfoils in two dimensions. A computer program has been developed to permit maximum exploitation of the new method of computation.

The wing configuration (consisting at most of a slat, a main element, and double-slotted flaps) is represented mathematically as an assembly of a large number of panels. The inviscid pressure distribution about a given configuration in the normal chord direction is determined with the aid of a two-dimensional potential flow program that is based on a vortex lattice technique. The boundary layer development over each element of a high-lift configuration is determined either by an integral or by a finite-difference boundary layer technique. Once the boundary layer development is known, a source distribution is determined as a function of the calculated boundary layer displacement thickness and pressure distributions.

The source distribution is included in a second calculation of the potential flow about the configuration and represents the effect of the boundary layer in the modification of the potential flow. The solution usually converges (after two to five iterations between the potential flow and boundary layer calculations). In subsequent computations, lift, drag, and pitching moments are determined as functions of the Reynolds number.

By using source distributions rather than the displacement thickness to represent the effect of the boundary layer on the potential flow, the influence coefficient matrix representing the geometry of the configuration needs to be inverted only once. This technique and the use of the iterative technique for matrix inversion help to reduce computer time for the overall analysis.

FORTRAN IV
100,000 Octal Words [Storage]

This program was written by Frank A. Dvorak and Frank A. Woodward of Flow Research, Inc., for **Ames Research Center.** *For further information, Circle M on the COSMIC Request Card.*
ARC-10790

Control System Design

Frequency domain models and parameter optimization for feedback controllers

A computer program has been written which optimizes the parameters in a feedback controller transfer function. Figure 1 represents the type of system for which the program can be used: a linear feedback system having a single control input, u, and one or two outputs in cascade, x_1 and x_2. The basic problem formulation has the control input u and an assembled disturbance d enter the system at the same point. The program allows the measured system outputs x_1 and x_2 to be corrupted with random noise v_1 and v_2.

The controller design problem was set up as a parameter optimization in the frequency domain and uses frequency response test data directly for the plant and actuator. Control effectiveness was evaluated in terms of a performance index which was obtained by integrating over frequency the absolute value squared of the system output x_1, the output rate $\dot{x}_1$, the control input u, and the control input rate $\dot{u}$. A modified conjugate gradient algorithm was used to search for the optimum controller parameters.

Figure 2 illustrates one gradient search sequence where the algorithm sequentially "tries" different parameter combinations in order to "slide down" the surface. Iteration stops at the surface minimum which is the point of best control. Such a search may typically require only a second or less of computer time and may be run on a small scientific computer.

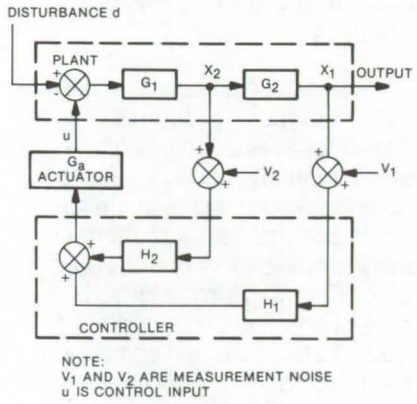

Figure 1. A **Typical Control System** for which the design program is written is a feedback system with a single control input, u, and one or two cascaded outputs, x_1 and x_2.

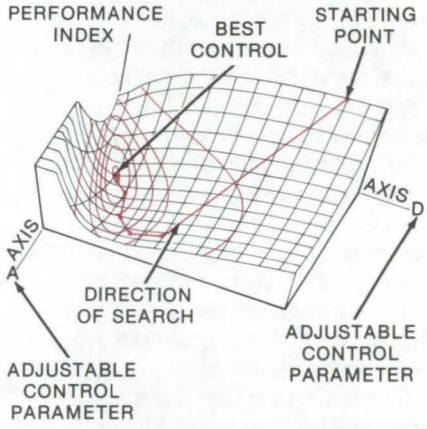

Figure 2. The **Control Optimization Procedure** is illustrated by the above surface. The algorithm "tries" successive points on the surface until a minimum is reached.

FORTRAN IV
IBM 360-67 TSS

This program was written by Robert C. Seidel and Bruce Lehtinen of **Lewis Research Center.** *For further information, Circle N on the COSMIC Request Card.*
LEW-12556

Machinery

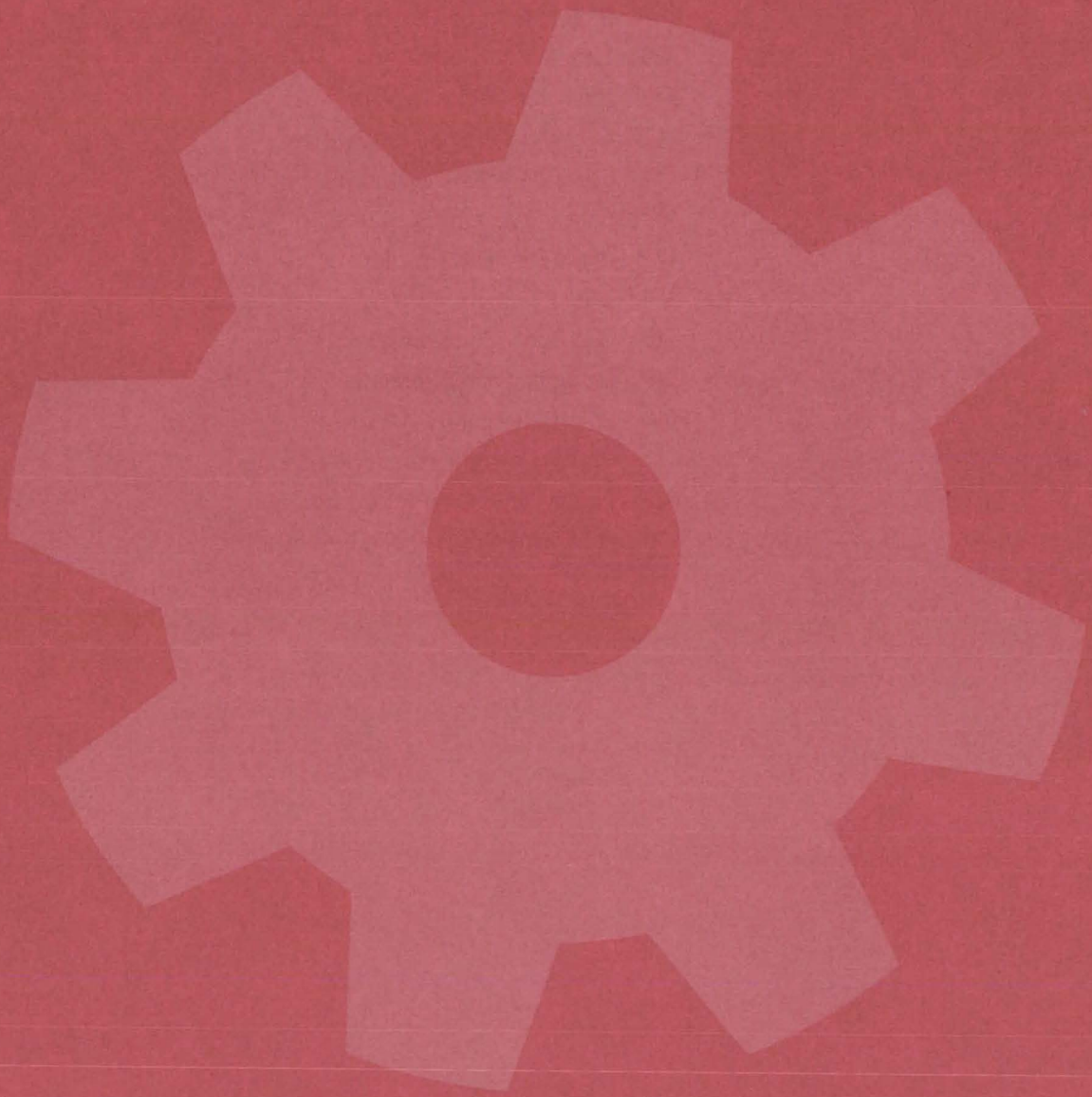

Hardware, Techniques, and Processes

High-Torque Open-End Wrench

The flexibility of an open-end wrench is combined with the high-torque close clearance of box and socket wrenches.

Caltech/JPL, Pasadena, California

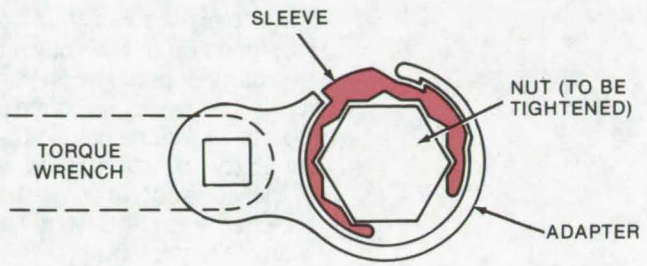

The wrench elements are set in place ready to tighten a nut (clearances are exaggerated for clarity).

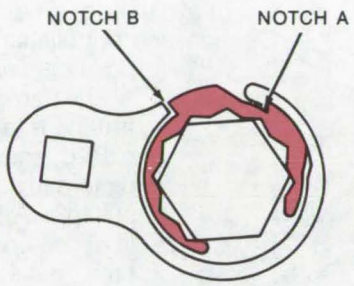

A very slight torque will engage notch A but not notch B.

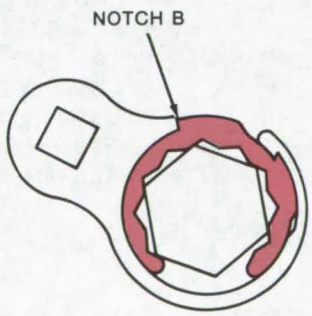

Slight additional torque engages notch B, and high torque can then be transmitted to the nut being tightened.

The **Two-Element Wrench** is shown as it is used to tighten a nut. When engaged in notch A, initial torque can be applied. When engaged in notch B, high torque can be applied.

It is often necessary to tighten closely-spaced gland nuts with sufficient torque to insure connections with no leakage. The usual socket and torque wrench cannot be used, and an open-end wrench thin enough to be used cannot transmit the required amount of torque without being bent out of shape.

A new two-element wrench has been especially designed for tightening closely-spaced nuts on adjacent tubing. It consists of two open-ended pieces, an adapter and a sleeve, that can engage a nut joining two pipes or other configurations not accessible to box and socket wrenches. The sleeve (see figure) is first slipped over the nut to be tightened, and then the adapter is slipped over the sleeve. As the wrench is tightened, notch A in the figure will engage first. As the amount of torque is increased, notch B engages, and a high torque can be applied to the nut.

A single adapter and sleeve are used to tighten and loosen a nut (one flat surface of the adapter is stamped "on," the other "off"). The proper surface faces upward as required for the operation to be performed. The configuration can be designed as an adapter for use with all available ratchet and torque wrench handles. In one embodiment the new wrench transmitted over 750 inch-pounds (85 J) to a steel gland nut on a 3/4-inch (1.9-cm) tube.

This work was done by Harold Behimer, James M. Dame, and Anthony Giandomenico of **Caltech/JPL.** *For further information, Circle 79 on the TSP Request Card.*
NPO-13541

Frame for Daylight Photocopying

Make quick copies of photographs in room light.

John F. Kennedy Space Center, Florida

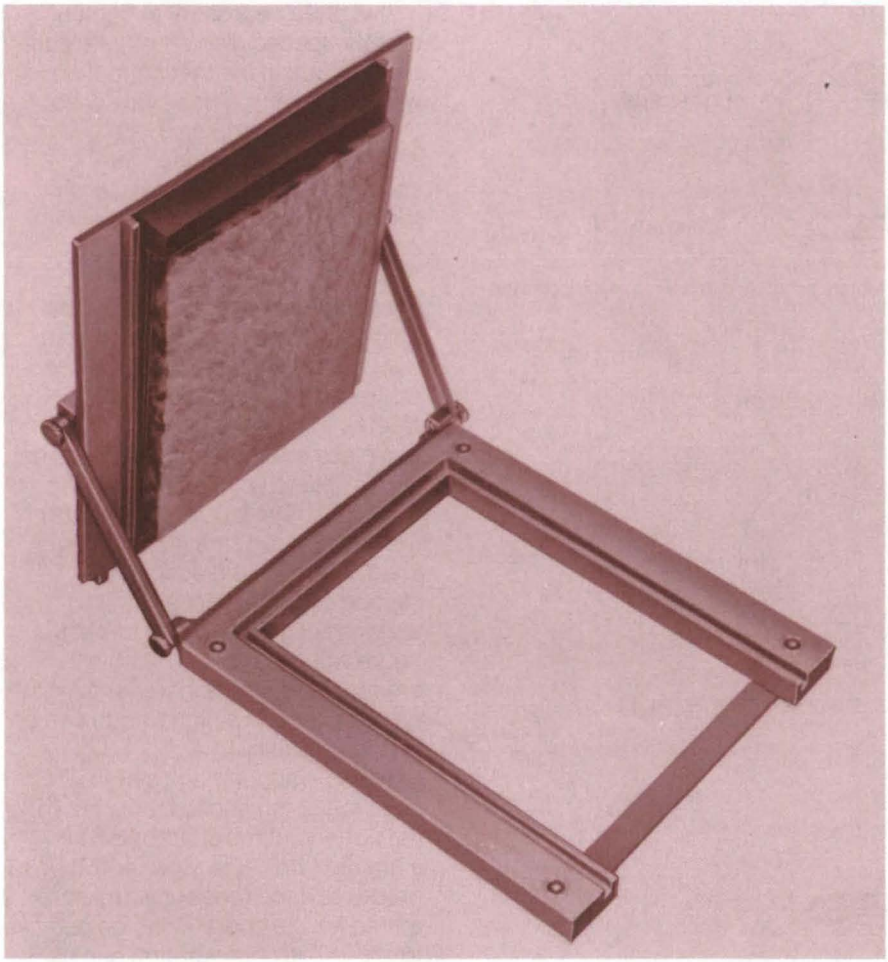

The **Printing Frame** holds 4-by-5-in. instant-developing film for copying photographs or pictures in daylight.

An inexpensive fixture has been designed for making quick copies of a picture or photograph (film positive or film negative) without a darkroom. The frame holds Polaroid 58 or 55 (or equivalent) film, which is exposed to obtain an on-the-spot color or black-and-white reproduction of the photograph.

The photograph to be copied is placed over a light source with a color temperature approximating that of daylight (or a filter may be used). The source should have a controllable intensity and an exposure timer.

The frame, as shown in the illustration, is loaded with the film, is closed, and is placed over the picture to be copied. Then the tab is pulled out of the film, the light source is turned on for the desired exposure time, and the tab is reinserted in the film pack. Finally, the film is developed in a standard Polaroid filmholder.

This work was done by James W. Dalton of **Kennedy Space Center.** *For further information, which includes design drawings of the contact printer, Circle 80 on the TSP Request Card.*
KSC-11026

Slotted Bolts and Studs for Vacuum Systems

Modification reduces
outgassing from installed fixtures.

Lewis Research Center, Cleveland, Ohio

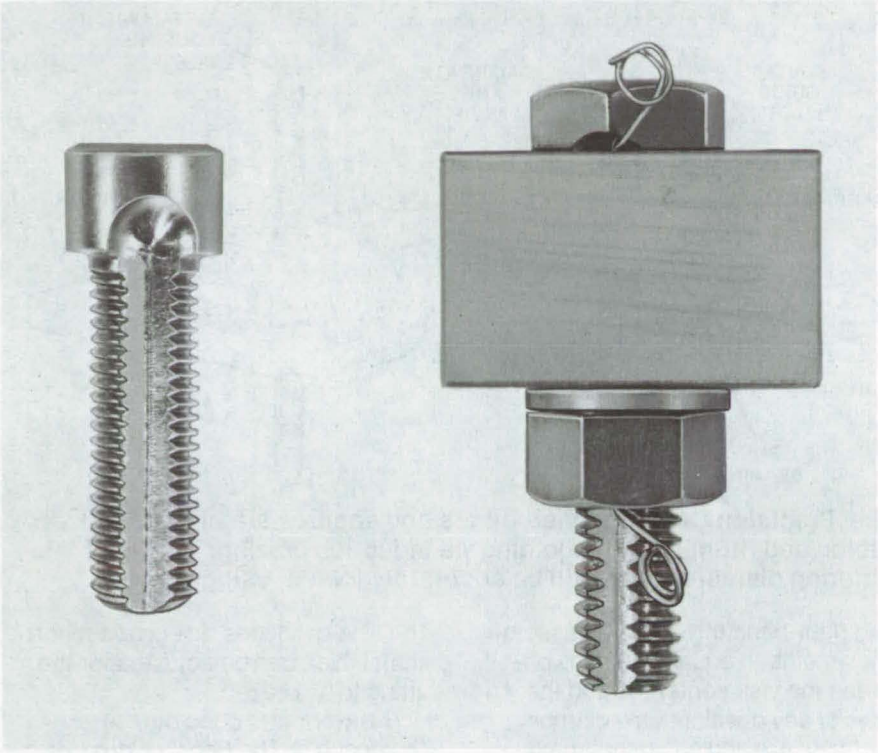

The **Slotted Bolt and Stud** shown can be used in vacuum systems where they allow gas trapped during installation to escape outside the vacuum.

Bolts and studs used inside of vacuum systems and apparatus were found to be a source of comparatively slow outgassing. This outgassing resulted from gas being trapped between the threads of the bolts or studs and the threads of the mating nuts or threaded parts during assembly. Under vacuum conditions, this trapped gas would work its way out into the vacuum chambers.

The problem was solved by slotting or grooving the bolts and studs longitudinally with a "ball end mill." The use of a ball end mill produced a smooth, clean groove similar to tap slots (see photograph). Bolts and studs slotted in this way were easy to assemble, and under vacuum conditions, the gas trapped in the threads is evacuated much more quickly via the slots. These grooved bolts and studs are recommended for attaching brackets, fixtures, components, and parts within vacuum systems.

This work was done by Fred E. Zellner of **Lewis Research Center.** *No further documentation is available.*
LEW-10391

Soft Seat A-N Fitting for Vacuum Use

An inexpensive
leaktight connection

Lewis Research Center, Cleveland, Ohio

Commercially available A and N fittings have been modified to make them suitable for use in vacuum systems. The modification consists of machining a groove in the tapered nose of the fitting and installing a Teflon O-ring in the groove. This modification is shown in the figure.

Initially, O-rings were made of Teflon material and slipped into the groove. Teflon O-rings of the proper size are presently available commercially.

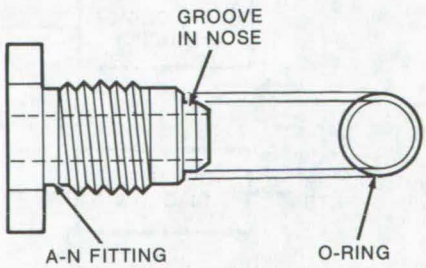

The **Soft Seat A-N Fitting** has a grooved nose for installing an O-ring.

A and N fittings modified in this way have been used in vacuum systems with excellent results. This modification increases the uses of A and N fittings and makes available leaktight vacuum connections at a low cost.

This work was done by Andrew B. Szuhai of **Lewis Research Center.** *No further documentation is available.*
LEW-10130

Precision Centering Vise

Tubing is accurately alined and secured during induction-brazing

John F. Kennedy Space Center, Florida

Stainless-steel tubing and fittings joined by induction brazing must be held securely, and the tubing centerlines must be alined accurately to insure the reliability and quality of brazed joints. However, it is difficult to secure tubing ends with available equipment. One of the most common reasons for quality rejection of brazed joints is traced to haphazard tubing alinement and/or tubing movement during setup and brazing.

A new vise automatically alines tubing ends regardless of differing diameters. It is lightweight and allows setups at virtually any angle. The tubing is held without crushing or deforming the walls, and the tool is particularly handy in remote areas where existing structures, walls, or other permanent fixtures cannot be used to anchor the tubing holder.

As shown, the centering vise consists of two vise assemblies, dual lockable jaws, and two vise carriages. Both jaw assemblies are opened and closed with a threaded adjusting screw that has left-hand and right-hand threads. The assemblies maintain equal distances between the vise centerline and the jaws at any position. Jaw clamping surfaces are angled so that the closing pressure of the jaws will center the tubing laterally and seat it firmly. A series of six screws position the jaws and lock them in place. The vise carriages ride on a support shaft which can be adjusted for the fitting to be brazed.

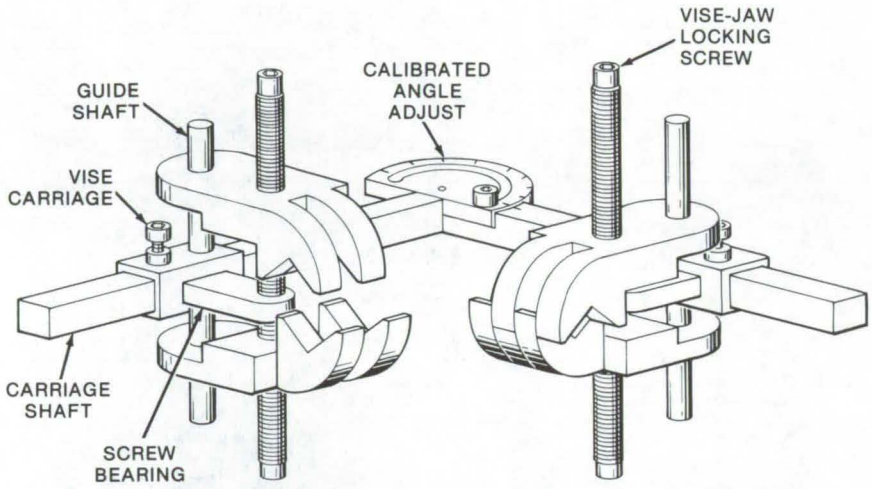

The **Precision Centering Vise** alines and secures stainless-steel tubing and fittings prior to joining via induction brazing. Tubing of differing diameters can still be accurately joined, using the vise.

This work was done by J. A. Thompson of The Bendix Corp. for **Kennedy Space Center.** *No further documentation is available. KSC-11041*

Sustained-Arc Ignition System

Long-duration sparks allow leaner and cleaner combustion.

Lewis Research Center, Cleveland, Ohio

A sustained-arc ignition system is being developed for use with lean fuel-to-air-ratio internal-combustion engines. The use of this system results in arc duration increases of 2 to 4 times and arc power increases of approximately 4 to 10 times the levels occurring in conventional systems. Test results show significant improvement over conventional ignition systems.

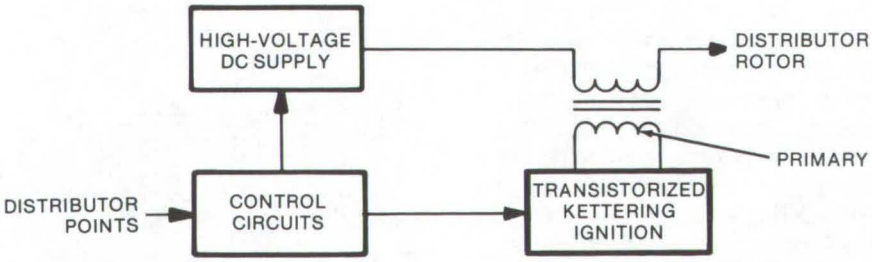

The **Sustained-Arc Ignition** for internal-combustion engines allows extremely-low fuel-to-air ratios. The arc requires 10 to 30 kV for initiation but only 1 to 3 kV to maintain.

One way to reduce emissions of a spark-ignition internal-combustion engine is to operate at extremely low ratios of fuel to air (lean). Lean operation of conventional spark-ignition engines has, however, been limited by available ignition systems. Lean operation will increase engine efficiency and reduce pollutants, but experiments show that it requires a long-duration high-energy spark. Conventional Kettering-ignition and capacitor-discharge systems currently used are limited in pulse duration. Multiple-discharge systems, although an improvement, do not produce the necessary continuous spark. This newly-developed sustained-arc ignition system, however, is not limited by available energy-storage devices and can produce a continuous spark of as long a duration as desired for optimum engine operation.

The sustained arc, once started, is powered by a high-voltage dc source. The arc is initiated by interrupting a current flow in the primary of an ignition coil as in a conventional Kettering ignition. The magnetic energy stored by the ignition coil produces a high voltage in the secondary which starts the arc. At the same time that the primary current is interrupted, the high-voltage dc supply is also turned on. The ignition coil secondary is returned to ground through the dc supply, so the high-voltage dc supply output will appear across the spark plug with the ignition coil secondary in series as an arc-stabilizing impedance. The arc will continue until the high-voltage dc supply is turned off or disconnected from the plug. The high-voltage supply needs only to supply the 1 to 3 kilovolts required to maintain the arc instead of the 10 to 30 kilovolts required to initiate it.

The system can be easily modified to operate on engines not using distributor points by modifying the control circuits to accept the available timing signal. It can also be used with conventional Kettering ignitions. The high-voltage dc supply can be a dc-to-dc converter to allow operation from a low-voltage battery.

This work was done by Arthur G. Birchenough of **Lewis Research Center.** *For further information, Circle 81 on the TSP Request Card.*

Inquiries concerning rights for the commercial use of this invention should be addressed to the Patent Counsel, Lewis Research Center [*see page A8*]. *Refer to LEW-12444.*

Powered Wheel for Aircraft

A single, integral, unit includes the motor, gearbox, and clutch.

Langley Research Center, Hampton, Virginia

A powered aircraft wheel includes a fluid-drive motor of the type patented by The Bendix Corporation under the name Dynavector. The Dynavector has been modified to provide a two-speed capability by supplying high-pressure fluid to alternate chambers only during high-speed low-torque operation. This modification has the same effect as shifting gears since it permits multiple-speed operation for a given fluid-flow rate (NASA Tech Brief B75-10258, "Reducing Flow Requirements of Fluid Actuators").

The unit, when mounted on the wheel axle, is housed completely within a wheel hub and provides not only locomotion but also a supplementary braking capability inherent in the system design. While it could be used on many types of machinery, it has been specifically designed to power the main landing gear of a Boeing 737-100 aircraft. It can also be used to spin the wheels of the aircraft prior to landing. A much smaller unit could be used solely for this purpose.

The wheel drive unit is bolted to the aircraft-brake mounting flange. Some of the bolts that retain the drive unit and brake have been modified to serve as fluid inlet and outlet ports. All other flow passages are machined into the wheel drive housing.

The drive unit receives power from fluid pumps within the aircraft and is controlled from the cockpit. Multiple drive units can be operated independently and in a forward or reverse direction. During ground operations the wheel reduces fuel consumption, minimizes atmospheric and noise pollution, and conserves airport space. The advantages of this drive unit are:

- It fits within the aerodynamic contours of the aircraft.
- It operates with an onboard power source (auxiliary power unit).
- It engages and disengages when either stopped or moving.
- It adds very little inertia to the wheel when disengaged.
- It does not interfere with the normal functioning of the landing gear.
- It reduces the use of regular brakes in congested areas.

This work was done by Moses J. Long and Stephen C. Irick of **Langley Research Center** *and R. K. Van Ausdal of The Bendix Corp. For further information, Circle 82 on the TSP Request Card.*

Inquiries concerning rights for the commercial use of this invention should be addressed to the Patent Counsel, Langley Research Center [*see page A8*]. *Refer to LAR-12053.*

Safety Brake for Tape Reels

An all-mechanical brake senses the end of a tape and stops the reel, even in the event of electronic-system failure.

Goddard Space Flight Center, Greenbelt, Maryland

A friction brake has been designed for stacked coaxial magnetic-tape reels. It functions by stopping both reels when either reel is fully wound. Because it is all mechanical, the brake will work even if the electronics fail. Thus it may be used as a primary brake or as a backup to an electronic brake.

In a stacked-reel tape recorder, for which this brake is designed, two parallel reels are placed one above the other with a common center axis. Tape is played out from one, through a series of guides and rollers, and up or down to the other reel on which it is wound. The general principle of the mechanical friction brake can be seen in Figure 1, which is a side view of two stacked reels.

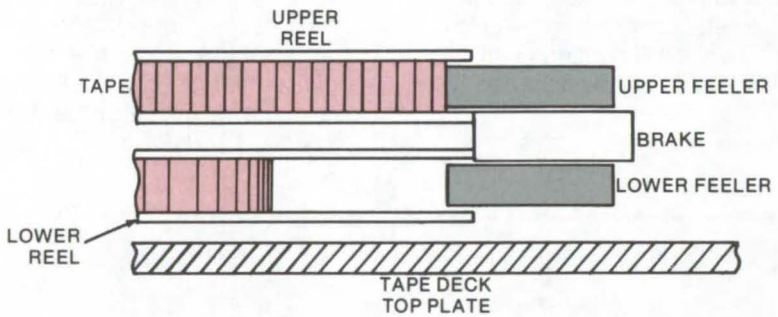

Figure 1. The **Mechanical Braking Concept** utilizes a pair of feelers. When either reel is sufficiently wound to contact a feeler, a braking surface will be forced against the hubs of both reels simultaneously.

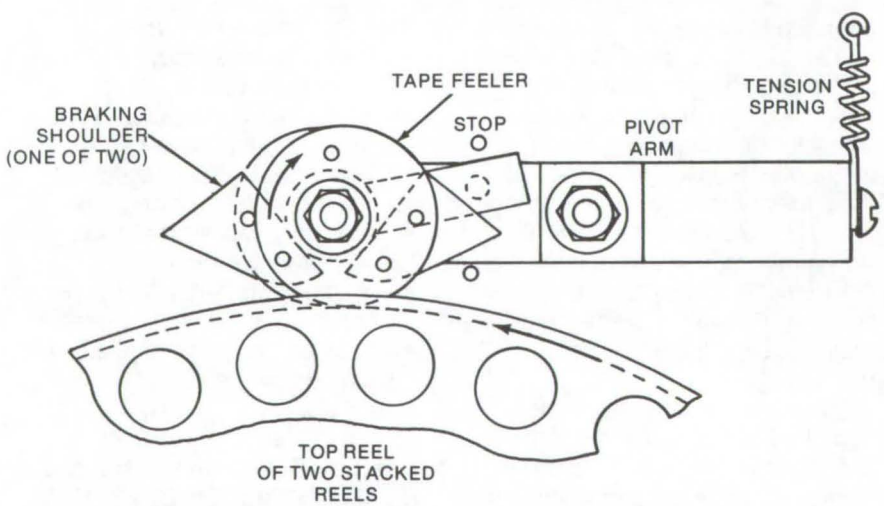

Figure 2. The **Friction Brake** is shown attached to the top deck of a tape recorder. Referring to the text and the figure above, assume that the top reel of the recorder is moving counterclockwise. The fully wound tape will contact the eccentrically mounted feeler and cause it to move clockwise. This motion forces one neoprene braking shoulder against the reel hub. The operation is similar when the bottom reel becomes full while rotating in the opposite direction.

The brake includes two feelers; when either one comes into contact with the tape on a fully wound reel, a brake shoulder is forced against the hub of the reels to stop rotation. The way in which this is implemented can be seen more clearly in Figure 2.

The three main components are the feeler, the braking shoulders, and the pivot arm. The pivot arm is attached to the top plate of the recorder by an assembly mount pin, about which the pivot arm is free to rotate. At one end of the pivot arm a tension spring pulls on the arm and causes its other end to move in between the reel hubs a preset distance.

As the tape fills up, the feeler contacts the tape. Two things happen at this point: (1) The force of the tension spring is overcome, and the sensor is pushed away from the reel axis; and (2) the feeler is rotated by the tape, forcing the braking shoulder into contact with the hub of the reel.

The assembly includes a stop to prevent the brake from overriding the tape. There is also (not shown in the drawing) a recentering mechanism used to return the brake to a neutral position after the torque is removed from the reels.

This work was done by Clinton E. Carle of **Goddard Space Flight Center.** *For further information, Circle on the TSP Request Card.*

This invention is owned by NASA, and a patent application has been filed. Inquiries concerning nonexclusive or exclusive license for its commercial development should be addressed to the Patent Counsel, Goddard Space Flight Center [see page A8]. Refer to GSC-11960.

Improved Load Handler

An easily made device lowers people or equipment at a constant speed.

Marshall Space Flight Center, Alabama

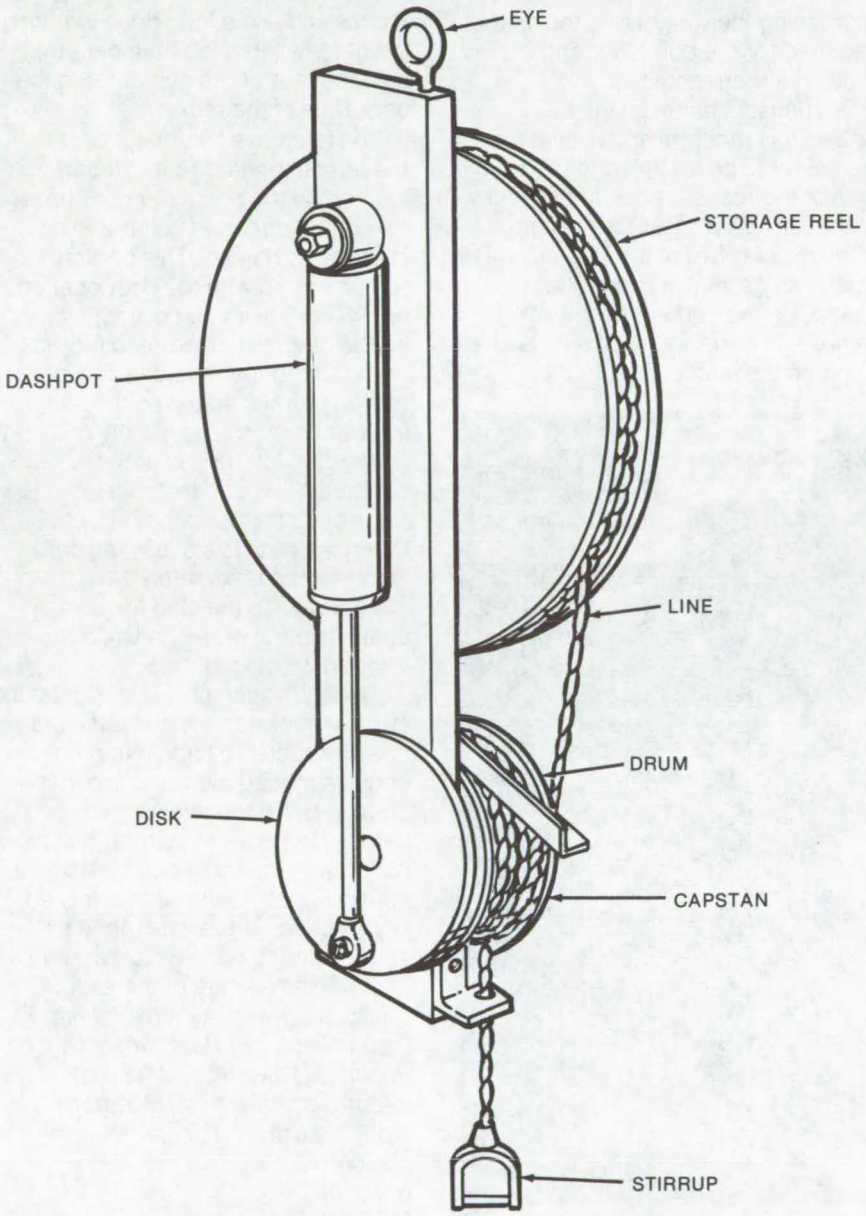

The Load Handler has a double-acting dashpot connected with the capstan for controlling the angular velocity of the capstan.

A new load-handling device is quite simple to manufacture and use. It is a rope-and-pulley arrangement that unwinds at a rate fairly independent of the weight attached to it. As such, it is particularly suitable as an emergency escape device or in other applications requiring built-in control of the rate of descent.

The load handler, as shown in the figure, consists of a rope-storage reel and a capstan. To control the velocity at which the stirrup on the end of the rope is lowered, a double-acting dashpot is connected to the drum and the capstan.

Since the number of turns of line around the drum is constant, the diameter of the drum is constant, and the moment arm imparting rotation to the disk remains constant. Therefore by adjusting the dashpot (for force dissipation) the velocity can be controlled. Greater velocity control is possible with the use of several dashpots. The load handler is easy to install and employ and fabrication is economical.

This work was done by Peter H. Broussard, Jr., John L. Burch, and Calvin Mueller of **Marshall Space Flight Center.** *For further information, Circle 84 on the TSP Request Card.*

Inquiries concerning rights for the commercial use of this invention should be addressed to the Patent Counsel, Marshall Space Flight Center [see page A8]. Refer to MFS-23233.

Door Latch With Through-Access Hole

A quick acting latch has an access hole that allows adjustments to be made through the latch.

Lyndon B. Johnson Space Center, Houston, Texas

During the design of a storage container that was to be loaded, latched, and later installed in a recess, a problem arose with the installation procedure. Because the container would be fully loaded when installed, it would not be possible to bolt the back of the container to the back of the recess. One solution, placing the mounting fasteners on ears and attaching the container to the wall surrounding the recess, had the disadvantages of increasing the weight and the space required for the container and making it more complex.

An unusual latch design has solved this problem and allows the container to be fastened to the rear wall of the recess, although it is fully loaded. This latch has a through-access hole; two of the latches are installed, as shown in the photograph, on the corners of the container. This arrangement allows one to place the latched box in the recess and use a long drive wrench to tighten allen head fasteners that hold the rear of the container to the back face of the recess.

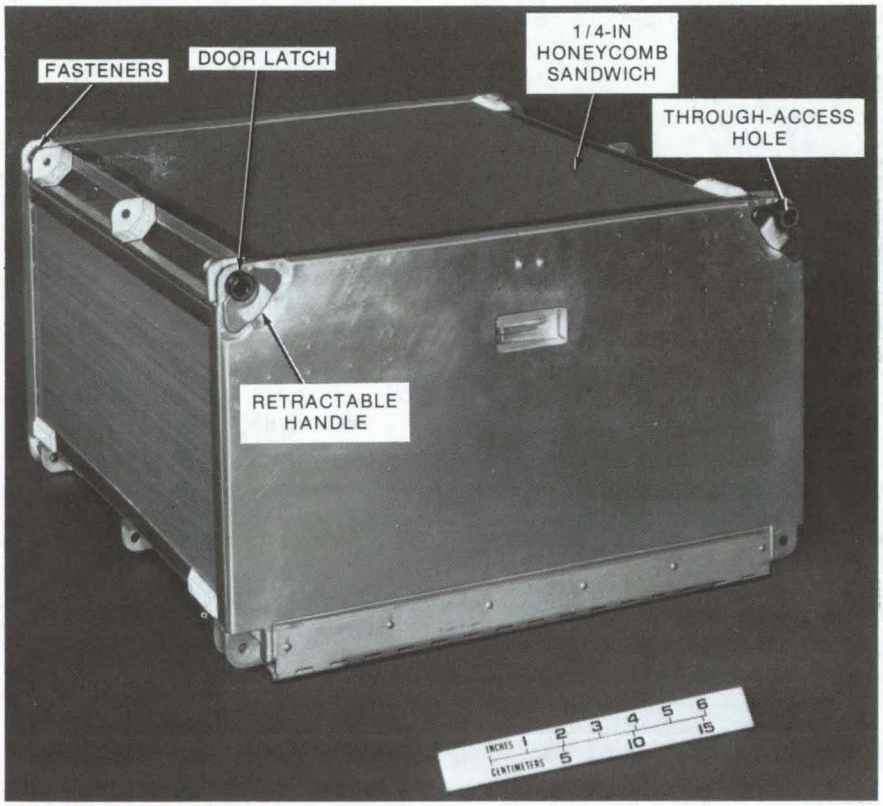

Door Latch With Through-Access Hole permits insertion of a drive wrench through the door of the container, permitting the mounting fasteners to be located within the container envelope.

The latch has two major parts; the female portion (captive nut) located on the container door has a quad-lead threaded collar and a retractable handle. This portion remains flush with the door opened or closed. The male portion, a hollow stud with quad-lead threads and a spring-loaded adjusting nut (which permits adjusting the stud to an exact dimension, greatly relaxing production tolerances in the container, lid, and fastener) is secured to the container structure. When the door is closed, the collar is rotated approximately 1-1/2 turns, drawing the stud forward against spring pressure while the door draws closed.

The latch assembly is designed to carry shear and tension loads and has a retractable handle that engages a mating tab recessed in the door. When engaged, the handle is trapped to restrict any rotation of the collar or stud, and it can be visually verified whether the door is locked or unlocked. There is no need for self-locking threads which would limit the service life of the lock.

This work was done by William F. Dixon, Robert P. Pritchard, and Robert E. Woodfill of Rockwell International Corp. for **Johnson Space Center.** *For further information, Circle 85 on the TSP Request Card.*
MSC-19634

Gas Boost Compressor

A free-piston compressor, driven by a relatively low-pressure gas, can boost compression four times the initial pressure.

Lyndon B. Johnson Space Center, Houston, Texas

A new type of boost compressor requires fewer controls and valves than conventional devices and is driven entirely by the "low-pressure" gas supply. It was originally designed to transfer oxygen from a supply at 6.2×10^6 N/m² (900 psia) to smaller tanks pressurized at 27.6×10^6 N/m² (4,000 psia). It could be used with other pressure ratios, such as filling scuba tanks, where speed is not a prime consideration.

In essence, the compressor uses the adiabatic expansion of a gas against a large surface area to drive a smaller surface area, resulting in an increase in pressure. The essential components of the device are shown in the illustration.

Gas supplied at a relatively slow rate enters the compressor from the low-pressure supply and is routed to two places: (1) to a capacitive chamber where a sufficient head is built up to drive the motor piston and (2) to a compression chamber where it will later be compressed for storage in a high-pressure tank.

When sufficient energy is stored in the capacitive chamber, an automatic cycling valve opens and allows the gas to enter the driving chamber where it expands adiabatically and moves the motor piston. The force on the motor piston, equal to that on the smaller compression piston, results in a higher pressure in the compression chamber. The high-pressure gas is driven through a one-way (check) valve into the high-pressure tank. At the end of the stroke, the lower pressure in the driving chamber causes the automatic cycle valve to close, and the spring-operated motor valve opens to exhaust the driving chamber and return the pistons.

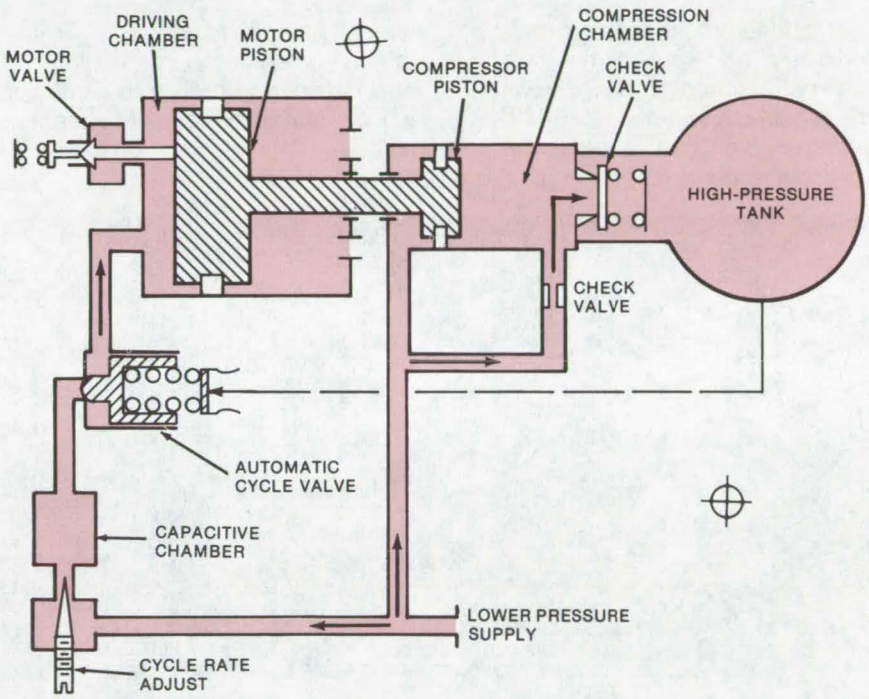

The **Boost Compressor** is driven by the same "low-pressure" gas supply that it transfers to a higher-pressure tank. The amount of boost depends on the ratio of the areas of the motor and compressor pistons. The rate of compression depends partly on the rate of gas supply from the supply source and is controlled by the automatic cycle valve as described in the text. The pressure required to open this spring-operated valve is less than that required to keep it open, allowing sufficient gas to flow from the capacitive chamber to operate the motor piston.

The efficiency of the illustrated compressor can be improved by using the gas force that returns the motor to set the capacitive release pressure. In this way, the release pressure becomes a function of the pressure in the compression tank.

This work was done by Les S. Terp of The Garrett Corp. for **Johnson Space Center.** *For further information, Circle 86 on the TSP Request Card.*

This invention is owned by NASA, and a patent application has been filed. Inquiries concerning license for its commercial development should be addressed to the Patent Counsel, Johnson Space Center [see page A8]. Refer to MSC-14757.

Dynamic Load Attenuator

A small dynamic attenuator does not produce loose particles.

Lyndon B. Johnson Space Center, Houston, Texas

An attenuator for dynamic loads consists of a special bolt head that cuts material from a splined washer. The required shear and tensile forces absorb kinetic energy. The cut-away material is retained by the shearing action, making this attenuator of special interest for applications where the production of loose metal particles is not acceptable.

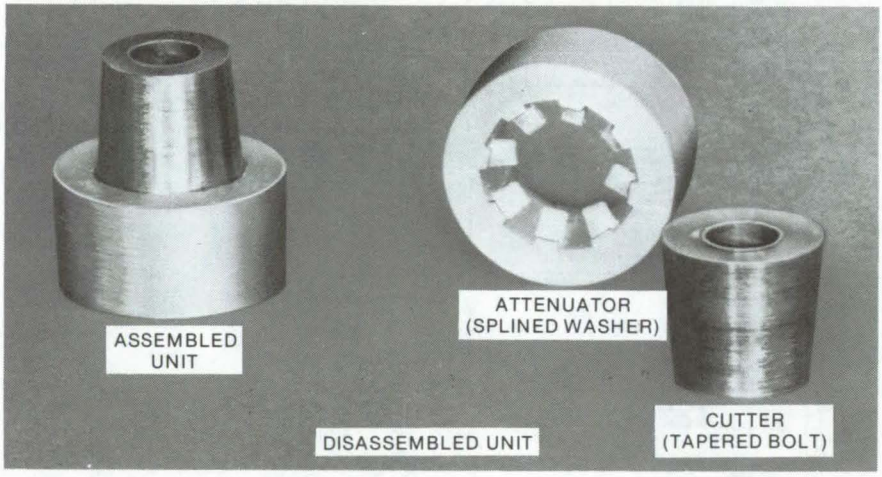

The **Dynamic Load Attenuator** consists of a tapered-bolt cutter that fits inside a splined washer. The work required to cut material from the washer attenuates loads applied to the bolt. The arrangement of the assembled unit prevents the dispersal of loose metal particles around the attenuator.

The special bolt and washer are mated to serve as a cutter and an attenuator block. The assembled unit is capable of absorbing 400±44.5 N (900±100 lb) in a 0.76-cm (0.3-in.) stroke, and it is smaller in height and diameter than most devices with equal attenuation capabilities.

The cutter and attenuator are illustrated in the photograph. The cutter is a tapered bolt made from an Inconel 718 steel bar. The bolt head is undercut with a radius blending into the shank to provide a cutting edge; it also has an internal bar relief for wrenching.

The attenuator block is a splined washer made from 6061-0 aluminum bar QQ-A-225/8, with a step for the bolt cutting edge. The splines adjust the load-carrying capacity. The spaces between the splines accommodate material sheared from the splines, when the unit is subjected to loading.

This work was done by Phillip N. Crum of Rockwell International Corp. for **Johnson Space Center.** *For further information, Circle 87 on the TSP Request Card.*
MSC-17472

Spin-Rate Control Device

An inexpensive technique eliminates the need for a driver, sensor, and interface logic.

Ames Research Center, Moffett Field, California

A vehicle in free fall within an atmosphere may be spun intentionally about an axis for a variety of reasons, for example, to increase the probability of impact at a given point or to cause onboard sensors to scan an area about the path of descent. In the latter instance, it is often desirable to have the spin rate remain within a narrow range of values by using an array of aerodynamic surfaces inclined to the direction of movement of the vehicle. If the surfaces are fixed, the spin rate varies as the velocity of the vehicle (which is an inverse function of the density of the atmosphere). However, when the density range of a planetary atmosphere is so great that fixed fins produce a spin-rate variation that is unacceptably high, it becomes necessary to provide some sort of spin-rate control.

Typically, spin-rate control can be obtained by the use of devices that change the angle of incidence of the spin-inducing aerodynamic surfaces so as to compensate for spin-velocity variations. Ordinarily, spin control is obtained by moving the

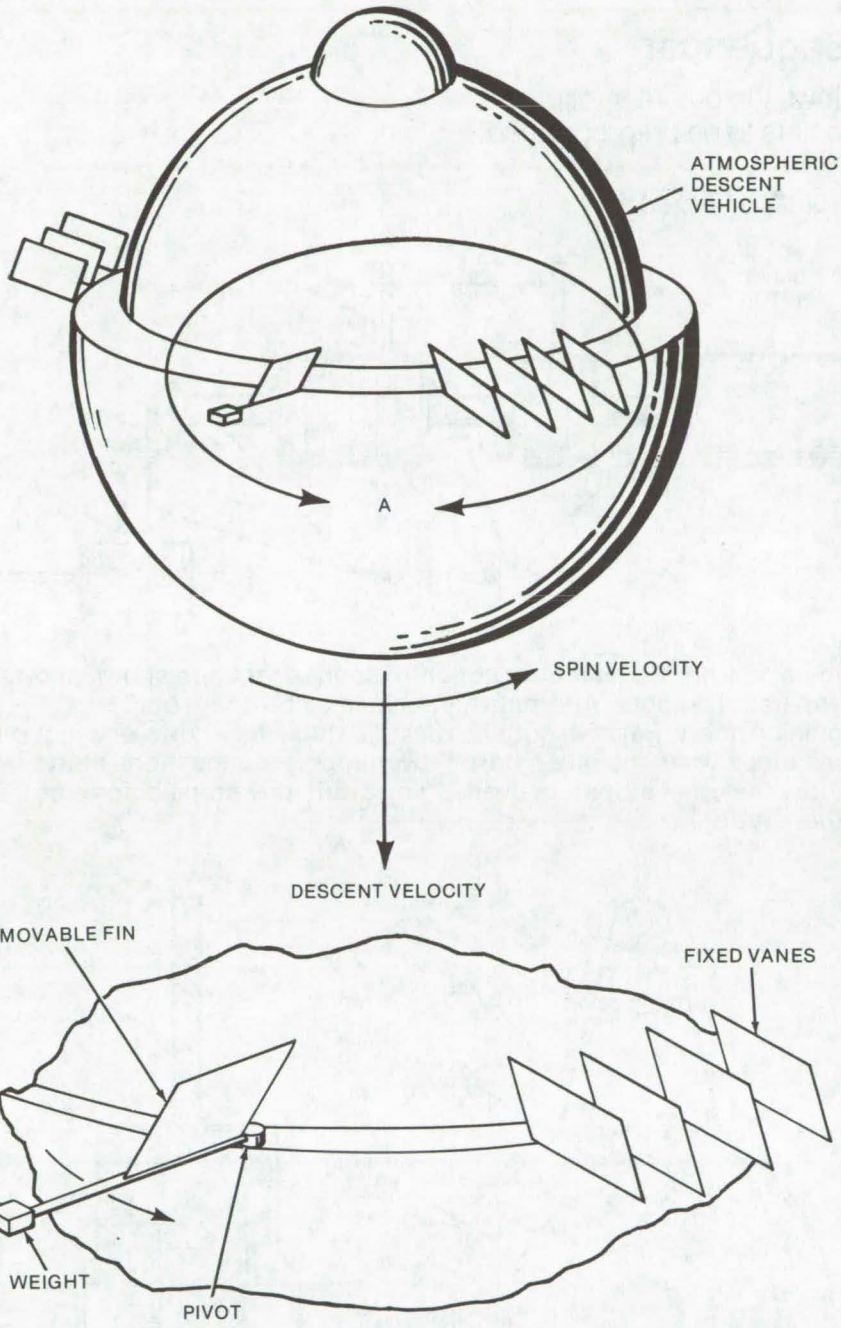

The **Passive Spin-Rate Control Device** consists of two elements. Fixed vanes provide the basic spin force that varies as the velocity of the body and inversely as the density of the atmosphere. To compensate for a high spin rate, movable surfaces with a variable positioning angle are employed.

aerodynamic structures electrically or mechanically over a preprogramed range of positions, but it is preferable that they be moved by a system controlled by an onboard rate sensor.

A relatively-inexpensive spin-rate control device has been designed to eliminate the need for driver, sensor, and interconnecting logic circuits. The new device combines the simplicity of the fixed-fin concept (which can provide large spin-rate excursions) with the precise rate control provided by an active flight-control system. The device comprises two sets of aerodynamic surfaces (see figure): (1) fixed vanes which provide the basic spin force and are set at an angle that can provide spin rates much higher than desired and (2) extendible fins angled so that they can selectively oppose the spin caused by the fixed vanes.

The extendible fins are pivoted at their inner edges and have small masses attached to their outer edges so that they are kept extended into the airstream by centrifugal forces. As altitude decreases, the spin force provided by the fixed vanes decreases, but the spin rate is kept nearly constant by a compensatory change of the angle of the movable fins. With the new device, the change in rate of spin is quite small, for example, about 20 percent for a factor of 20 change in airstream density. In contrast, a fixed-fin system allows the spin rate to vary by as much as a factor of 4.5 over the same density range.

This work was done by Leo J. Nolte of Hughes Aircraft Co. for **Ames Research Center.** *For further information, Circle 88 on the TSP Request Card.*
ARC-10884

Heavy-Duty Mechanical Sequencer

A modular sequential mechanism allows the output stroke angle and the location of start/stop points to be preprogramed.

Lyndon B. Johnson Space Center, Houston, Texas

A sequential mechanism (see Figure 1) capable of being connected to similar mechanisms in a stacked or modular configuration has a single continuous input from a rotary shaft. The sequenced rotary output, depending on the number of stacked mechanisms, can be end-to-end, overlapping, dwell, or simple linear motion. Operation of the sequencer is similar to that of a Geneva mechanism, but its output can be preprogramed for variable output stroke angle and the location of start/stop points. Output torques are higher than typical Geneva mechanisms, are constant throughout the cycle, and have a moment equal to that of the power source.

The sequencer uses a free roller set that moves radially for latching and moves circumferentially for driving. Two (or more) sequencers may be connected to the same input power shaft as shown in Figure 2. The output crank and drive fittings are integrated to balance system loads. The centrally located crank with twin drive fittings on both sides reduces free play between the input and output crank.

In the left (front) view of Figure 2 the drive fitting is at the transition point; i.e., clockwise motion will move the crank; counterclockwise motion locks the roller set to the housing by bringing the circular portion of the drive fitting under the roller set and keeping it from descending out of a locking notch that forms one end of the track in the housing. The roller set is shown in this locked position. Assuming counterclockwise motion, the crank has just stopped at the instant shown, and the rollers have just reached the fully locked position with the circular portion of the drive fitting just beginning to move under the rollers.

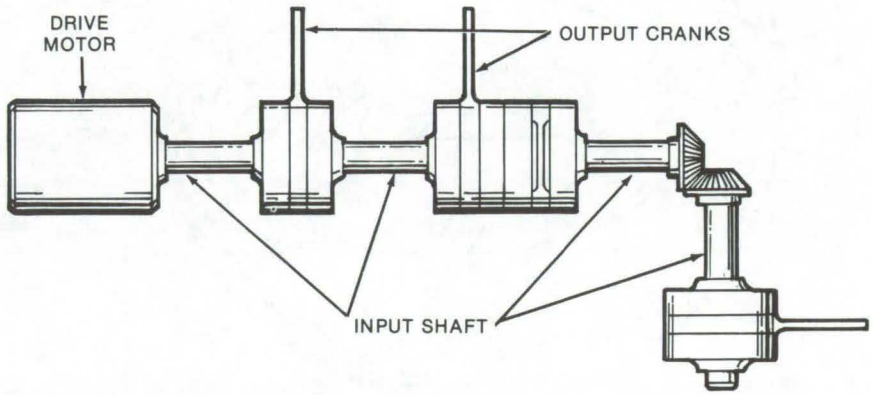

Figure 1. The **Modular Connection** of sequencer units shown allows nonparallel outputs. Alternatively, units may be connected by a common shaft. Relative outputs are adjustable for end-to-end motions (one stops when the other starts), overlapping motions (one starts before the other stops), or overlapping dwell (one stops before the other starts).

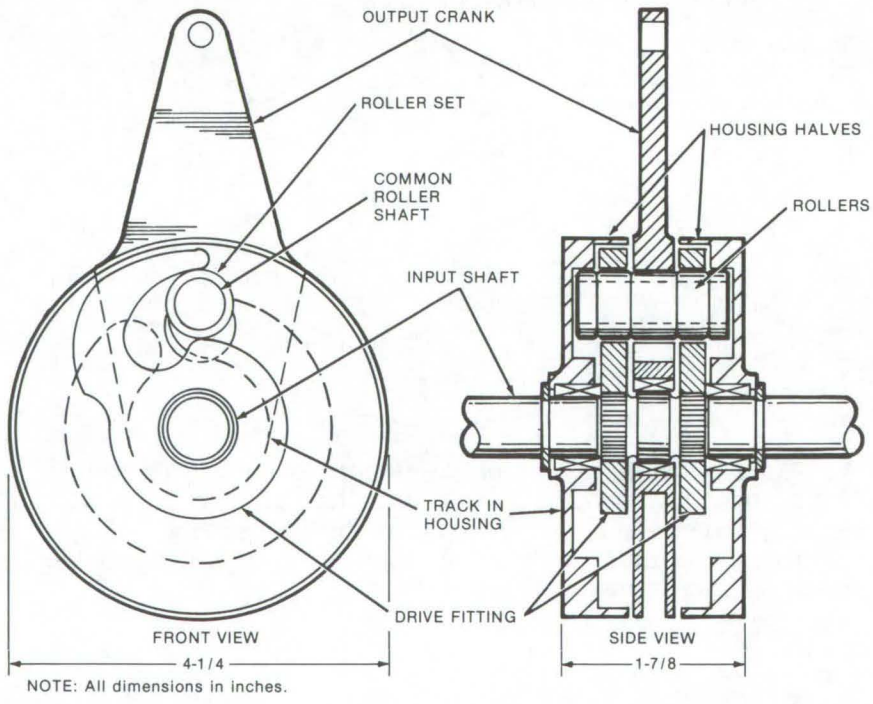

Figure 2. The **Mechanical Sequencer** has an input shaft splined to two drive fittings. In the left (front) view the drive fitting is shown touching a set of rollers that pass through the output crank. The roller set, consisting of five rollers on a common shaft, engages the two housing halves and the crank. The two outer rollers engage a track in the housing halves. The two adjacent rollers engage the drive fittings when the crank is in motion. The center roller engages the crank.

Assuming clockwise motion of the drive fittings, the rollers immediately begin to descend out of the housing-track locking notch and into the cam-shaped notch in the drive fittings. As they bottom (reach the lower end) in the drive-fitting notch, they enter the circular portion of the housing track. The output crank begins to move with the first clockwise motion of the drive fitting from the position shown as the center roller bears against a slot in the crank, requiring it to move with the roller. The slot length, which is radially oriented, permits the required radial displacement of the roller set as it moves in and out of the housing-track locking notch. Cam action, which occurs only in the transition region, starts and terminates crank motion by accelerating from (or decelerating to) zero sinusoidally, thereby preventing shock loads on the mechanism.

This work was done by Walter T. Appleberry of Rockwell International Corp. for **Johnson Space Center.** *For further information, Circle 89 on the TSP Request Card.*

This invention is owned by NASA, and a patent application has been filed. Inquiries concerning nonexclusive or exclusive license for its commercial development should be addressed to the Patent Counsel, Johnson Space Center [see page A8]. *Refer to MSC-19536.*

Energy-Absorbing Attenuator

A simple one-shot load absorber is inexpensive and easy to install.

Lyndon B. Johnson Space Center, Houston, Texas

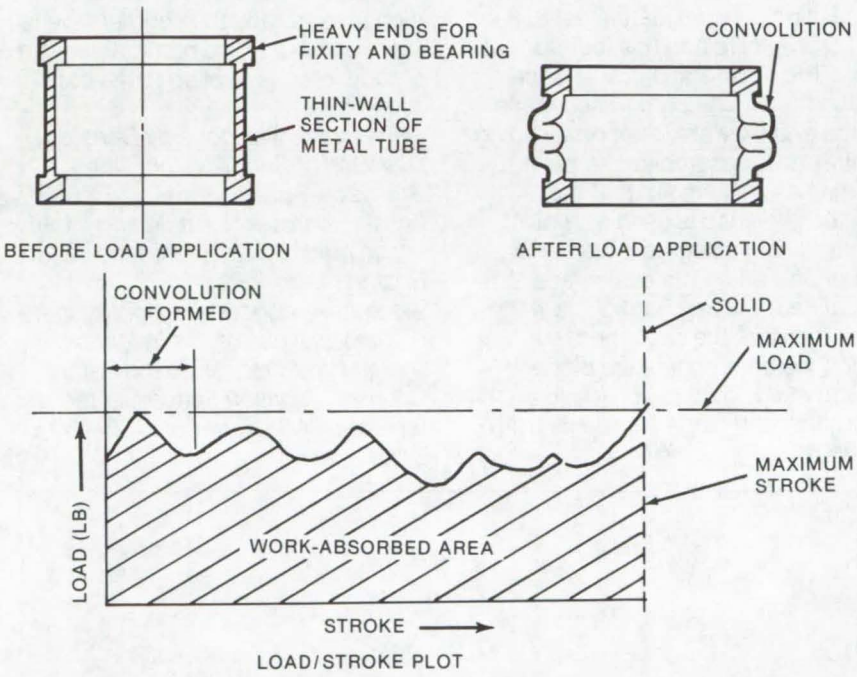

The **Energy-Absorbing Attenuator** is a simple one-shot device that absorbs energy through deformation of a metal tube. As can be seen from the Load/Stroke Plot, energy is absorbed somewhat regularly throughout the compression of the tube.

A one-shot high-energy absorption device (see illustration) uses a thin-walled soft-metal tube to absorb kinetic energy by controlled buckling. When an applied load exceeds the yield capability of the material, the tube compresses uniformly, forming convolutions and absorbing energy. The energy-absorption characteristics are similar to those of crushable honeycomb, but devices of this class can be made smaller and lighter in weight.

This work was done by Peter Galovich and Joseph C. Wilkowski of Rockwell International Corp. for **Johnson Space Center.** *No further documentation is available. MSC-17473*

Jet Engine Stator-Blade Removal Tool

Stator blades are removed from the J-85 engine without damage to blade segments or compressor case.

Lyndon B. Johnson Space Center, Houston, Texas

Considerable difficulty is experienced when attempting to remove stator blades from jet engines having 400 hours or more operating time. When the engines are used in humid atmospheres with a high salt content, corrosion tends to lock the blades to the slots within the compressor. Stator segments located toward the final-compression stages in the engine are further subjected to extreme heat. Previous methods used to remove the stators from the slots began with soaking and ultrasonic vibration to loosen the blades before the use of a driving tool. However, even after the soaking and ultrasonic preparation, the removal tool lacked sufficient mechanical advantage to grasp the blade.

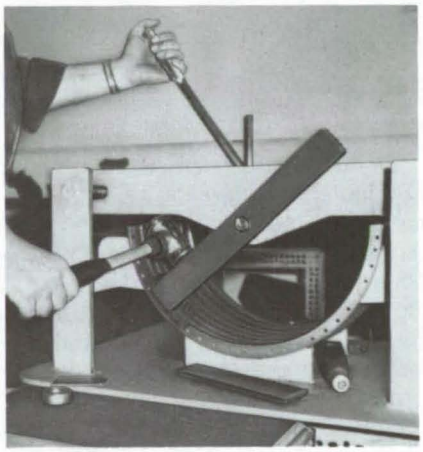

The **Stator Removal Tool,** designed for the J-85 engine, is shown in use. The operator is applying force to a breakover bar to dislodge the stator blade.

A new tool removes individual stator-blade segments from the J-85 jet engine without deforming the blades or the engine casing. The tool base is made from plate steel 3/8 in. (0.95 cm) thick and has four upright legs. The legs form a cradle upon which the engine compressor case rests, and they also support a sliding main-frame assembly. The main frame has a rotary shaft at the center; the shaft is used as a pivot for attaching a segment die and a drive tool. When the casing and tool are alined, the segment die is inserted so that the die fingers surround the base root of the blade to be removed. Torque applied to the tool slides the blade segments from their slots. There is no damage to either the casing or the blades.

In use the jet engine compressor case is set into position in the tool. The proper segment die is selected and attached to the blades. The movable main frame is slid into position so that the segment die is engaged with the first segment to be removed. The segment die is swung around on its axis to assure blade alinement. A breakover bar is used to extricate the segment. In instances where extreme torque must be applied, a breakover bar extension is used, and the segment die is tapped with a brass hammer while a steady force is applied to the bar (see figure).

This work was done by Donald D. Diamond of Serv-Air, Inc., for **Johnson Space Center.** *For further information, including a tool usage guide, Circle 90 on the TSP Request Card.*

Inquiries concerning rights for the commercial use of this invention should be addressed to the Patent Counsel, Johnson Space Center [*see page A8*]. *Refer to MSC-16000.*

Fabrication Technology

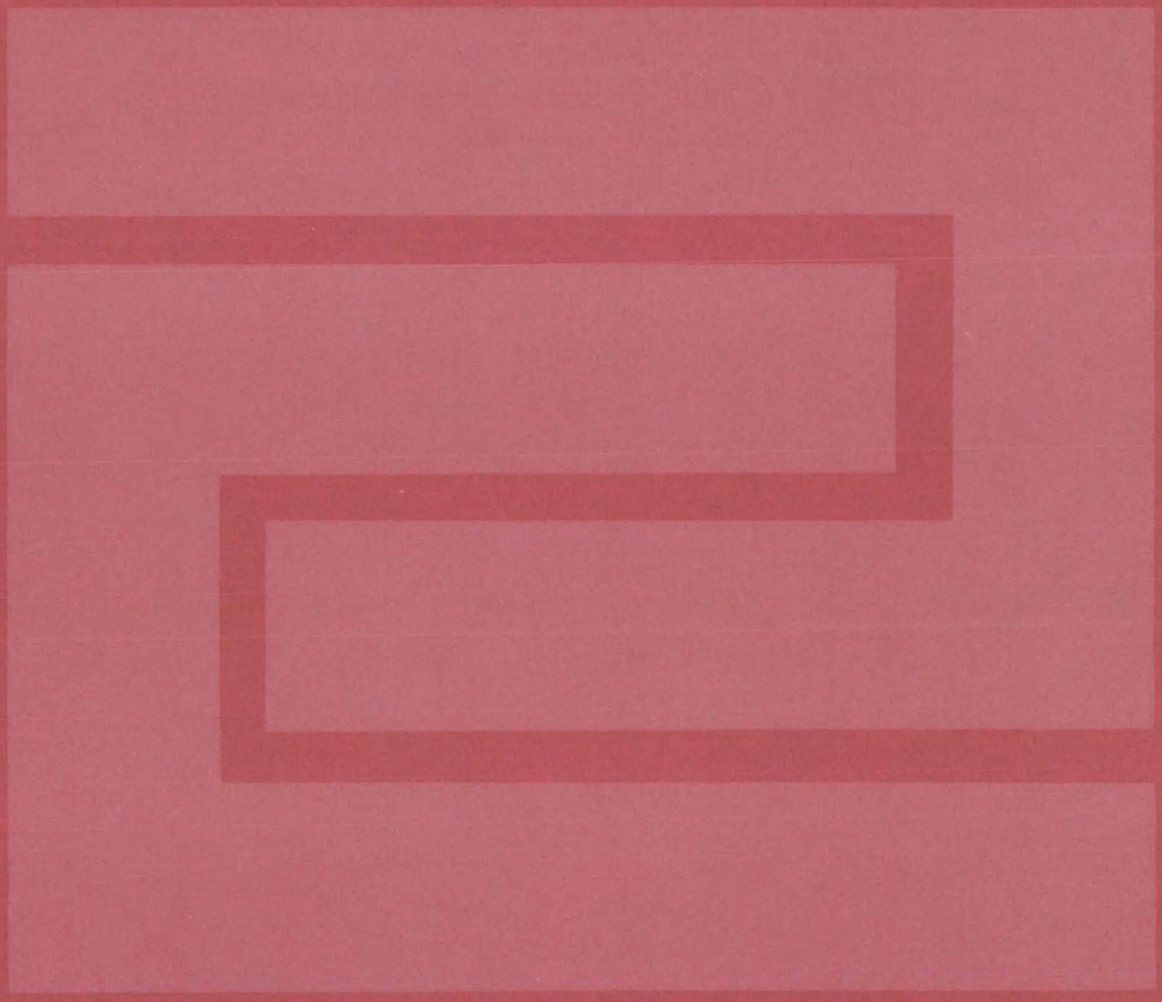

Hardware, Techniques, and Processes

Modular Multipurpose Panel Support

A modular support for large contour panels is inexpensive, adjustable and easily moved.

Lyndon B. Johnson Space Center, Houston, Texas

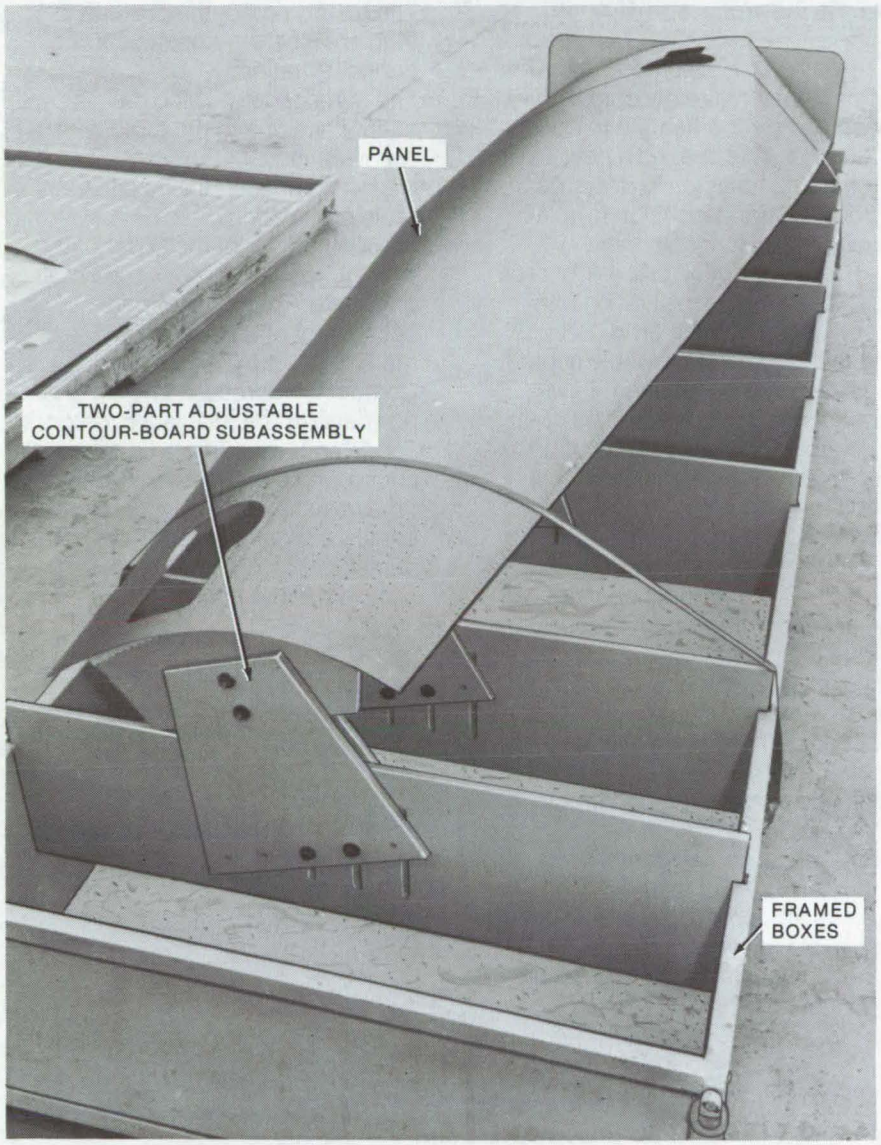

The **Plywood Modular Support** consisting of framed boxes is designed to support a variety of adjustable interchangeable contour-board subassemblies.

Many industries fabricate large formed panels that require fitted contour support during trimming, countersinking, polishing, cleaning, painting, riveting, temperature shaping, and storage. A set of modular semirigid box structures can serve as a multipurpose support for many different types of thin panels. The fixture (see figure) has been designed to hold several different, but interchangeable, two-part adjustable contour-board subassemblies. The boards can be rotated and moved vertically and laterally before being clamped into place. The angle-framed plywood boxes are automatically adjusted for minor floor-level variations when the cross supports are adjusted to minimize twisting and bending in the supported panels.

By combining modules, any number of fixtures can be bolted together to accommodate any length of skin or panel. Skins and panels of various shapes, sizes, and contours can be supported by using different sets of contour boards. The actual contours are determined with a new three-point coordinate system, used with an automatic tape-controlled drafting machine. In addition, contour-board sets are designed to accommodate right-handed or left-handed parts by merely turning the contour boards 180° while otherwise maintaining the same relative position of the boards. A rocker arm attached to the contour boards accommodates the ribbon effect of the skins, and standardization of the boards allows them to be interchanged with the basic module.

This work was done by Marvin R. Daun and Larry A. Maring of Rockwell International Corp. for **Johnson Space Center.** *For further information, Circle 91 on the TSP Request Card.*
MSC-19641

Containerless Processing of Tungsten

Simultaneous electromagnetic levitation and electron-beam heating allow contaminationless melting of tungsten.

Marshall Space Flight Center, Alabama

To improve service properties of tungsten (for uses such as X-ray targets) at room temperatures and at elevated temperatures, interest in a high-purity single-crystal tungsten or in a fine-grained high-purity tungsten had led to a technique of containerless processing (for the control of solidification morphology). Present techniques in single-crystal growth of tungsten are unable to meet these objectives economically.

A facility has been designed to permit the levitation melting of tungsten through electromagnetic levitation (this has not been done before because of the high melting temperature of tungsten, 3,410° C) with electron-beam heating. Electromagnetic levitation was used to levitate 10-gram specimens of tungsten and heat them to 2,600° C. Electron-beam heating was then employed to melt and superheat the levitated specimens above the melting temperature of tungsten. Through the use of the electron beam, the levitation force and the temperature of the levitated tungsten were independently controlled. The solidification of molten tungsten while levitated produced single crystals and bicrystals. Among the applications for this new technique of growing tungsten crystals is the production of X-ray targets.

It was also possible to vapor deposit tungsten directly onto molybdenum by superheating to about 3,600° C. This opened a new way of fabricating tungsten X-ray targets through vapor deposition from a superheated tungsten melt.

The construction of a 4-foot drop tube enabled the evaluation of a freely-falling molten drop. Results indicated that considerable supercooling could be attained. Fine-grained material obtained by grain refinement through solidification of supercooled melts resulted in another method for X-ray target production.

Of the three ways to produce tungsten X-ray targets economically, the vapor deposition process offers the most promise, with single-crystal tungsten being the second most promising. Some advantages of containerless processing of metals especially for the high-melting-temperature and reactive metals are:

- Sources of contamination from the crucible are eliminated.
- Large amounts of supercooling are possible in very pure metals due to the elimination of sites for heterogeneous nucleation.
- The melt is homogeneous due to efficient electromagnetic stirring during levitation.
- The homogeneity of the melt is maintained due to the rapidity of solidification.
- High-vacuum conditions allow rapid purification.
- A large number of melts per day with a large number of varied melt parameters can be attained because of rapid heating and melting.
- Compacts of pressed and sintered powders are rapidly consolidated.
- Tungsten X-ray targets can be produced with enhanced exposure lifetime, greater fracture stregth, and enhanced room temperature ductility.

This work was done by N. Beser, R. T. Frost, E. C. Okress, D. J. Rutecki, and G. Wouch of General Electric Co. for **Marshall Space Flight Center.** *For further information, Circle 92 on the TSP Request Card.*

Inquiries concerning rights for the commercial use of this invention should be addressed to the Patent Counsel, Marshall Space Flight Center [see page A8]. *Refer to MFS-23509.*

Acoustic-Energy Shaping of Meltable Metals

A containerless shaping technique is applicable to machining metals technology.

Caltech/JPL, Pasadena, California

A method of contactless machining of meltable metals in suspension utilizes acoustic-energy shaping (see figure). By varying the power ratio in any pair of acoustic transducers used for positioning an object in an acoustic suspension chamber, a resultant force is applied to the object. The force will produce a deformation in the material (in the plastic state) that is retained after solidification. Intricate noncontacting machining can be produced by varying the power ratios in pairs of transducers on selected axes. Metals melted in such an environment have improved properties, since impurities are not introduced from the container walls or floor.

To suspend an object within an acoustic chamber, it is sufficient to have equal acoustic power on the extremities of the three axes to the object (the three axes being orthogonally disposed to each other). More than one opposed pair of transducers could be utilized in any particular plane, such as for example the x-y plane. Twelve or more opposed transducers could be utilized, not only for suspension; but by providing the capability of adjusting the power ratio in any pair of transducers, pressure could be exerted in any direction by a pair of opposed transducers to shape the molten metal.

This work was done by Daniel D. Elleman and Taylor G. Wang of **Caltech/JPL.** *For further information, Circle 93 on the TSP Request Card.*

This invention is owned by NASA, and a patent application has been filed. Inquiries concerning nonexclusive or exclusive license for its commercial development should be addressed to the Patent Counsel, NASA Resident Legal Office-JPL [see page A8]. Refer to NPO-13802.

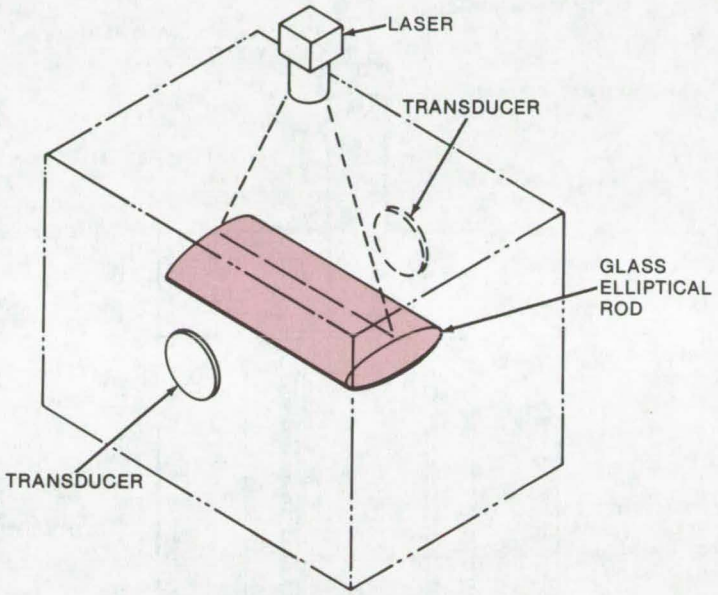

DRAWING FROM AN ELLIPTICAL ROD

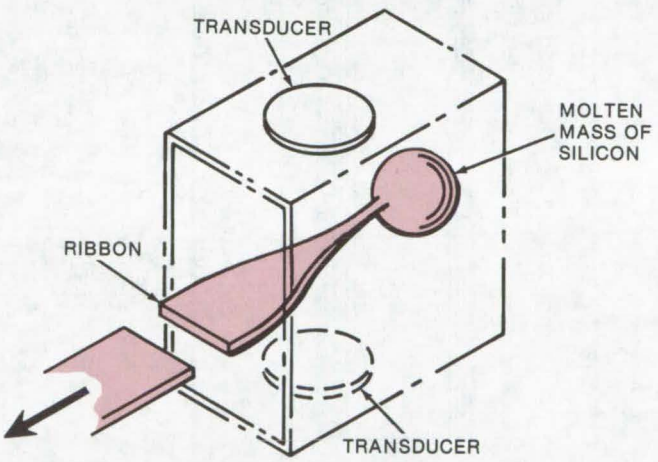

DRAWING FROM A MOLTEN MASS

Acoustic Shaping of Silicon as shown above could be used to make optical fibers or solar-cell ribbons. A flat ribbon can be formed from a thread drawn from a molten mass of silicon as it passes between a pair of transducers that generate sound of high intensity to flatten it. An elliptical glass rod is heated along its middle portion by a laser. The shape of the product is determined by the placement of the acoustic transducers. If they are placed at the top only, the ribbon will be flat. Lateral transducers could be used to squash the middle of the mass so the glass can be drawn into a long fiber with bulges along its top and bottom.

All-Tantalum Electrolytic Capacitor

Volumetric efficiency is increased by using a single-compression seal.

Marshall Space Flight Center, Alabama

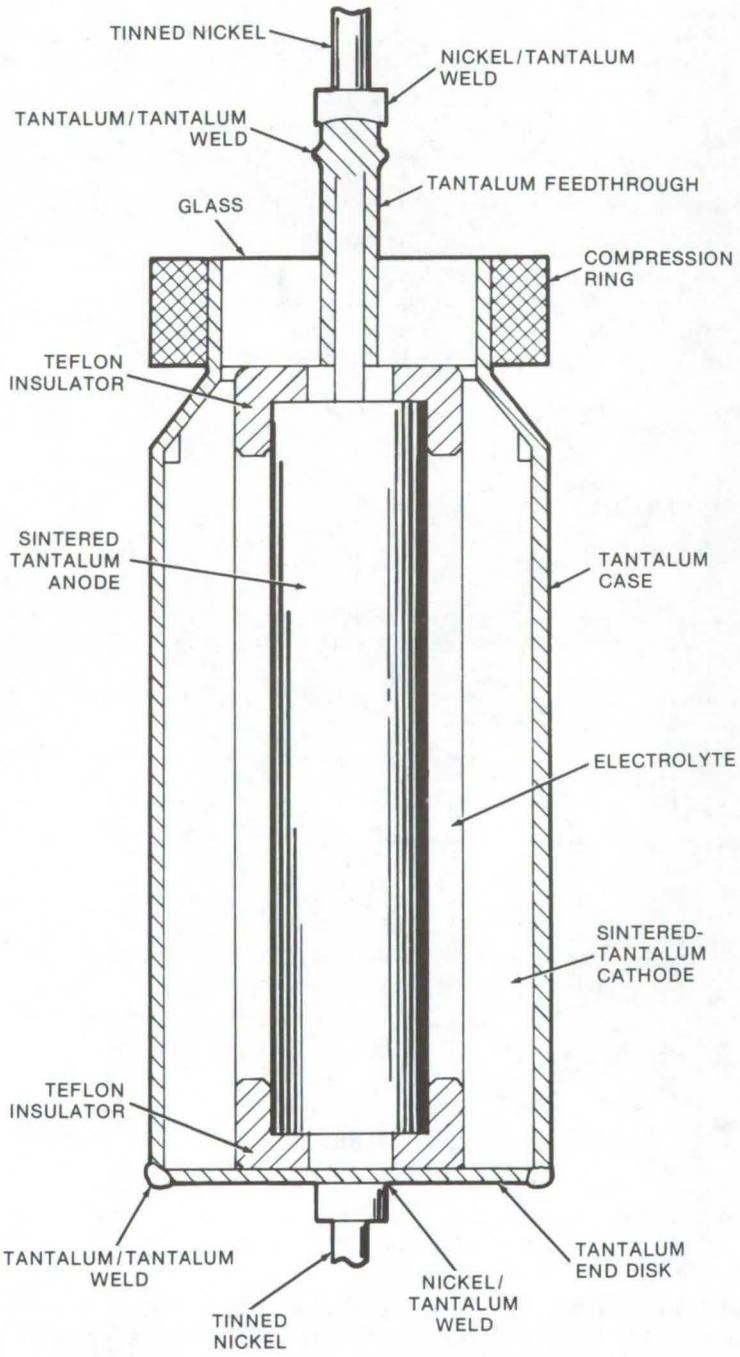

All-Tantalum Electrolytic Capacitor uses a single-compression tantalum-to-glass-to-tantalum seal. The case is tantalum, as are the cathode and the anode.

An all-tantalum electrolytic capacitor uses a single-compression tantalum-to-glass-to-tantalum seal. The capacitor case material is tantalum, and the cathode has a dielectric film sufficient to handle negative voltages up to 3 Vdc, thus eliminating capacitor degradation caused by the plating action in silver-cased capacitors. The single-compression seal allows better utilization of the volume within the capacitor. Volume gained is occupied by a lengthened cathode.

The capacitor uses a sintered-tantalum cathode as well as a sintered-tantalum anode. A pair of Teflon insulators are used to mechanically locate and support the anode. The tantalum end cap is welded to the case and the cathode, and the tantalum feedthrough is welded to the tantalum anode riser wire. Nickel leads are welded to the anode and cathode ends of the capacitor. The electrolyte is sulfuric acid, but all internal materials used are inert in the electrolyte.

As a result of the all-tantalum case and the lengthened cathode, the electrical parameters, particularly equivalent series resistance and capacitance stability, are significantly improved over the silver-cased capacitor.

This work was done by Gilbert E. Green, Jr., of Aerotron, Inc., for **Marshall Space Flight Center.**

For further information on wet-slug tantalum capacitors, Circle 94 on the TSP Request Card.

Inquiries concerning rights for the commercial use of this invention should be addressed to the Patent Counsel, Marshall Space Flight Center *[see page A8]*. *Refer to MFS-23462.*

Low-Pressure Low-Temperature Molding Process

Graphite/epoxy laminated parts are bonded, using pressure generated by an expanding rubber mandrel.

Lyndon B. Johnson Space Center, Houston, Texas

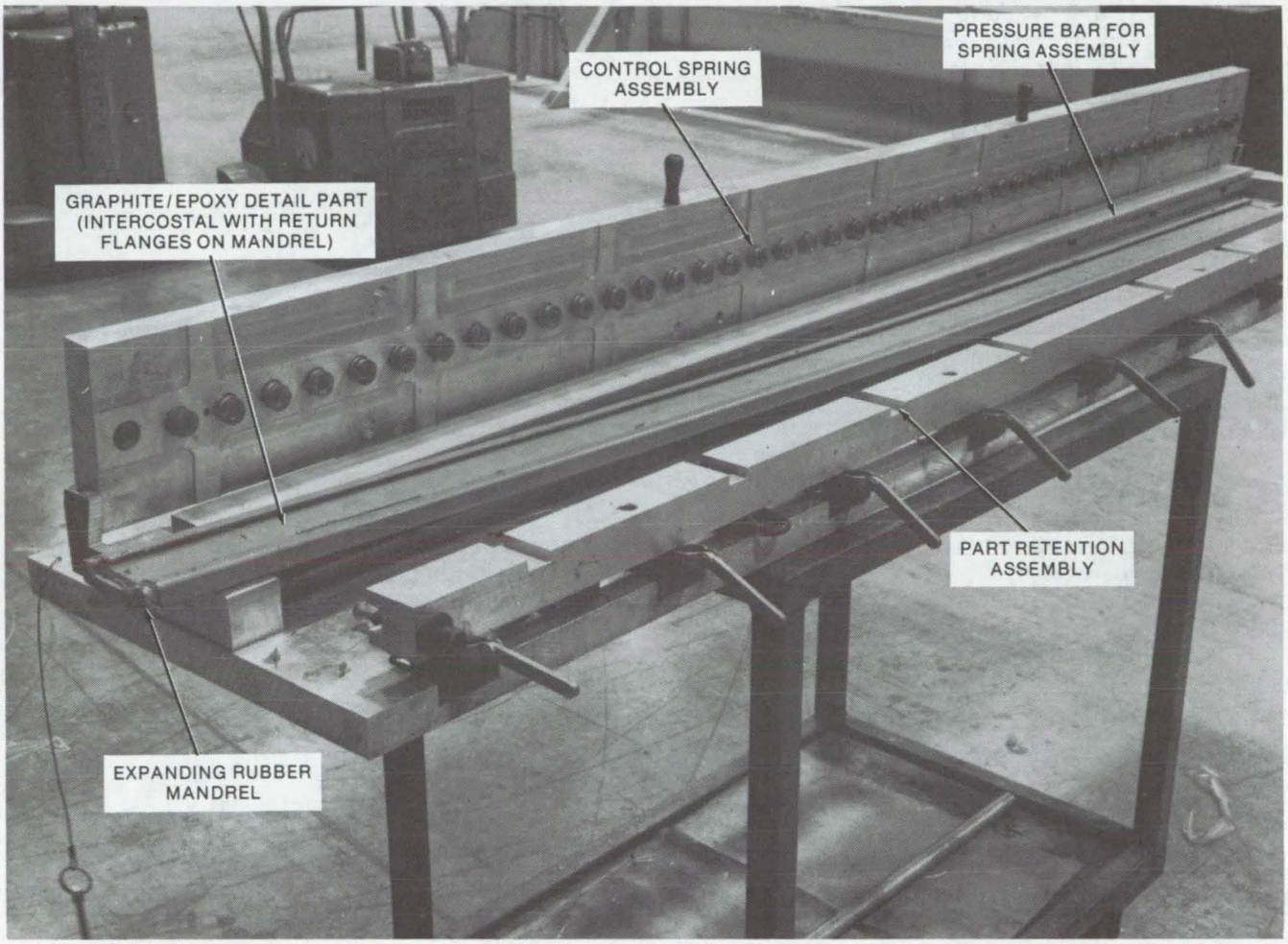

The **Expanding Rubber Mandrel** presses the laminate against the mold. Generated pressure is controlled by using a spring-loaded mechanism which sets the upper limit of applied pressure. Without the limiting mechanism, up to 1,000 psi (6.9×10^6 N/m^2) can be generated.

By using a mandrel, graphite/epoxy laminated parts may be cured in an oven instead of an expensive autoclave. When laminating parts in the oven, mandrel bonding pressure may be reduced to the range of 80 to 100 psi (552×10^3 to 690×10^3 N/m^2). Since resin contact is manipulated by precise control of the mandrel-generated pressure, a complex bleeder system is not required.

Details are laminated by using channels with return flanges. The outer mold line of a detail is controlled by a heavy-duty two-piece aluminum mold which limits deflection. The mandrel comprises, in part, an RTV type J silicone compound which is formulated with a controlled expansion rate. The compound is sized to fit within the channel and to provide 85 to 100 psi (586×10^3 to 690×10^3 N/m^2) at a temperature of 350° F (176° C). The area between the two return flanges is fitted with a pressure plate which is backed up with die springs that are calculated to oppose the compound-induced pressure. The laminate detail is positioned on the mandrel which is placed in the tool and heated to 350° F to cure.

This work was done by Eldon L. Bowman of Rockwell International Corp. for **Johnson Space Center.** *No further documentation is available.*
MSC-19778

Fuel-Cell Powerplant Insulation

A thermal blanket is optimized for minimum weight and heat loss.

Lyndon B. Johnson Space Center, Houston, Texas

Heat loss from a fuel-cell powerplant must be properly controlled to obtain maximum performance and minimum fuel consumption regardless of the environmental conditions. A new type of insulation blanket to limit heat loss has been developed for the Space Shuttle fuel-cell powerplant and may be useful with other fuel cells and applications requiring a flexible lightweight insulator.

The multilayer blanket was designed to insulate the power section, water trap, hydrogen pump, and motor of the fuel-cell powerplant. The blanket, shown in cross section, is constructed of an outer casing of rubberized glass cloth (SRG 0607, or equivalent) containing eight layers of borosilicate glass mat and seven layers of polyimide (Kapton, or equivalent) gold film.

This work was done by Robin J. Guthrie of United Technologies Corp. for **Johnson Space Center.** *No further documentation is available.*
MSC-16012

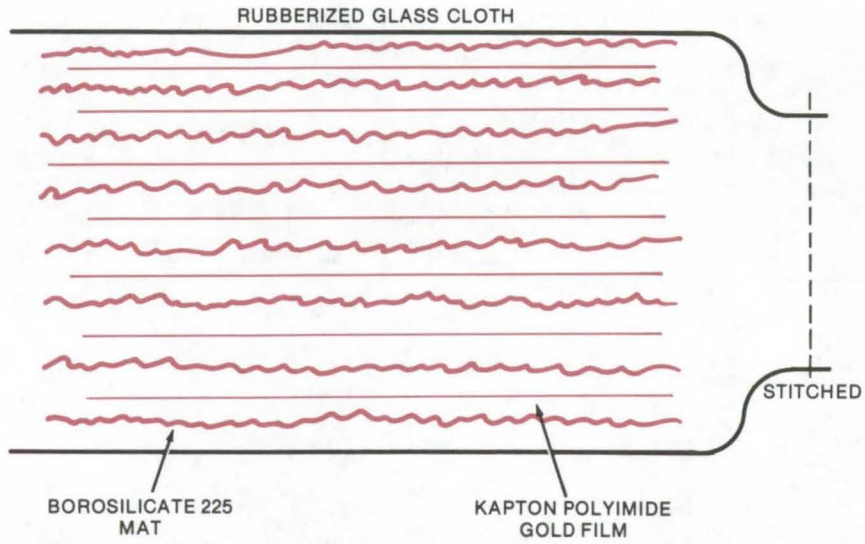

Powerplant Insulation Blanket consists of 8 layers of borosilicate mat alternated with 7 layers of polyimide gold film. Mat and film are sandwiched between rubberized glass cloth. The blanket is an excellent insulator.

Reduced Costs for Solar-Cell Modules

Production costs are reduced by new techniques, including printed circuits.

Lewis Research Center, Cleveland, Ohio

A process has been developed that reduces solar-cell-module production costs by embossing the encapsulating plastic film to position and hold the cells in place and also by printing the electrical circuitry onto the encapsulating plastic sheets so that the electrical connections are made at the same time the cells are encapsulated.

Current procedures are tedious and time consuming. The electrical contacts to the solar cells are made individually and in separate operations. The contacts are made much thicker than necessary in order to withstand the necessary handling. The printed metal-film circuitry can be much thinner than the conventional contacts because of the support provided by the plastic cover sheet.

The new process can be used for either standard-contact or wraparound-contact solar cells. For wraparound solar cells, the plastic film is heated and pressure molded to yield an embossed surface with an appropriate number of solar-cell-shaped depressions for a particular application. The solar cells are placed face down into the depressions. A flat sheet of plastic for the back surface of the module, printed with the interconnecting circuitry, is placed over the assembly. The embossed plastic sheet, solar cells, and the plastic sheet with the printed circuitry are then laminated together. The electrical interconnections are made during the lamination process by thermocompression bonding.

For standard-contact solar cells, the procedure would be the same except that the circuitry would be printed onto the embossed sheets as well as on the flat cover sheets. In this way, the packaging of solar cells into modules can be accomplished with less handling than present methods and is suitable for development with automatic processing. The individual steps of the process have been demonstrated successfully.

This work was done by Americo F. Forestieri and Evelyn Anagnostou of **Lewis Research Center.** *No further documentation is available.*

Inquiries concerning rights for the commercial use of this invention should be addressed to the Patent Counsel, Lewis Research Center [*see page A8*]. *Refer to LEW-12185.*

Improved Bonding of Honeycomb Panels

Bonded-on metal braces allow fast, strong, inexpensive, and attractive interconnection of panels.

Lyndon B. Johnson Space Center, Houston, Texas

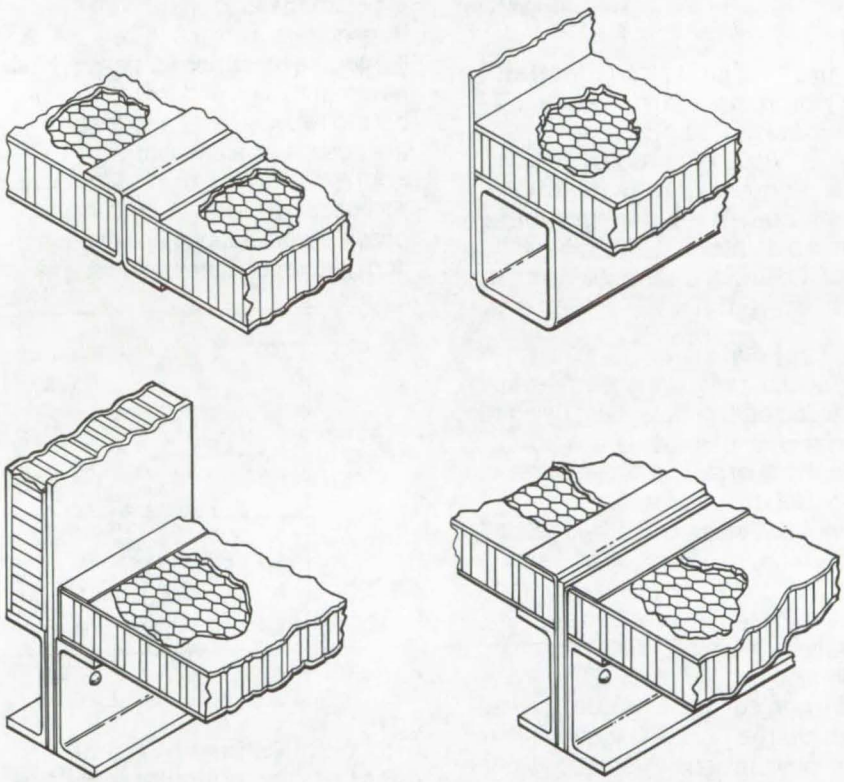

The **Metal Attachment Strips** are bonded to the panels with epoxy or other suitable adhesive. The strips shown were made from 6061-T6 aluminum alloy. Once bonded to the panels, the strips may be bolted or riveted together to form a strong and attractive connection.

One of the major problems in the fabrication of structures from honeycomb panels, fiber-reinforced composites, foam panels, or similar materials is the joining of the panels. Bolts and rivets produce weak points near or at the joints, and adhesive bonding is an expensive labor-intensive process.

A simple and inexpensive technique, using angular metal braces bonded onto the panels, can lower the cost of construction using honeycomb panels and composites. As illustrated, the braces may be made in various shapes, depending on the panel size and the angle at which they are to be joined.

This technique has been used to join the floor panels for large platforms. It was found to improve the overall structural strength, lower assembly time, and reduce construction costs.

This work was done by Stefan A. Sobkiewicz of Rockwell International Corp. for **Johnson Space Center.** *No further documentation is available.*

MSC-19560

Fabrication and Applications of Electrets

Improved fabrication techniques and applications in contamination studies suggest new markets for electrets.

Marshall Space Flight Center, Alabama

Electrets are dielectrics, usually polymers, with a permanent surface charge that gives them properties analogous to those of magnets. A recent study of ways of making electrets and of their properties suggests more economical and effective fabrication techniques and several new applications. Possible uses include particle filtration (pollution control), low-power sensors, and illumination control.

Fabrication Techniques

Electrets are classically made by placing a polymer between two parallel electrode plates, heating it until it softens, and applying a high-voltage direct current across the electrodes for several hours. Three new techniques discussed below are very much faster, can produce electrets of any size and shape, and result in improved properties.

Charge Injection

A dielectric sheet is passed through an oven; as it emerges, a corona discharge is induced over the surface by applying a high-voltage current to a metal wire brush that is kept a short distance from the dielectric. Charges are injected on the dielectric, polarizing it. The sheet then passes through a grounded, air- or water-cooled plate to freeze in the injected and polarized charge. Usually, charges of opposite polarity are produced on opposite sides of the sheet.

Tesla Coil Charging

A heated dielectric is charged with a high-frequency ac potential derived from a Tesla coil. The sheet is cooled by passing it over a grounded metal plate.

Molten Spray

A molten dielectric is sprayed through a corona discharge that is maintained between the spray gun and a cooled surface. The thin layer of deposited dielectric exhibits a permanent surface charge.

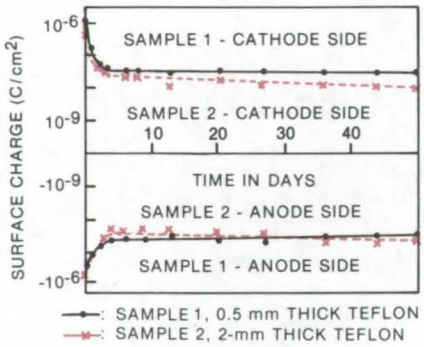

Figure 1. The **Teflon Electret,** for which the charge decay characteristics are shown above, was prepared by the brush-corona charge injection technique. The polarizing voltage was 15 kV, temperature was 180 ° C, and the sample was stroked 10 times.

Electret Materials

Several materials were investigated as electret substances, using the new techniques described above. Surface charge and decay rates were determined for numerous samples. Teflon, polyethylene, polypropylene, Plexiglas, Mylar, and polycarbonates were investigated, and of these, Teflon electrets showed the best stability and charge retention up to 200° C. Using the charge injection technique, a surface charge of 10^{-6} C/cm^2, higher than any previous electret, has been achieved, using Teflon electrets. (See Figure 1.)

Other interesting materials studied include mica and fused quartz which were found to be polarizable at relatively low temperatures and suitable for application at extremes of temperature, pressure, and humidity. Polarized quartz may be useful in quartz crystal microbalances for contamination studies.

Metal-impregnated Kapton can be used to make strong electrets with varying charge distributions. Single crystals of pure substances were also investigated, and for the first time, a single-crystal crystal electret (gadolinium molybdate) has been reported. Charge decay properties are shown in Figure 2.

Applications

Electrets are currently used in electrostatic measuring and recording instruments, microphones, transducers, prosthetic devices, and numerous other applications. These new techniques and materials will help to reduce costs and expand their use in existing markets. Furthermore, as part of this study, additional work has been done on possible applications in air pollution and general contamination studies.

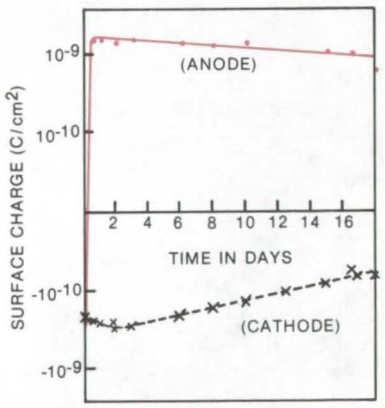

Figure 2. A **Single-Crystal Electret** of gadolinium was prepared, and its charge decay characteristics are shown above. The 1.35-mm-thick sample was polarized at 200 ° C with a field of 69 kV/cm for 7 hours. Thin sheets of mica were placed between the crystal and electrodes during the corona charging.

Electrets were shown to be efficient devices for collecting, detecting, and controlling gases and vapors of substances, such as SO_2, acetone, alcohols, and benzene. In studies of rocket exhaust effluent, electrets have been used to collect exhaust particles which were later analyzed by X-ray microprobes. The electrets were also found to be excellent collectors of dust and charged or uncharged particulate matter.

This work was done by P. K. C. Pillai and Edward L. Shriver of **Marshall Space Flight Center.** *For further information, Circle 95 on the TSP Request Card.*
MFS-23437

Cleaning Large Tanks and Gas Bottles

A solvent-vapor technique is economical and effective.

Lyndon B. Johnson Space Center, Houston, Texas

High-pressure gas bottles and large cryogenic storage tanks are normally cleaned with trichlorotrifluoroethane (CCl_3CF_3) solvent to remove hydrocarbon, halocarbon, and silicone contaminants. The procedure is awkward, and the solvent is not very effective. Gas bottles are cleaned by adding the solvent and agitating. In this procedure some areas remain contaminated because the solvent does not reach them. On the other hand, when a large tank is cleaned, a number of workers must enter inside to wash its interior wall. This by itself adds contamination. In addition, artificial breathing equipment must be used in this type of work.

These disadvantages are overcome by using a vapor solvent, trichloromonofluoromethane (CCl_3F). This vapor is more effective than CCl_3CF_3, and there is no need to enter the tank. The technique is less expensive because less solvent is required and the solvent can be easily recycled.

Removal of hydrocarbons, halocarbons, and silicones from the internal surfaces of the cryogenic tanks and high pressure GN_2 bottles depends upon the fact that vapor phase solvent will condense into a liquid on chilled surfaces. If sufficient vapor is present, it will eventually form drops of liquid which drain from the surface. It is this "distillation" process that is used to clean large-volume vessels.

Trichloromonofluoromethane (CCl_3F) is used as the solvent for several reasons:

- It is a better solvent for hydrocarbons, halocarbons, and silicones than trichlorotrifluoroethane (CCl_3CF_3), the commonly used solvent.
- Its normal boiling point is 23.8° C (74.8° F). This permits the use of a simple low-temperature boiler to produce solvent vapor, using water as the heat-exchange medium between the heaters and the solvent.
- Its freezing point is -111° C (-168° F). Therefore, evacuation of the tank or bottle will easily remove residual solvent that cannot be drained from the tanks. Under normal conditions the solvent will not freeze during the evacuation operation.
- The solvent is easily distilled to purify the trichloromonofluoromethane for reuse.

This work was done by Irwin D. Smith of the White Sands Test Facility for **Johnson Space Center.** *For further information, Circle 96 on the TSP Request Card.*
MSC-14966

Design of Redundant Systems

An algorithmic approach aids the design of systems with multiple noisy inputs. It could be used with circuits, chemical processes, and machinery design. When transfer functions and parameter tolerances are known, the probabilities of failures for various designs may be determined.
(See page 417.)

Catalytic Oxidation of Waste Materials

A new technique for catalytic oxidation of waste materials employs a soluble ruthenium salt that is introduced upstream from the reaction chamber. In the reaction chamber, heat causes the soluble salt to be deposited as an insoluble ruthenium black catalyst on the internal surface of the reactor. Thus no soluble catalyst exits the reactor to contribute to pollution of the treated water. Because the soluble salt is introduced external to the reactor, the system may be "recharged" while the purification is in process.
(See page 381.)

Molecular Beam Generator

A molecular beam generator for heavy organic molecules may be used as a laboratory instrument or to deposit organic coatings. The generator has a nozzle and aperture designed especially for beams of heavyorganic molecules. Deposition rates are from 6 to 15 Å/min.
(See page 380.)

Graphical Methods for Variable Sampling Plans

A simplified technique can be done quickly and without machine assistance.

Lyndon B. Johnson Space Center, Houston, Texas

Previously, variable sampling plans (MIL-STD-414) required extensive computations and were rarely used by floor-level inspection personnel. With a new graphical analysis, which simplifies the necessary calculations, variable sampling can now be utilized with a minimum of training. Compared to attribute sampling (MIL-STD-105), it provides more accurate quality-level information for given sample sizes.

In cases where the number of samples is limited, the cost of inspection is extremely high, or the inspection is destructive, the variable sampling plans are a logical choice. In cases where the quality levels of the product items usually exceed the requirements, the graphical method for applying variable sampling plans may be used in place of 100 percent inspection to reduce inspection cost. These procedures give a close approximation of the results otherwise obtained by the computations of MIL-STD-414.

The graphical method is done on standard probability paper (see figure). The ordinate is used to represent quality levels, and the abscissa values are probability percentages. For a given lot size, the appropriate sample size is determined from a table. Using the sample size, a set of P values is found in another table, and these are marked on the abscissa at the assigned probability-percentage points.

Horizontal lines are drawn representing the maximum and minimum specification levels. (For instance, for a resistor, they might be 650 ohms maximum and 600 ohms minimum.) The samples are then tested, and the quality levels are plotted in ascending order against the P values. A best-fit line is drawn through the points.

The intersection of this line with the horizontal specification lines gives percentages of defective parts. These percentages are added, and the lot is acceptable if their sum does not exceed the M value found in the appropriate table. For single-limit specifications, the single intercept is compared with the appropriate published K value.

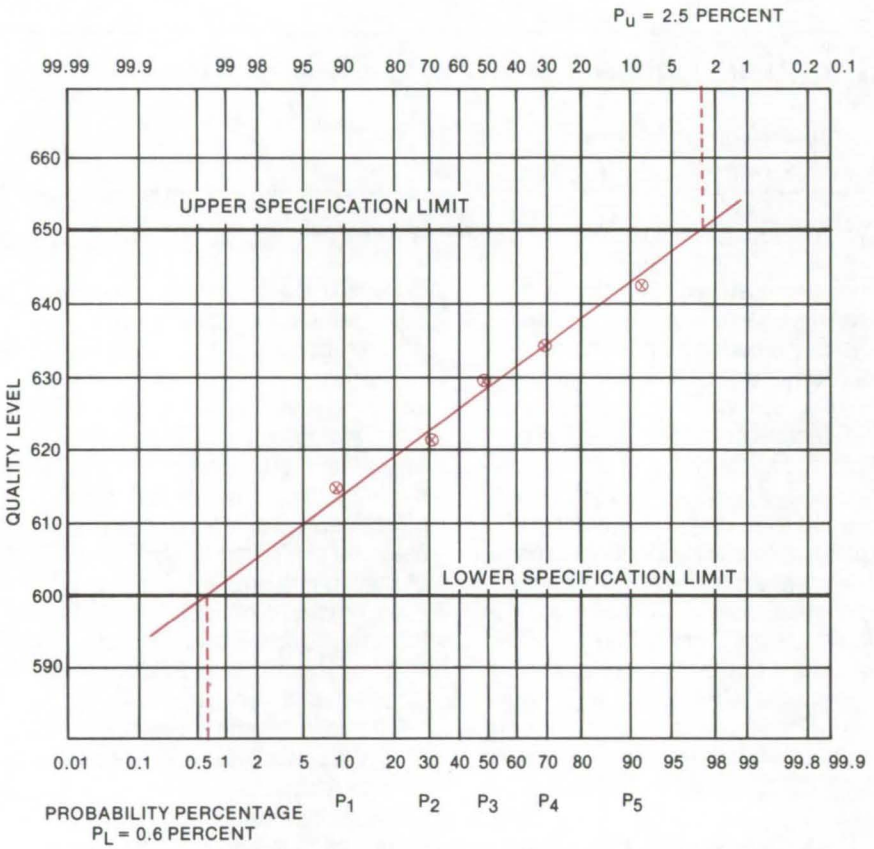

The **Graphical Method** for determining whether a production lot meets required specifications is carried out with standard probability paper with coordinate values determined from a set of tables. The procedure is described in the text.

This work was done by Kuniyoshi Teramura of Rockwell International Corp. for **Johnson Space Center.** *For further information, Circle 97 on the TSP Request Card.*
MSC-19279

Controlled Linear Clamper/Loader

A tool used to clamp odd-shaped parts to nonuniform surfaces

Goddard Space Flight Center, Greenbelt, Maryland

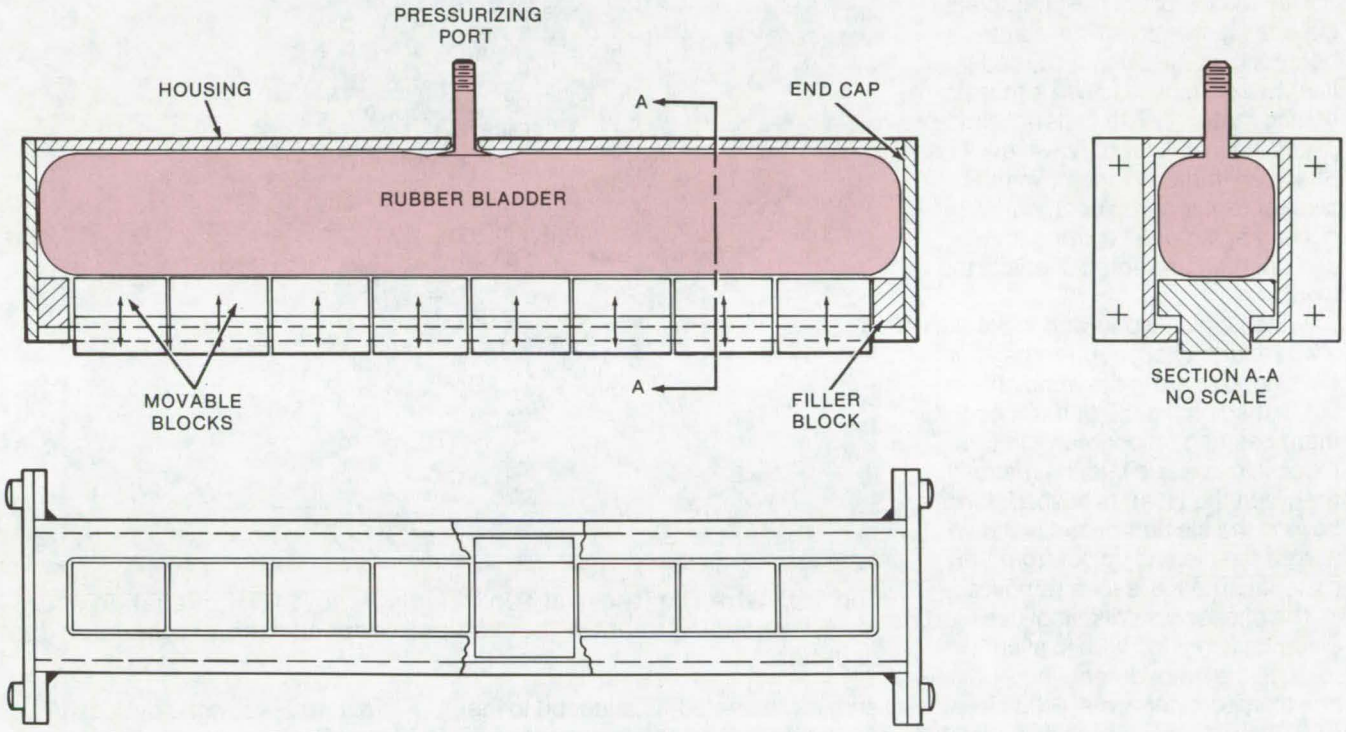

Controlled Linear Clamping Tool is placed over parts and is pneumatically (or hydraulically) pressurized via the port. A rubber bladder exerts a common force on each of the movable blocks; housing shape or size is thus limited only by practical size of the enclosed bladder.

Tools used to clamp or load odd-shaped or delicate hardware to nonuniform surfaces during manufacture include C-clamps and straps. However, this type of hardware, besides asserting clamping forces only at discrete points, depends on the skill of the operator to set and apply the forces correctly. The new tool shown in the figure aids in clamping hardware to any shape surface and applies a uniform load over the clamped surface. The clamp consists of a housing and end caps, an enclosed rubber bladder, and movable blocks through which the clamping force (or linear load) is applied.

The clamp is positioned over the parts which are located on a baseplate. Controlled pneumatic or hydraulic pressure is applied to the pressurizing port. The bladder expands, exerting an equal force on each movable block which, in turn, bears on the parts. The clamp may also be attached directly to individual parts and pressure applied to achieve a similar result.

The clamper/loader is shown with a rectangular cross section, but the use of a rubber bladder allows it to be made in most any required shape. It can also be as short or as long as needed, and it can be made from nonmagnetic materials for use in magnetic-field test environments.

This work was done by Robert M. Steudl of **Goddard Space Flight Center.** *No further documentation is available.*
GSC-12105

Hot-Wire Tile Removal Tool

Tiles held in place by heat-activated bonding agents can be released without damage to the tile or to the agent.

John F. Kennedy Space Center, Florida

One means of bonding flat, planar objects (such as heat-resistant ceramic tiles, flooring tiles, and the like) to a surface is to use a thermosetting material. The material simplifies tile installation; however, it is often very difficult to remove the tiles for repair or replacement without damaging or destroying them and creating unwanted debris in the work area.

A tool, which works and looks like a wire-blade cheesecutter, has been developed to aid in tile removal without damaging the tile or harming the thermosetting embedment. In use, the tool is inserted into the material (between the tiles), is pushed down beyond the tile depth, and is drawn across the tile and up out from the material. The tile is then removed.

The cheesecutterlike tool uses an electrically heated wire to slice through the embedment. Two beryllium/copper arms [0.030 in. (0.076 cm) thick], which hold the wire, fit between the tiles to pull the wire through the thermosetting compound. The heated wire is Nichrome 0.025 in. (0.064 cm) in diameter and, as illustrated, is attached to the arms for removal or adjustment as required. The wire is powered via an external voltage regulator which sources it with 6.5 volts at 9 amperes.

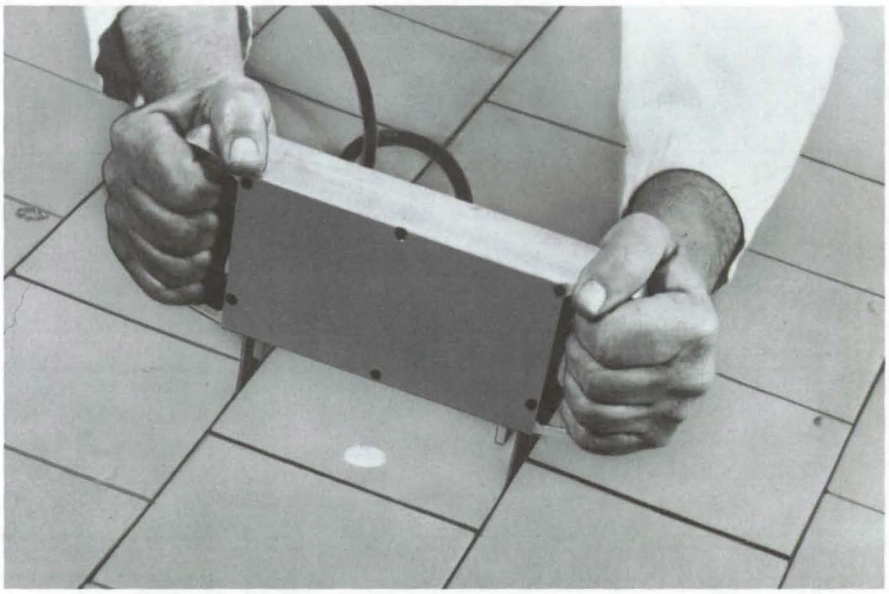

The **Hot-Wire Tile Removal Tool** rapidly removes flat, planar objects from the bonding agent without adjustment and without producing dust or debris.

This work was done by Jack W. Holt of Rockwell International Corp. for **Kennedy Space Center.** *For further information, Circle 99 on the TSP Request Card.*
KSC-11043

Mathematics and Information Sciences

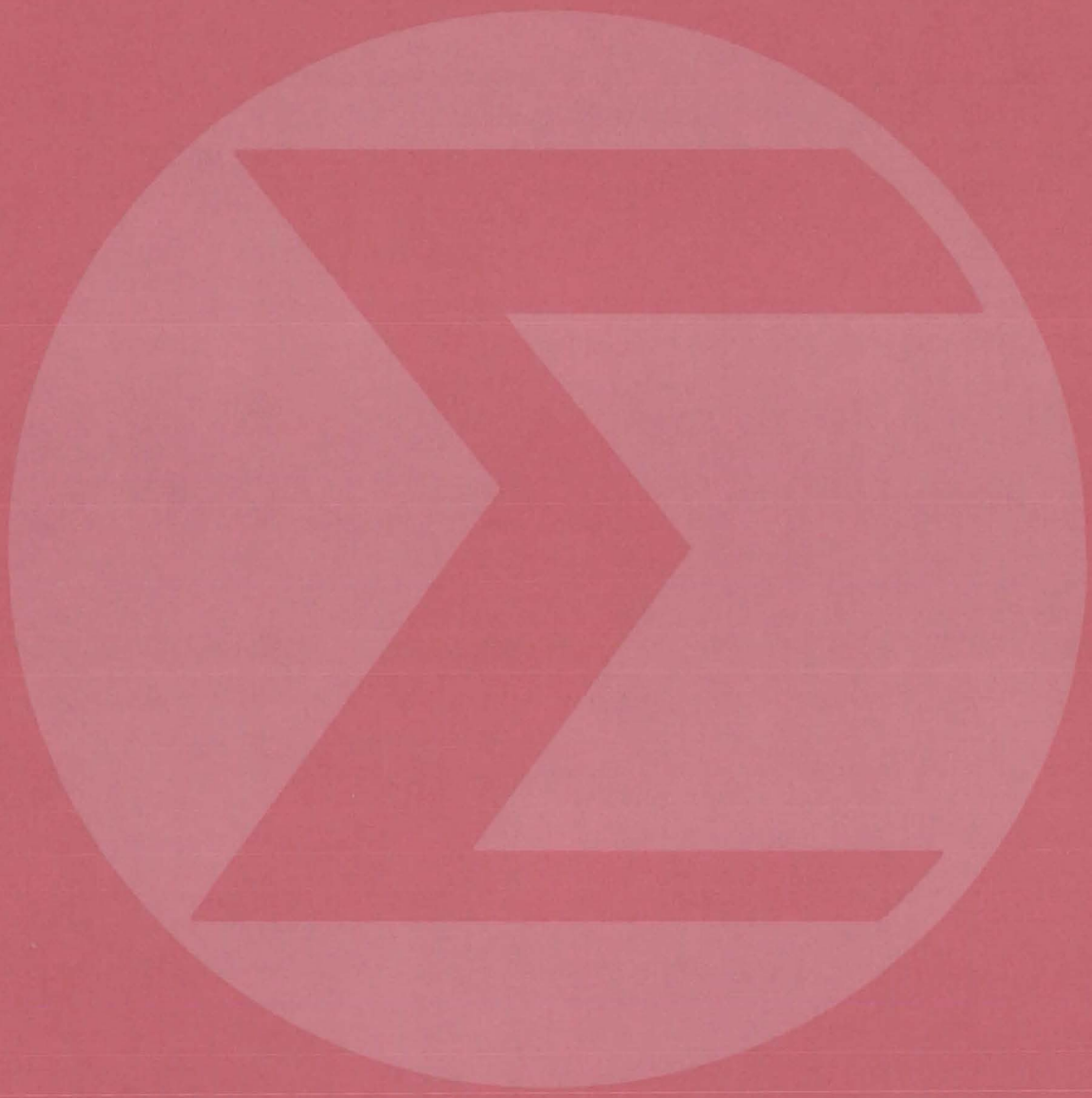

Curvilinear Bicubic-Spline-Fit Interpolation

A modified interpolation technique is suited to circular systems represented by polar grid patterns.

Langley Research Center, Hampton, Virginia

When complex surface mapping problems (e.g., the equiphase surface of an electromagnetic wave, optical lens design, ray tracing, potential distribution, and structural surface deformation) are to be solved by a digital computer, the computer solution requires the construction of a suitable grid-point pattern over the surface region. The computed values then are obtained at the discrete grid points. However, when a continuous function is solved by the computer, a reliable interpolation technique is needed to obtain intermediate values between the grid points.

The bicubic spline-fit interpolation technique is often used for this purpose. It precisely interpolates functions up to the third degree in each coordinate axis and is sufficient to interpolate a physical surface that is expressible by the double Laplacian equation (or lower-order differential equation)

$$\nabla 2(\nabla 2\Psi) = 0$$

provided that the surface region is subdivided into a number of small enough patches.

When the geometry of the system is circular, as it is for practically all optical systems, a polar grid pattern is usually preferable to a rectangular or a triangular grid pattern, especially when the behavior of the computed function is strongly dependent on the boundary conditions along the system circumference. However, the currently-available rectangular bicubic spline-fit interpolation is not adaptable for use with the circular boundary region; a modified interpolation scheme for the polar grid pattern must therefore be devised.

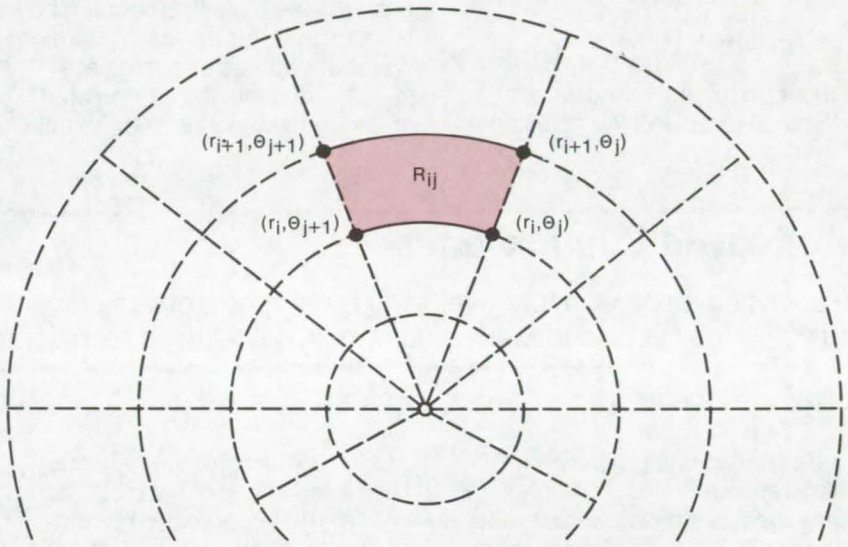

Figure 1. **Patch Regions** (R_{ij}) are defined by radius and arc length. Differentiation is performed with respect to arc length instead of angle.

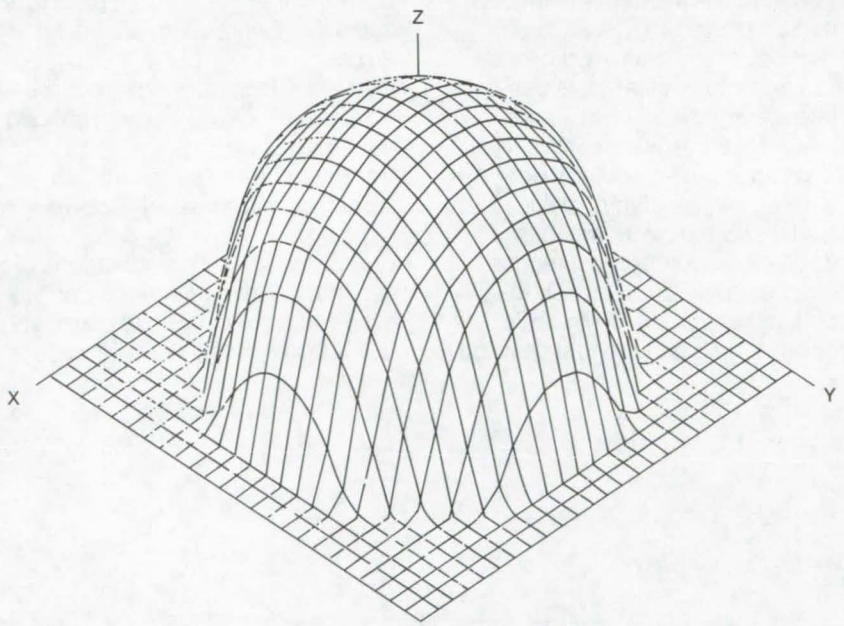

Figure 2. The **Hemisphere** shown above is based on interpolated values between polar grid points.

A curvilinear interpolation has been developed in which the variables are transformed to radius and arc length. Differentiation then is with respect to arc length instead of angle and so is physically a more meaningful quantity. The region of the polar patch is defined by

$$R_{ij}: r_i \leq r \leq r_{i+1}, \theta_j \leq \theta \leq \theta_{j-1},$$

as shown in Figure 1, and within each patch is defined the curvilinear bicubic polynomial,

$$T(r,\theta) = \sum_{m=0}^{3} \sum_{n=0}^{3} C_{mn} (r-a)^m (r\theta - a\eta)^n$$

where a, η are constants.

The isometric drawing (see Figure 2) shows a hemisphere which is based on the interpolated values between the polar grid points. The isometric plotter moves in a straight line in a rectangular coordinate system and plots the interpolated values of the function at given intervals. Each interpolated value was computed using the curvilinear bicubic spline-fit formulas and was then supplied to the plotting machine. The isometric drawing illustrates the working of the interpolation on a qualitative basis.

This work was done by Chang H. Chi of The Perkin-Elmer Corp. for **Langley Research Center.** *For further information, Circle 100 on the TSP Request Card.*
LAR-11391

Interleaved Cyclic Codes

An analytical approach for developing burst error correction and detection cyclic codes does not require shortening techniques.

John F. Kennedy Space Center, Florida

A distributed computer system configuration requires a complex communications network to provide computer-to-computer communications. A common memory is the coordination point for all subsystem data communications and allows the interconnection of up to 64 minicomputers. The system is designed so that a breakdown at some point will not cause the entire system to fail. In order to facilitate this design an interleaved cyclic (16,8) code was developed. Advantageous use of burst error cyclic codes is employed without weakening basic codes by shortening techniques.

Modified b-adjacent techniques are applied to a Bose-Chaudhuri-Hocqnenghen (BCH) (7,4) single error correcting code to first develop a BCH (8,4) alpha-squared code. Then interleaving of the modified BCH (8,4) to degree two gives a code with the capability of correcting adjacent bit errors for bursts up to and including (N-k)/2 bits.

The codes meet the following requirements:

- Correct all single random bit errors and detect all random double bit errors.
- Correct at least all single, double adjacent bit errors on an even/odd hardware boundary.
- Detect an "all ones" or an "all zeros" condition as an uncorrectable error.
- Detect at least all combinations of second, double adjacent bit errors over the same even/odd boundary.
- Easily convert to a code capable of correcting four adjacent bit errors on an even/odd hardware boundary.

With the use of successive b-adjacent interleaving of the (8,4) code, any half-rate code (n,n/2) can be derived that displays the characteristics of cyclic codes of defined length. The derived code detects 94.4 percent (1,533 out of 1,624) combinations of possible adjacent errors of three, four, five, or six bits resulting from three hardware chip failures, where each chip contains two bits per chip on an even/odd boundary.

This work was done by R. W. Hockenberger of IBM Corp. for **Kennedy Space Center.** *For further information, Circle 101 on the TSP Request Card.*
KSC-11040

Computer Programs

These programs may be obtained at very reasonable cost from COSMIC, a facility sponsored by NASA to make new programs available to the public. For information on program price, size, and availability, circle the reference letter on the COSMIC Request Card in this issue.

Contouring Randomly Spaced Data

A program contours data points too numerous to fit into a rectangular grid.

By using a triangulation contouring technique, randomly-spaced input data can be contoured without first fitting the data into a rectangular grid. Each data point of the function to be contoured consists of an X, a Y, and a Z value. The X and Y values correspond to the independent coordinates to be plotted, and Z = Z(X,Y) is the function value to be contoured. The contouring process begins by forming a convex region composed of triangles from the set of X-Y data points. After the triangles are arranged, each Z value is assigned to its corresponding X-Y vertex in each triangle. An interpolating plane which fits the vertexes exactly is then calculated for each triangle.

If a chosen contour level lies between the Z values for any triangle, the two contour points that lie on the sides of the triangle are computed from the interpolating plane. These contour points are calculated for each specified contour level. The contour points for any given contour level may then be connected by straight lines to yield a polygonal approximation to the required contour, or a cubic-spline function under tension can be used to fit a smooth curve to each set of contour points.

Several output options are available to the user, such as: controlling which value in the data record is to be contoured, whether contours are drawn by polygonal lines or by a spline under tension, and controlling the contour level labels which may be suppressed if desired. Using random access procedures, the program can handle up to 56,000 data points and provides for up to 20 contour intervals for a multiple number of parameters. The program requires 42K octal storage locations plus the larger of: 24 times the maximum number of points in each data partition or 2K plus 4 times the total number of points to be plotted.

FORTRAN IV
CDC 6000 Series
CALCOMP Plotting

This program was written by James F. Kibler and W. Douglas Morris of **Langley Research Center** *and Roy W. Hamm of Computer Sciences Corp. For further information, Circle R on the COSMIC Request Card.*
LAR-12044

Meta-assembler

A "machine-independent" cross-assembler program

The meta-assembler, a cross assembler with a high degree of machine independence, can produce object modules for a variety of computers. It is a single assembler program capable of being reconfigured by a data set supplied at assembly time. The data set includes a target computer definition of all required machine characteristics and a definition of the assembler input language.

The purpose of the meta-assembler is to produce object modules for various computers. Input to the program is a data set describing the configuration of the target computer (computer on which the output object module will be loaded) and the user-supplied program in meta-assembler code. These input functions are performed on a host computer which may be any machine with FORTRAN IV implementation and word size of 32 or more bits. The output is an object module of the user's program for the target computer. A variety of individual target computers may be specified by reconfiguring the input data set.

FORTRAN IV
Batch Mode
IBM 360/65

This program was written by B. C. Hodges of **Marshall Space Flight Center** *and A. J. Edwards of McDonnell Douglas Corp. For further information, Circle P on the COSMIC Request Card.*
MFS-23449

Processing Equations for State-Space Models

Calculation of Matrix Stability and Frequency Response

Three computer programs comprising six efficient subroutines have been used to process state variable equations for systems of high order. High-speed digital computers have made matrix state variable methods for system analysis practical. But for large systems, the required execution time and the cumulative effect of roundoff errors make it increasingly important to employ efficient algorithms.

The first of these three computer programs obtains the characteristic

equation of a system matrix by the method of Danilevsky. This program includes a Gauss pivotal element condensation scheme to increase its accuracy.

The second computer program determines the stability of the characteristic equation by the Routh-Horwitz alternate formulation method.

The third computer program obtains the system transfer function using the method of Bollinger. A transformation by Davison is used in conjunction with Bollinger's method to obtain the transfer function between any input and output. The transfer function can then be evaluated to obtain its frequency response.

FORTRAN IV
IBM 360-67 TSS

These programs were written by Robert C. Seidel of **Lewis Research Center.** *For further information, Circle Q on the COSMIC Request Card.*
LEW-12555

SUBJECT INDEX

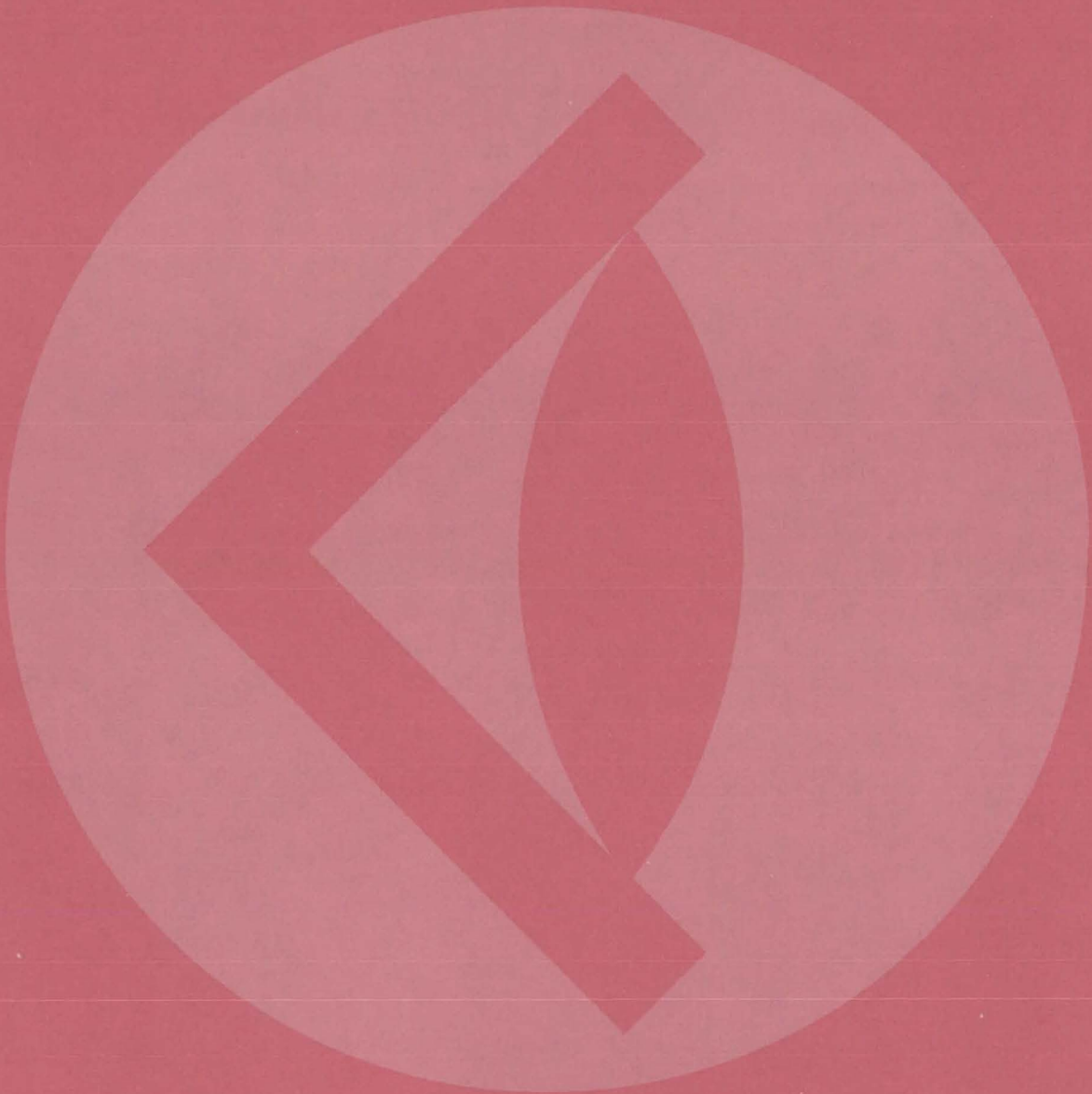

National Aeronautics and
Space Administration

Washington, D.C.
20546

NASA

Computer programs available from COSMIC have been used to determine chemical-equilibrium data needed for the design of pollution-abatement plants and equipment.